Principles of 2-D and 3-D Seismic Interpretation

Presented by

Dr. Bruce S. Hart, McGill University

Cairo/Sharm El Sheikh – December 5-9, 2004

Course Contents

Chapter 9: Advanced Methods

- Amplitude variation with offset (AVO)
- Seismic attributes
- Time-lapse (“4-D”) seismic
- Multicomponent seismic
- Seismic inversion

Seismic Interpretation

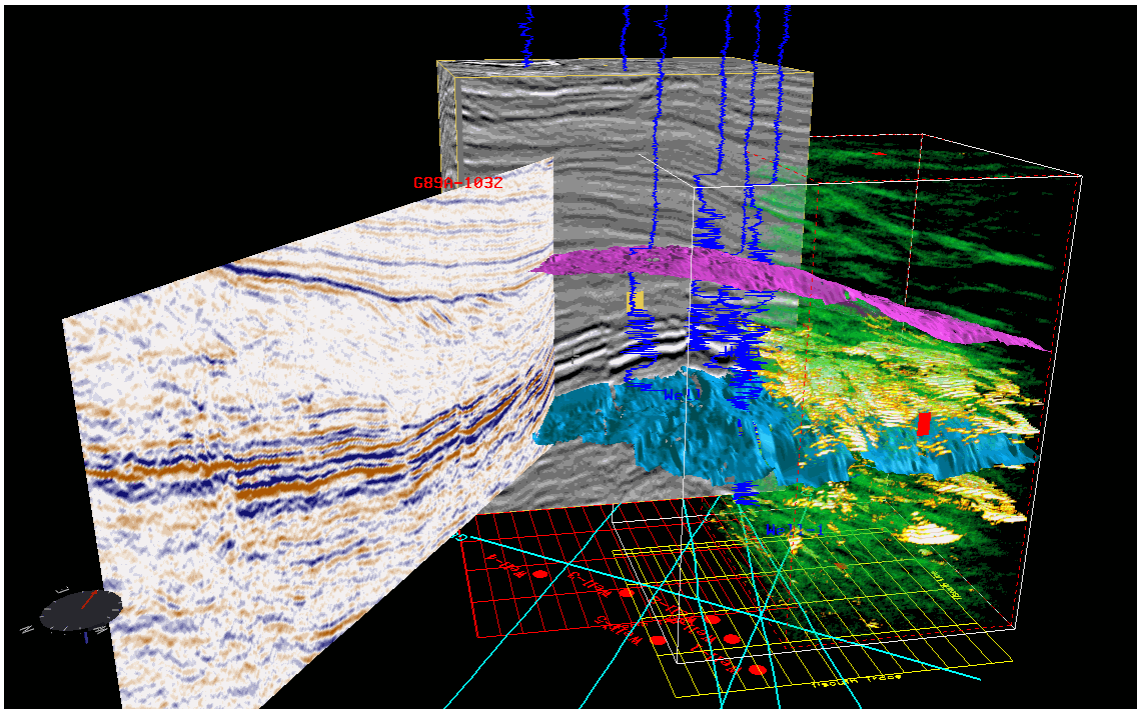

- Seismic data, in particular 3-D seismic data, are a mainstay of the petroleum industry
- These geophysical data provide subsurface images and other information that may be used by geophysicists, geologists and engineers alike to identify and effectively drain hydrocarbon reservoirs
- Seismic data should not be interpreted in a stand-alone fashion. Both geological and geophysical (and, arguably, engineering) expertise and data need to be included in a “complete” interpretation

Course Content

- This course will emphasize the geological interpretation of seismic data for the exploration and development of hydrocarbons. A complete interpretation requires the integration of geological, geophysical and engineering data and concepts. Consensus growing that the interpretation truly starts at the survey design phase, and continues up through processing
- Objectives are to provide a basic tool set and workflow for interpretation
- Will touch on certain aspects of acquisition and processing. Full treatment of these two topics is beyond the scope of this course
- Focus will be on the principles underlying the interpretation process. The nuts-and-bolts of how to use specific software applications will be discussed in other courses
- Course will begin by reviewing the physical basis of the seismic method, including the convolutional theorem
- Acquisition and processing parameters have a big impact on data quality, and so on the interpreter's ability to work with the data. Post-stack processing can improve data interpretability. Coherency volumes are often prepared for structural interpretation.
- Basic tools when preparing for interpretation include synthetic seismograms, seismic modeling, velocity data,
- Both 2-D and 3-D seismic methods have uses, particular characteristics and pitfalls. Techniques for viewing seismic data can help interpreter
- Let regional tectonic environment be you guide when undertaking structural interpretation
- Depth conversion takes seismic interpretation from geophysical world into geologic/engineering world. Different methods available, each with advantages/disadvantages.
- Stratigraphic interpretation may range from regional to reservoir scale.
- Knowledge of other topics, e.g., volumetric interpretation, amplitude variation with offset (AVO) and time-lapse methods, will be briefly discussed
- Interpretation workflow summarises concepts

3-D Seismic Data

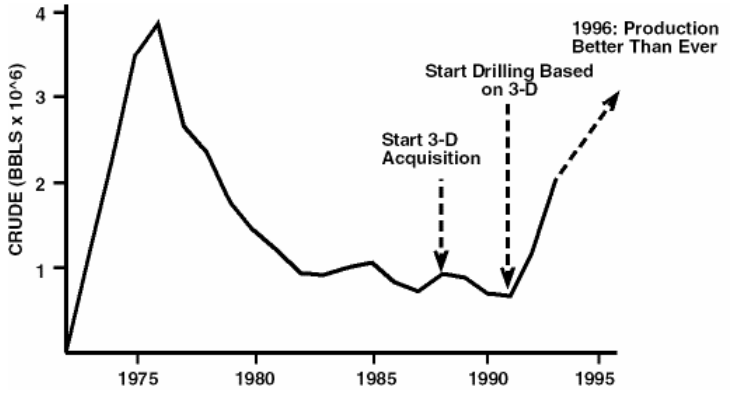

- Much of course content focuses on 3-D seismic data
  - The tool of choice in the petroleum industry
- 3-D seismic data provide the most accurate, continuous volume of information that can be obtained to image subsurface stratigraphy, structure and rock properties. Routinely, interpretations based on 2-D seismic or log data are shown to be incorrect, to varying degrees, once 3-D seismic data become available for interpretation
- Figure above, showing annual production data for a field in the offshore Gulf of Mexico, is a classic example of the benefits of 3-D seismic data:
  - First production in 1972
  - Production peaks in 1974, then begins to decline
  - Workovers and other efforts temporarily slow down decline
  - First 3-D data collected in 1988
  - Drilling based on 3-D data begins in 1991
  - Reversal in field's production decline is immediate
- Similar results have been obtained in many other places, although there are places where 3-D seismic data have not resulted in large improvements in drilling success. In this course we will learn why.

Keys to Success with 3-D Seismic Data

- Good quality data
- Integrated, accurate database
- Multidisciplinary integration (acquisitionplanning to reservoir management)
- Clear understanding of capabilities and limitations of methods/software
- Insight - Asking the right questions! (Geological/geophysical/engineering)

Seismic Interpreters

- Ideal interpreter: “integrated geoscientist”, combining geologic training, geophysics training, computer skills and engineering concepts. Unfortunately, no (?few) universities train “integrated geoscientists”, instead they train geologists or geophysicists. Integrated geoscientists typically emerge after industry cross-training

- According to Sternbach, (TLE, Oct. 2002) as interpreters, geologists are commonly “play finders”. They have skills in pattern recognition and an understanding of geologic models (“What should it look like?”). They prepare “plausible models” integrating all data types. Geophysicists are commonly ‘pay finders”, using direct-detection software to find prospects. They focus on quantitative measurements and data analysis

The Seismic Method

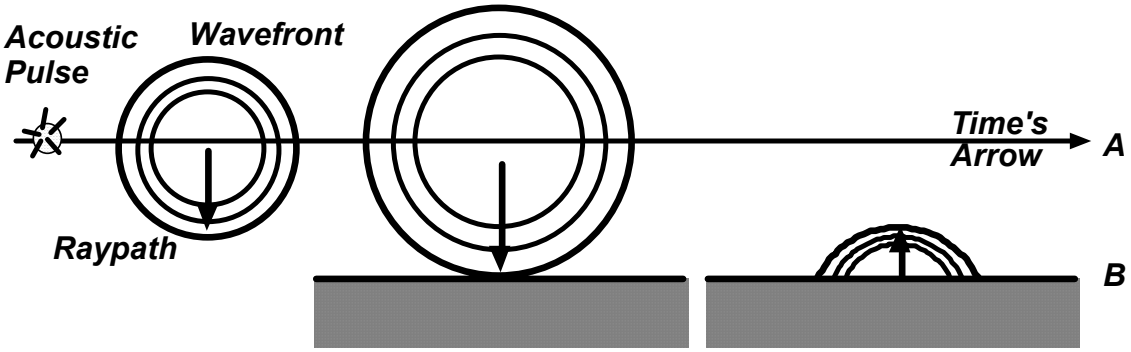

- Conventional reflection seismic technology uses acoustic waves (“sound”) to image the subsurface
- Conceptually, as shown above, we begin by generating a bang. The sound travels down into the earth, some of it gets reflected off buried interfaces, and we record the reflected energy (“echoes”)
  - The distance from the surface to buried horizons is measured in time – (two-way traveltime - TWT)
  - If we know the velocity of sound in the propagating medium we can derive true depths
- In practice we need to determine the optimal source of acoustic energy for the situation at hand, there is more than one interface in the subsurface and we need to repeat the exercise many times in order to generate a seismic profile or volume
  - Ship-towed airguns used at sea
  - Dynamite or vibroseis used on land

P & S Waves

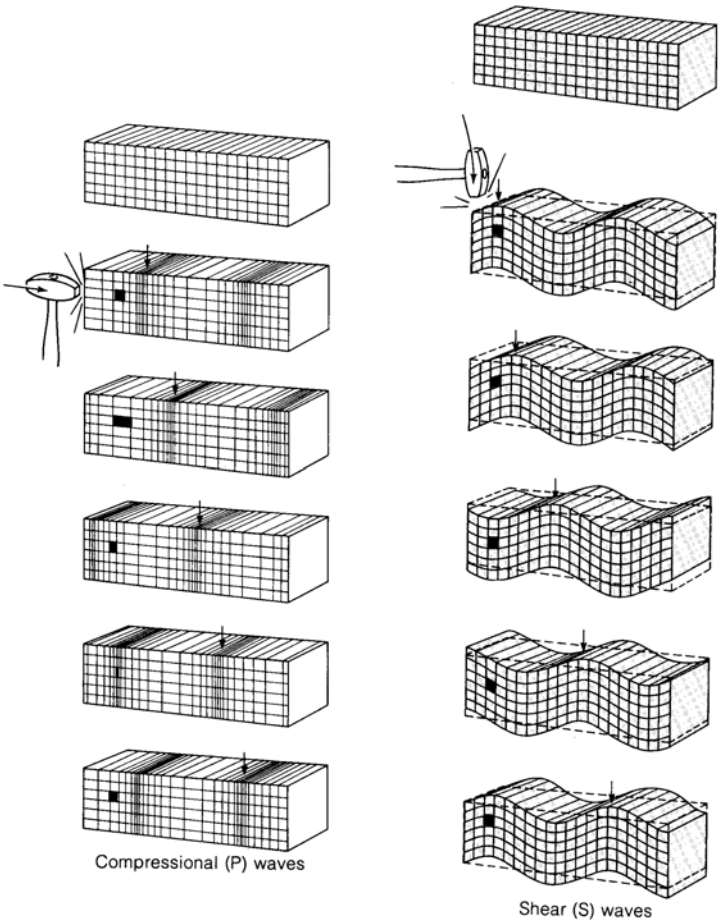

- As just noted, most seismic surveying is conducted with acoustic, a.k.a. “compressional” waves
  - Abbreviated as “P” waves
- Shear waves are another type of wave
  - Abbreviated as “S” waves
  - Cannot propagate through fluids
- In this course we will focus on P-wave seismic methods, the most common case
  - Multicomponent surveys seeing increasing use/interest

The Seismic wavelet

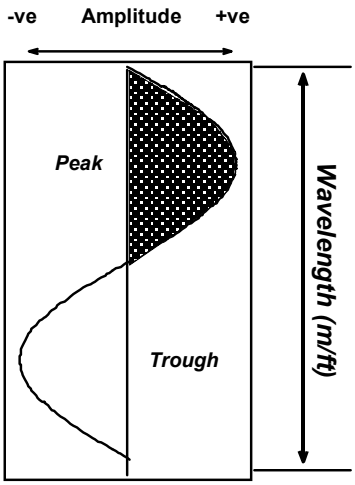

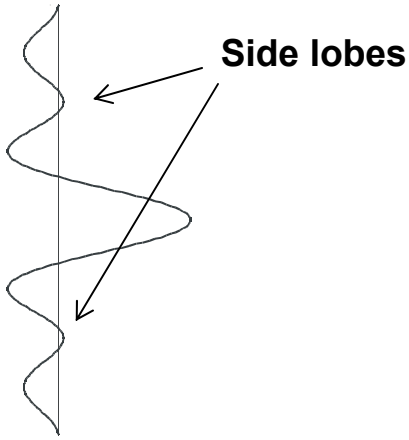

- Wavelets may be measured/described in a variety of ways:
  - Wavelength (λ)
    - Distance between successive repetitions of the waveform
    - Meters/feet
  - Amplitude
    - Positive values (“peaks”)
    - Negative values (“troughs”)
  - Frequency (F)
    - Number of wavelets that pass by a given point in a given time
    - Cycles/second – Hertz
- Key relationship:

$$\lambda = V/F$$

V – Velocity

- Real seismic wavelets more complex than simple sinusoid shown at left
  - More realistic, but nevertheless still “idealized” wavelet shown at right

Seismic Data Frequency Content

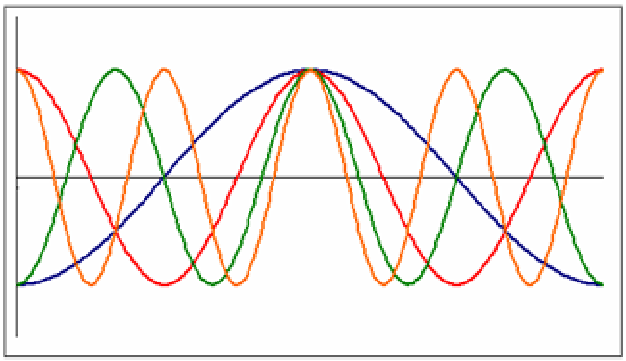

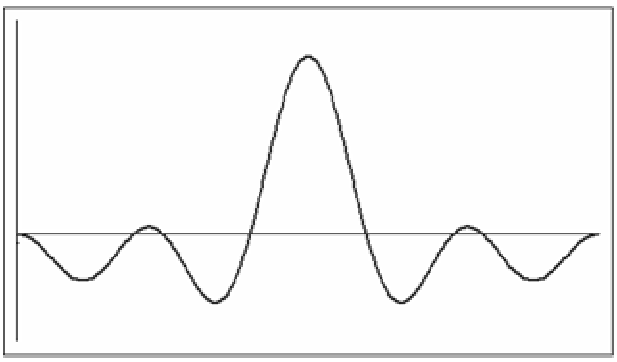

- The seismic wavelet contains a range of frequencies, rather than just one. The image at top shows how several frequencies are combined to produce a single wavelet.

- The frequency content of seismic data may be derived in a number of ways. One is visually, counting the number of cycles present in the data in a specific time interval. This provides an estimate of the dominant frequency of the data at that level. The other main method involves the Fourier transform. A particular range of data is selected by the interpreter and the software displays an amplitude spectrum for that interval. A sample amplitude spectrum is shown below.

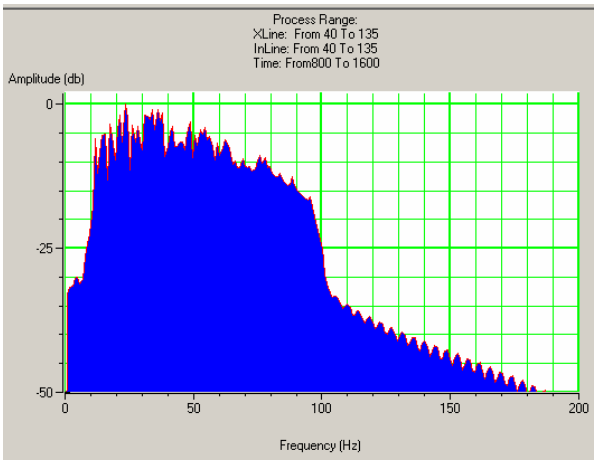

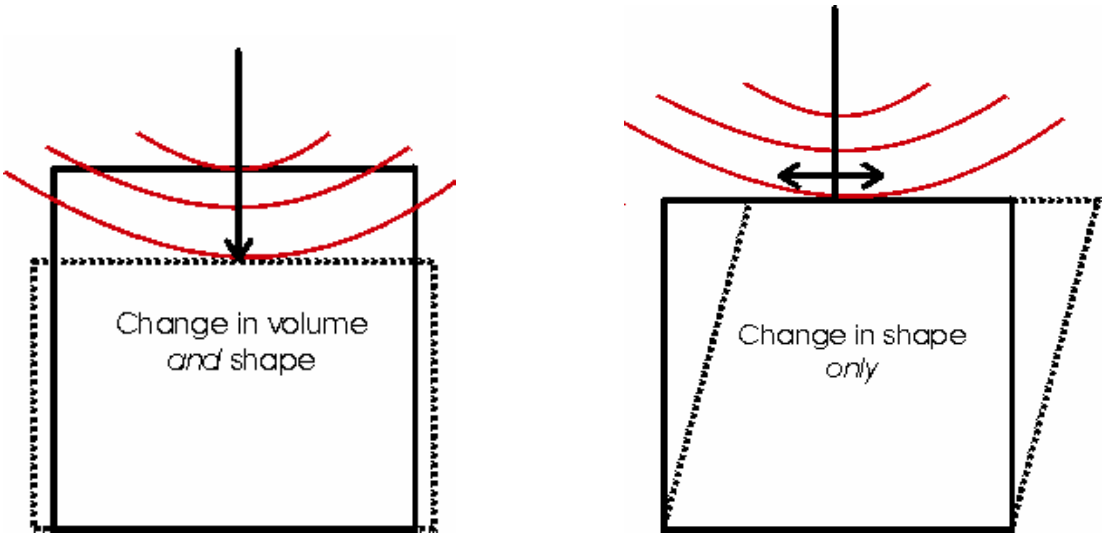

Scott-Pickford

•When a compressional wave (p-wave) travels through a body (left), the body undergoes changes in both volume and shape. When a shear wave (s-wave) travels through a body (right), the body undergoes a change in shape only.

•The p-wave velocity through a body is given by:

$$v_p = \sqrt{(\kappa + 4(\mu/3))/\rho}$$

•The s-wave velocity through a body is given by:

$$v_s = \sqrt{\mu/\rho}$$

•Where κ is the bulk modulus, μ is the shear modulus and ρ is the density.

•The bulk modulus, is a measure of the compressibility of a body (e.g., rocks or fluids). It is the stress-strain ratio under simple hydrostatic pressure, and measures the body's propensity to change volume (it is sometimes called the "incompressibility"). The shear modulus ("rigidity") is the stress-strain ratio for simple shear, and measures a body's reluctance to change shape. It provides information about the rock matrix.

•Importantly, from an AVO perspective, The shear modulus of a rock does not change when the fluid is changed. However, the bulk modulus changes significantly when the fluid changes. As such, the p-wave velocity of a rock will change as hydrocarbon saturation changes whereas the s-wave velocity will change relatively little (there is a slight density effect). Therefore, if we look at the V_p/V_s ratio of rocks we should be able to predict pore fill.

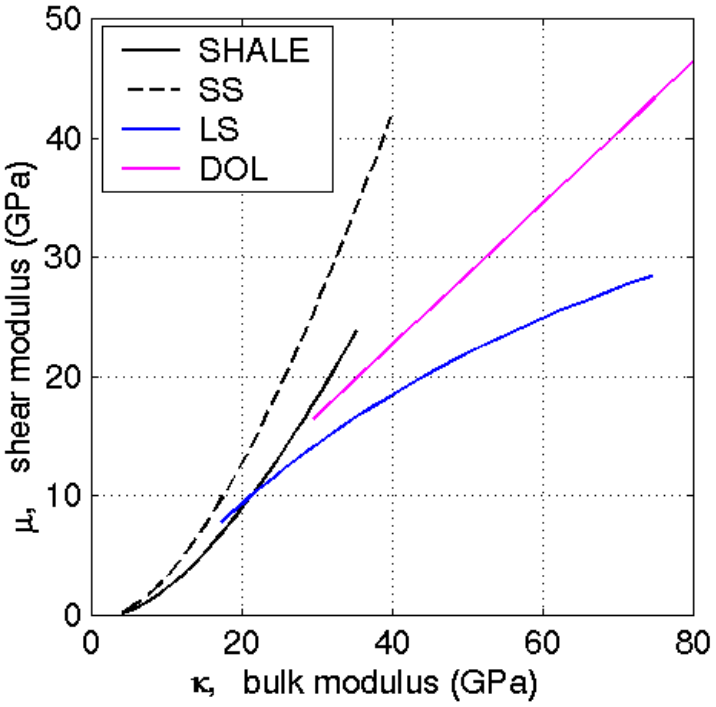

With increasing:	Compressional velocity	Shear velocity	Density	Incompressibility	Rigidity
Temperature	↓	↓	—	↓	↓
Pressure	↑	↑	↑	↑	↑
Pore Pressure	↓	↓	—	↑	↓
Porosity	↓	↓	↓	↓	↓
Clay content	↓	↓	—	↓	↓
Gas Saturation	↓	↑	↓	↓	—

•These two images, courtesy of Scott Pickford, illustrate relationships between bulk and shear moduli for different rock types (top), and how they, density and p- and s-wave velocities change as a function of various variables (bottom).

•The cross-plot at top shows how different lithologies may be distiinguished on the basis of their elastic moduli. The values are for brine-filled rocks/sediments. Unconsolidated materials (e.g., mud, unconsolidated sand) 0plot in the lower left, and highly consolidated materials plot in the upper right. The presence of gas in pore space will decrease the bulk modulus but not the shear modulus. Therefore the curves will be shifted to the left as gas saturation increases.

•The chart shows how changes in temperature, overburden pressure, pore pressure, porosity, clay content and gas saturation will affect elastic moduli (incompressibility – bulk modulus, rigidity – shear modulus), density and hence p- and s-wave velocity. Note that changes in gas saturation do not affect rigidity and only have a slight effect on the shear wave velocity.

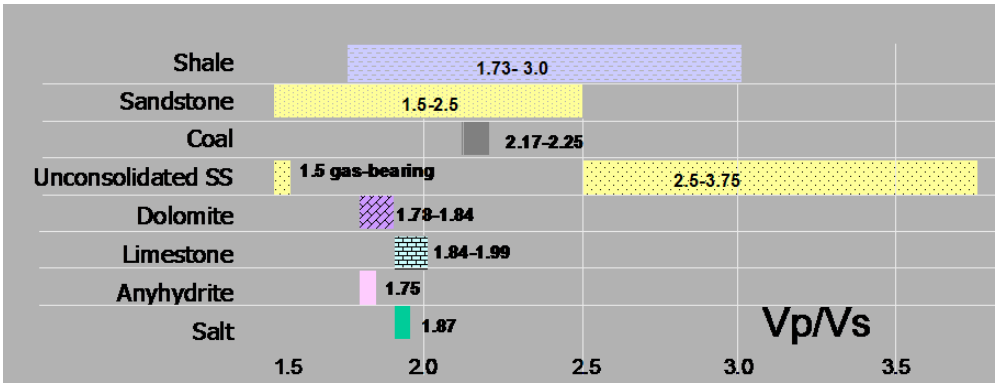

•The images on the previous page suggested that compressional- and shear-wave velocities are a function of several variables, including lithology and pore-filling fluids. This leads to the possibility of using the ratio of those two velocities to define lithology and gas content. This figure shows V_p/V_s ratios for various lithologies. There is some overlap between rock types, but each has its own characteristic range. Note the large change in V_p/V_s ratio for unconsolidated sand when the pore fill contains gas.

•Poisson's ratio (σ), a measure of the compressibility of a material perpendicular to applied stress, can be defined as:

$$\sigma = \frac{1 - 2\gamma^2}{2(1-\gamma^2)}$$

•where:

$$\gamma = \frac{V_S}{V_P}$$

•The images below show Poisson's Ratio versus Vp and versus porosity for different rock types. Note the difference between clastic and carbonate behaviour, and gas effect.

•All images on this page courtesy of Scott Pickford.

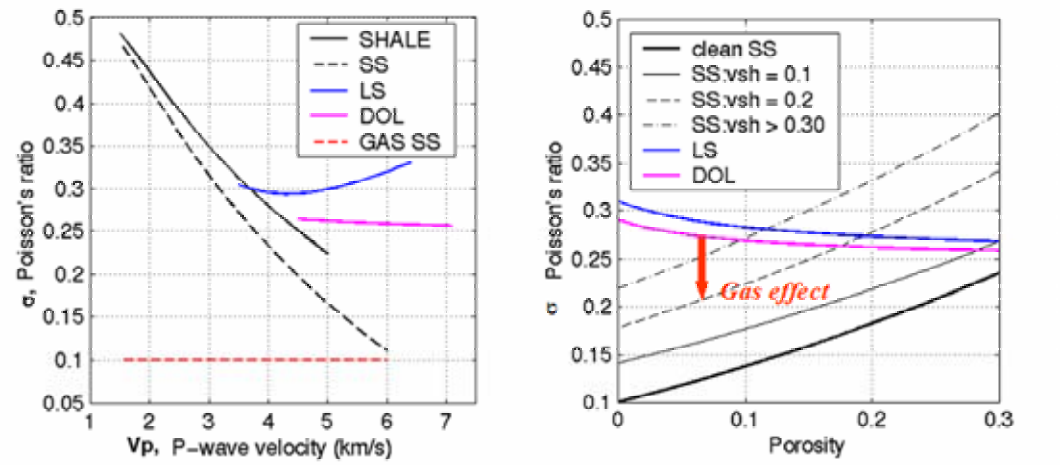

Rock Properties I

Rock	Density (g/cm^3)	Velocity (ft/s, (m/s))
Sandstone (Unconsolidated)	2.1	<17,000 (5,180)
Sandstone (Semi-consolidated)	2.2	18,000 (5,490)
Sandstone (Consolidated)	2.6	19,000 (5,790)
Shale	1.9 – 2.7	6,000 – 16,000 (1830 – 4880)
Limestone	2.6	21,000 (6,400)
Dolomite	2.8	23,000 (7,010)
Anhydrite	2.98	20,000 (6,100)
Halite	2.03	15,000 (4,575)
Coal	1.17 – 1.80	1,600 (490)

- Acoustic energy traveling through the subsurface will be reflected from interfaces associated with a change in physical properties from one layer to the next
- Physical properties of interest are bulk density (RHOB, ρ) and p-wave velocity (V_p or simply, since we will be working primarily with compressional waves, V)
  - Density a function of mineralogy, porosity and pore-filling fluids
  - Velocity a function of mineralogy, porosity, pore-filling fluids, cementation, pressure, temperature, etc.
- Table above lists density and velocity for some common rocks of interest

Rock Properties II

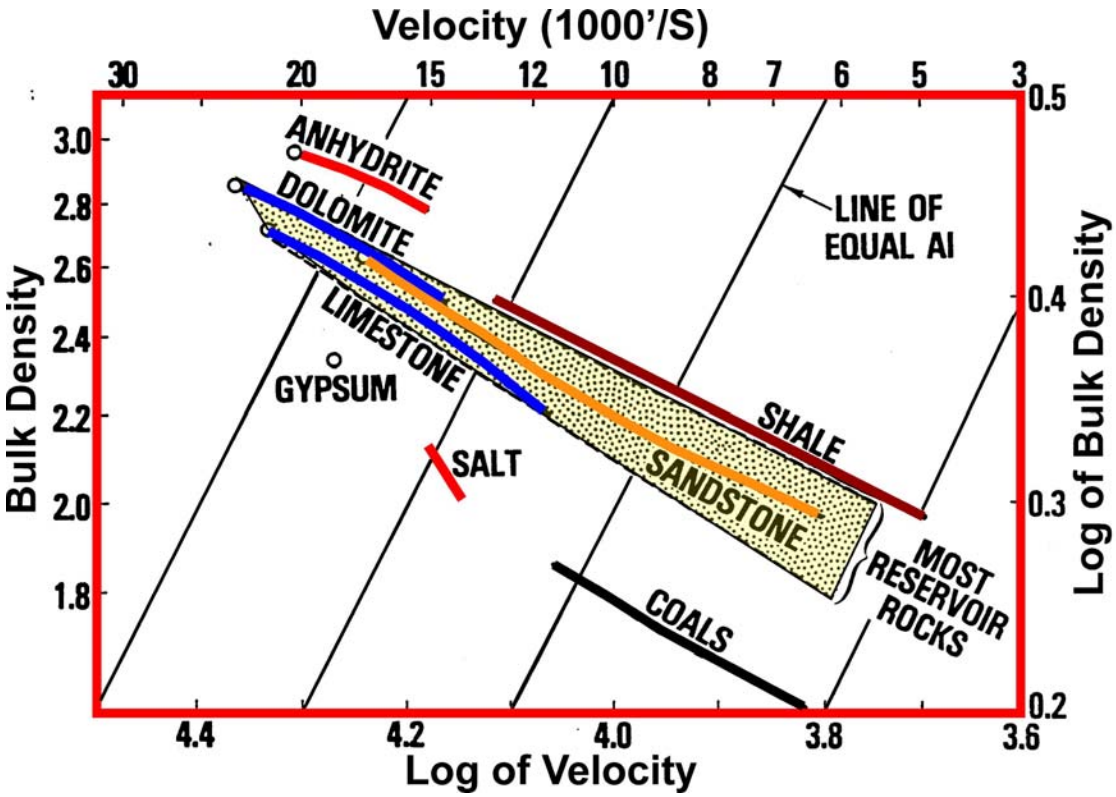

- Acoustic energy responds to the product of density and velocity (ρV) – known as the acoustic impedance (AI)
- Figure above shows how acoustic impedance varies for some common sedimentary rocks
  - A range of AI values may characterize a single lithology
  - Different lithologies may have identical AI

Reflection Coefficients

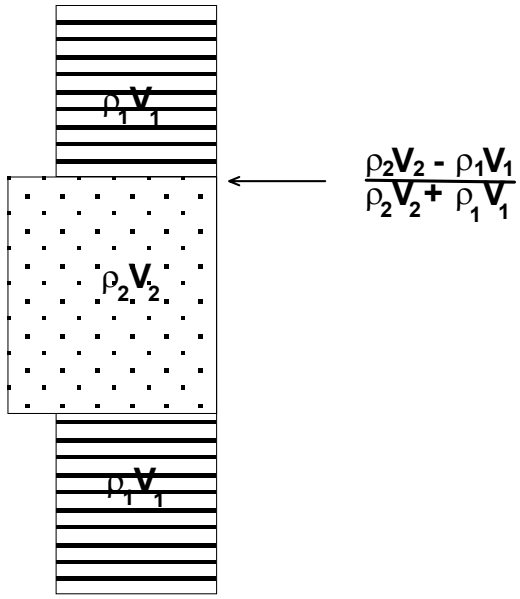

- Where there is a change in AI, some of the incident acoustic energy will be reflected at the interface and some will be transmitted
- Amount reflected (amplitude of reflection) will depend on the relative difference in physical properties across the interface
  - Define reflection coefficient (RC)

$$RC = \frac{AI_2 - AI_1}{AI_2 + AI_1}$$

  - If $AI_2 > AI_1$ – positive RC
  - If $AI_2 < AI_1$ – negative RC
- Not all changes in lithology associated with change in AI. Changes in fluid content in a single lithology can give rise to relfections
- Different combinations of layers lithologies can have the same RC
  - Seismic “non-unique”
- Seismic data image *interfaces* – we observe changes in AI across an interface, not properties of layers themselves

Convolutional Theorem

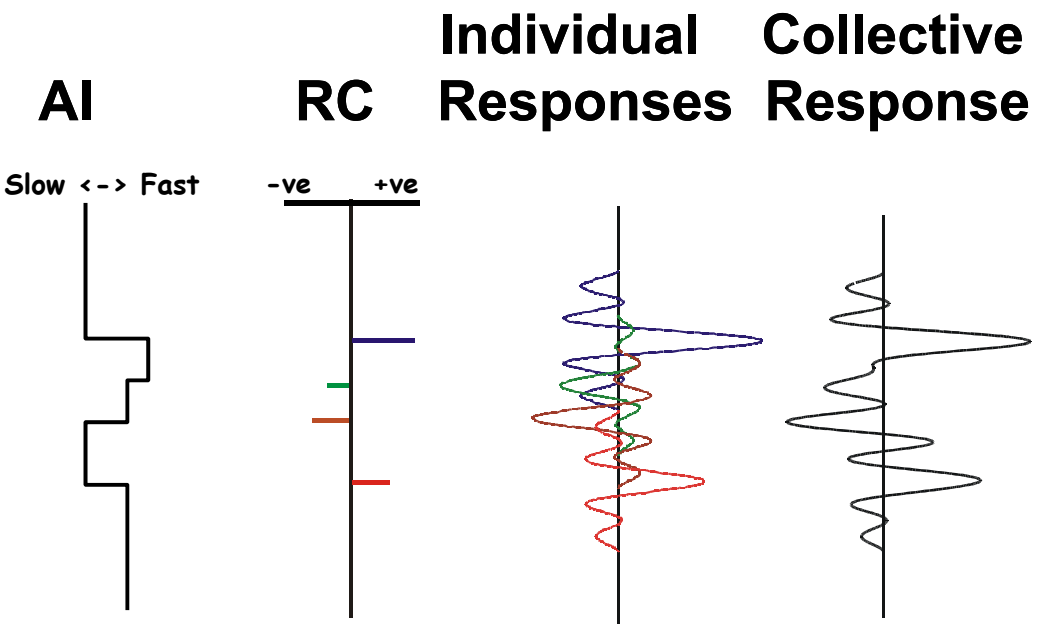

- We can think of the subsurface at any one location as consisting of a one-dimensional series of reflection coefficients
- Each RC will give rise to a separate reflection event, the amplitude of which is proportional to the change in AI across the interface
- As shown above, the final image we will record for that location may be thought of as the algebraic sum of all the individual reflections
- Mathematicians say that we “convolve” the wavelet with the series of reflection coefficients

Resolution

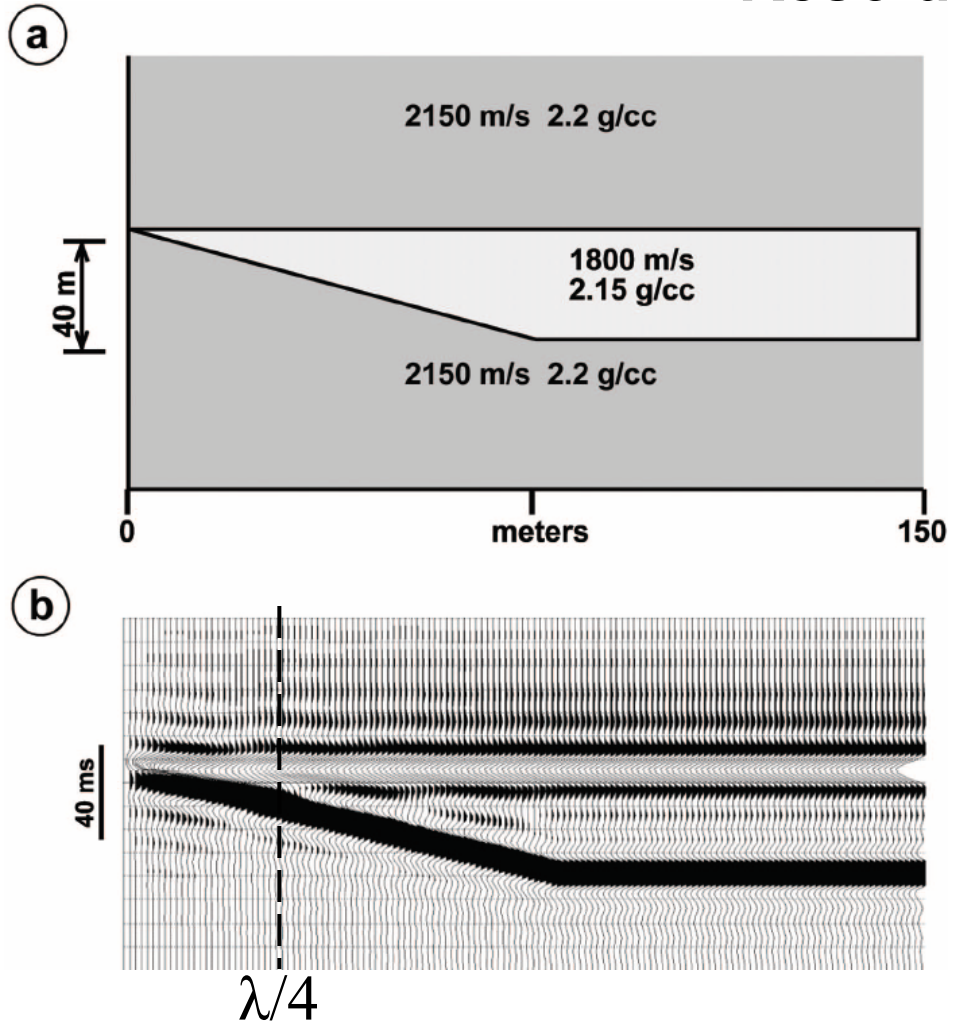

- Imagine a wedge of low AI sandstone encased in relatively high AI shale. When bed is thick enough (right), reflections from top and base of sandstone are separate and peak/trough distance provides a reliable indicator of bed thickness
- As bed thickness decreases to ¼ λ, peak/trough distance remains a reliable indicator of bed thickness, but below that thickness peak/trough distance no longer changes, i.e. it is no longer an indicator of bed thickness.
- The ¼ λ criterion defines the resolution of the seismic data. Note that it is still possible to *detect* a bed that is below tuning, even if technically it cannot be resolved. Detection limit depends on factors, such as signal-to-noise ratio.
- Beds less than ¼ λ are known as seismic thin beds
  - Many reservoirs are seismic thin beds

Controls on Seismic Visibility

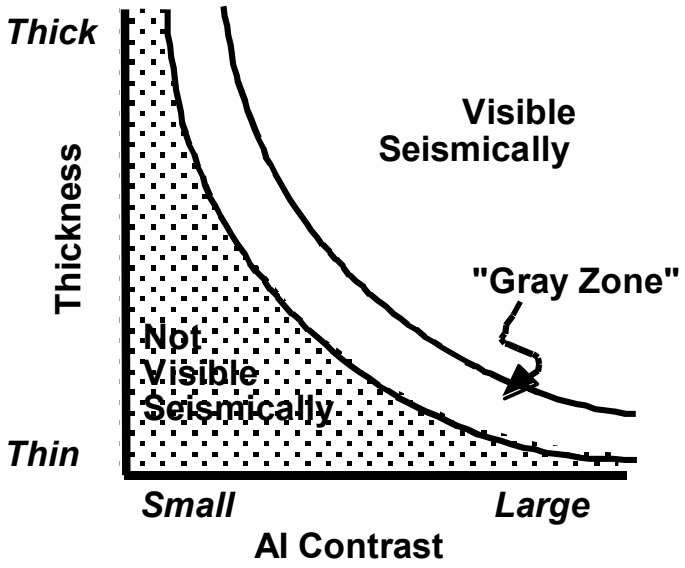

- The two fundamental controls on whether a bed will be visible seismically are bed thickness and AI contrast with surrounding layers
  - "Thick" beds with large AI contrasts will be visible, whereas "thin" beds with small AI contrasts will not be visible
  - A bed with small AI contrast may be visible if it is thick enough
  - A "thin" bed may be visible if the AI contrast is very high
  - Thickness measured with respect to wavelength
  - Gray zone a function of signal-to-noise ratio, interpreter's skill, etc.

Resolution Changes with Depth

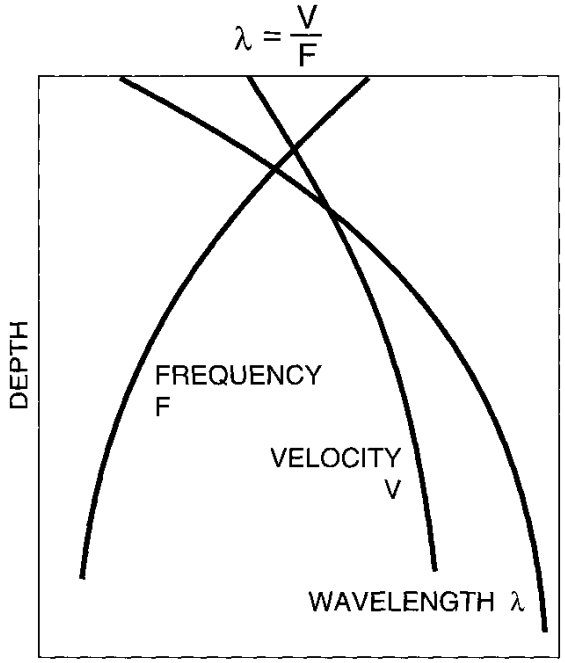

- As a general rule, velocity increases with depth
  - Porosity decreases with depth, pressure increases
- High frequencies in seismic signal attenuated as signal propagates through earth
  - Analogous to stereo in neighbor's apartment: base makes it through wall but high frequencies (cymbals, etc.) do not
- As a result, wavelength increases with depth and vertical resolution is reduced

Effects of Frequency on Stratigraphic Resolution

Effects of frequency content on seismic stratigraphic relationships

Input Geology

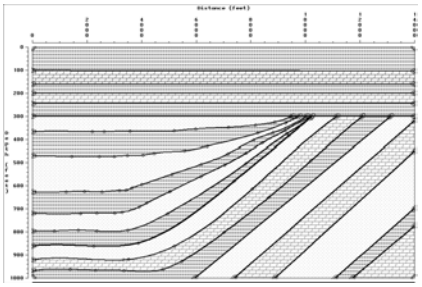

75 Hz Ricker Wavelet

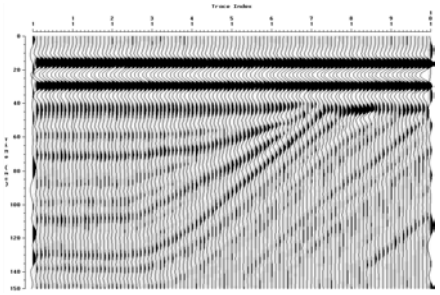

25 Hz Ricker Wavelet

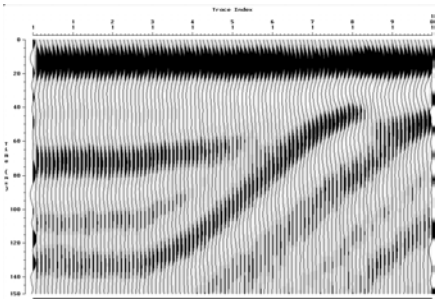

- Frequency content of seismic data affects resolution *and* apparent seismic stratigraphic relationships.
- Image at upper right shows stratigraphic relationships for an imaginary area
- Image at lower left shows how geology would be imaged with relatively high frequency data. The true stratigraphic relationships are imaged.
- With lower frequency data (lower right) true stratigraphic relationships are not apparent.

Lateral Resolution

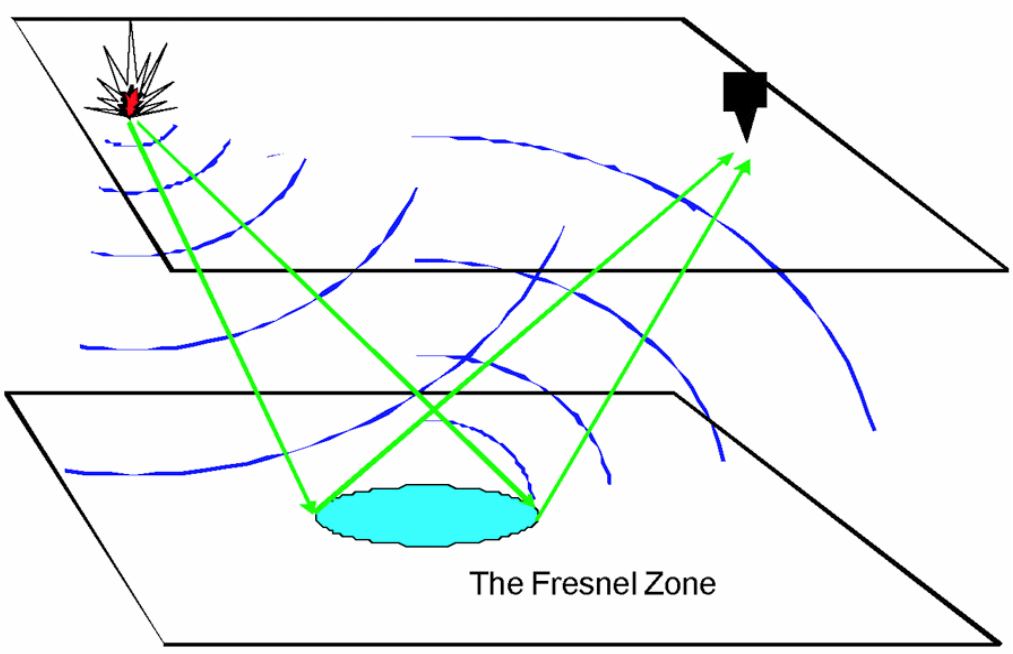

- Lateral resolution described by Fresnel Zone
  - Seismic data image (“illuminate”) an area, rather than a single point as might be suspected from examination of raypath diagrams
- The diameter of the Fresnel zone (F) depends upon three key variables:
  - Average velocity down to the horizon of interest (v)
  - Two-way travel time (t)
  - Dominant frequency (f)

$$F = v\,(t/f)^{1/2}$$

- Fresnel zone will be shrunk by migration of the data during processing.

Exercises 1

1. If V = 7000 m/s (e.g., carbonate) and F = 50, what is the wavelength?

2. If V = 3000 m/s (e.g., young shale) and F = 50, what is the wavelength?

3. What is the tuning thickness for both of the examples above?

Exercises 2

4. What is the dominant frequency of the seismic data in the interval between 1500 and 1600 ms? If the velocity is 5000 m/s, what is the tuning thickness? If it is possible to detect a bed down to 1/16 of the wavelength, what would that be?

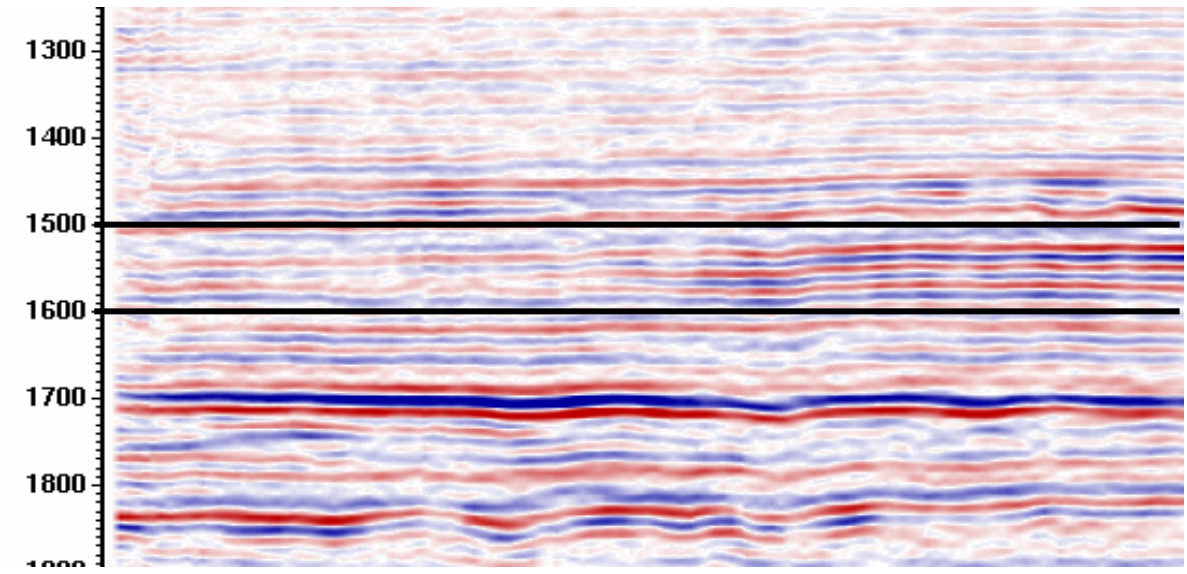

Exercises 3

5. Calculate the reflection coefficients at each of the interfaces: Would each interface be represented by a peak or a trough? What convention are you using? What is the likely lithology represented by each layer (can you tell)?

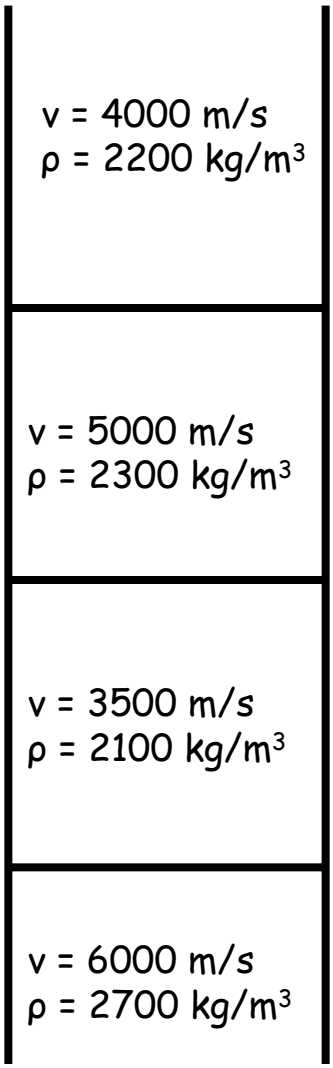

Exercises 4

6. Calculate the pre-migration Fresnel zone radius for a TWT of 2.0 seconds, dominant frequency of 25 Hz and average velocity of 2440 m/s.

Effects of Acquisition and Processing on Interpretation

Content

- Introduction
- 2-D seismic acquisition and processing
- 3-D seismic acquisition and processing
- Reprocessing, post-stack processing
- Coherency processing
- Exercises

Acquisition and processing parameters have a significant impact on the quality of the seismic images available for interpretation and for what the images show (e.g., apparent structure). In this chapter we examine simplified acquisition and processing flows, and illustrate the effects of changing these parameters on real datasets.

Target depth and dimensions, subsurface structure and other factors will need to be assessed when designing a seismic survey. Survey design, 2-D or 3-D, is commonly a compromise between what *should* be done and what *can* be done. Restrictions on seismic data acquisition include cost, surface problems (environmental, cultural, etc.), hardware limitations, crew availability etc.

The data recorded in the field are not optimized for interpretation. To produce an interpretable image, we must attempt to remove artifacts associated with the way the data were acquired, eliminate noise, and correct for the raypaths taken by acoustic energy on its way from source to receiver. These manipulations are known as seismic data processing. Processing is a mixture of both art and science.

We begin by focusing on 2-D seismic acquisition and processing because the concepts are easier to introduce for that data type. We then examine 3-D seismic acquisition and focus on how 3-D migration improves subsurface imaging. Most seismic data used in the petroleum industry are collected via the common mid-point method. As such, we focus on that approach.

Although 3-D seismic data has become the tool of choice in the petroleum industry, there are some cases where 2-D data may be encountered. These include: 1) frontier or exploration areas, 2) old pools ("legacy" data), 3) areas where difficult terrain/logistical difficulties make collection of 3-D economically unfeasible, 4) other economic conditions.

The images on the next page show transects from two different, but overlapping, 3-D seismic surveys. Although the transects do not show exactly the same portion of the subsurface, the geology does not appreciably differ from one area to the next, hence the differences in image content and quality are primarily due to differences in acquisition and processing flows between the two surveys. Which would be most useful for defining reservoir properties?

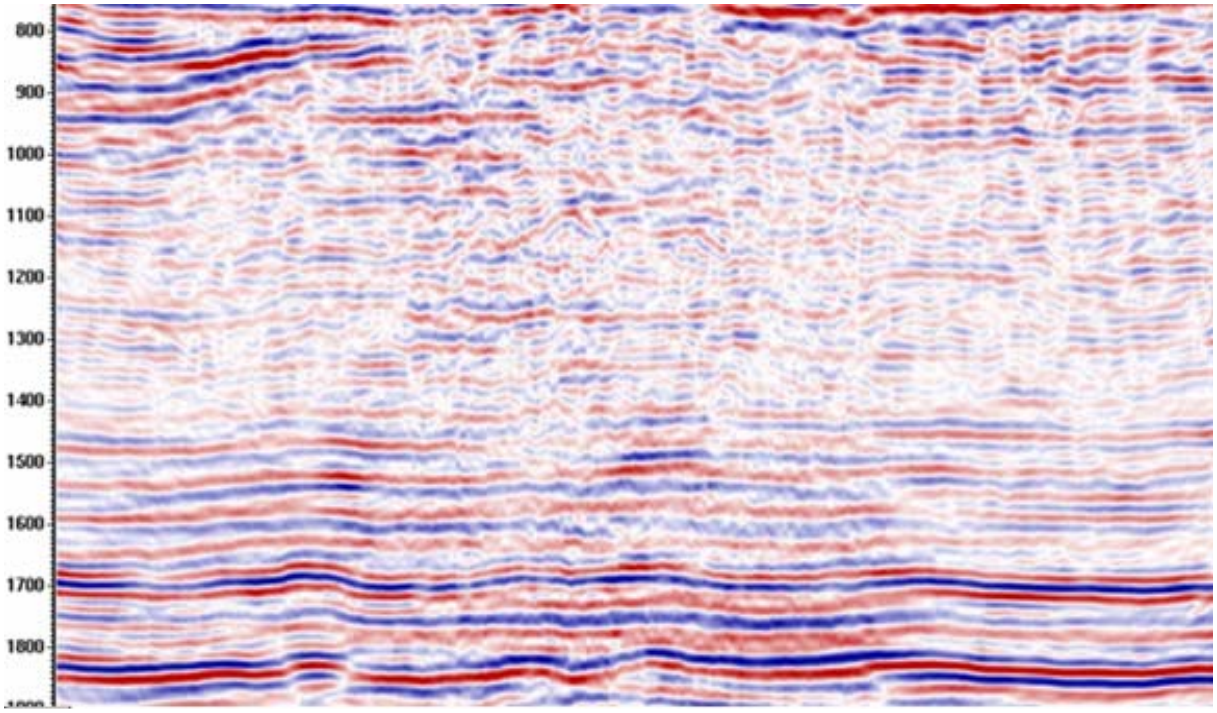
800
900
1000
1100
1200
1300
1400
1500
1600
1700
1800

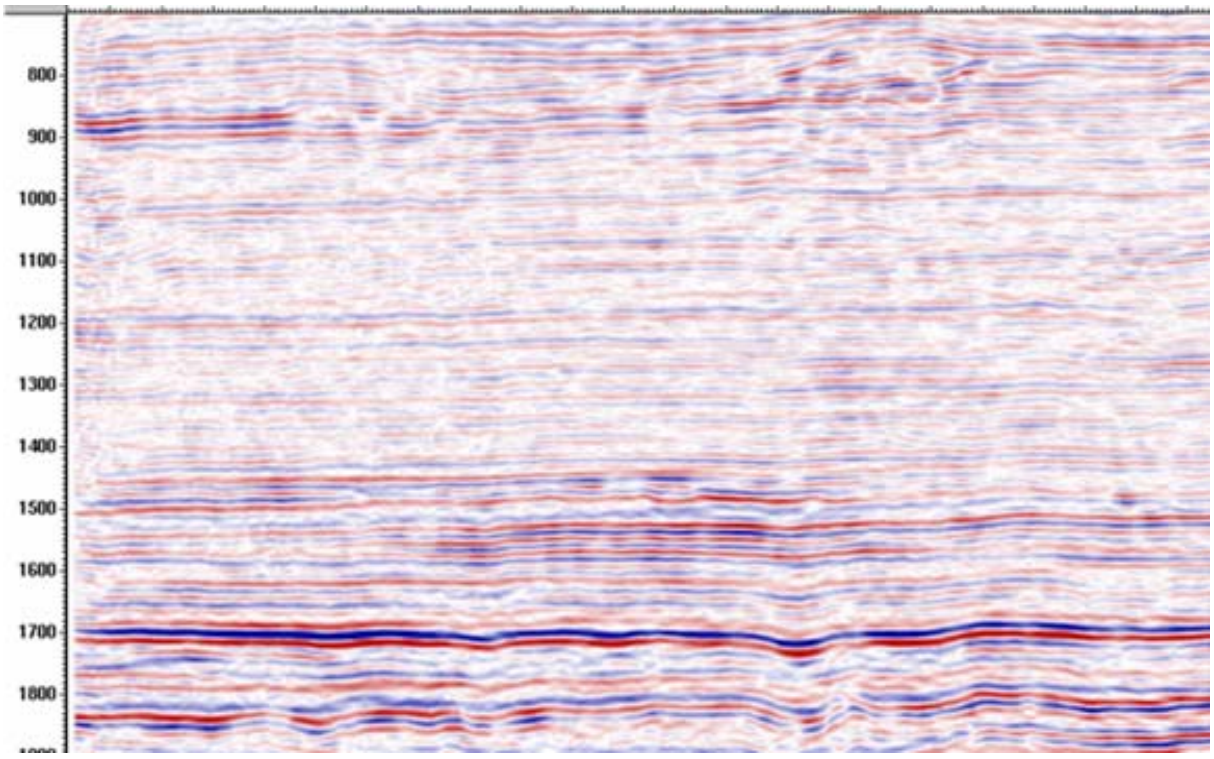
800
900
1000
1100
1200
1300
1400
1500
1600
1700
1800

2-D Seismic Profile

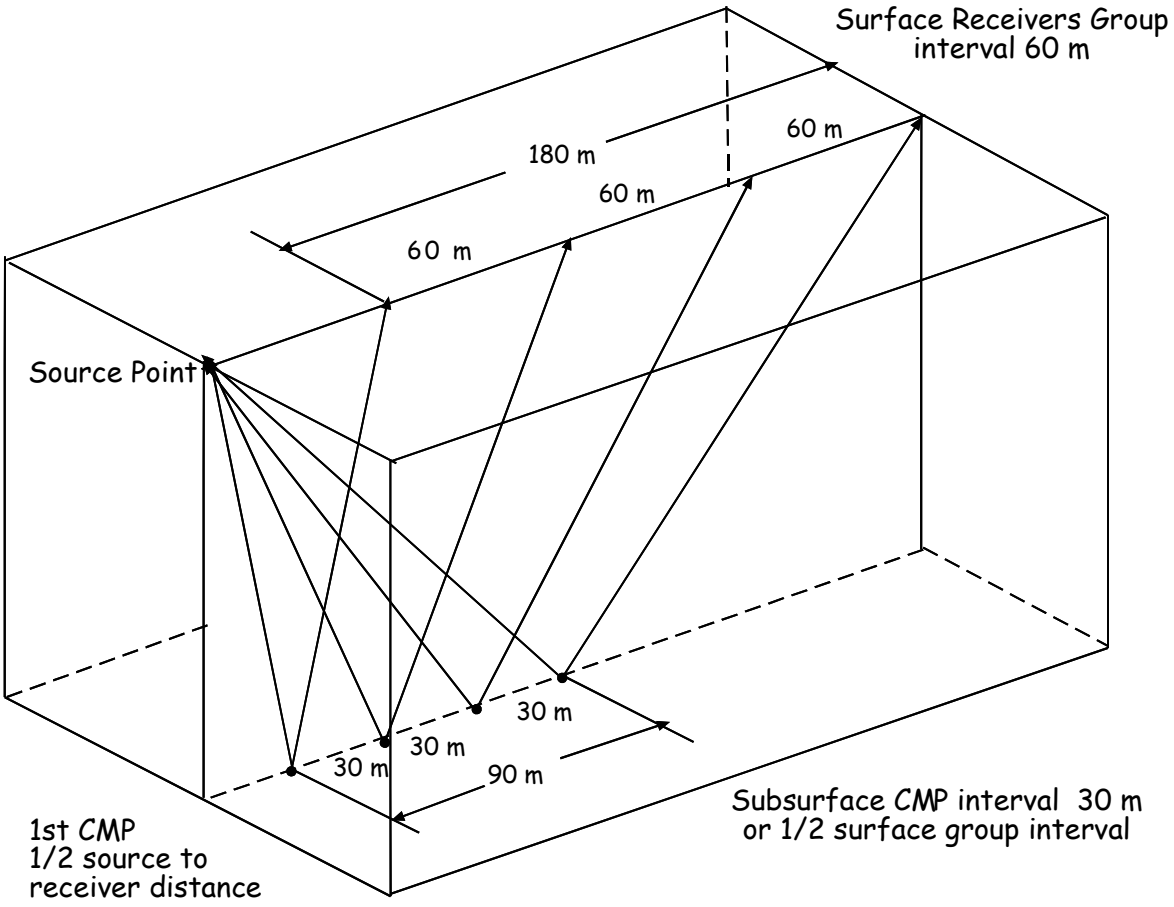

The image above shows an idealized layout for 2-D seismic data collection. Energy from a single shot travels through the subsurface, is reflected off an interface and returns to the surface where it is recorded by receivers (geophones on land, hydrophones at sea). More than one receiver is present at each location, defining a "receiver group". The distance between a source and receiver group is known as the offset. The reflection point is mid-way between the source and the receiver group, and the distance between midpoints (CMP – common midpoint) is half the distance between the receiver groups.

Simplifications made in the above image include: a) only one interface is present, b) the interface is horizontal, and c) only a small number of receiver groups are shown (for clarity).

The farthest offset should be at least equal to the target depth but less than twice the target depth. For example, if the main target is at 3 km depth, the farthest offset should be between 3 km and 6 km.

The use of more than one receiver group to record the reflected energy is known as multi-channel recording.

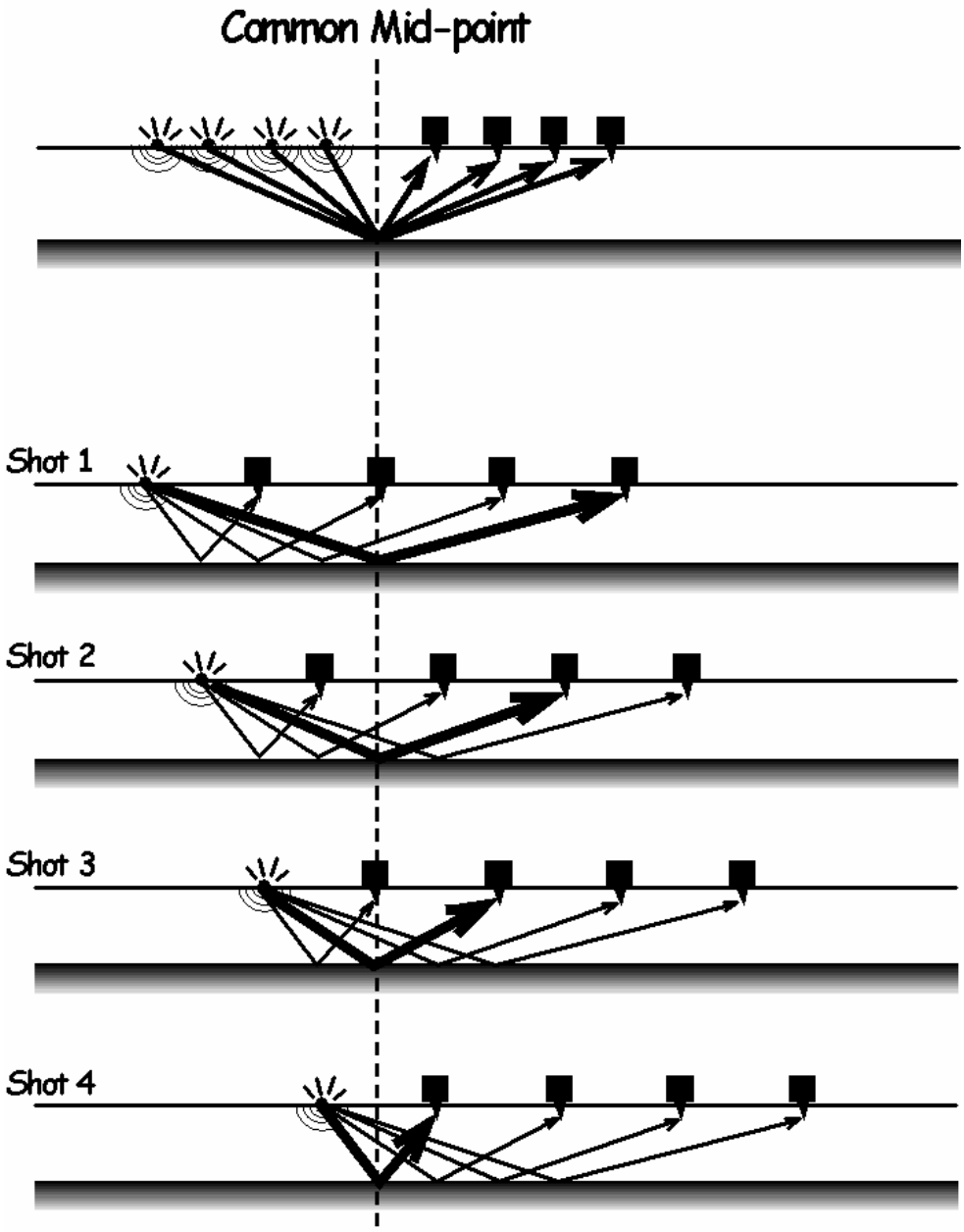

The previous slide showed a single shot with reflected energy being recorded by four receiver groups. That exercise might be “Shot 1” shown above. To collect a seismic profile, we repeat the exercise but move the locations of the shotpoints and receiver groups each time. In the figure above, we show four shots and the raypaths that link the sources to the receivers. The distance that we move each time is kept fixed, and is known as the move-up.

Inspection of the image above shows that four combinations of shot-receiver have imaged a common mid- point (CMP) in the subsurface. The raypaths associated with this mid-point are shown as bold lines for clarity. During processing, seismic processors sort through all the combinations of sources and receivers to find those that share a common mid-point.

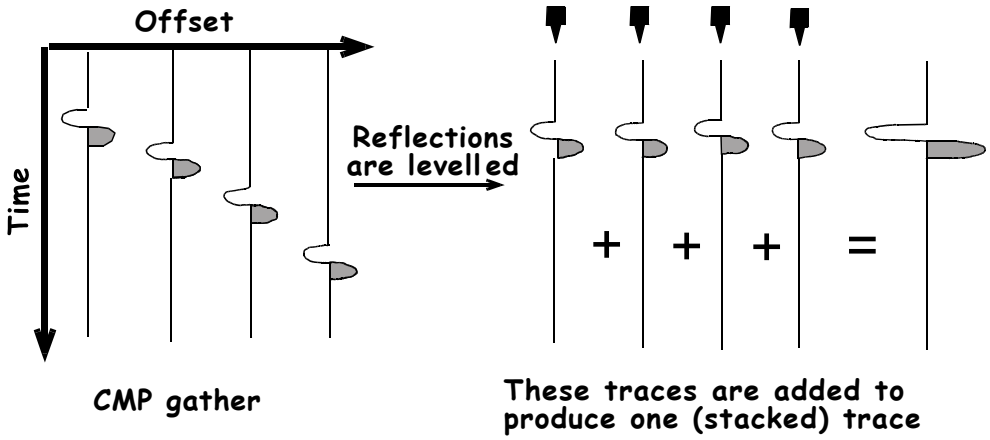

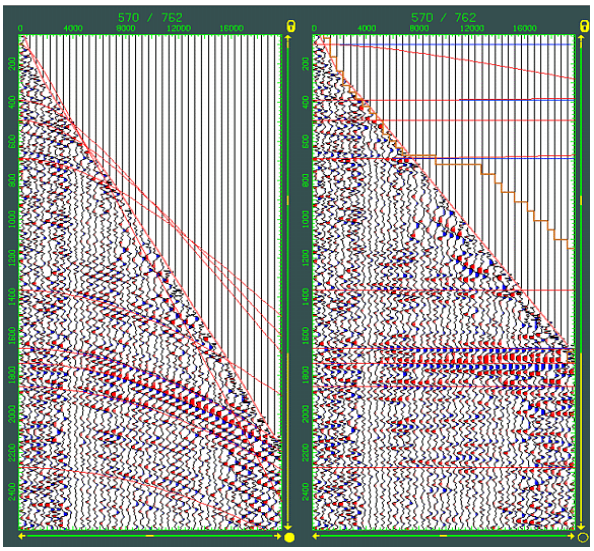

The previous slide showed four source-receiver combinations that image a common mid-point (CMP). The distance traveled by the sound increases with source-receiver offset. As such, if we plot the seismic records from each of the geophones side-by-side, we will see (top left) that the recorded reflection time increases with offset (Time 0 is when the shot occurred). This is known as normal moveout (NMO). The NMO defines an hyperbola that corresponds to a particular average velocity between the ground surface and the reflector.

To help enhance the signal-to-noise ratio (the reflected energy is commonly relatively weak compared to sources of noise) we need to combine the reflections, and to do so we need to first level them out. We correct for NMO ("NMO corrections") by estimating the appropriate velocity (velocity analysis) then correcting the data to level out the reflections. The individual traces are then added together (stacked) to produce a single stacked trace that will show the seismic response of the Earth at the CMP location. The number of traces added together is known as the stacking fold. In the upper example, the stacking fold would be four.

The lower images show NMO corrections applied to a real dataset. More than one reflecting horizon is present in and the hyperbolae corresponding to these horizons are shown by red curves at left; a different stacking velocity will need to be derived for each hyperbola. At right the horizons have been leveled and the data are ready for stacking. The stacking fold in this example would be 40.

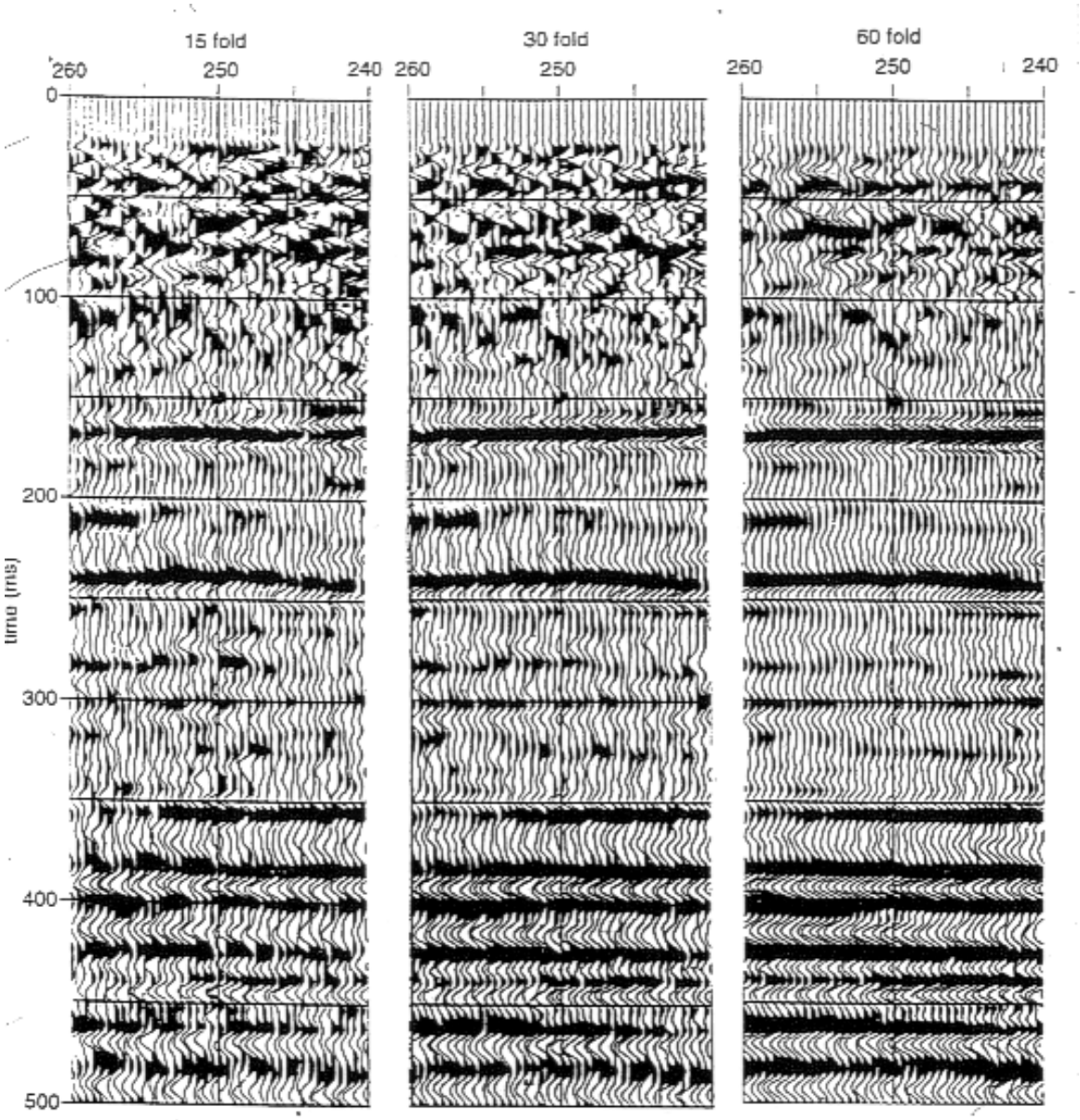

All else being equal (e.g., geology, acquisition methods, processing parameters), the higher the stacking fold the better the data quality. This improvement in signal-to-noise ratio is shown in these images. These 2-D data were collected to produce 60-fold data (right). As an experiment, the processors then decimated the data before stacking to produce various versions of the data. The middle image was derived by stacking every second trace (stacking fold = 30) and the image at left was derived by stacking every fourth trace (stacking fold = 15). Note the degradation in image quality (decrease in reflection continuity, increase in noise) as the fold decreases.

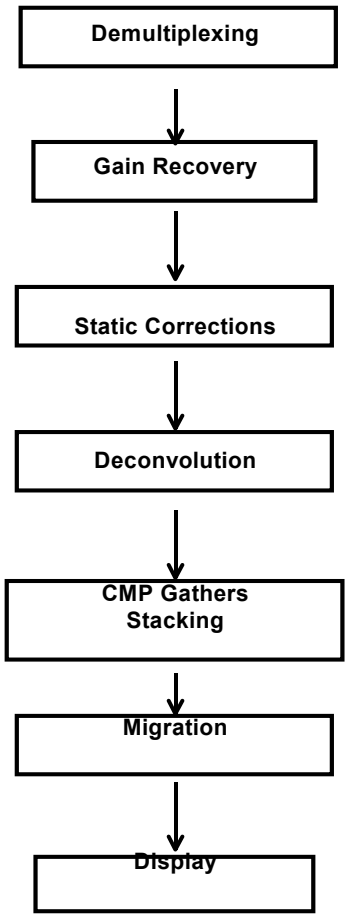

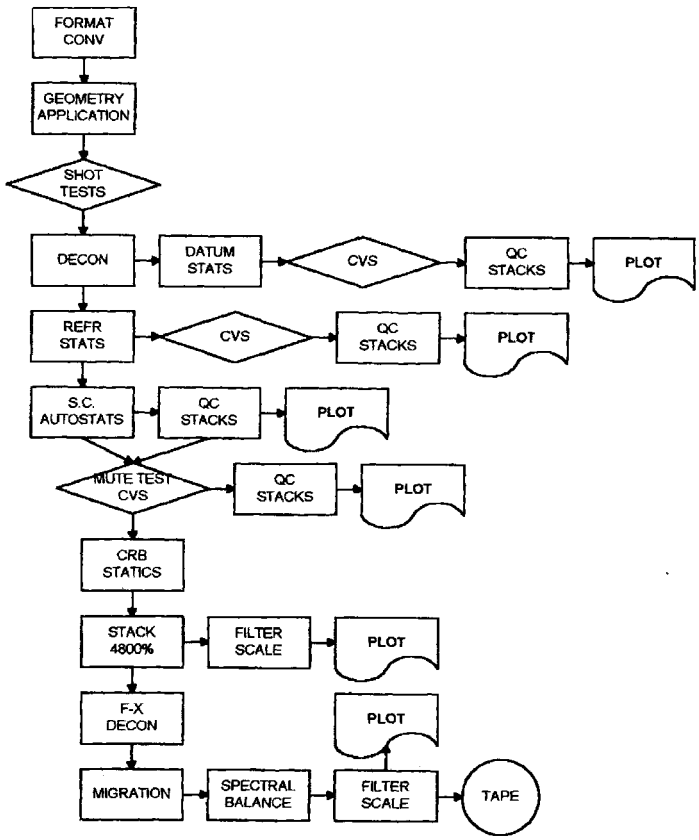

In reality, the normal moveout corrections and stacking just examined are only part of the processing flow. The image at left is a simplified workflow that shows some of the more important processing steps, including (from top to bottom): a) demultiplexing (initial sort through the data to identify which data were recorded by which receivers for each shot), b) gain recovery (to account for loss of energy associated with spherical divergence, attenuation, etc.), c) static corrections (accounting for uneven topography, near-surface velocity corrections), d) deconvolution (replacing the original “messy” wavelet with a “clean” wavelet whose characteristics are known, e) CMP gathers and stacking (just described), f) migration (repositioning reflected energy to its true position in the subsurface), and g) display (hardcopy images and/or digital data to be displayed on computer workstation).

In the following pages we will briefly review static corrections, deconvolution and migration.

The image at right shows a real processing sequence. Processing steps are not always applied in the same order.

Processing - Gain

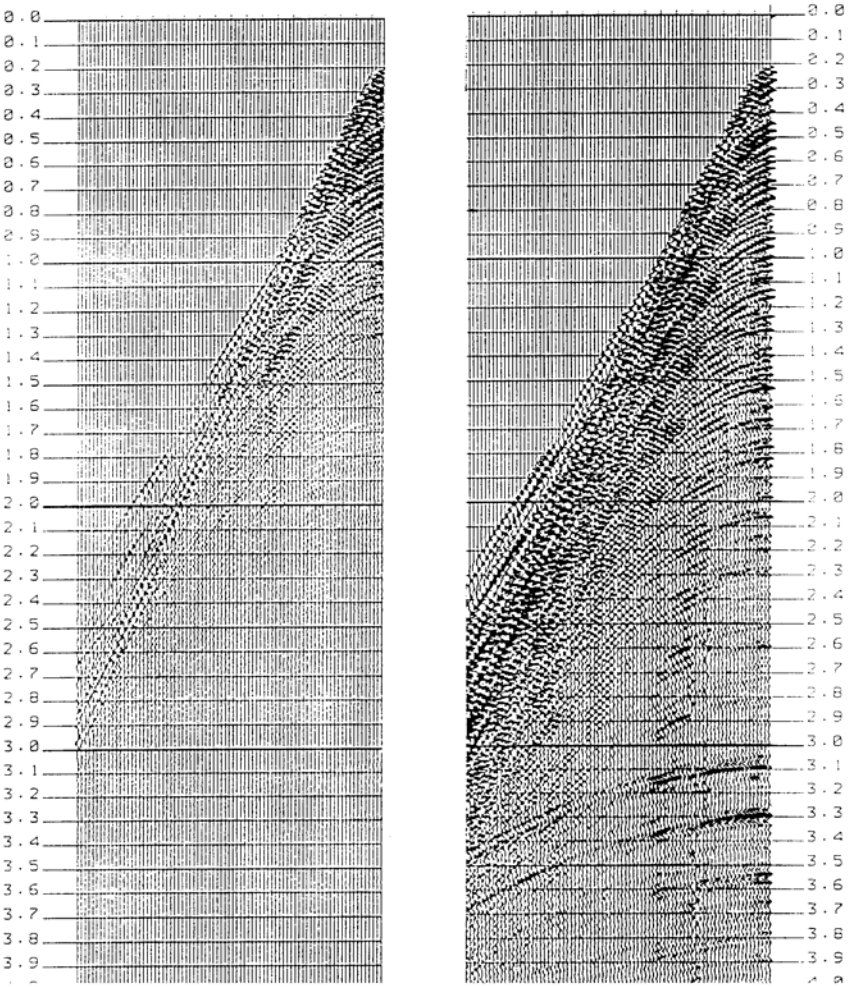

- Geometric spreading and attenuation loss combine to cause a rapid decay of the seismic signal with time (depth). If these losses are left uncorrected, only the uppermost reflectors would be visible on the final section.
- The two images shown above show a shot gather as originally recorded (left), and the same gather after gain has been applied (right).

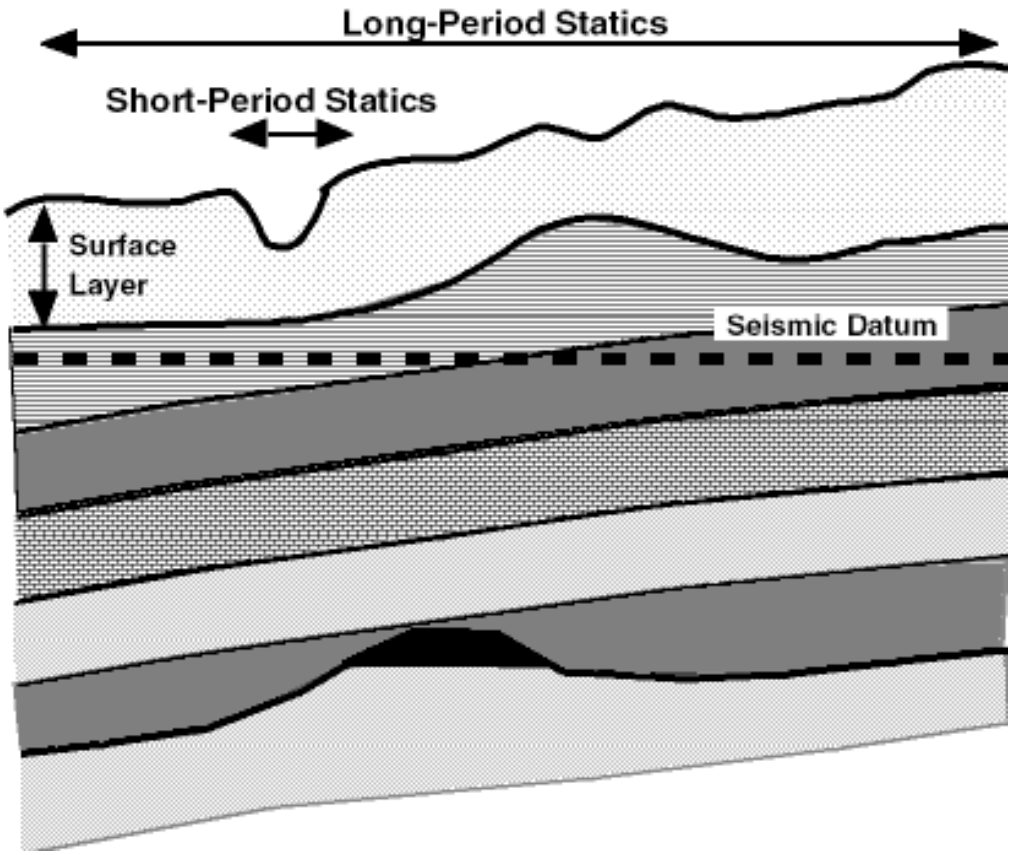

Data collected on land need to have the effects of changes in ground surface elevation removed and, potentially, the effects of changes in thickness (and velocity) of the "surface layer" (low-velocity weathered rock, till, aeolian dunes, etc.). An arbitrary seismic datum is defined at this time. These processes are collectively known as static corrections ("statics"). In addition to defining the near-surface velocity, the elevation of sources and receivers must be known.

Short-period statics occur within the length of the spread, whereas long-period statics are associated with lateral velocity variations that are longer than the length of the spread.

Static corrections may be undertaken in two steps. Field statics ("refraction statics) are traveltime corrections to account for irregular topography and near-surface weathering layer. They remove a significant part of distortions (especially long-wavelength anomalies), but not all. Residual statics are applied later and account for rapidly varying near-surface effects.

Failure to account for statics problems can lead to poor stacking (next slide) and to false structures at depth (see later).

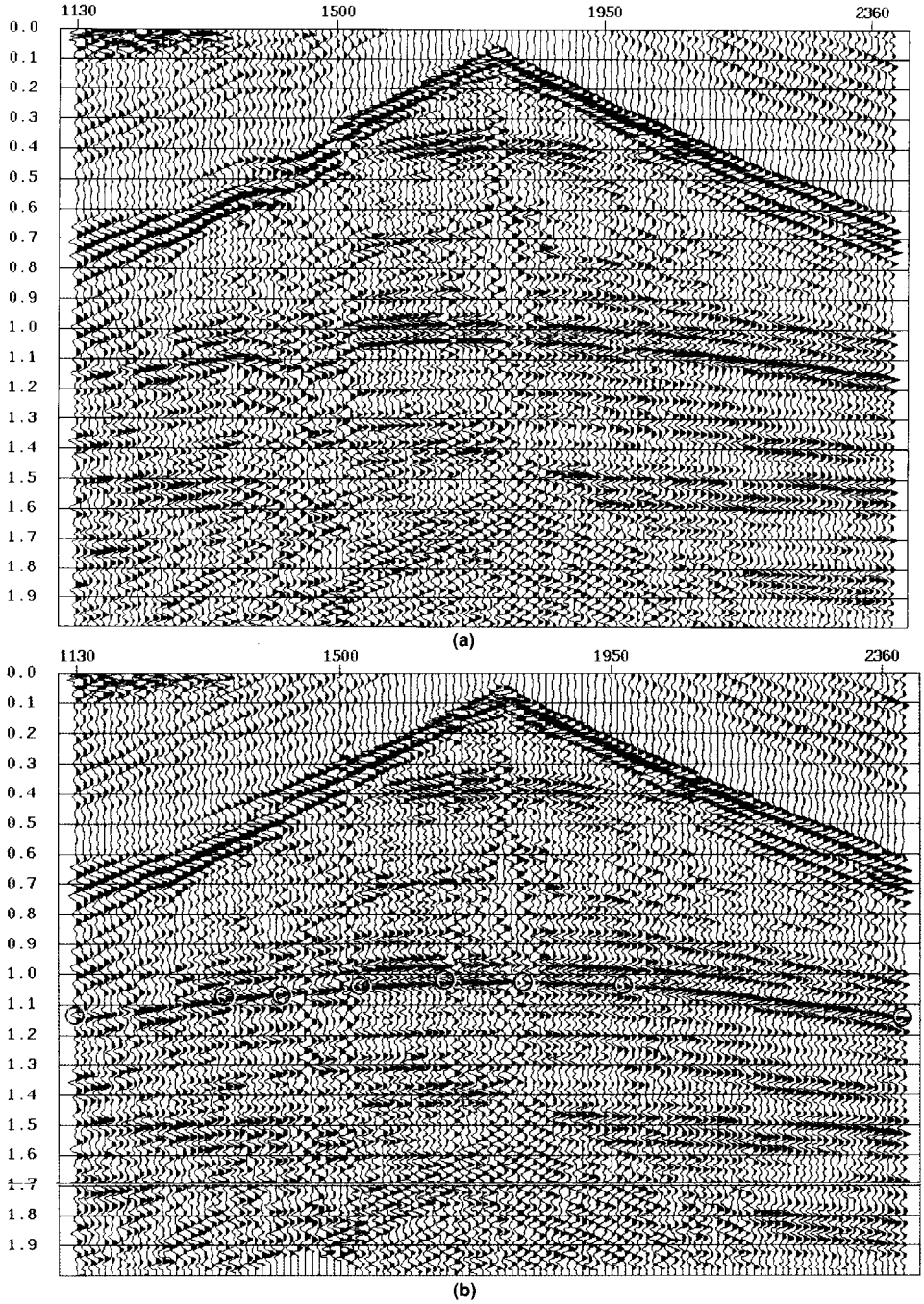

Duncan, 1992

The upper image shows a gather with a prominent "valley" to the left of station 1500. The "valley" persists throughout the length of the section. These data will stack poorly after NMO corrections are made and the final image will not be clear.

The lower image shows the same gather after static corrections have been applied. This version of the data will stack better, giving a more interpretable image.

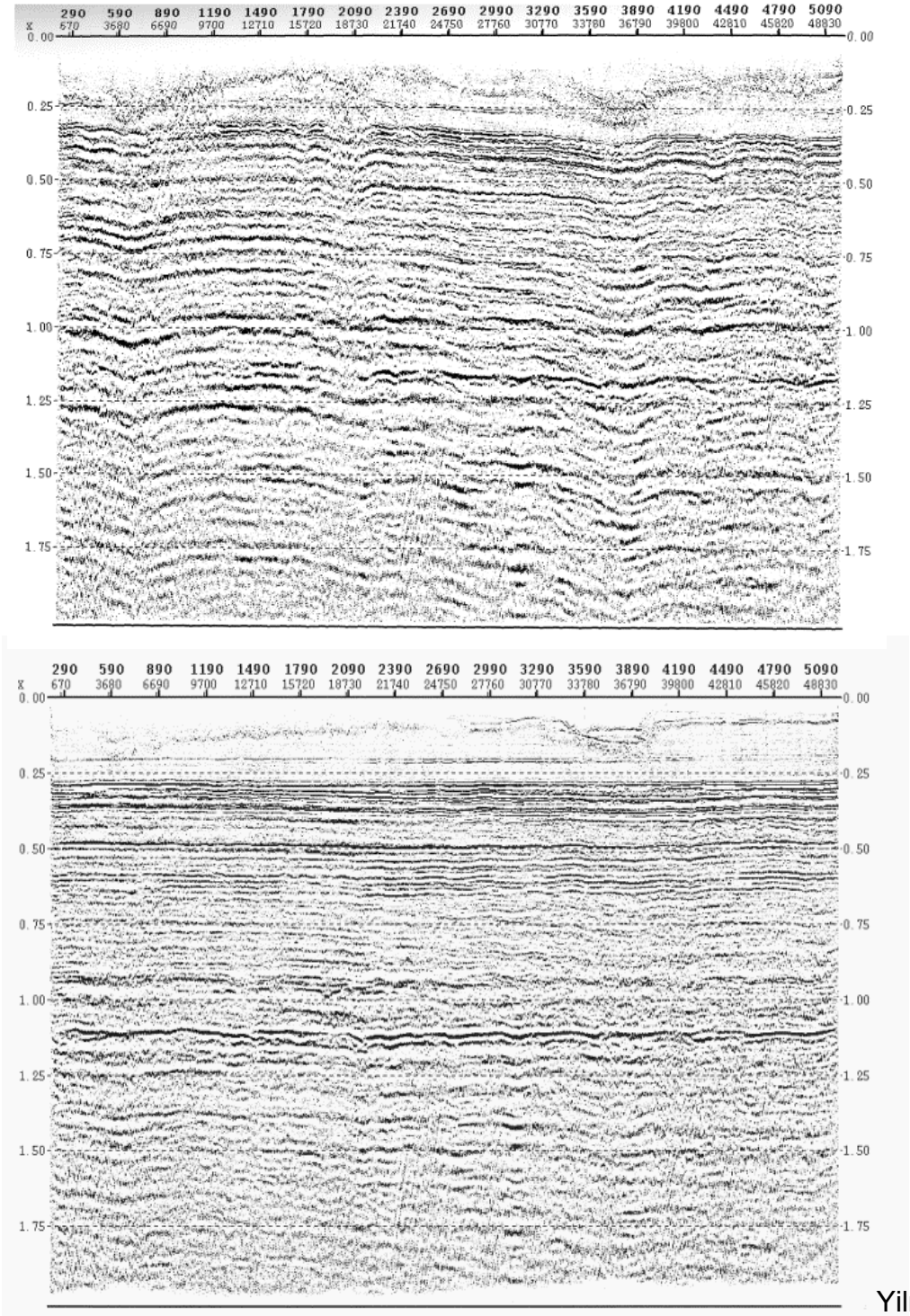

Yilmaz, 2001

These two images show the effects of static corrections on data quality and the apparent subsurface structure. The upper image shows a stacked seismic section without static corrections. The lower image shows the same data but with static corrections applied. Note the improvement in data interpretability in the lower image and the disappearance of some low-amplitude structures seen in the upper image; these were due to statics problems.

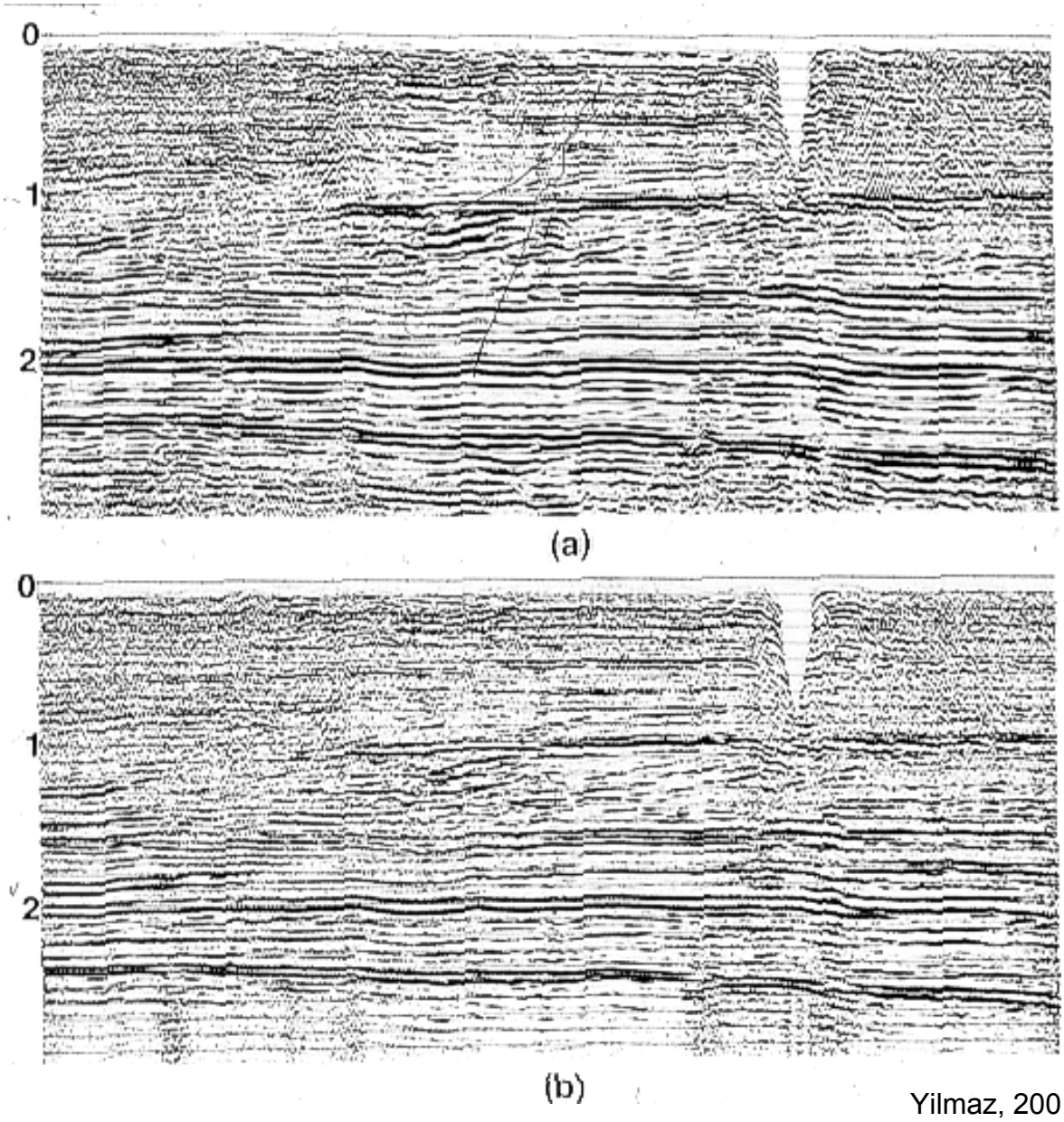

Yilmaz, 2001

As the seismic wavelet travels from the source to reflecting interface and back to a receiver, its shape is modified by a variety of factors, including loss of certain frequency ranges, interference effects (including short-period multiples), noise, etc. The receivers themselves have a characteristic response function and the wavelet generated is not an infinitely sharp pulse. Because of these problems, reflections are smeared out over a period of time and the true position of the reflecting interface may not be clear.

Deconvolution refers to seismic processing techniques that attempt to correct for these problems. The objectives are to: a) compress the basic wavelet, b) attenuate reverberations ("ringiness" of the data), c) attenuate short-period multiples, and d) wavelet shaping (produce a wavelet with known phase). The result will be improved temporal (i.e., stratigraphic) resolution.

The images shown above compare a stacked section without deconvolution (top) with a stacked section after deconvolution (bottom). Stratigraphic features are clearer in the lower image.

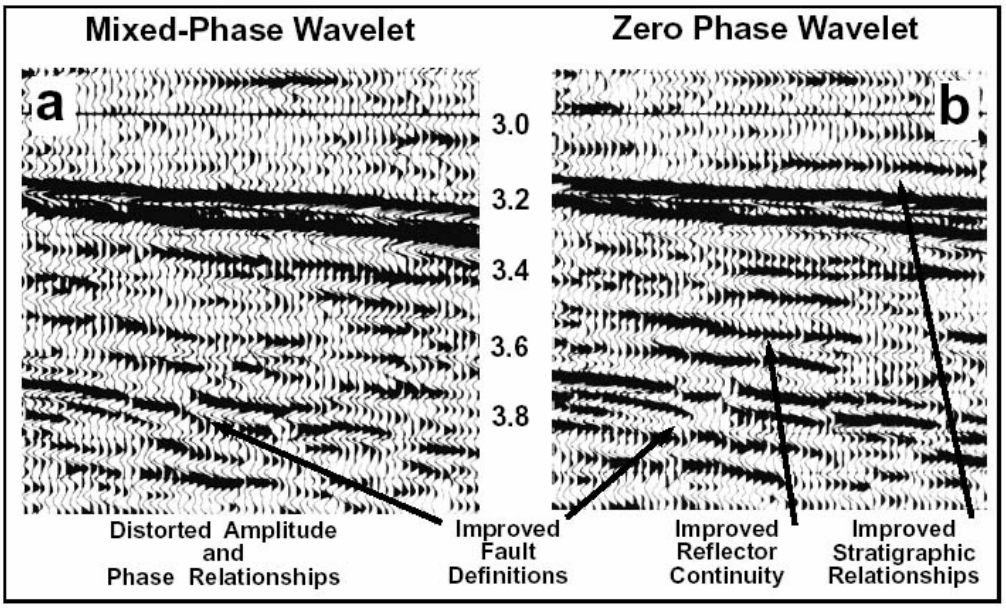

Henry, 2001

Different types of deconvolution are available. Statistical deconvolution assumes that the source wavelet was minimum phase and that the subsurface reflectivity is random. If these two assumptions are not valid, the result will be a mixed-phase wavelet. For signature deconvolution the source wavelet must be known, but the result will be a zero phase wavelet.

The images shown above, from Henry (2001), compare seismic data processed using statistical deconvolution (left) with signature deconvolution (right) that produced mixed-phase and zero-phase wavelets respectively. The zero-phase data have improved definition of faults and stratigraphic features.

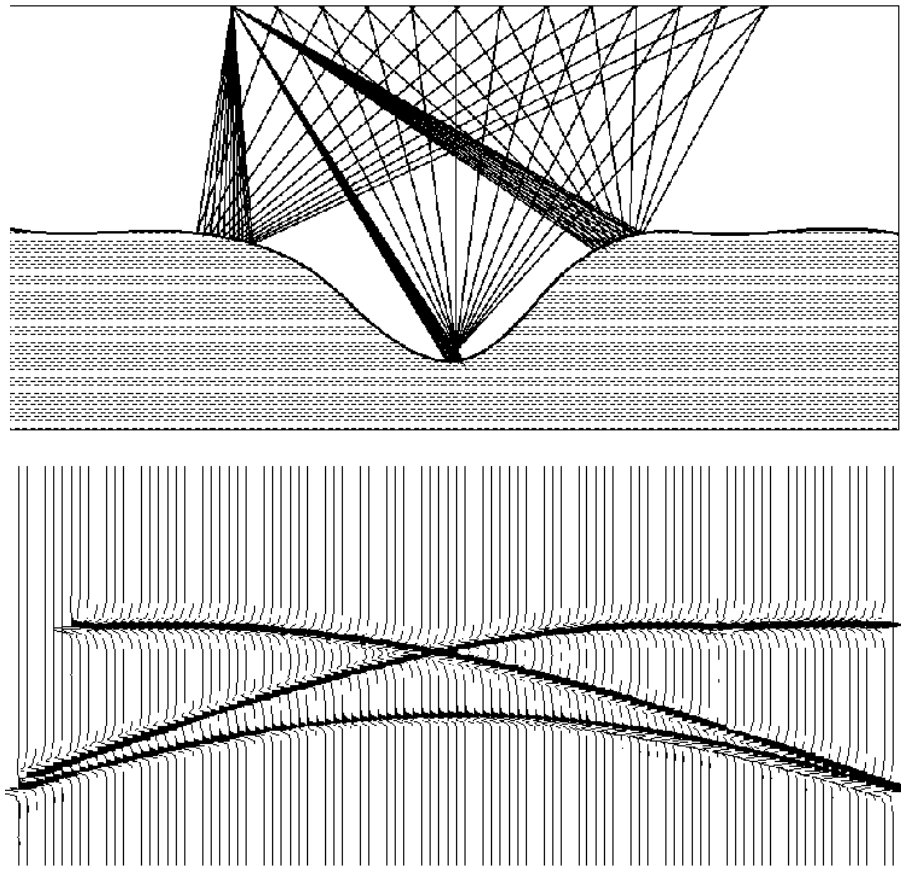

Most areas of interest to petroleum geoscientists are not characterized by layer-cake geology. Subsurface structures are present, and these can lead to problems using the seismic method. The figure above shows one such problem. The upper panel shows a buried channel. The lines show raypaths from source (at left) to receivers (at right). Notice that reflections do not come from half way between source and receivers (as expected using the common midpoint method) and that a receivers record reflected energy from three places along the interface. The expected seismic expression of the channel is shown in the lower image. Note the classic "bowtie" appearance.

Properly accomplished, seismic migration accomplishes three objectives: 1) repositioning reflected energy to its true subsurface location, 2) collapsing diffractions, and 3) shrinking the Fresnel zone.

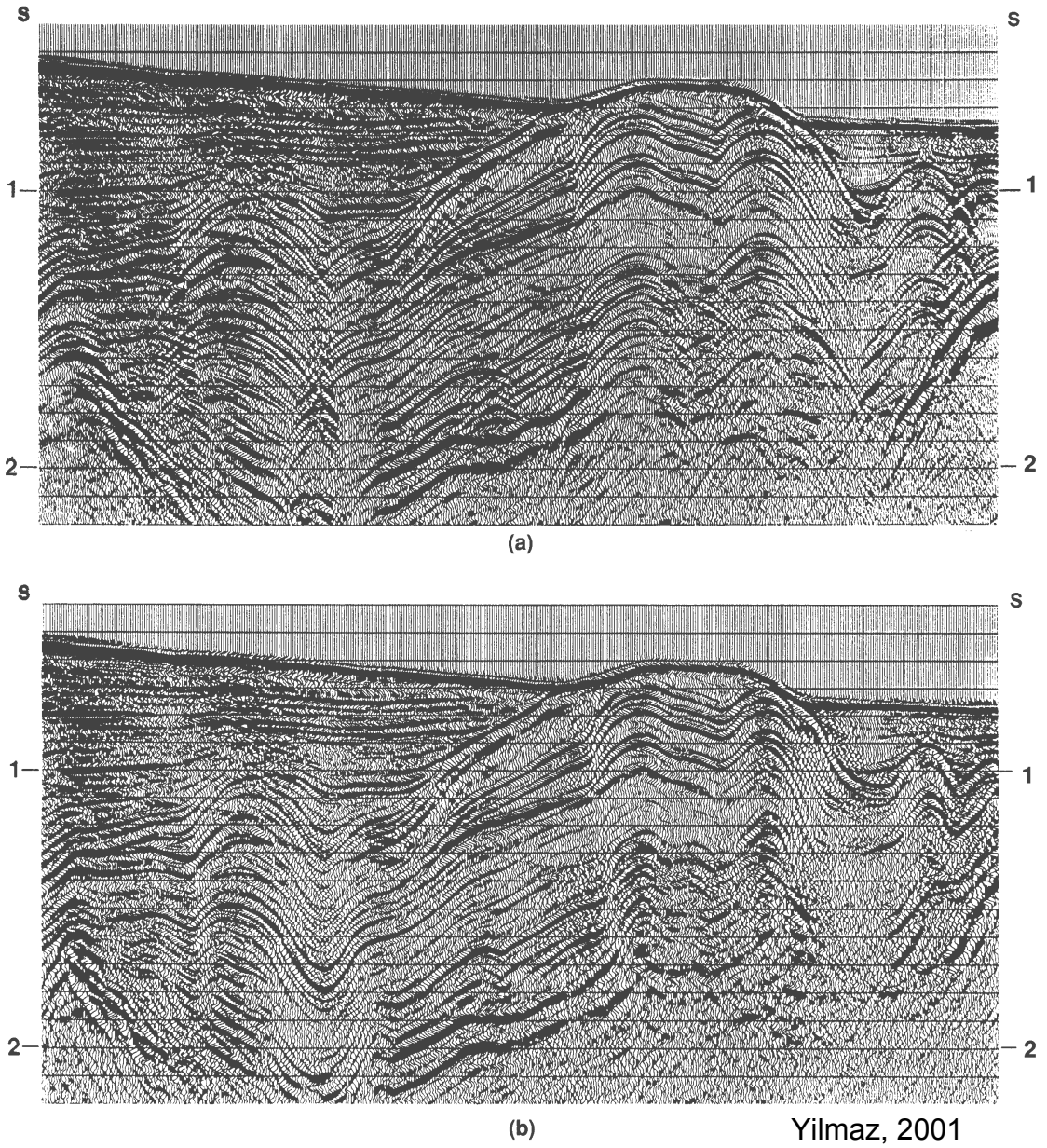

Yilmaz, 2001

These images show the impact that seismic migration can have on a seismic image. The upper image is a stacked section without migration, the lower image shows the same data but migrated. Note that the “bowties” evident at left in the upper image have disappeared and the anticlines in the right-center portion of the image are smaller (“tighter”) in the migrated image.

Migration is typically one of the last processing steps. Different types of migration are available with the commercial cost being proportional to the amount of computer time required for the work. To migrate seismic data, processors need to know, or be able to estimate, the subsurface velocity field. The accuracy of the results of implementing any migration algorithm will be dependent on the accuracy of the velocity model used.

Different types of migration algorithms are available. We will come back to these following the section on 3-D migration

Processing: Effects on Interpretability

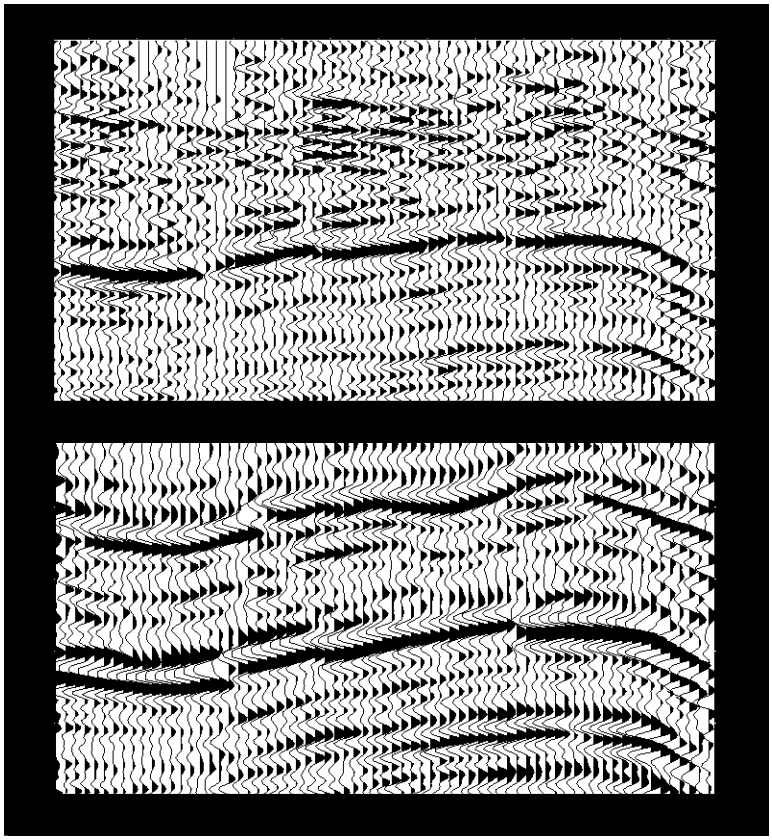

- Processors' capabilities have improved with time as hardware and software capabilities have developed. Accordingly, many older datasets are commonly sent out for reprocessing before interpretation.
- Images above show two differently processed versions of the same data. They illustrate how much the choice of processing flows can have a major impact on data interpretability. Note the dramatic improvement in reflection continuity in the upper part of the section.
  - Principal processing differences:
    - Dip moveout in lower image (to account for steep dips)
    - Filtering out higher frequencies in lower image (reduce high-frequency noise)

3-D Seismic volume

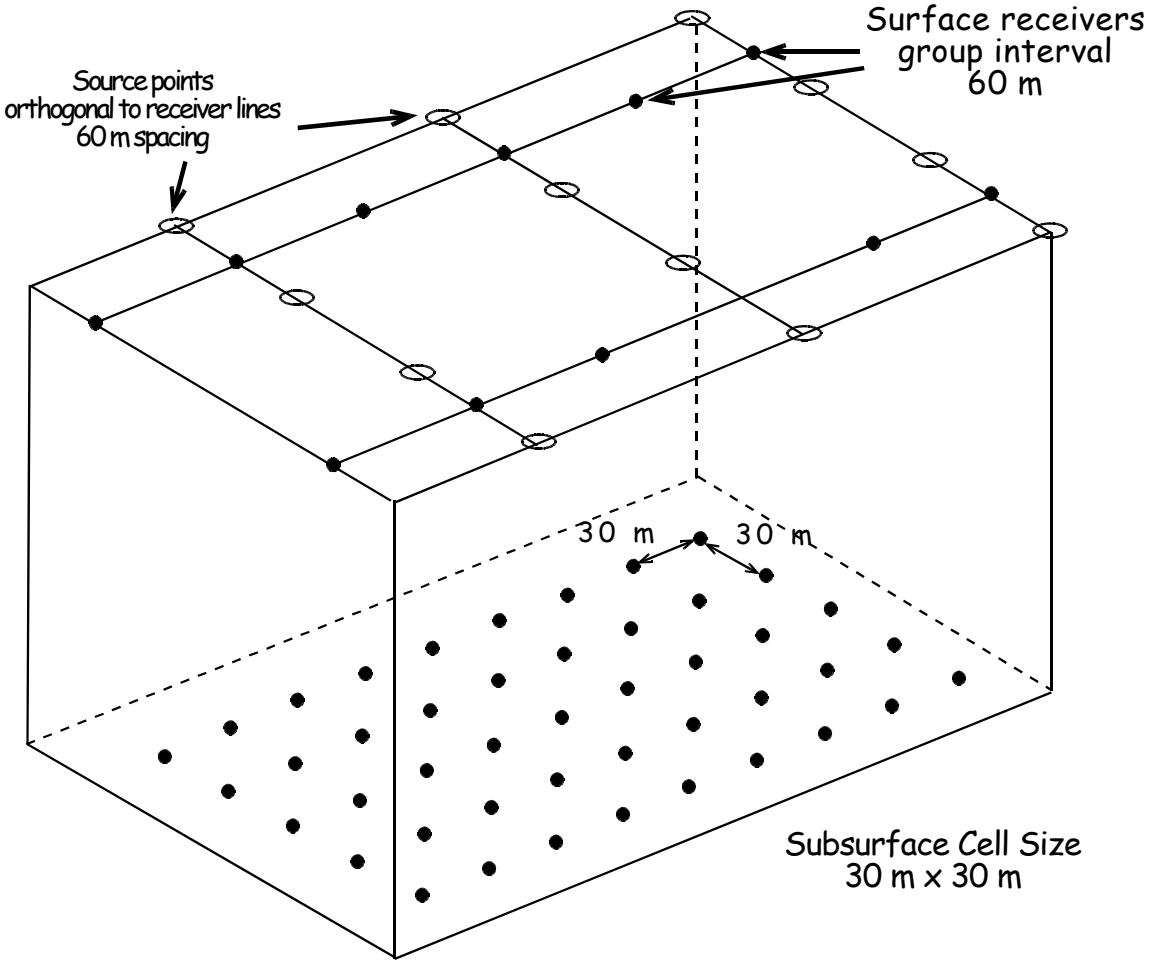

3-D seismic acquisition differs from 2-D acquisition. The image above shows an idealized layout for a land 3-D survey. Lines of source points are perpendicular to lines of receivers (or, more likely, receiver groups) forming an orthogonal grid. As shots are made at different points throughout the grid, sound travels down in 3 dimensions and a grid of mid-points is generated. The distance between CMPs will be half the distance between source points in that direction, and half the distance between receiver groups in the other direction. For example, if (as shown) the distance between source points is 60 m, and the distance between receiver groups is 60 m, the CMPs will form a grid that is 30 x 30 m.

In the 3-D seismic volume, each trace is considered to represent an area rather than a single location (i.e., the CMP location). This area is known as a bin and, as shown above, bin size is a function of acquisition geometry. In the example above, bins have dimensions of 30 x 30 m and would be centered on the CMP locations.

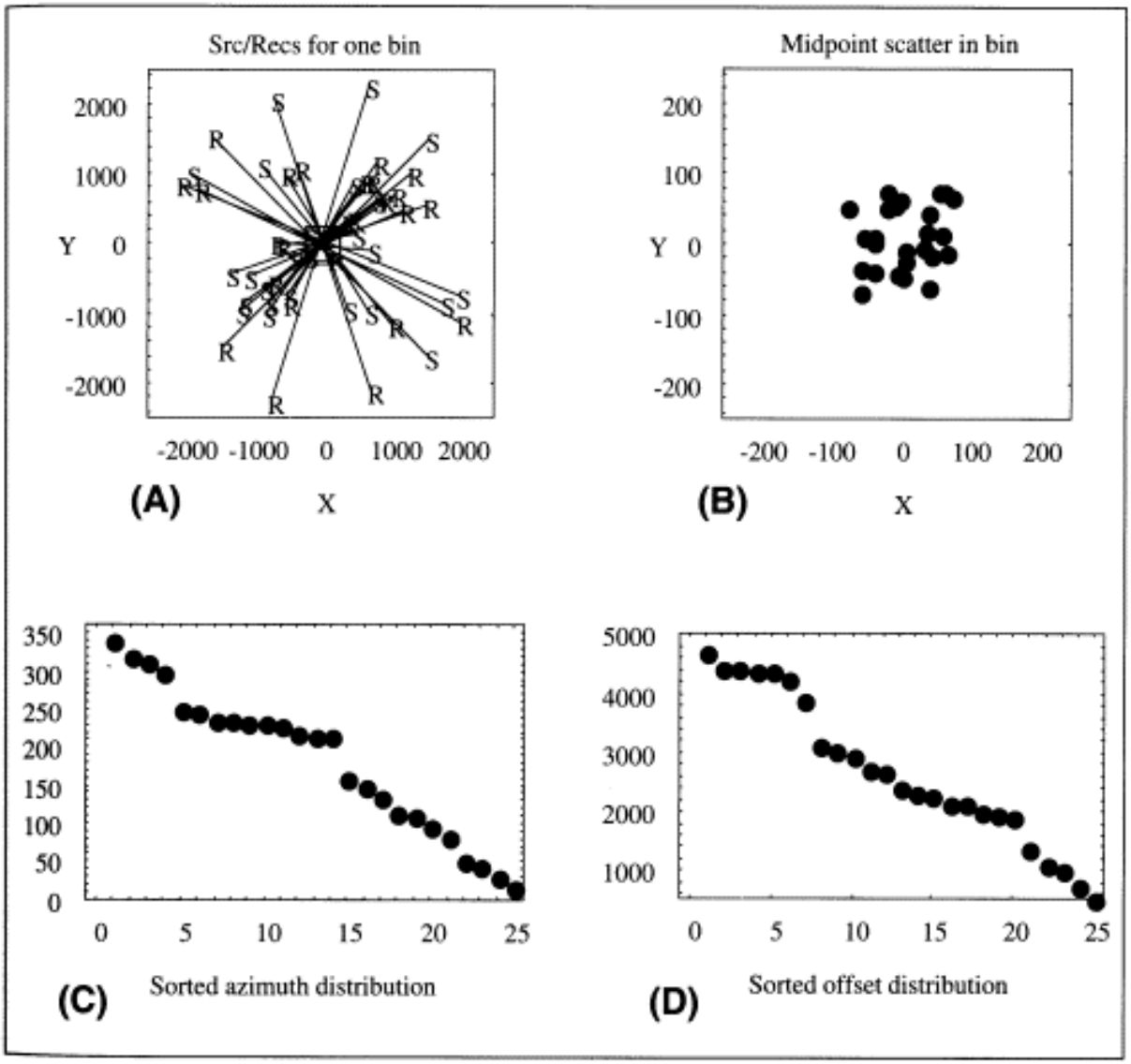

(Liner, 1999)

With knowledge of the subsurface structure it is possible to predict how, for each bin, different combinations of sources and receivers will interact. A) Map view showing lines joining source (S) – receiver (R) combinations whose mid-points fall within the same bin. B) Zooming in on the bin, the dots show a tight cluster of midpoints near the center of the bin for the source-receiver combinations in A. C) The dots show a broad range of azimuths (0 - 360°) for the source-receiver combinations in A, and D) The dots show a broad range of offsets for the source-receiver combinations in A.

When designing a 3-D survey, it will ideally be possible to ensure that uniformity of coverage (e.g., azimuths, offsets, fold) is present throughout the entire area. Otherwise acquisition artifacts may be present in the data and the utility of the data for some advanced analytical techniques may be compromised..

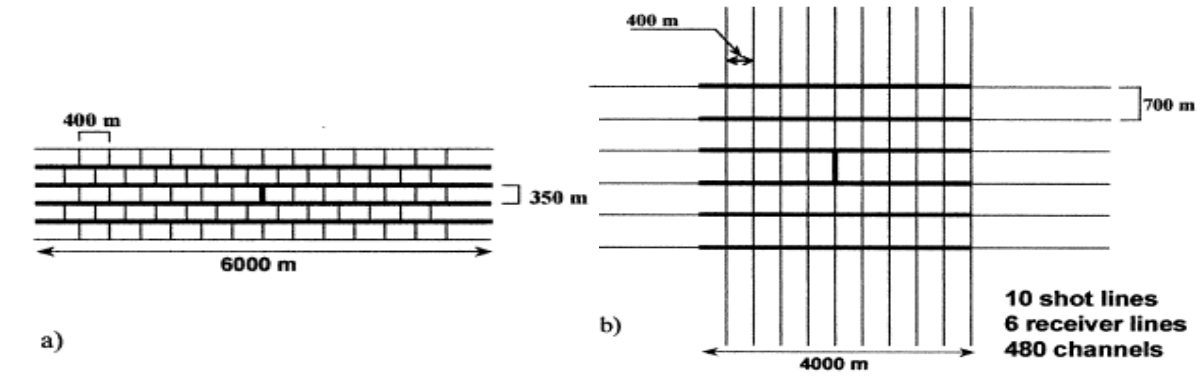

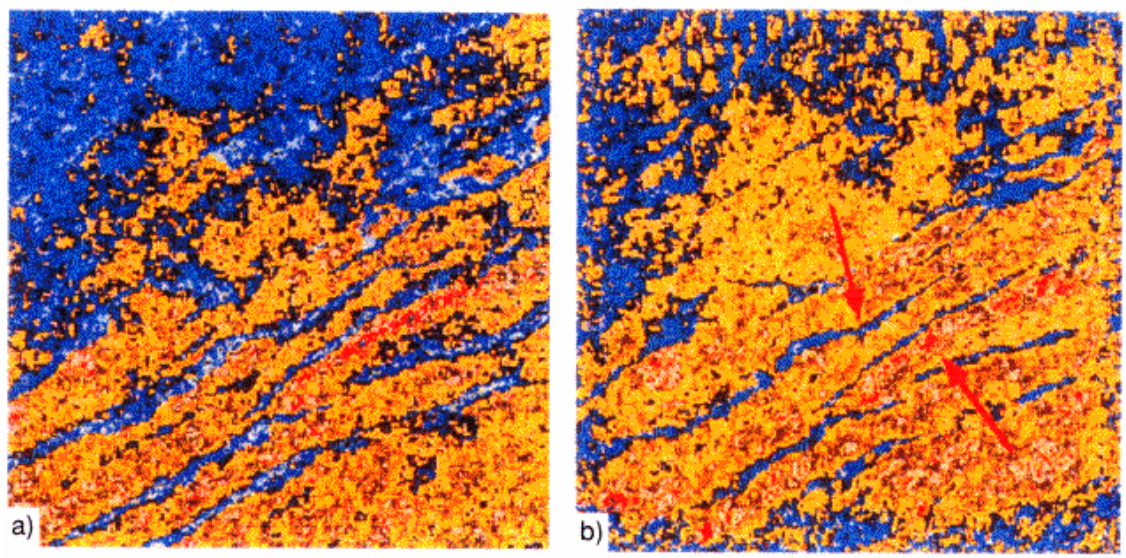

Vermeer, 2002

Many different 3-D acquisition geometries have been proposed. Vermeer (2002) showed the results of a deliberate test of two different geometries, a “brick” geometry (upper left) and a “cross-spread” geometry (upper right). The lower two images show amplitude maps for the target horizon. The faults are more clearly defined in the cross-spread volume (lower right) than in the brick volume (lower left). Note also the differences in amplitudes in the upper left corner of the two surveys.

These results show that acquisition geometry can be an important control on data interpretability.

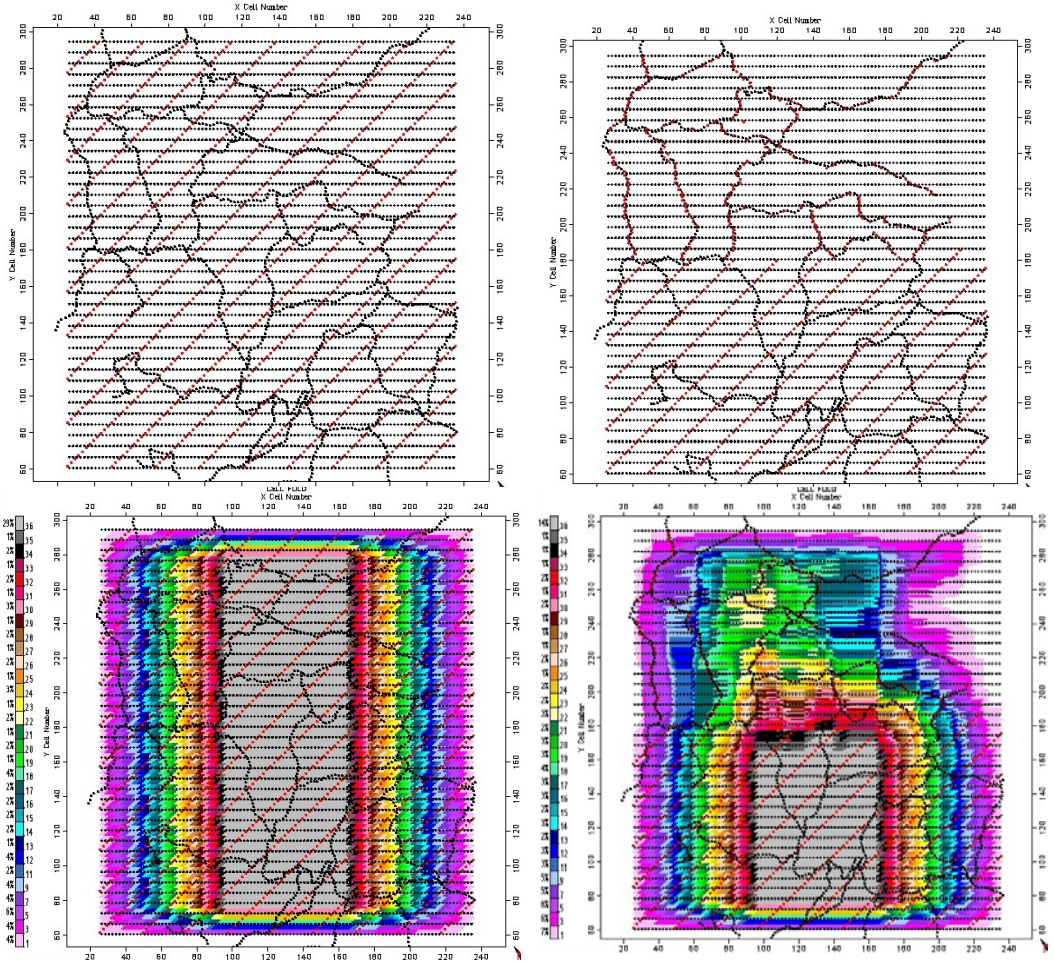

Courtesy Western Geophysical

At times, logistical considerations prevent or discourage a company from acquiring a 3-D survey using a regular grid of source and receiver locations. Compromises might be made. Using acquisition planning software, it is possible to predict the effects of the changes. For example, the survey design at upper left shows a non-orthogonal survey design with receiver lines in an E-W pattern and vibroseis (source) lines running NE-SW. The predicted fold at the target depth using this design is shown in the image at lower left. High fold (grey) is predicted for the entire area in the middle of the survey. Perhaps because of permitting, environmental or other problems, the company might decide that it is impractical to have the trucks continue the NE-SW source lines in the upper half of the survey. Instead, they have the trucks run along the roads (black lines) where permitting is not a problem (upper right). The image at lower right shows the predicted distribution of fold at the target depth. Notice that the fold is no longer evenly distributed in the north. The company can expect problems (e.g., changes in amplitude, time structure, etc.) in this area that will restrict their ability to properly interpret the data.

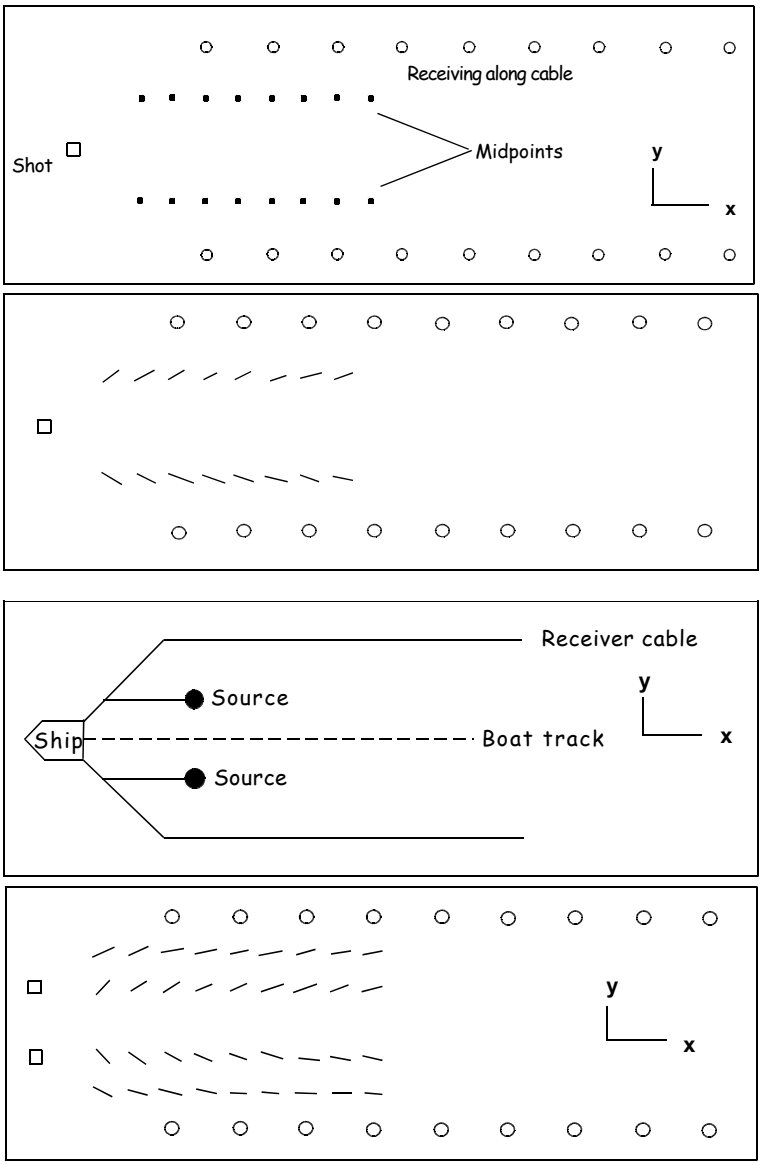

In marine settings, 3-D data are collected using a source array ("shot" in top image) and streamers being towed behind the survey vessel. Receivers (hydrophones) are spaced at regular intervals along the streamers. The distribution of midpoints for an idealized single shot is shown in the top image. The next image down shows the distribution of azimuths for each midpoint. As the ship moves through the water, different combinations of sources and receivers will have the same midpoint, although each will have a different azimuth. Note though that only a limited range of azimuths is generated this way.

The lower two images show a dual cable, dual source acquisition geometry. The source arrays are fired alternately, in a "flip-flop" manner. More midpoints are generated for each survey line and a better range of azimuths is also generated using this approach.

Other, more complicated, acquisition geometries (e.g., using two ships) are also possible.

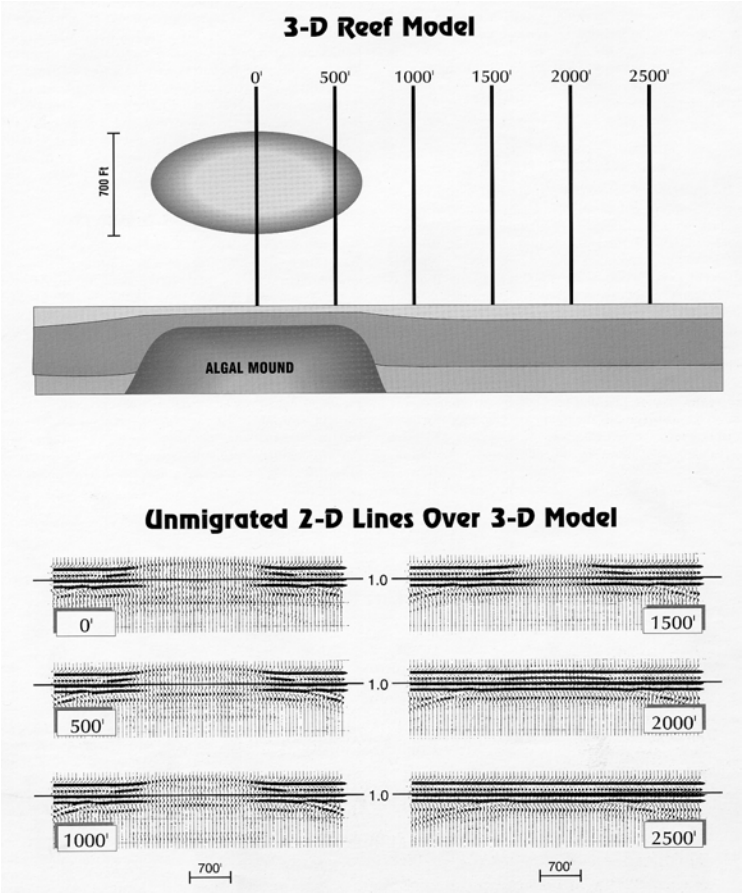

Hilterman 1975

Sound travels out as a 3-D wavefront from a shot, not as a 2-D raypath that is restricted to traveling in the plane beneath the source and receivers in 2-D seismic acquisition. As such, reflections can come from objects that are off to the side of the line, and these reflections are known as “sideswipe”. They appear to be real reflections, and processing cannot remove them from 2-D seismic data. Although this problem has been known for many years, it was not until 3-D acquisition and processing became feasible (~1970s) that the issue could be addressed.

The image above shows the results of some seismic modeling. An oval-shaped carbonate buildup (algal mound) is imaged in a series of 2-D seismic lines spaced various distances from the crest of the buildup. The mound appears in seismic images for lines that do not even cross the buildup because of sideswipe problems. The images have not been migrated, but 2-D migration would not be able to remove the sideswipe problem.

The images on the next page show the impact of 3-D migration. A geophysical company collected “spec” 3-D data and then processed using a typical 3-D processing flow including 3-D migration. They then, as an academic experiment, extracted a single line to be processed using 2-D migration. The line with 3-D migration is shown at top, and the version with 2-D migration is shown below. Notice the remarkable difference in structure and data quality lower in the images. The 3-D version should be providing a better subsurface image.

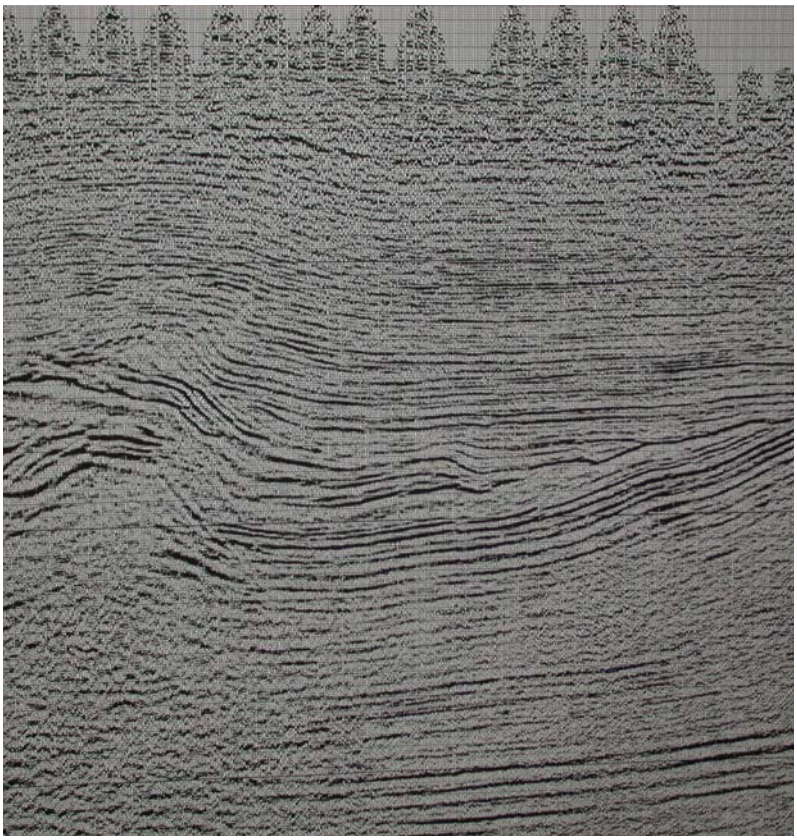

3-D migration

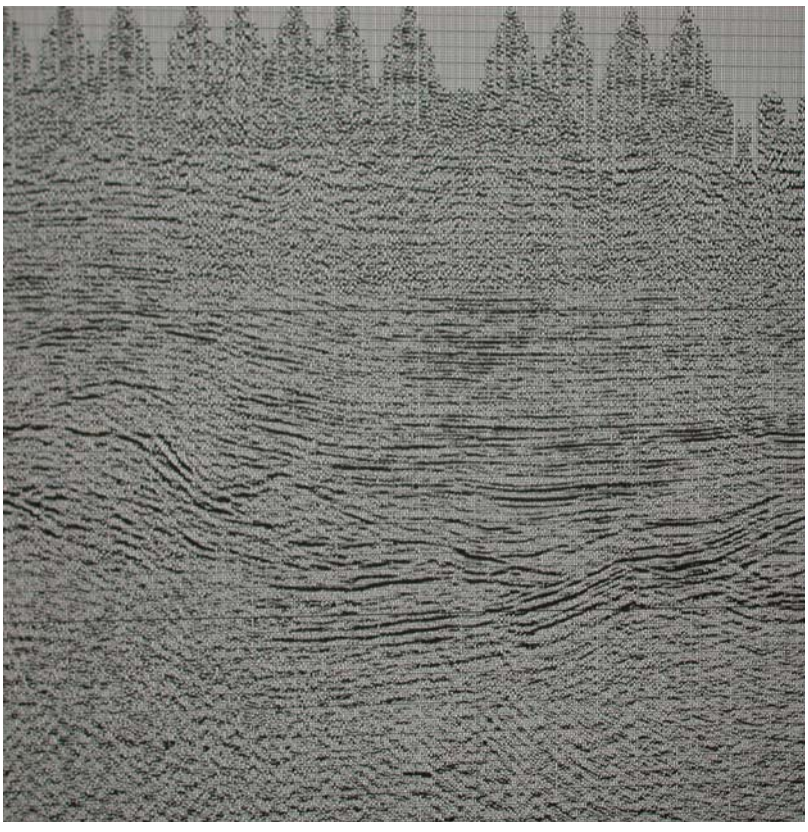

2-D migration

Courtesy Western Geophysical

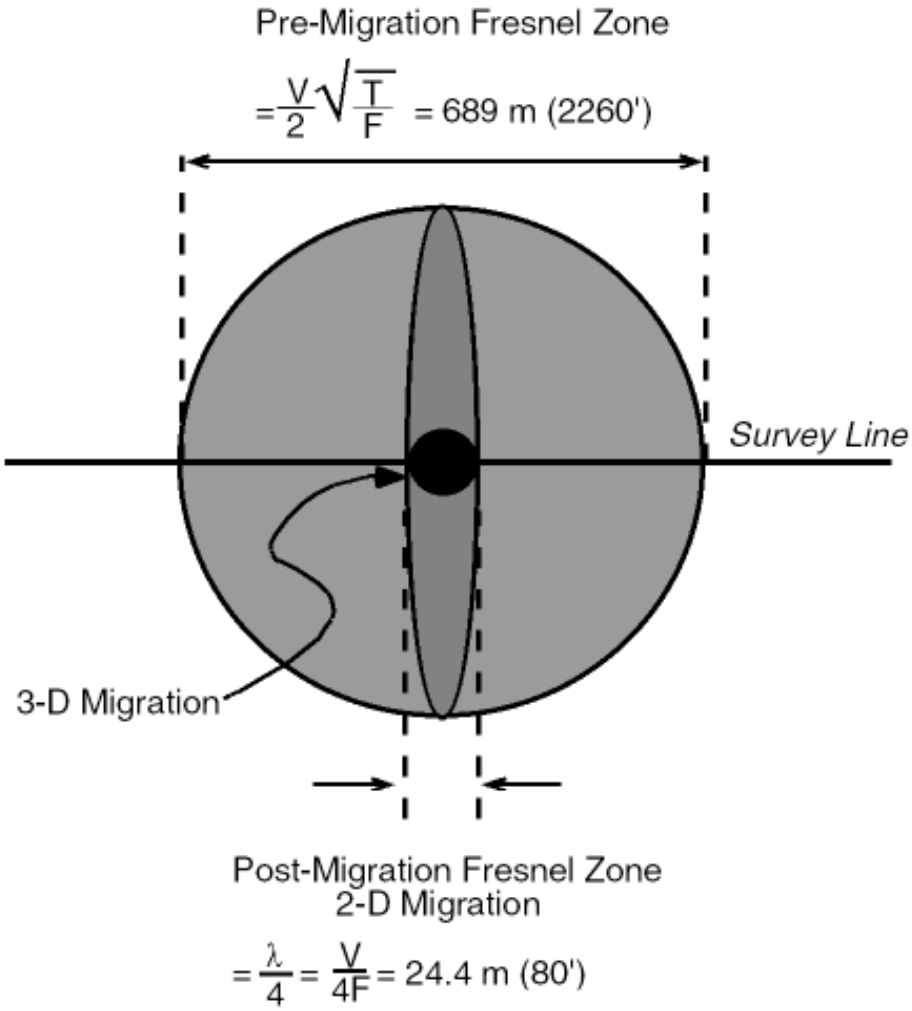

Example parameters:
T = 2.0 s
F = 25 Hz
V = 2440 m/s = 8000 ft/s

3-D migration shrinks the Fresnel zone in 2-D. The image above, showing a map-view image of the Fresnel zone, illustrates this point. The horizontal line shows the trace of a 2-D transect, with a CMP in the middle of the image. 2-D migration compresses the Fresnel zone in the direction of the line, but cannot compress it in the direction perpendicular to the line. As such, the seismic image will "see" a good distance off to the side of the line and sideswipe is still a problem. Given the example shown above, the dimensions of the Fresnel zone will be 24.4 m x 689 m. Let us now assume that the CMP in the center of the image is from a 3-D survey. 3-D migration shrinks the Fresnel zone both parallel and perpendicular to the line orientation making it a smaller point. The dimensions of this point, given the input data above, would be 24.4 x 24.4 m.

3-D migration was originally a two-step procedure, with the first pass in the inline direction and a subsequent pass in the crossline direction. It is now a one-pass operation.

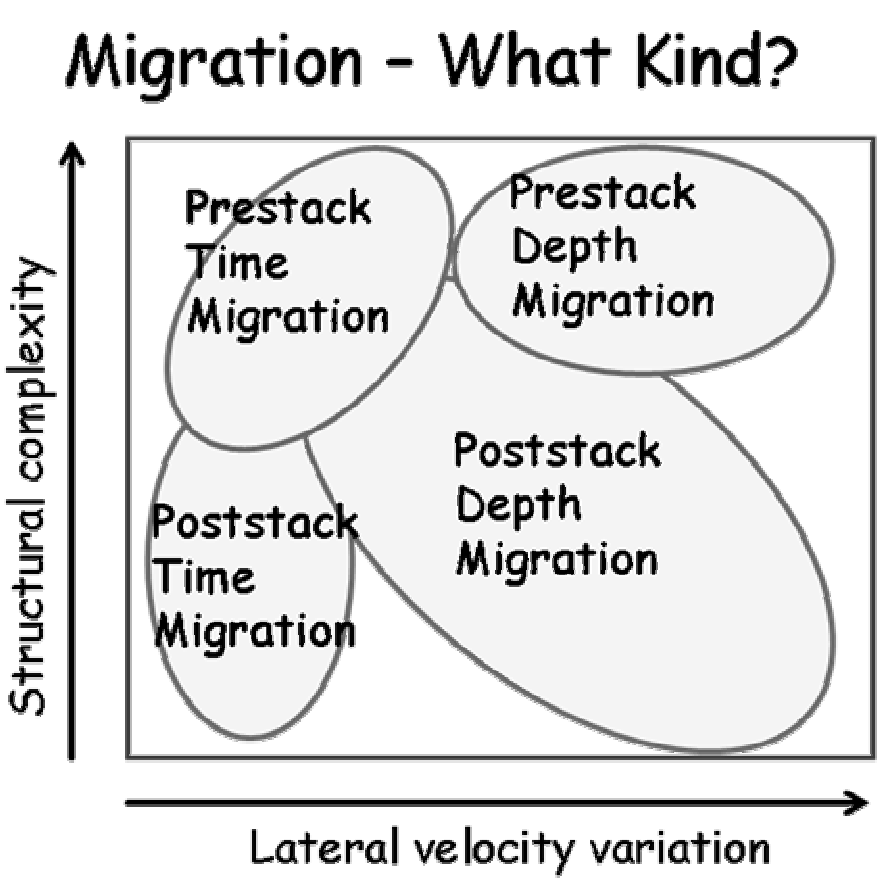

Different types of migration algorithms are possible. Two of the major decisions are: 1) should the migration be done before or after stacking, and 2) should the migration be done in the depth or time domain? Also (and obviously) 3-D data should have 3-D migration, and 2-D data can only have 2-D migration.

The figure above (redrawn from Liner, 1999) shows, conceptually, when different types of migration should be undertaken. For “simple” geology (i.e., little or no structure and small lateral velocity variations) conventional post-stack time migration is adequate. Pre-stack depth migration is preferred in structurally complex areas that have significant lateral velocity variations. Other options are possible.

Cost is an additional factor in determining what type of migration to choose. In general, cost increases as the amount of data increases or the complexity of the algorithm (i.e., the amount of physics) increases. Both of these factors will increase the amount of computer time necessary for the processing.

Kirchoff migration is the most commonly used 3-D prestack migration algorithm. It is fast and has other economic advantages. However it has: difficulties imaging complex geologic structures (e.g., beneath “rugose” horizons like faulted salt domes). Wave-equation migration provides more accurate results, but is computationally more intensive, resulting in higher costs.

The results of any migration method are only as accurate as the velocity model used to perform the migration.

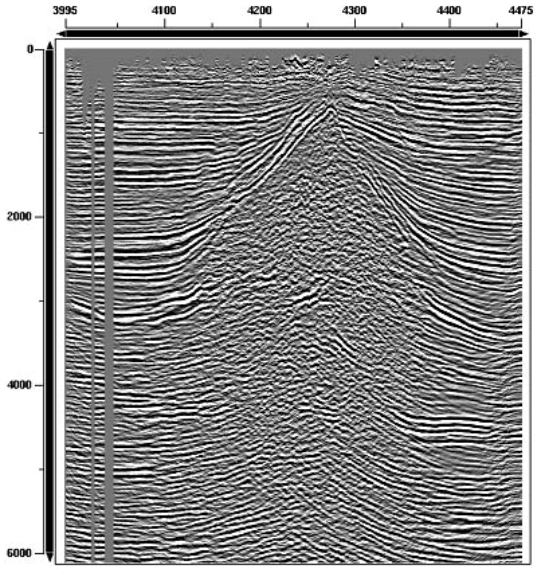

Figure 9: PSTM Section of Crossline 8180

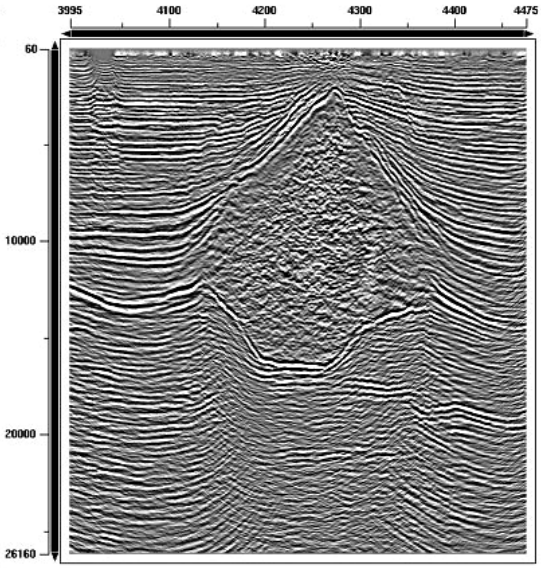

Figure 10: PSDM Section of Crossline 8180

These sets of images, courtesy of GXT, show the improvement in image quality brought about by pre-stack depth vs post-stack time migration. The images at top show changes in the seismic appearance of a salt dome. The pre-stack depth migrated image is at right.

Below, are images showing a carbonate reef and small “pop-up” structure. The pre-stack depth migrated image is at right.

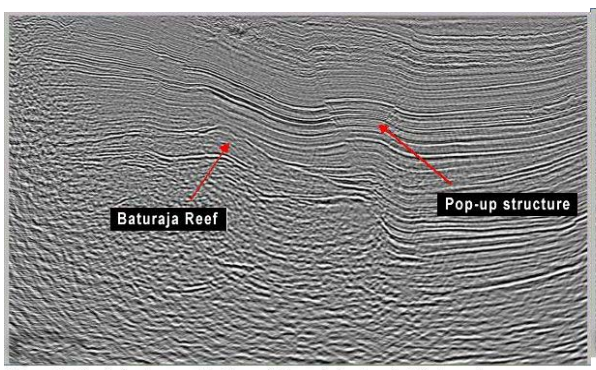

Time migration indicates a reef buildup, with low relief and an indistinct crest

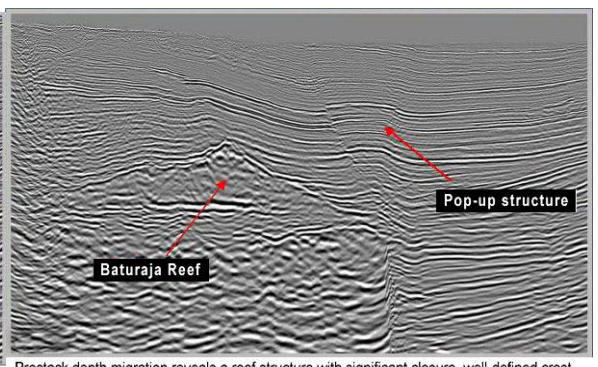

Prestack depth migration reveals a reef structure with significant closure, well-defined crest and flanks, and onlapping reflectors

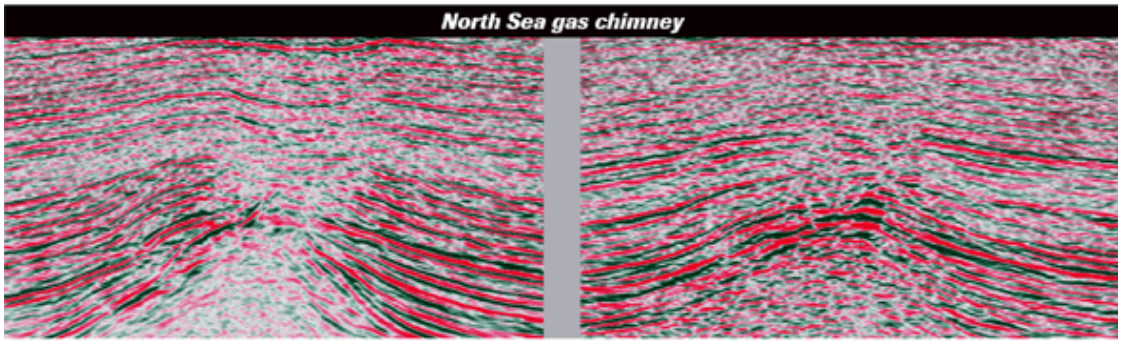

http://www.westerngeco.com/content/services/marine/multicomponent/index.asp

For some applications, it is desirable to put the receivers directly on the seafloor using ocean-bottom cables (OBC). The acquisition of shear wave seismic data is one such use. Shear waves do not travel through water, and so conventional marine sources do not generate them and hydrophones will not record them. However, part of the downgoing p-wave energy produced by an airgun will be converted to upgoing shear wave energy at a reflecting horizon (see chapter on AVO). Shear wave receivers placed on the seafloor will be able to record this mode-converted shear wave energy.

Applications of shear wave seismic technology in marine settings include seeing through gas clouds ("chimneys"). P-waves are scattered by gas clouds creating "no data" zones. S-waves are unaffected by pore fill, and so "see through" the gas.

The images above, from WesternGeco, show a gas chimney above a salt dome at Lomond Field in the North Sea. Conventional p-wave data (PP – p-wave down and p-wave up) at left show the gas cloud obscuring the structure above the dome. Unfortunately, this area hosts the principal reservoirs. The PS image (p-waves down and s-waves up, i.e., converted waves recorded with OBC technology) sees through the gas cloud and allows the structure to be mapped.

A poorly designed seismic survey (2-D or 3-D) will cost money but not provide the answers needed to make proper exploration or development decisions.

There are a variety of factors that need to be considered when designing a survey. Some of these are discussed on the following pages.

•When to collect 3-D seismic data?

- 3-D seismic data is commonly collected after a discovery has been made. This helps to reduce risk associated with questions such as whether a working petroleum system is present in an area. The survey is collected around the discovery well in order to delineate the field. The existence of at least one well in the 3-D survey area helps to calibrate the subsurface (lithology, velocity, etc.) for further analysis. The survey should be collected early in the life of a field because there will be fewer obstacles (pipelines, etc.), less noise (e.g., associated with working pumpjacks) and costs will be weighed against all future benefits (i.e., productive wells). At least 7 working pumpjacks are visible in the small area shown in this photo and a new well is being drilled. Is it worth collecting new 3-D data?
- Some large companies (with deep pockets) will collect 3-D seismic data for purely exploration purposes, especially in expensive offshore areas. This helps mitigate against the possibility of planning expensive wildcat wells using incorrect structure maps.
- Geophysical companies might collect non-exclusive surveys (“spec data”) in areas that are considered to be potentially interesting from an exploration perspective. They then seek to lease the data to E & P companies. Often these data are collected to cover large areas, and the bin sizes are large. This means that they can be of limited utility when trying to identify and map small-scale stratigraphic or structural features.

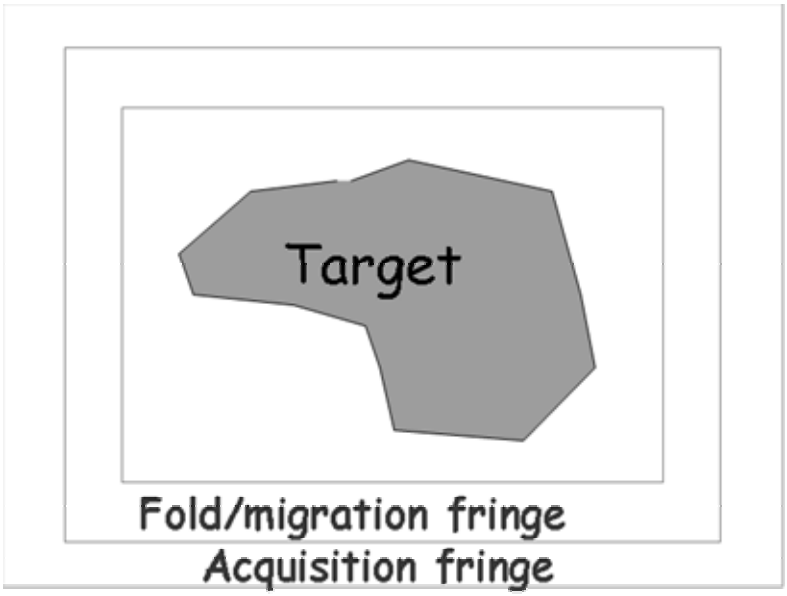

•How big does the 3-D survey need to be?

- The survey should be big enough so that the stratigraphic and/or structural limits of the field are completely covered by high-fold data (the “image area”. In order to do so, there need to be “fringes” around the survey area. These include (see image above): a) the acquisition fringe – an area which will have source and receiver locations but no CMPs will be generated there, and b) the fold/migration fringe – an area that has CMPs but less than adequate fold and less than adequate data for migration to work properly.
- The width of the acquisition fringe (A) may be calculated using: $A = z \tan\Theta$, where z is the target depth and Θ is the dip.
- A single large survey is better than collecting a series of small surveys with the thought of subsequently merging them. Less money is wasted (each small survey has its own fold and acquisition fringes) and artifacts almost invariably remain in merged surveys, making it harder to use them in quantitative analyses.
- Large surveys will give a bigger, and hopefully more useful, structural and stratigraphic image of the subsurface. However, larger surveys generally have a larger bin size in order to keep costs down. This means that they are less able to image small-scale features. The importance of this trade-off will vary from project to project.
- As a general rule, bigger is better, but costlier.

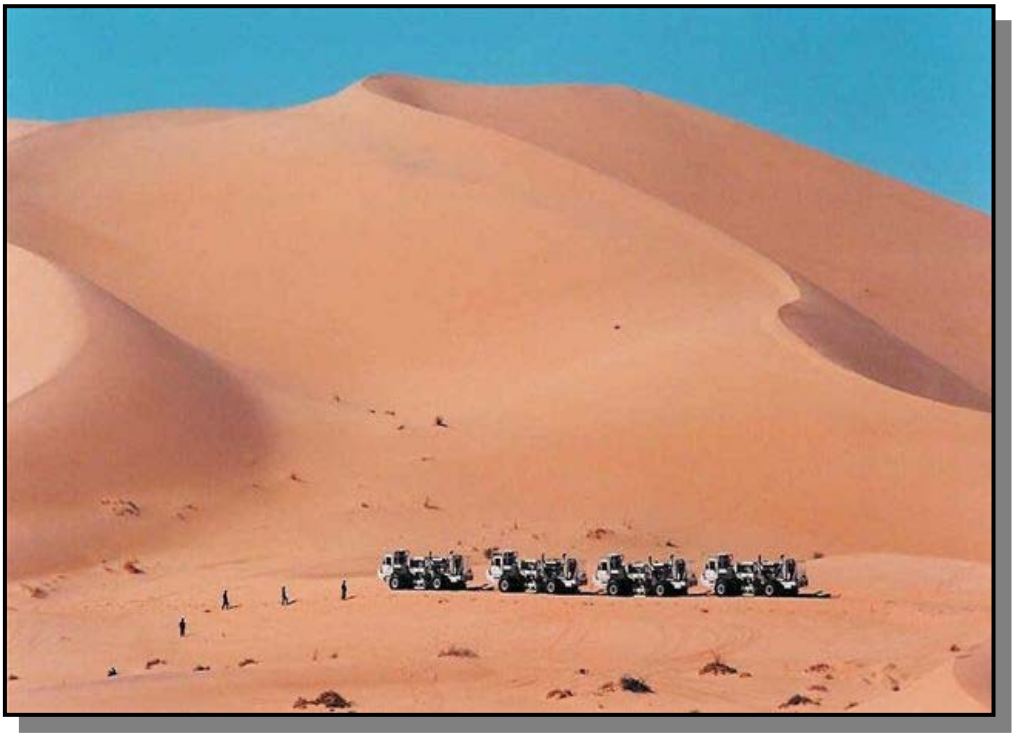

Courtesy François Gauthier

•What type of source to use? Choice of source will depend on:

- Marine (airgun arrays) vs land (dynamite, vibroseis) or transition zone acquisiiton
- Needed penetration (energy). More energetic sources are needed to obtain "'deep" images than "shallow" images.
- Bandwidth for required resolution. What is the expected thickness of the target(s)? What range of frequencies is needed to resolve the target(s)? Is it possible to get the desired frequencies down to the target level and back to the surface again or do the high frequencies get lost?
- Signal-to-noise characteristics (e.g., loose sand at surface)
- Environment (buildings, flora/fauna, etc.). For example, dynamite can generally not be used in populated areas.
- Crew availability and cost

Two methods for predicting the usable range of frequencies and energy likely to be obtained are source testing and examining existing seismic data

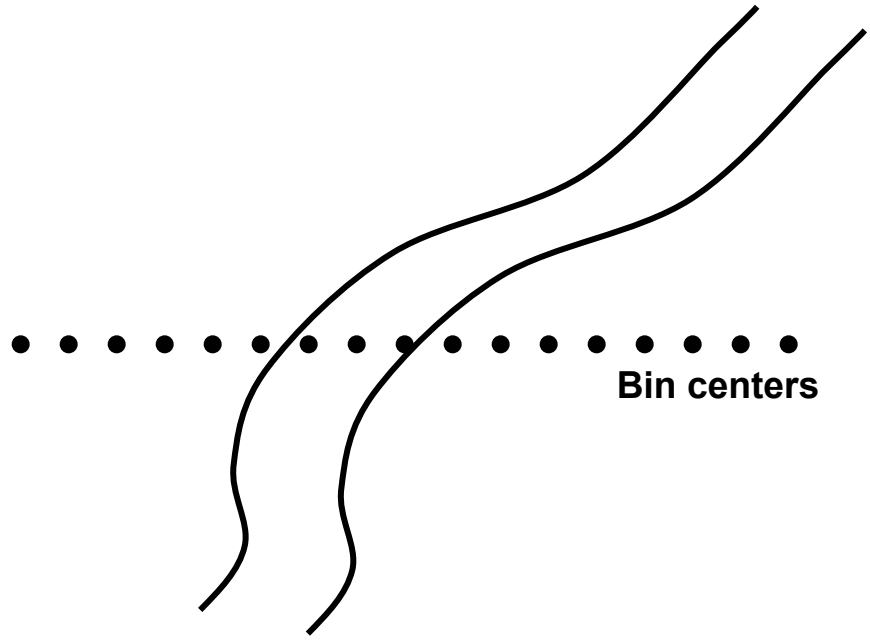

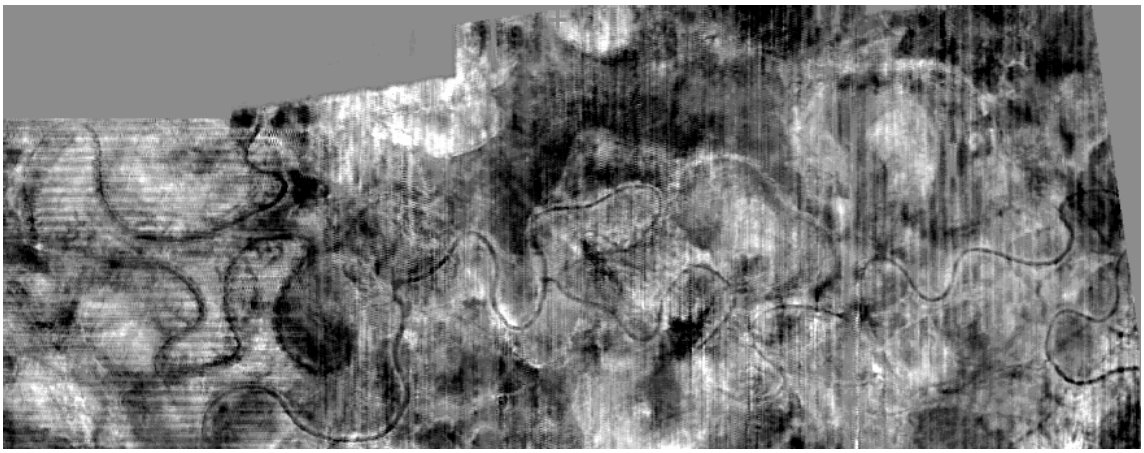

one km

Image courtesy H. Posamentier

•How big should the bins be?

- For consistency of interpretation, bin dimensions should be 1/3 to 1/4 the width of the narrowest feature to be resolved. For example, if the objective is to image channels that are 120 m wide, bins need to be no greater than 30-40 m across.
- Lateral resolution of 3-D data is determined by the largest of either: a) 3 x the bin size, or b) the post-migration Fresnel zone diameter (wavelength/2).
- Bins need to be small enough to avoid spatial aliasing (are dipping events "real"?). For a trace spacing (bin size) of X, spatial aliasing will occur when:

$$X > V/(4F\sin D)$$

Where: V = Interval Velocity near Target, F = Maximum Unaliased Frequency, and D = Structural Dip

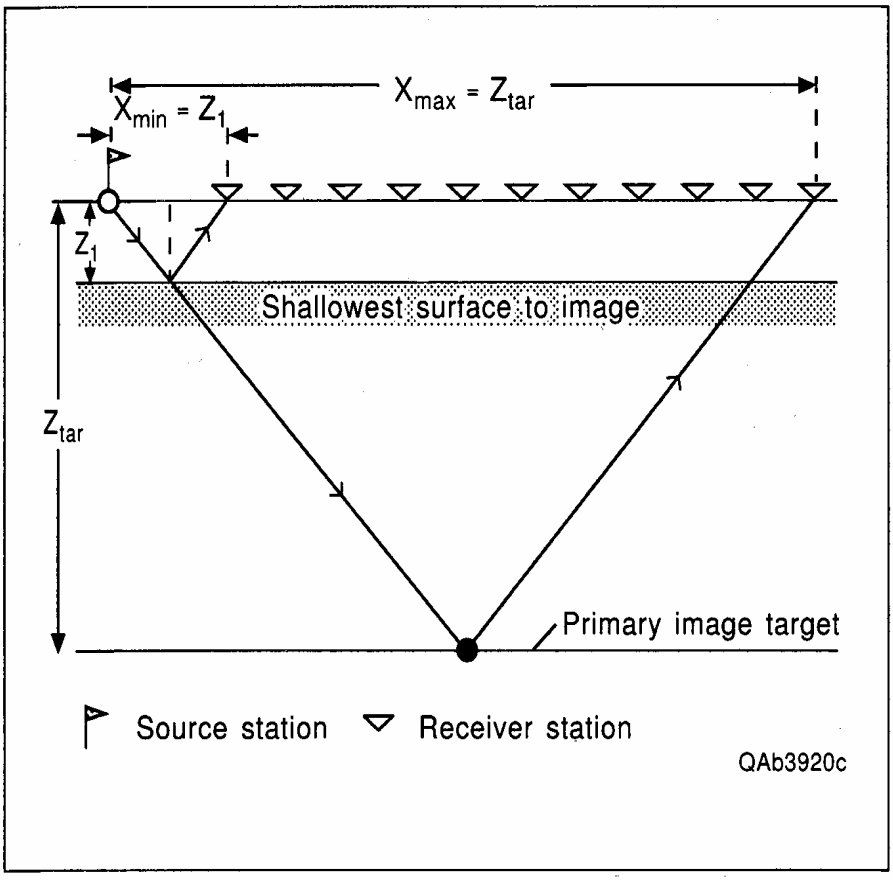

Hardage, 1997

•What depths are important?

- At least two depths are important: the shallowest target to be imaged, and the depth of the primary target
- The shallowest target to be imaged may be associated with a horizon that needs to be interpreted or simply one that needs to be imaged for geophysical (e.g., processing) reasons. It is not necessarily a drilling target. The source-line and receiver-line spacings should be approximately the same as, or less than, the shallow target depth, and the fold at that depth should be at least 3 or 4.
- The farthest offset should be at least equal to the primary target depth, possibly up to 2x target depth. This is because the NMO needs to be large enough for velocity picking (proper stacking and multiple attenuation). If distances are too large, NMO stretch may be a problem. Hardware limitations may impose limits on the length of the spread.

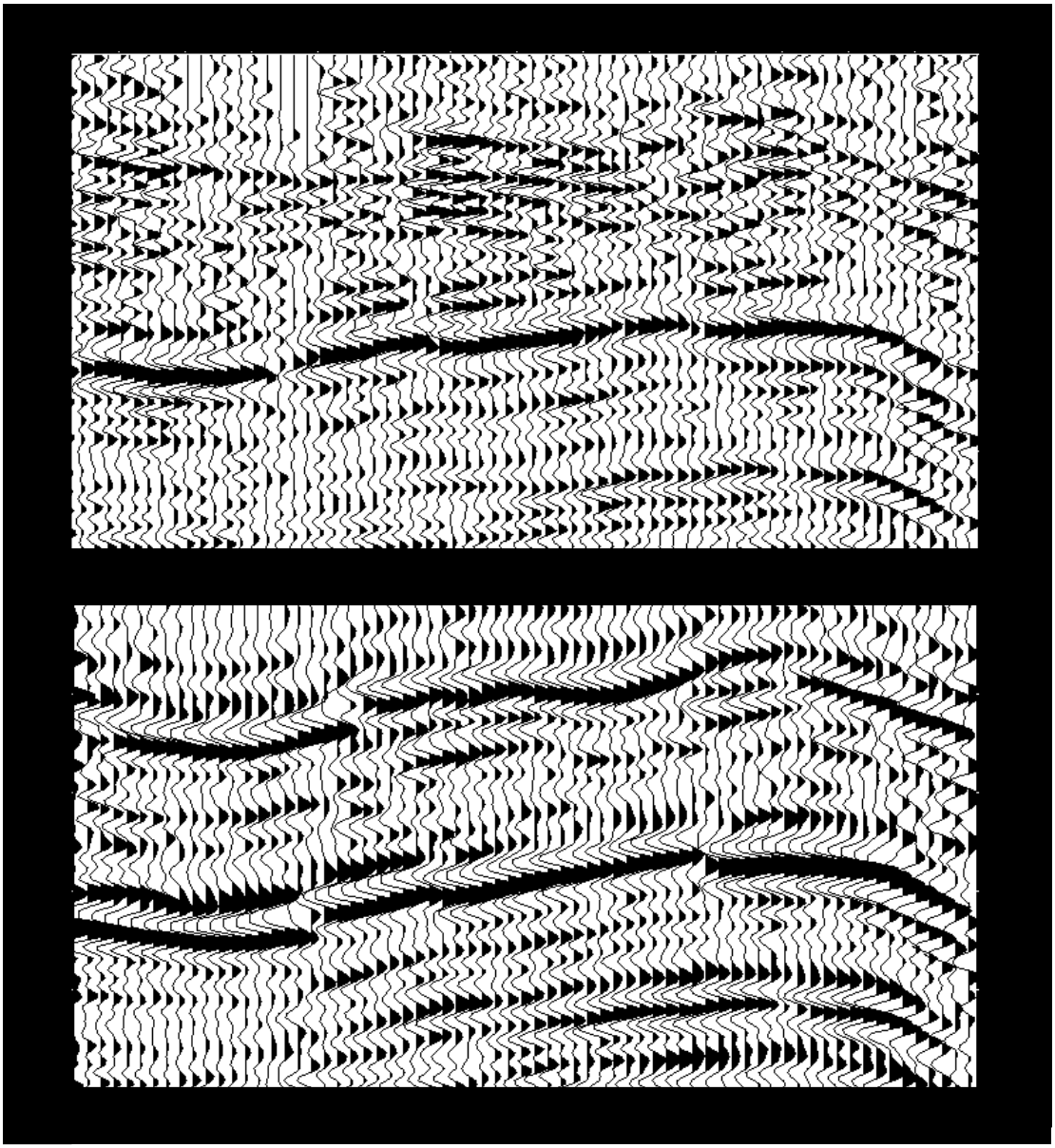

Improvements in seismic processing capabilities with time lead some companies to send data out for reprocessing in the hopes of getting more interpretable images. These two images show the impact reprocessing can have. The top image shows a transect through a 3-D volume that was acquired and processed in the early 1990s. The approximate level of the top of the target horizon is indicated. The data are very hard to interpret in this version. The lower image shows the same transect but after the data had been reprocessed. Note the improvement in data interpretability at the target level.

Raw seismic data are said to have a long “shelf life”, provided that they were properly recorded and archived.

Before

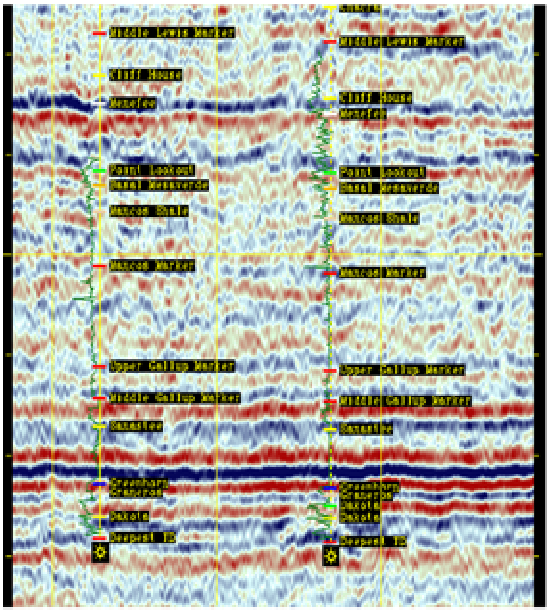

After

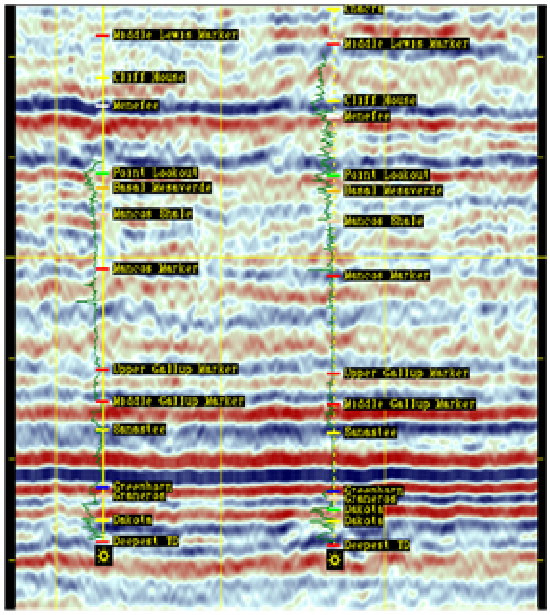

If data quality is less-than-perfect but sending the data out for reprocessing is not an option, a variety of post-stack processing techniques may be applied. The usual objective is to enhance data interpretability. Techniques include various types of filtering (bandpass, f-k, etc.), deconvolution, amplitude scaling, trace averaging, etc. These processes are chosen and applied by the seismic interpreter, with results being produced in near-real time (minutes, hours – depending on the processing flow selected and the size of the dataset).

The example above shows the improvement in data interpretability associated with a post-stack processing flow. Note the improvement in lateral reflection continuity.

Post-stack processing can be a double-edged sword. It can significantly (at least sometimes) enhance data interpretability, but it can also remove information and add artifacts to the data. It should be employed with caution.

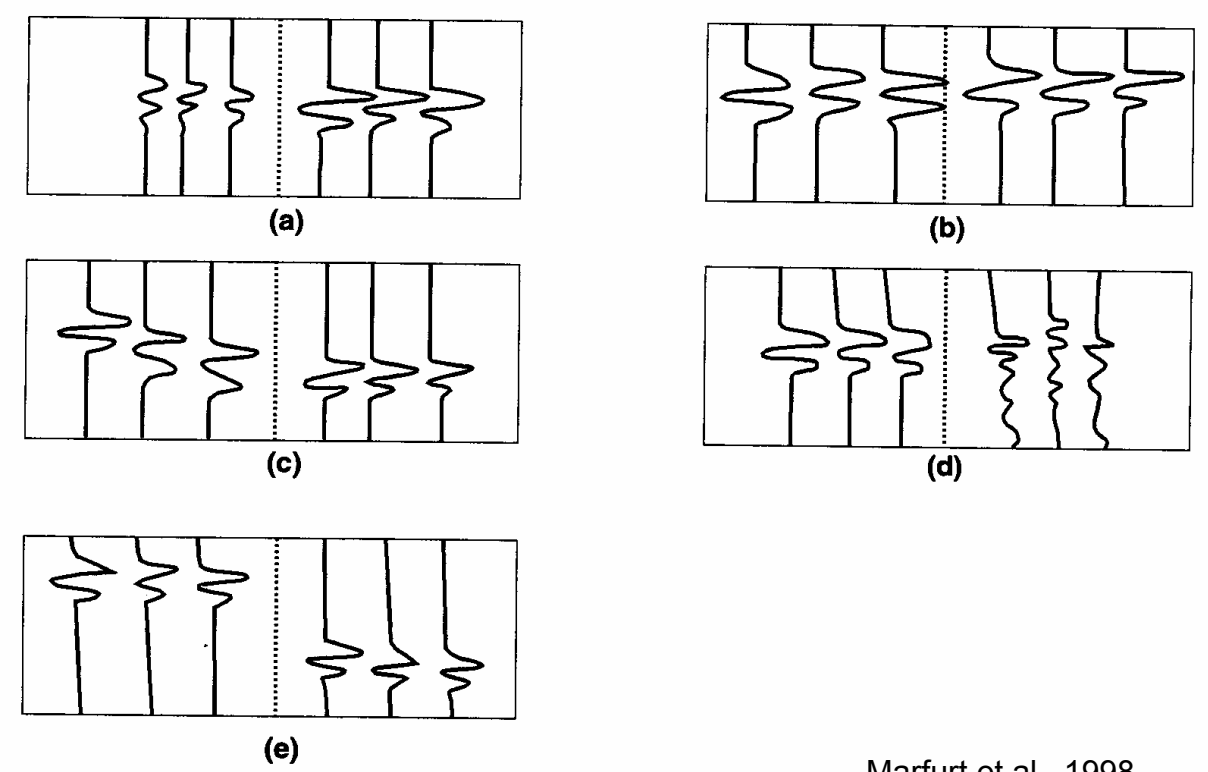

Marfurt et al., 1998

There are a number of ways in which faults may be recognized in seismic data. The images shown above illustrate several of these.

In a) the reflections change amplitude across the center line. The reflections on the right have higher amplitudes than those on the left b) There is a slight change in phase from the left to the right side of the figure. The Left side shows a symmetrical doublet, whereas the right the doublet is asymmetrical. c) Reflections on the left side are dipping whereas the reflections on the right are horizontal. There is a change in dip from one side of the section to the other. d) There is a change in noise level. The left side has "clean" reflections whereas the traces are noisy on the right. e) There is an offset from the left side to the right side.

In each of these cases (except the right side of D), the events are similar ("coherent") on each side of the fault, but the traces are different (low coherency) from one side of the fault to the other. By quantifying the coherency, it is possible to identify faults and other features.

This approach was originally developed by Amoco – spun off Coherence Technology Corp. Now, most software and seismic processing companies have developed some variant of this approach. Each vendor has a different name; here the word "coherency" is used to describe all such products.

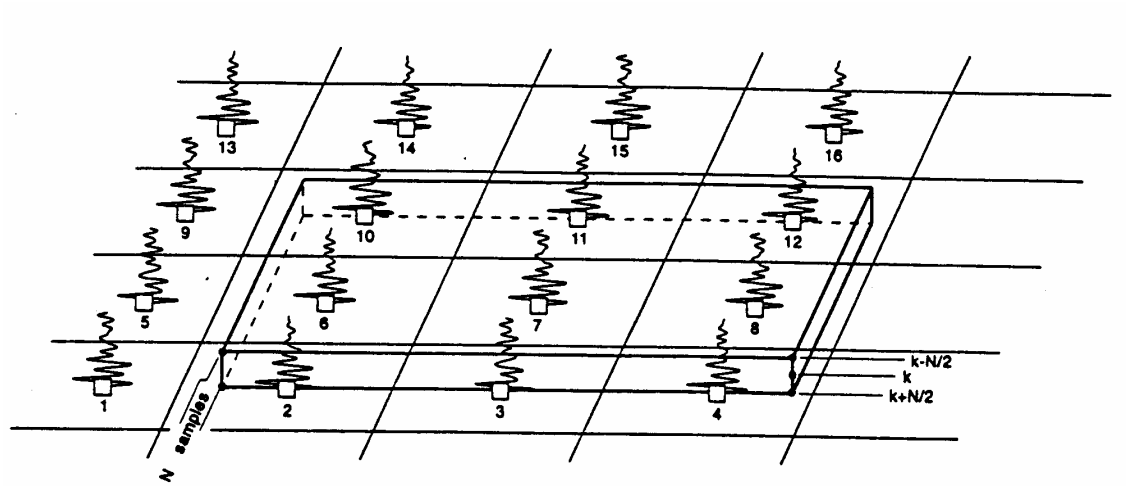

Courtesy Bob Hardage

Several different algorithms have been developed to produce coherency volumes. This figure illustrates the basic procedure.

Coherency is calculated for every sample on every trace in the 3-D survey. Let us consider trace #7 in the figure above. The square highlights the sample on that trace for which the algorithm is calculating coherency. We must tell the computer at least two things: a) how many neighboring traces to use for comparison purposes when generating the coherency volume, and b) over what time window to make the comparison (this will be a sliding window that moves down each trace as the volume is generated). We might tell the software to compare trace 7 with all 8 of its neighbors, four of its neighbors or two of its neighbors. If we decide on four or two traces for the comparison, we must specify the search pattern. A smaller number of traces will help to identify subtler features and take less computational time than if we pick a lager number. However, the results could be adversely affected by noise. Similarly, picking a large sliding time window will smooth out noise but may obliterate fine-scale structures.

Modern coherency algorithms are able to incorporate the presence of dipping reflections into the coherency calculations.

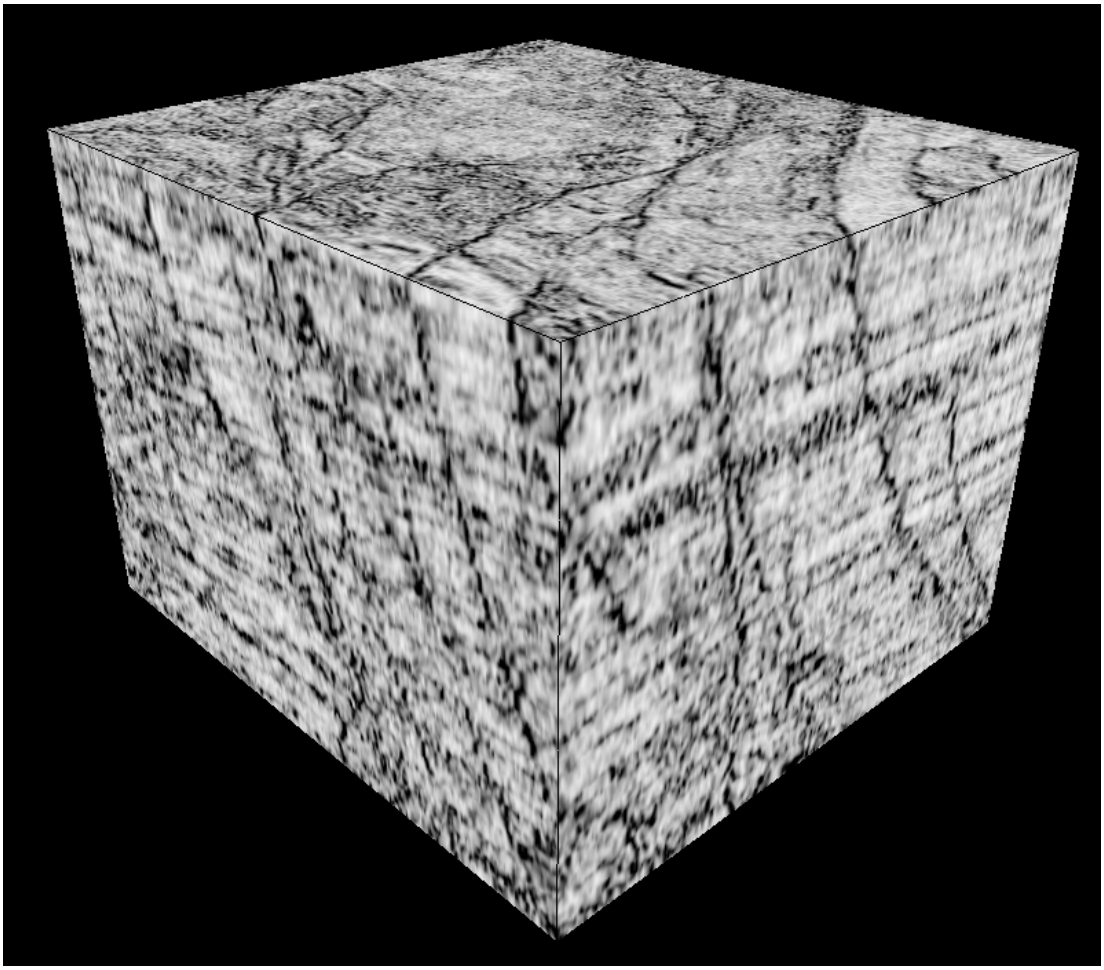

Courtesy GeoQuest

A coherence attribute cube. High values of coherency are shown in white, low values are shown in black. The low coherency values delineate faults that are clearly evident on the sides and top face of the cube. Faults may be picked on any face of the cube, but typically timeslice views (top of cube) are thought to be most useful.

Notice that some stratigraphic levels are characterized by higher coherency and others are characterized by lower coherency (black). Coherence volumes have proven to be useful for defining channels, reef margins and other stratigraphic features.

"Coherency cubes" are a common post-stack processing product. Most larger companies, and many smaller companies, routinely send their 3-D seismic data out to be processed into such volumes.

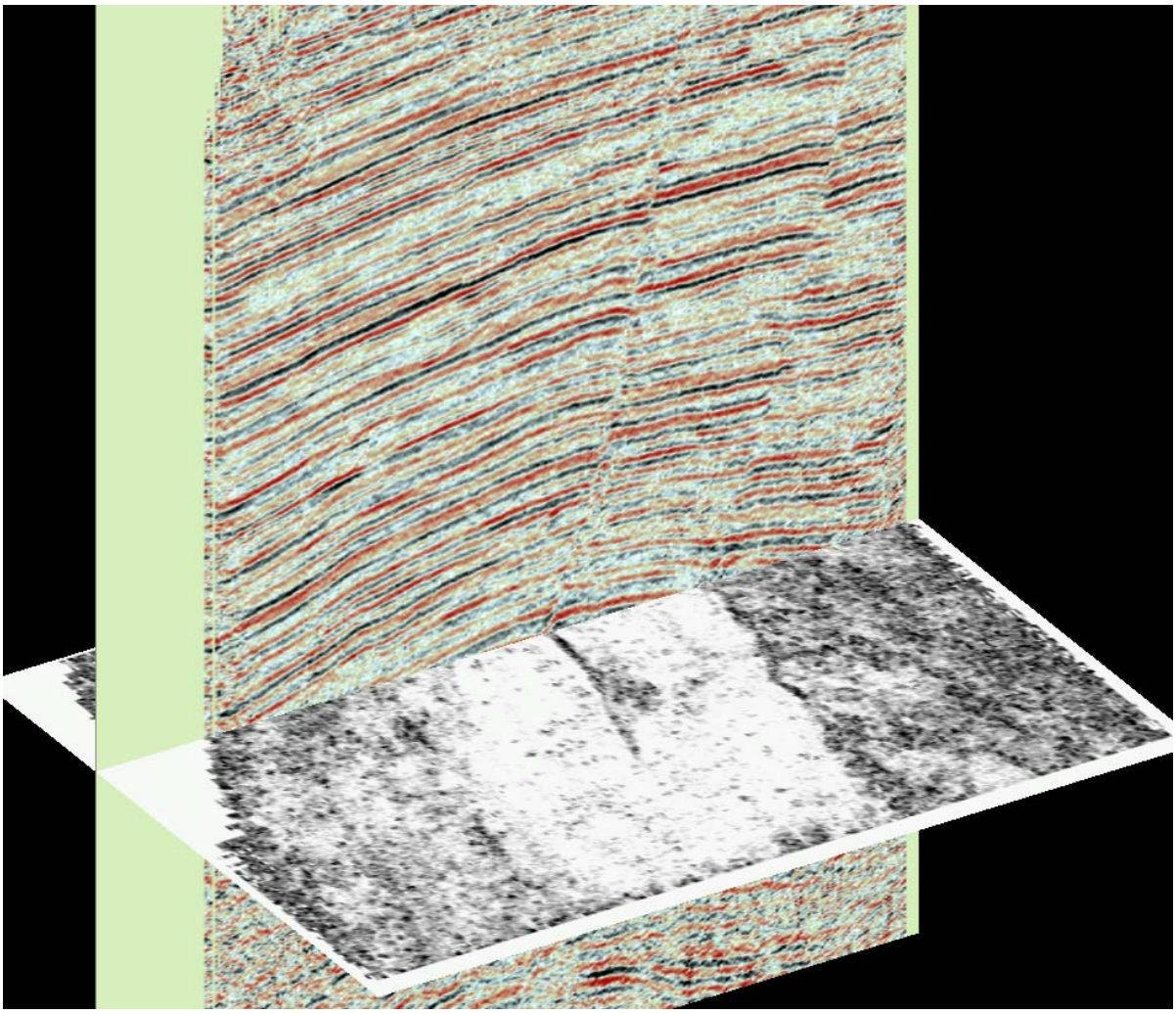

A seismic amplitude transect and coherency timeslice from a Tertiary clastic section with two normal faults. The fault on the left is defined by reflection offsets at the level of the coherency timeslice. Note the good definition of the fault trace on the coherency timeslice. The fault on the right is defined by changes in noise level and reflection offsets at the level of the coherency timeslice.

Fault picking is typically performed by looking at both coherency timeslices and vertical transects through amplitude volume simultaneously.

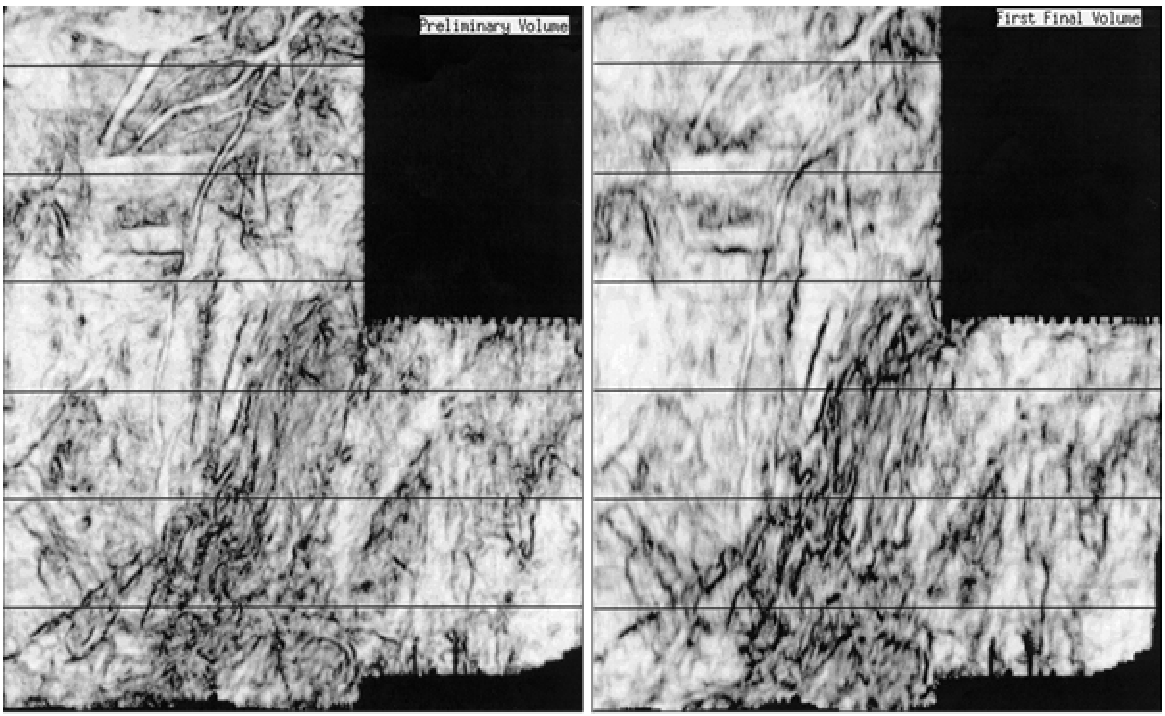

Scott-Pickford

Different methods are possible for evaluating the impact of different processing flows (statics, migration, etc.). Coherency volumes may be generated for this purpose. The idea is that faults and stratigraphic features will be sharpest in the data volume that has the best processing flow.

These two images show a timeslice through two coherency volumes derived from differently processed seismic volumes. Which processing flow resulted in the best image?

Exercises 1

1. What is the narrowest feature that can be resolved in a 3-D seismic data volume if the dominant frequency at a particular level is 50 Hz, the bin size is 15 m and the interval velocity is 2400 m/s?

2. The migration aperture needed to correctly image a dipping horizon can be estimated using the following equation:

$$A = z \tan\Theta$$

Where: A- aperture width, z – depth of reflector, Θ – bed dip

If the depth to a target is 2500 m and the bed dip is 30°, what does the migration aperture need to be?

Exercises 2

3. The image below shows a “side panel” for some seismic data that was collected about 20 yeas ago. Your management has requested that you try to integrate it into your interpretation. The prospect you are working on is at approximately 14,000’ depth. Comment on how useful the seismic data will be.

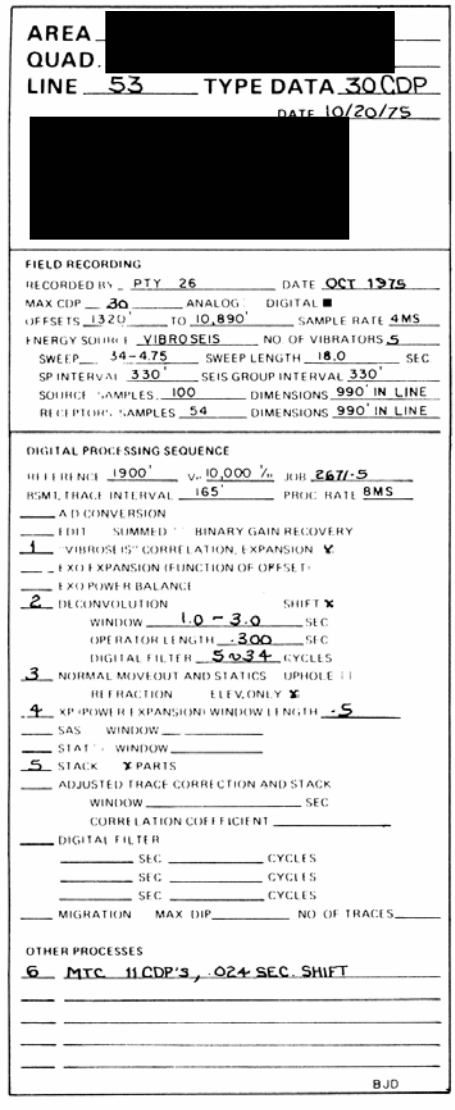

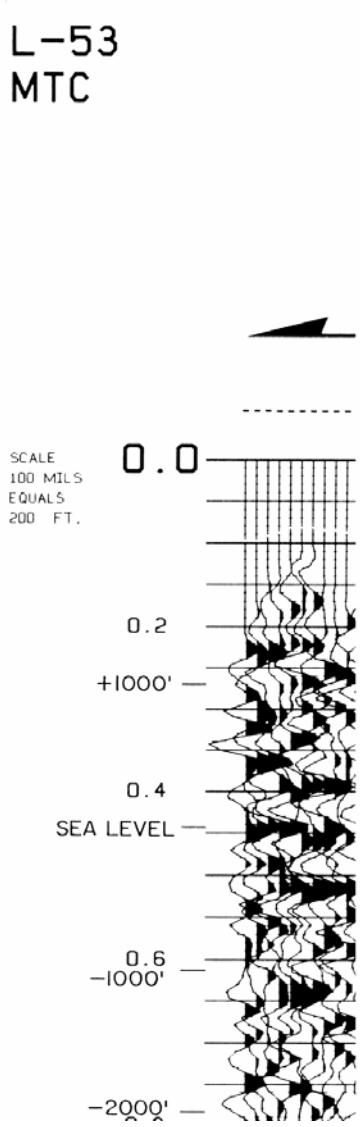

Exercises 3

4. The stacking fold of 3-D seismic data does not need to be as high as the stacking fold for 2-D data, largely due to the improvements resulting from 3-D migration. Krey (1987) determined that to obtain comparable data quality, the stacking fold for 3-D should be: 2-D fold X (frequency of interest)/100. If 30-fold 2-D seismic data produce an adequate image, and the frequency is 70 Hz, what does the 3-D stacking fold need to be to obtain a comparable image?

2-D vs 3-D Seismic Data – An Overview

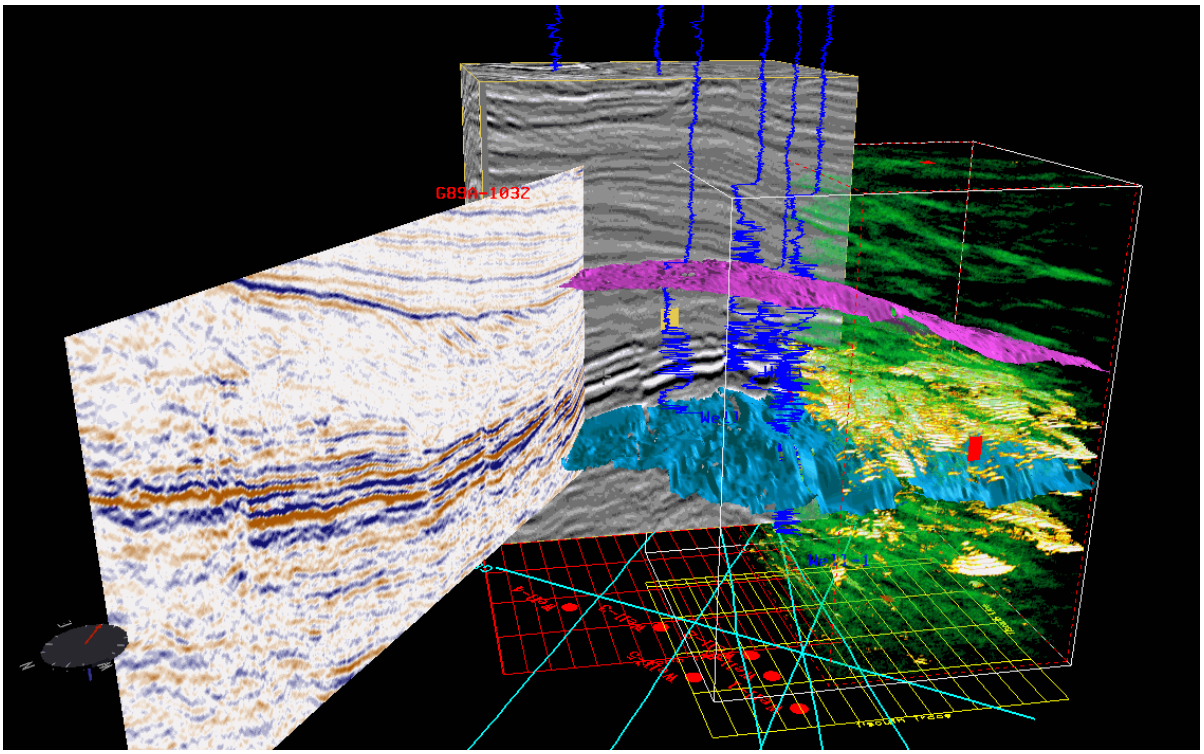

- Both 2-D and 3-D seismic data are collected and interpreted for the exploration and exploitation of hydrocarbons, although 3-D seismic have become the tool of choice in most cases.
- In this chapter, we will examine the characteristics, uses and pitfalls of each type of data.
- Seismic data are typically stored and interpreted in digital format using PC or workstation-based software (e.g., SeisWorks, SeisVision). These packages typically allow 2-D and 3-D seismic data (including multiple vintages of data) to be viewed and interpreted together (as shown above).

2-D Seismic Data - Acquisition

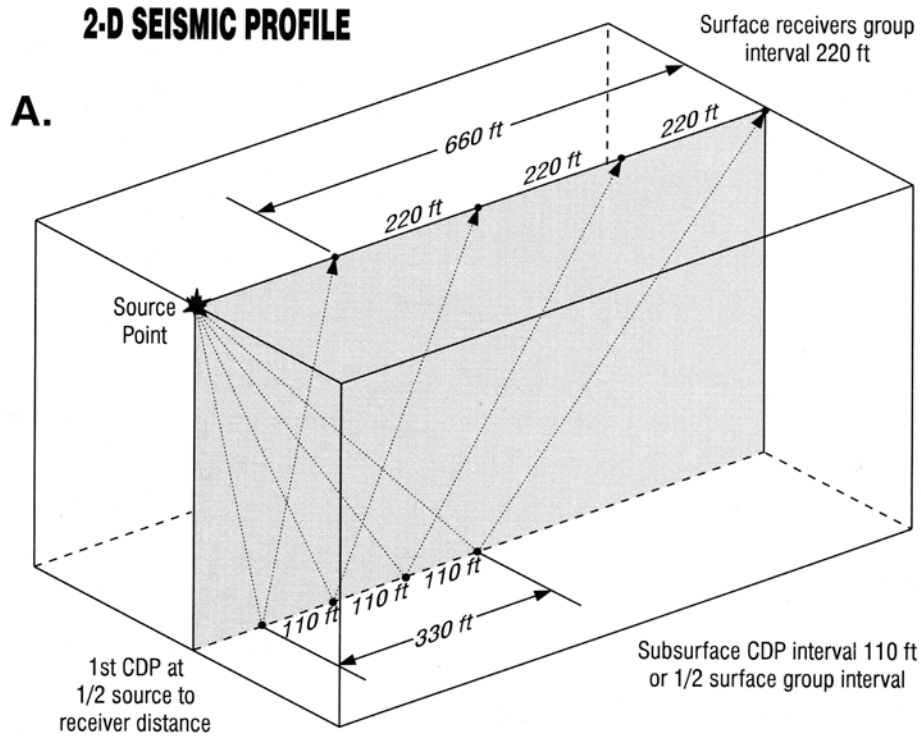

- As shown above, 2-D seismic data are recorded with the seismic source and receivers arranged in a line. In a simple layer-cake world, reflections come from locations that are mid-way between source and receivers (“mid-points”). The spacing between mid-points is half the distance between receiver groups at the surface.
  - The original terminology called common mid-points “common depth points” – CDPs (as used above)

2-D Seismic Grids

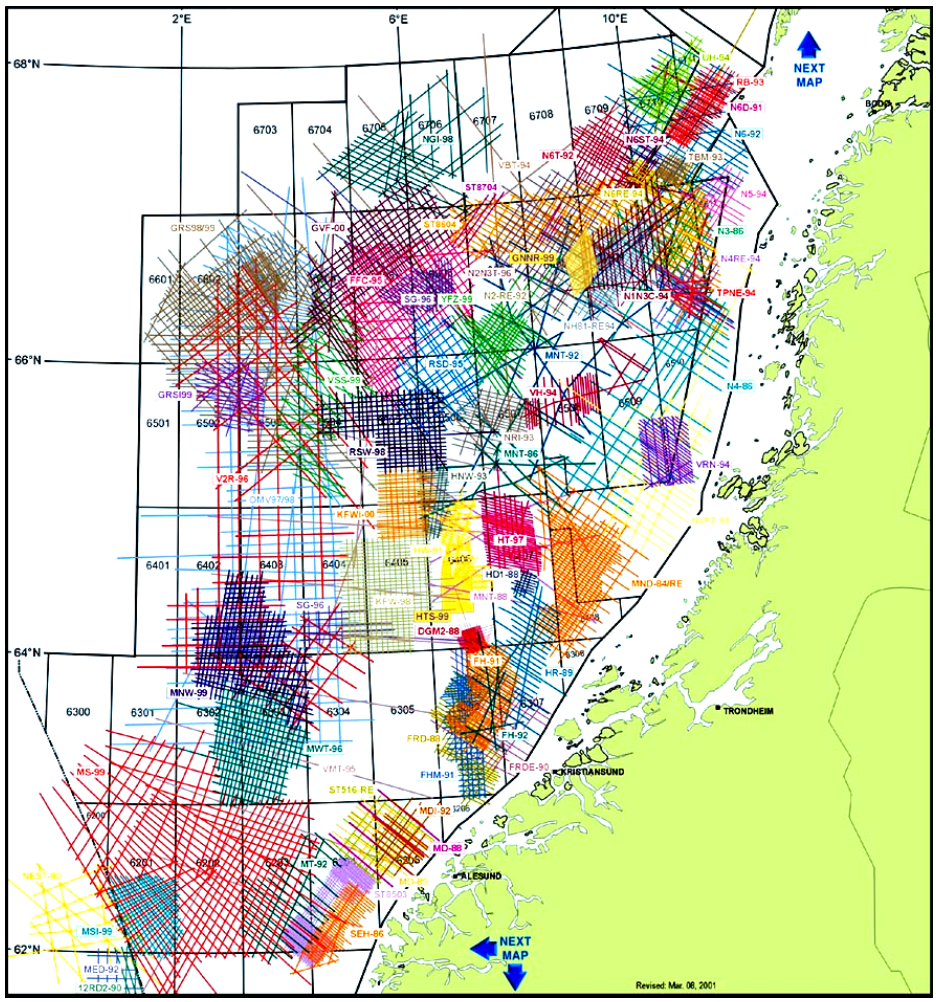

- Typically 2-D seismic data are collected as grids, the size and orientation of which are a function of variables such as the size of the structural or stratigraphic targets, the anticipated structural grain, and money available.
  - Multiple vintages of 2-D lines might be available from a particular area. Each might have different acquisition and processing parameters, and it can take considerable effort (e.g., adjusting amplitudes, frequencies, phase, static shifts) to make sure that all lines tie in a particular area (grid balancing).

2-D Seismic Data – Example

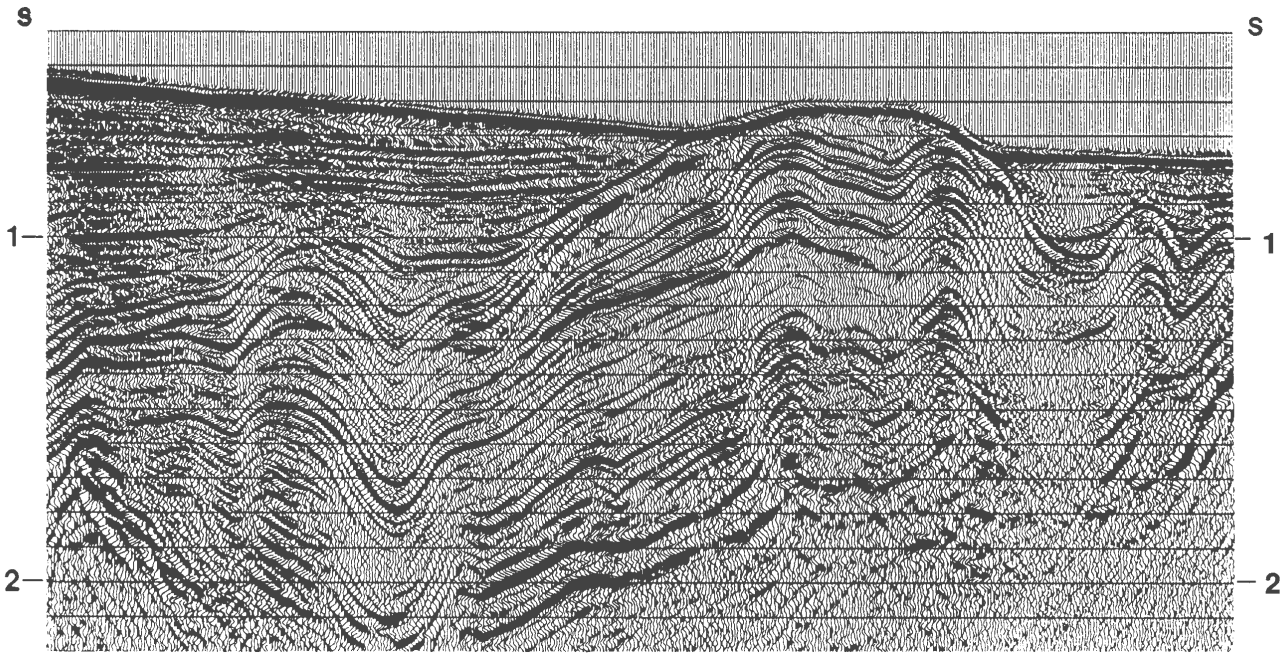

- The result of collecting 2-D seismic data is something that resembles (but isn't!!!) a geological cross-section through the earth.
- Our objectives might include definition of stratigraphic and/or structural features that are hydrocarbon reservoirs. To get there, we might need to use our knowledge of structural or sedimentary geology to reconstruct the geological history of the section being studied.

2-D Seismic Data – Uses

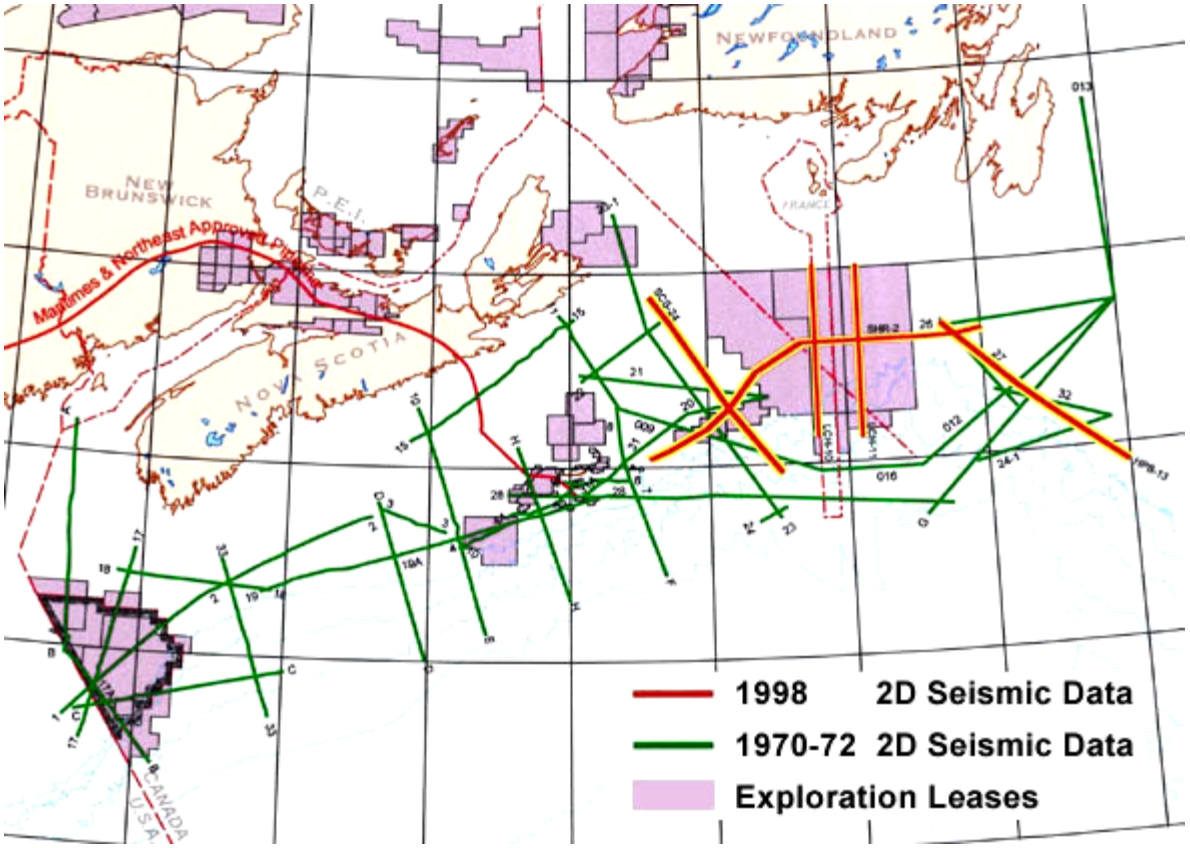

- Although most seismic data collected nowadays is 3-D, there is still a need to collect and interpret 2-D lines.
- Some cases where 2-D data may be encountered are:
  - Frontier (including many international) areas – where the objective is to cover large areas and define the “big picture”
  - Old pools – where 2-D data were collected prior to application of 3-D methods
  - Difficult terrain or other areas where logistical difficulties make collection of 3-D datasets economically unfeasible.
- Typically work with grids of 2-D lines of different vintages.

2-D Seismic Data – Pitfalls - Sideswipe

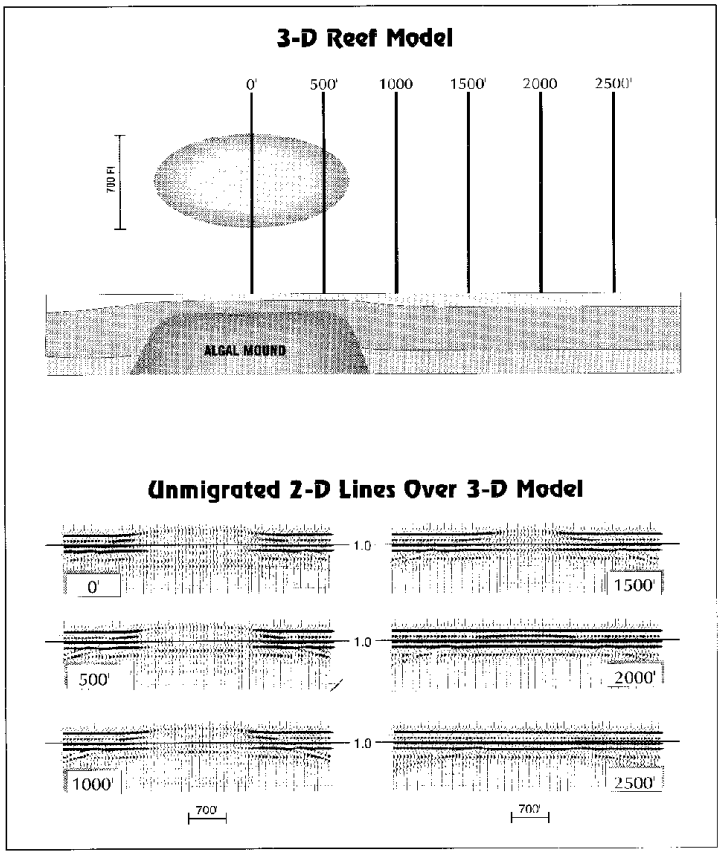

- One of the biggest pitfalls of 2-D data is that acoustic energy does not simply follow 2-D raypaths such as those shown previously. Sound expands out in 3-D in the subsurface. As such, geological bodies located off to the side of the line may be imaged ("sideswipe").
- The image shown above illustrates this point. The upper part of the figure shows a map view (top) and transect (below) through a geological model of a carbonate buildup. The locations of six 2-D seismic lines are also shown; the lower images show these seismic profiles. Note that the carbonate buildup is imaged, even on lines that do not cross the feature (e.g., 1500').

2-D Seismic Data – Pitfalls – Joining the Dots

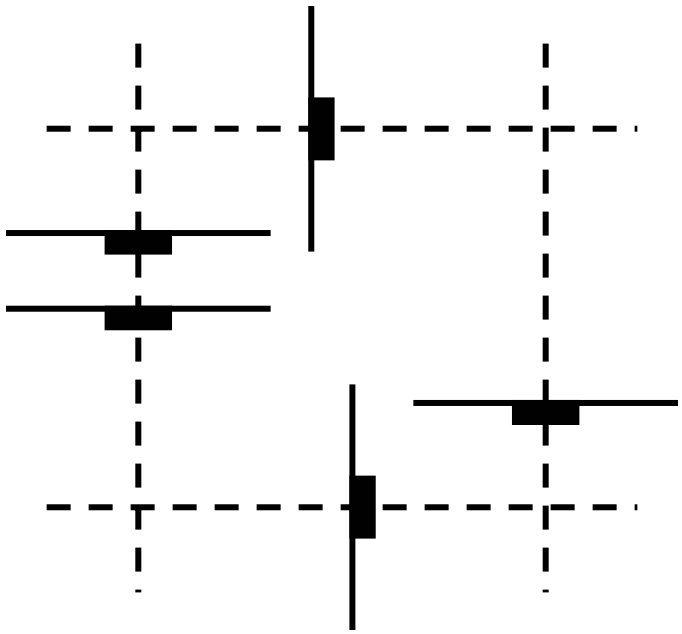

- Another problem when working with 2-D data is interpolating what happens between lines.
- For example, the illustration shown above shows a simple grid of four 2-D seismic lines (dashed) upon which the apparent senses of displacement on a series of normal faults are identified. How many different ways might it be possible to correlate the faults?
- The same type of problem may be encountered when working with other structural or stratigraphic features
- The limitations of 2-D seismic have been known for many years. Although some groups (e.g., Humble Oil) began investigating 3-D methods in the 1960s it was not until the 1970s that 3-D methods became commercially available.

3-D Seismic Characteristics

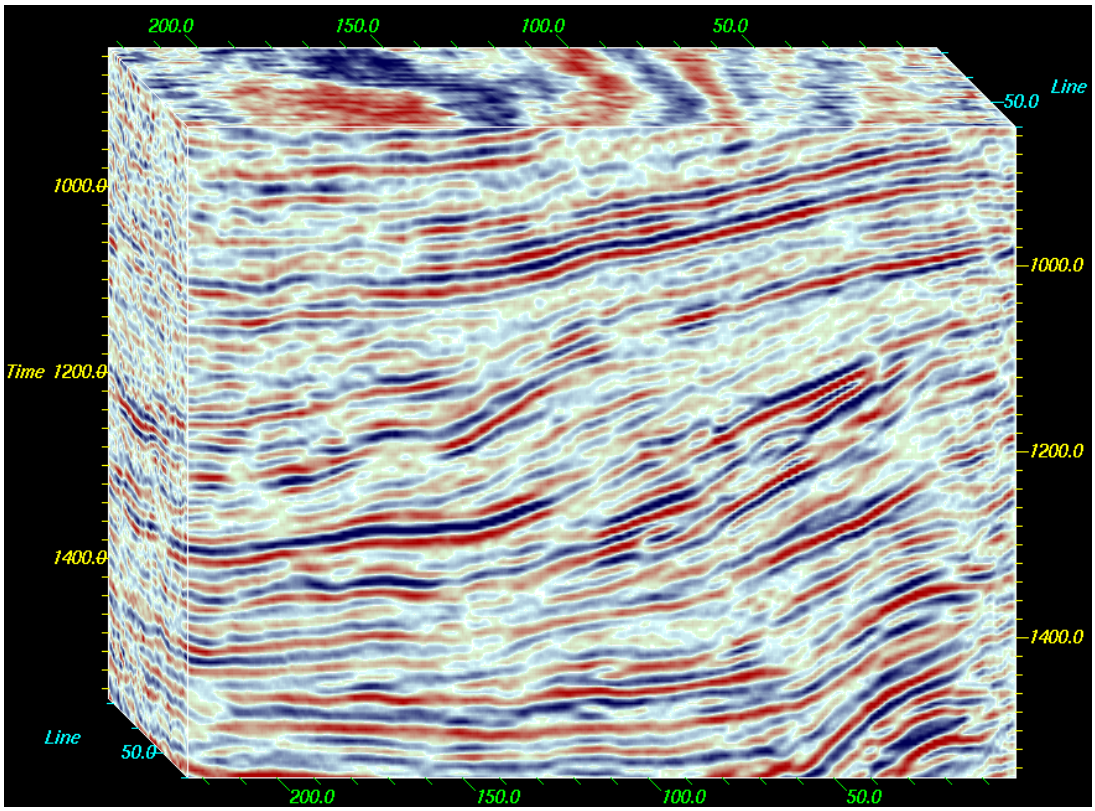

- Data volume stored digitally on a computer.
  - Interpretations also stored in digital format
- Complete coverage of a subsurface area
  - Lateral resolution (LR) defined by:

$$LR = \text{Max}[F_D, 3\text{Bin}]$$

- Geometrically accurate image, sideswipe eliminated
  - Need accurate velocity model for migration, otherwise image may not be accurate
  - Statics/velocity problems may still be present

Viewing 3-D Seismic Data

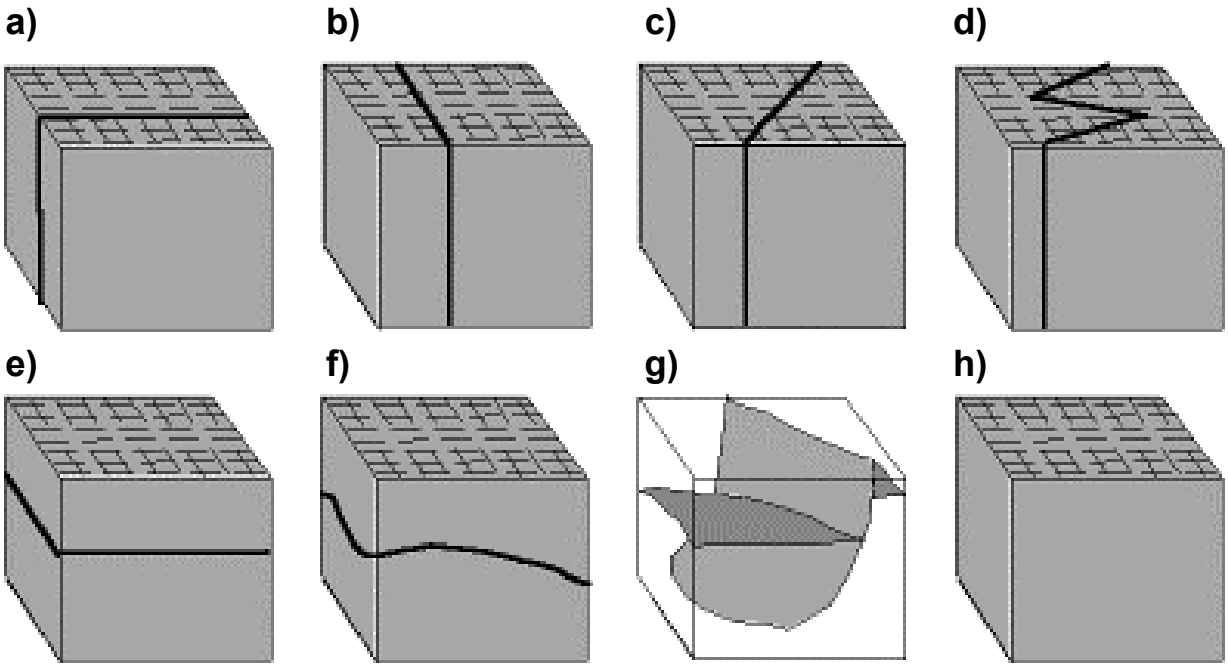

- Computer software allows 3-D data volume to be viewed from a variety of perspectives.
  - a) Line (“Inline”)
  - b) Trace (“crossline”)
  - c) d) Arbitrary Lines
  - e) Timeslice
  - f) horizon slice (“amplitude map”), stratal slice
  - g) Visualizations of interpretations (horizons, faults)
  - h) Cube, Voxel displays
- Learn how to use these views together, rather than alone, to help you with your interpretations.

Viewing 3-D Seismic Data– Vertical Transects - General

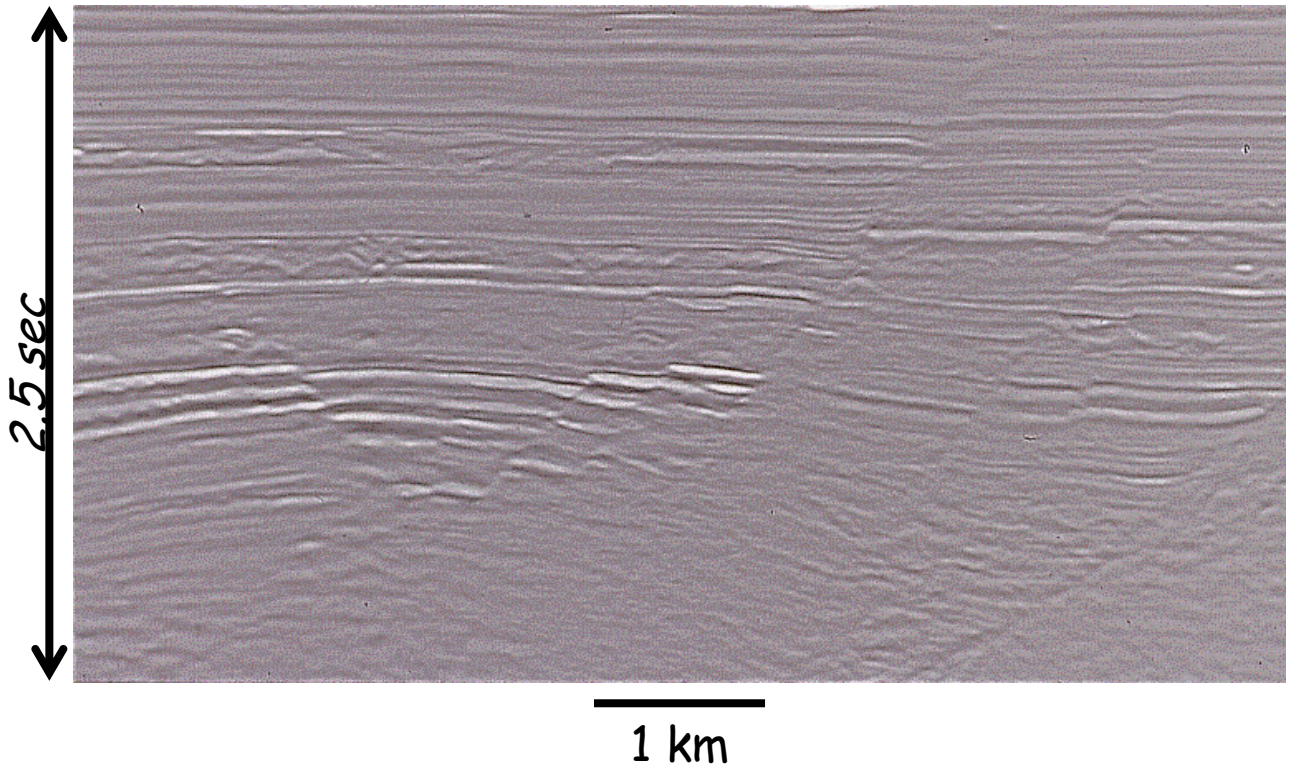

- 3-D seismic data may be viewed as lines (a.k.a. inlines) or traces (a.k.a. crosslines) or arbitrary lines cutting through the data volume. These transects look like 2-D seismic transects. One major advantage is that arbitrary lines may be viewed at any angle chosen by the interpreter. With 2-D lines the interpreter is constrained to view the data in the orientation that they were acquired. Another major advantage is that 3-D data have had 3-D migration applied.

Viewing Digital Seismic Data– Vertical Transects – Zooming in/out

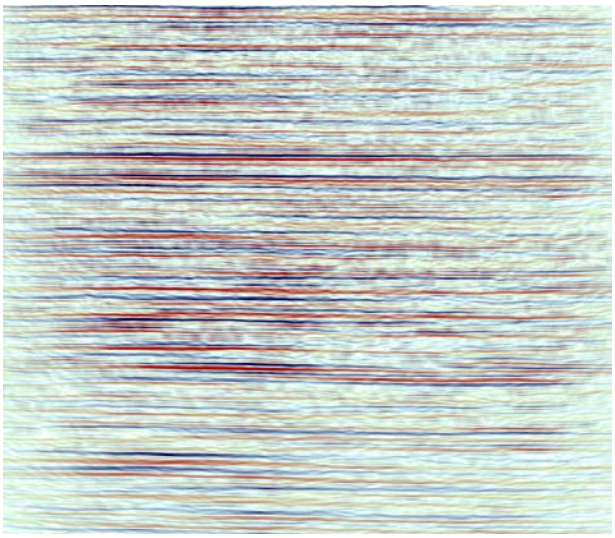

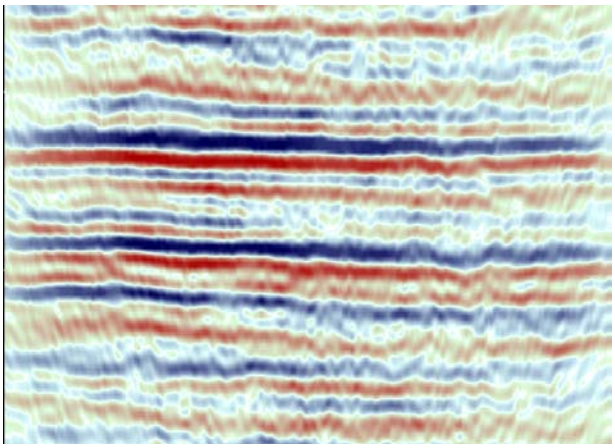

- Because the data are stored in digital format, the interpreter may chose to see as little or as much data as he/she sees fit. One might “zoom out” to look at the big-scale structural and stratigraphic setting, then “zoom in” to look at fine-scale stratigraphic/structural details.
  - Upper image shows 1.5 seconds of data and is ~ 4 miles long
  - Lower image shows same length of line, but zooms in on 150 ms in upper 1/3 of section
- Technique may be applied to viewing digital 2-D data as well.

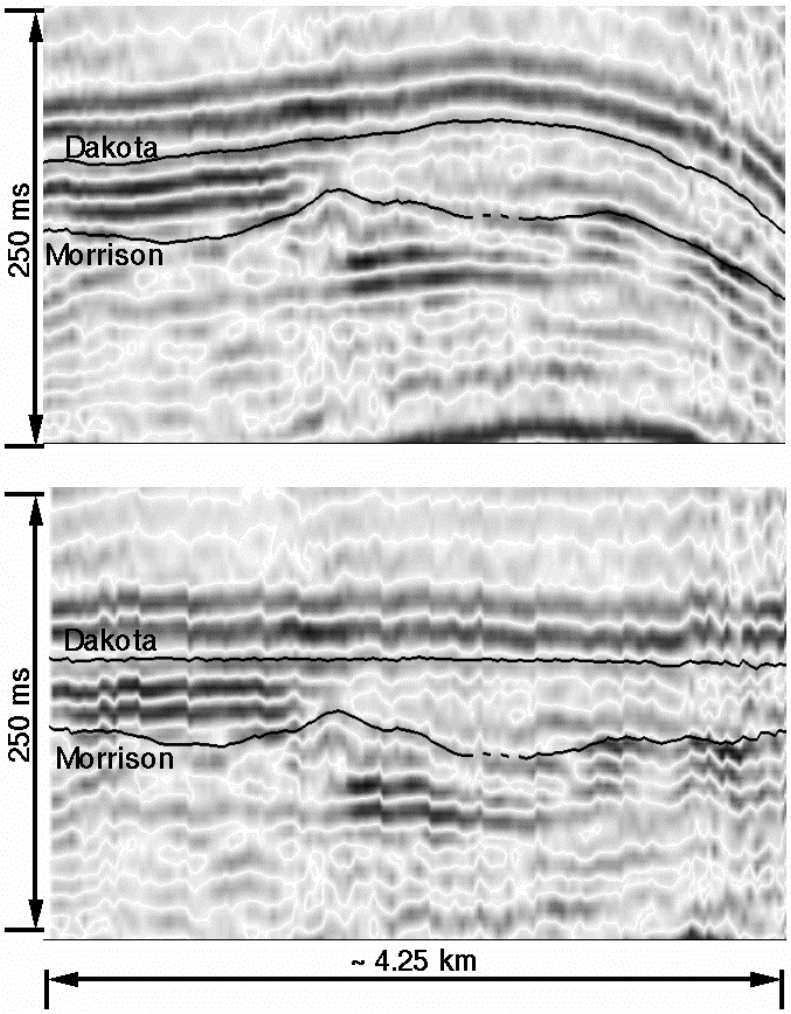

- Flattening seismic sections on horizons may be a useful technique for viewing features such as unconformities that have been structurally deformed. A horizon is picked in the seismic data and then all the traces are shifted vertically until the horizon pick is horizontal. The technique is similar to the way that geologists construct stratigraphic cross-sections using well logs. In that approach, the cross-section is constructed such that the logs are aligned with one of the log markers being horizontal. The original seismic image, prior to flattening, can be considered as being equivalent to a structural log cross-section.

- The image at top shows a transect through a 3-D seismic volume. The Dakota Formation is a Cretaceous unit in western North America that produces gas and oil in various places. It unonformably overlies the Jurassic Morrison Formation. The stratigraphy has been folded in this area. The lower image shows the same image flattened on the top of the Dakota. Note the improved image of the relief on the unconformity.

- Make sure that the surface you flatten on was originally a horizontal surface. The flooding surface at the top of the Dakota is a good choice, the unconformity would be a bad choice for flattening. Also, watch out for geometric pitfalls – the software applies a bulk shift to the traces, it does not unfold the stratigraphy.

Viewing 3-D Seismic Data – Timeslices

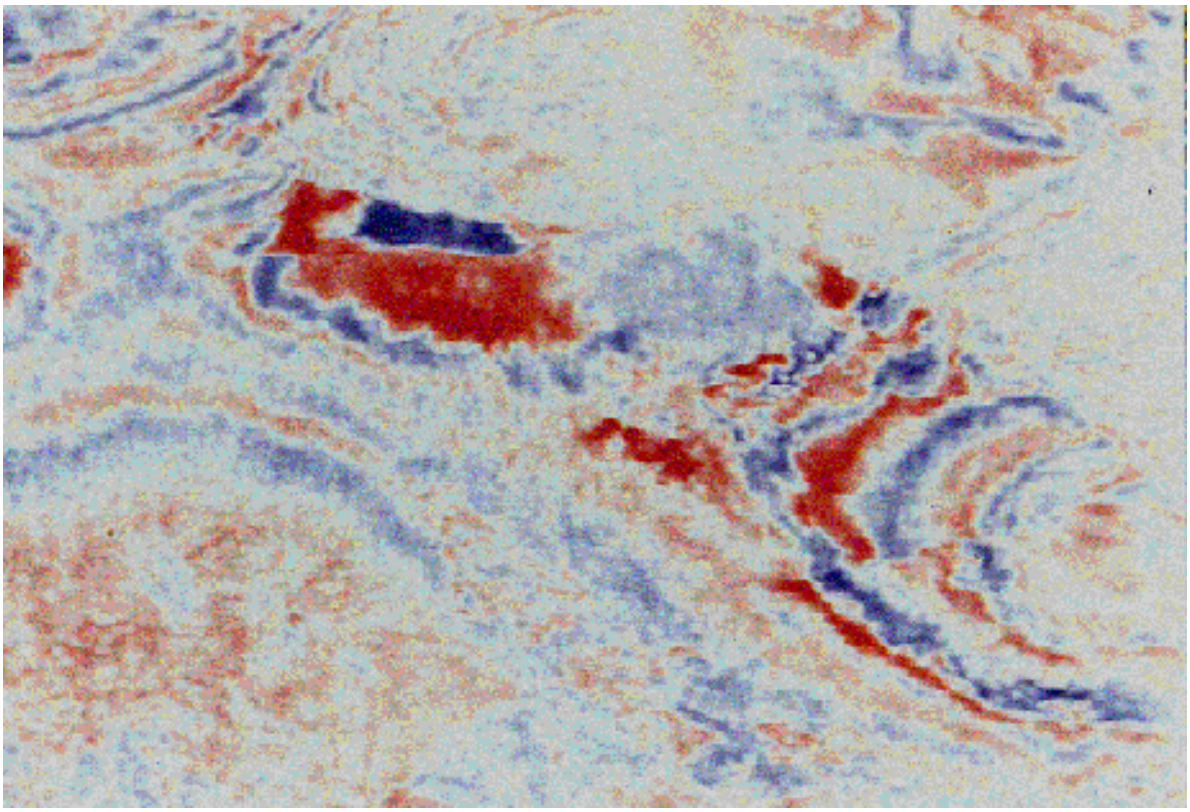

- Timeslices represent planes of constant two-way traveltime through the 3-D volume. They can be very useful for defining structural and stratigraphic features.
  - Recognize faults using offsets of reflections, changes in character, etc.
- Use timeslices in conjunction with vertical transects, not alone.

Viewing 3-D Seismic Data – Timeslices

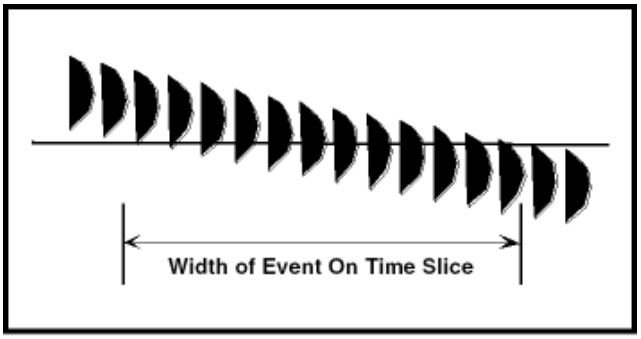

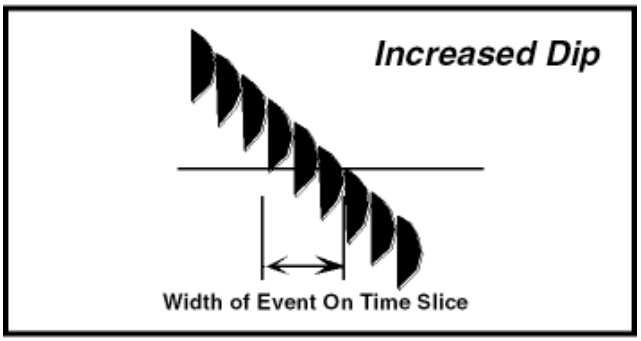

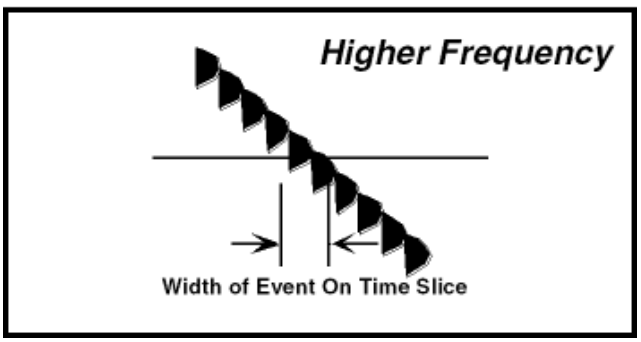

- The width of an event on a timeslice is a function of two variables:
  - Stratal dip
  - Frequency of the event

Viewing 3-D Seismic Data – Timeslices

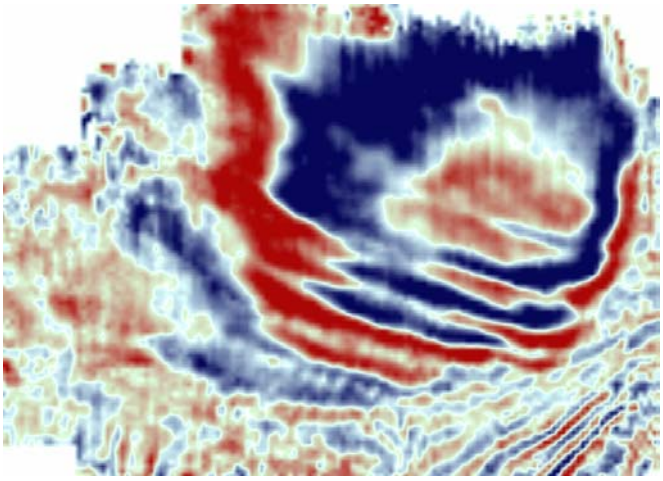

- Timeslices through coherency volumes are very helpful for mapping faults
  - The upper image shows a timeslice through an amplitude volume. Some faults are visible
  - The lower image shows the same timeslice through a coherency (“continuity”) volume. It is much easier to identify the faults.

Viewing 3-D Seismic Data – Horizon Slices

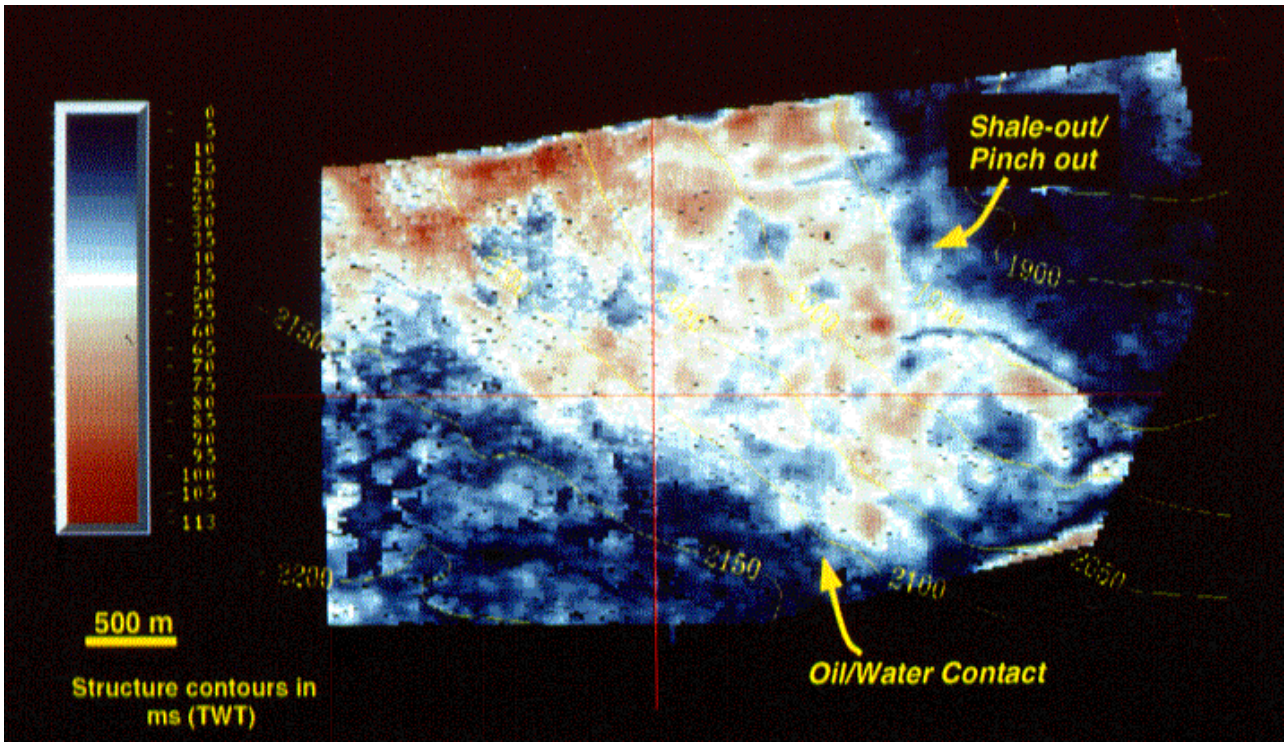

- Horizon slices show how amplitudes vary along horizons that have been picked in 3-D data volumes. This is one of the unique capabilities of working with 3-D data.
  - Sometimes known as “amplitude maps”
- Image above shows variations in amplitude along a Pleistocene sand from the Offshore Gulf of Mexico. High amplitudes shown in red. Mapping (using well logs) allowed interpreter to identify up-dip limit of bright amplitudes (to right) as a shale-out, and lower limit of bright amplitudes (to left) as an oil/water contact. Notice how lower limit of bright spot is approximately parallel to structural contours (yellow), helping to confirm it as a fluid contact.

Amplitudes as Direct Hydrocarbon Indicators (DHI) – A Digression

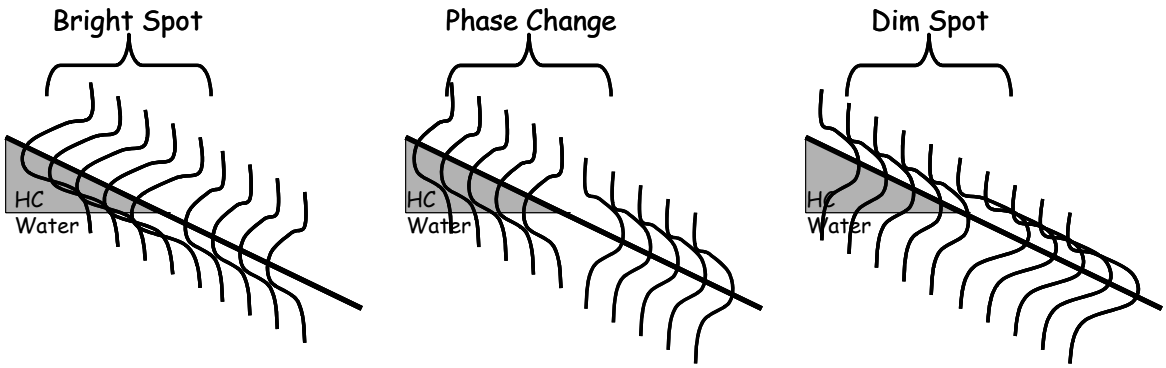

- There are three general cases for using amplitudes as direct hydrocarbon indicators (DHIs):
  - In some areas, such as the Offshore Gulf of Mexico or other "young" clastic successions, water-filled reservoir sands are slower and less dense than the surrounding shales. When hydrocarbons (gas, or "live" oil) fill the pore spaces, the sands become even slower and less dense than the surrounding shales and, accordingly, the reflection amplitude increases (above, left). These are "bright spots" such as those shown on the previous page.
  - In other areas, wet sandstones are slightly faster/denser than the surrounding shales, yielding a positive reflection coefficient. When hydrocarbons are in the sands, they become slower/less dense than the surrounding shales, yielding a negative reflection coefficient. The result is that the polarity of the reflection changes at the fluid contact, yielding a phase change (above, center).
  - Finally, in "old" rocks, a strong positive reflection coefficient may be present at the top of a wet, porous unit. When the unit is charged, the reflection coefficient stays positive, but is reduced somewhat (above, right). This is a "dim spot".
- Use petrophysical modeling (porosity, saturation, fluid properties, etc.) to determine whether an amplitude effect might be observed.

Viewing 3-D Seismic Data – Horizon Slices

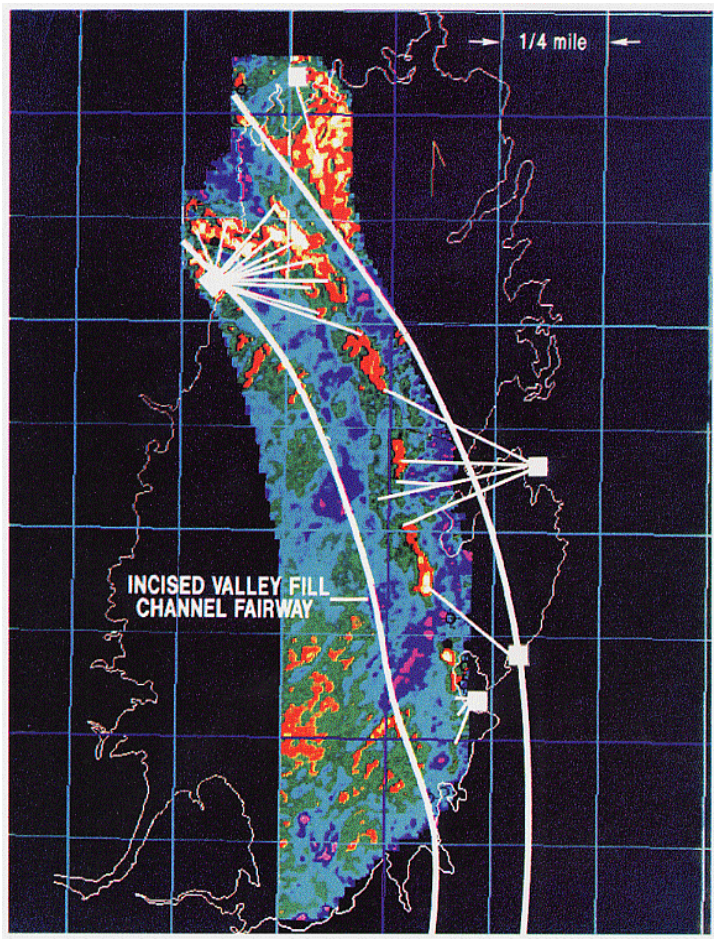

- Amplitudes on horizon slices do not always show hydrocarbon effects. Physical properties (porosity, lithology, etc.), thickness (tuning) and acquisition parameters (e.g., fold) may also affect amplitudes. Seismic- and petrophysical modeling may help to identify these controls.
- Image above shows amplitude variations along a Cretaceous horizon from the Alberta Basin. High amplitudes (red/whites) in this image show location of clean (charged) fluvial sandstones within an incised valley.

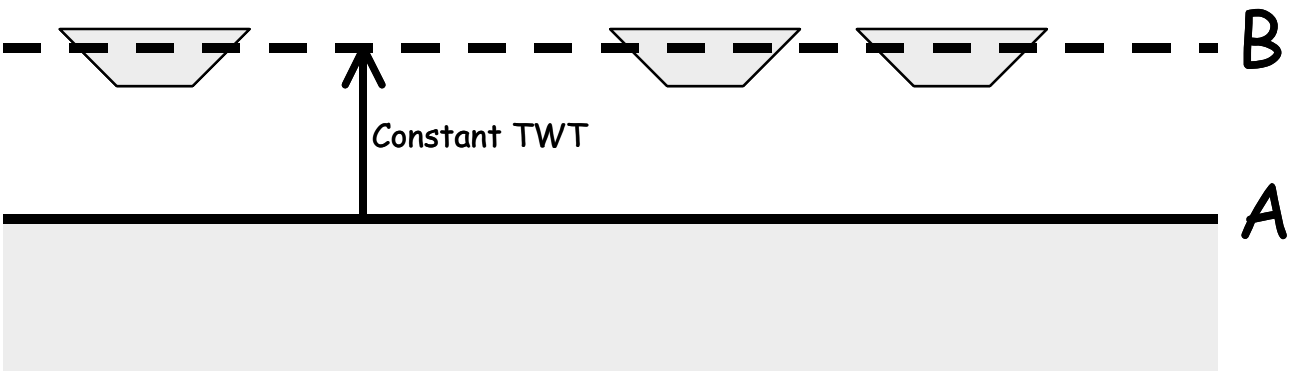

Stratal slicing is an approach for examining discontinuous stratigraphic features that are associated with levels that cannot be mapped directly in the seismic data. The illustration shown above shows why this might be necessary. A series of sand-filled channels might be present at a particular stratigraphic level in an otherwise shaley succession. No continuous seismic reflection is present at this level because there is no consistent change in acoustic impedance.

To “find” this horizon, the interpreter picks a nearby reflection (e.g., “A”) that corresponds to a continuous horizon. A horizon “B” is then generated by subtracting a constant amount of time from the original horizon. The interpreter can then see how seismic amplitudes change along the new horizon. Note that, if desired, a horizon could be generated below the original pick by adding a constant TWT to that horizon.

The technique works best when the stratigraphy is parallel. This is most likely to be the case when subsidence was constant in an area and there are no unconformities between the original horizon and the stratigraphic level that is being sought.

The images below show a comparison of a conventional timeslice (left) and a stratal slice for imaging a tidal channel in an slightly dipping area. Note the better definition in the stratal slice.

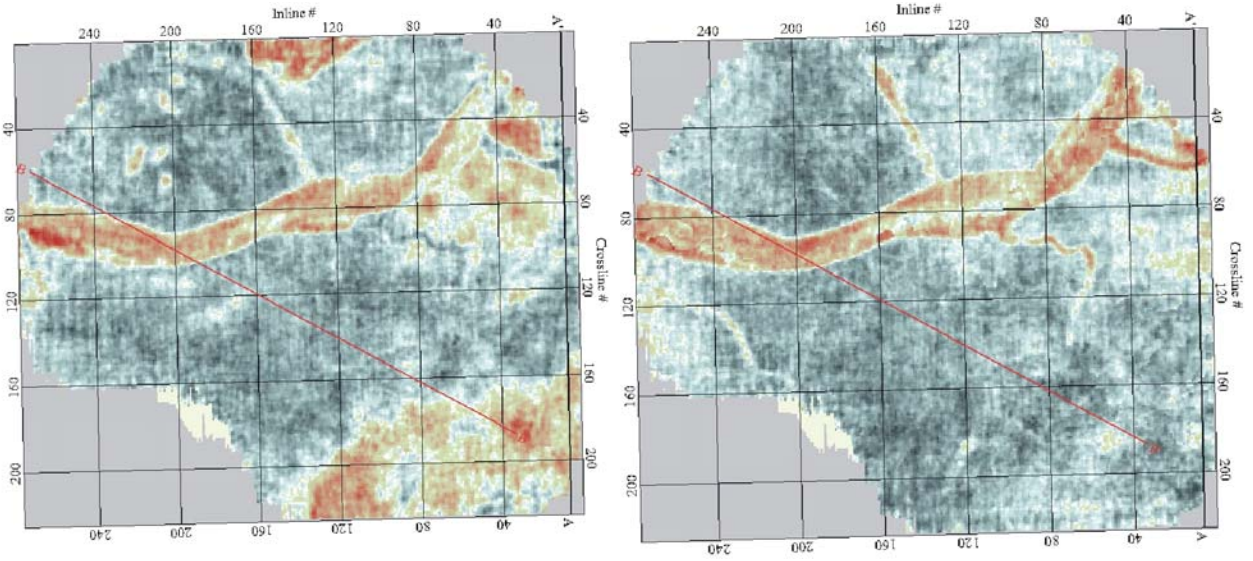

Viewing 3-D Seismic Data – Stratal Slices

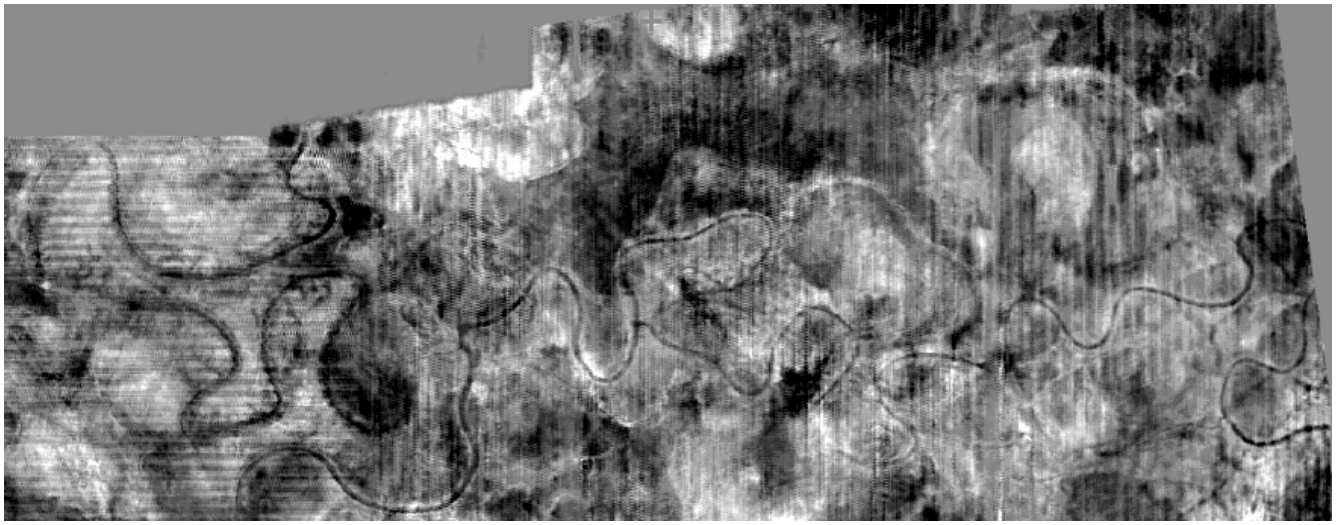

Henry Posamentier

- This stratal slice shows meandering fluvial channels

Viewing 3-D Seismic Data – Map Views of Interpretations

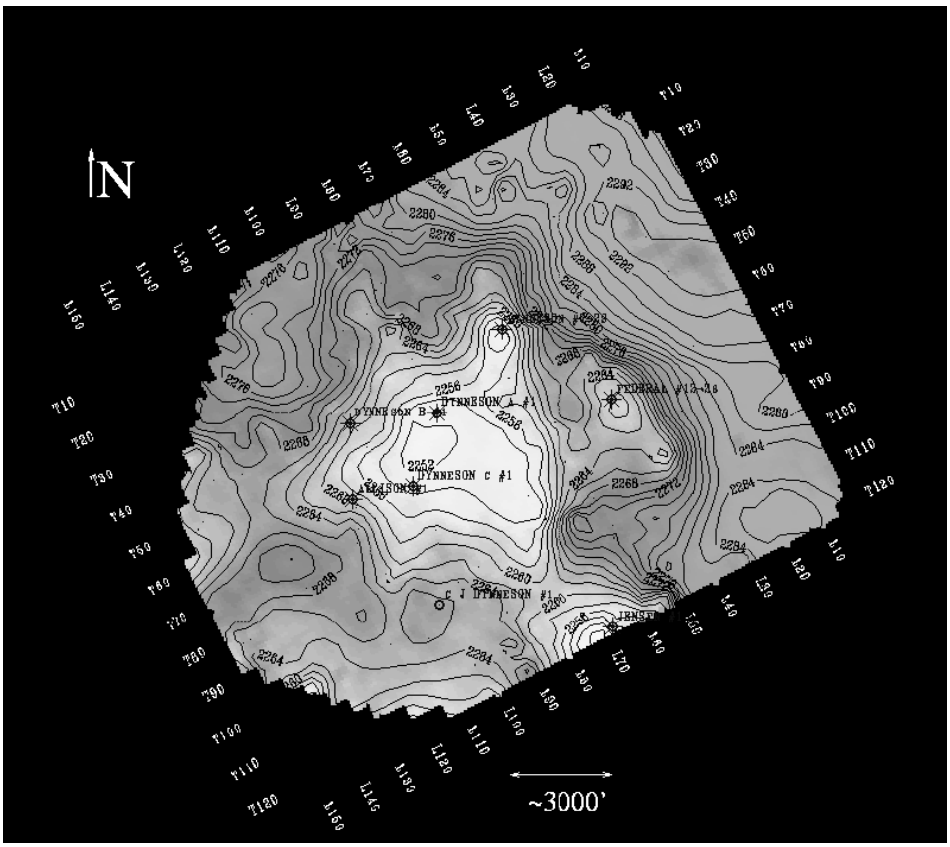

- The traditional way of viewing seismic interpretations has been to generate maps (time-structure maps, isochron maps, amplitude maps, etc.).
- Working with 3-D seismic data in digital form allows the interpreter to quickly produce, modify and update these maps.
- Image above shows a time-structure map of an Ordovician Red River field from the Williston Basin. It shows the Line and Trace grid, a scale bar, a North arrow and well locations. Ideally it would show other cultural data such as Section, Township and Range, roads, rivers, etc.

Viewing 3-D Seismic Data – Map Views of Interpretations

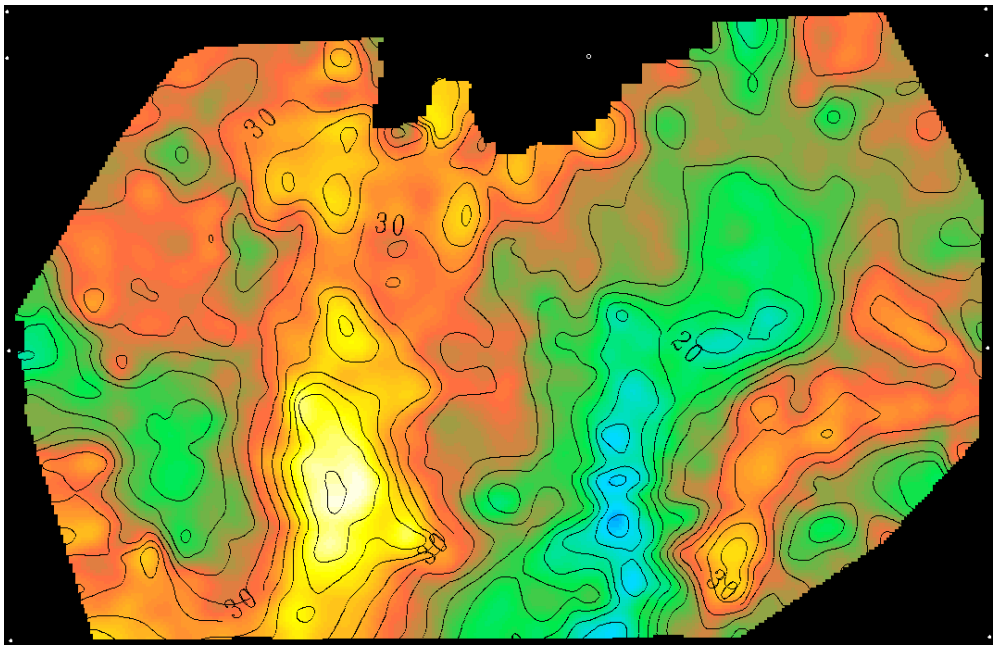

- This image shows a contoured isochron map (in ms TWT) of a lowstand fan unit from the Permian Basin. Thick areas are in “hot” colors, helping the viewer to recognize them as potentially prospective areas.
  - Learn to use color judiciously to highlight features of interest.

Viewing 3-D Seismic Data – Map Views of Interpretations

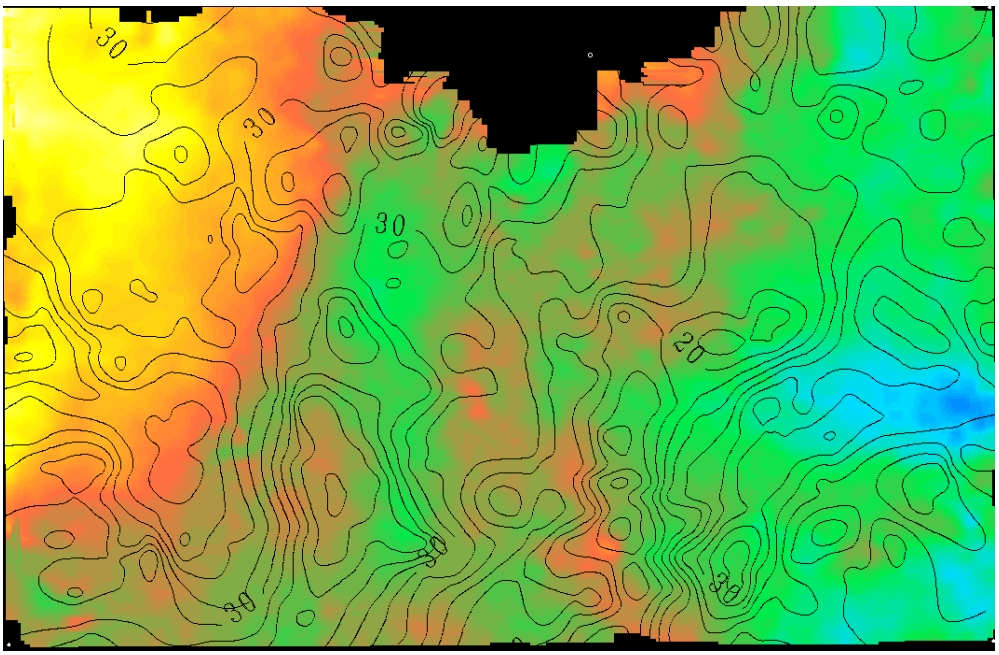

- Maps may be used to combine information from two different horizons. This map shows the isochron contours from the previous slide superimposed on a color background showing the time-structure of an underlying unit (yellow = structurally high areas, blue = structurally low areas). The objective was to see whether pre-existing structures affected deposition. Do you think that they did? Why?

Viewing 3-D Seismic Data – Visualizing Your Interpretations

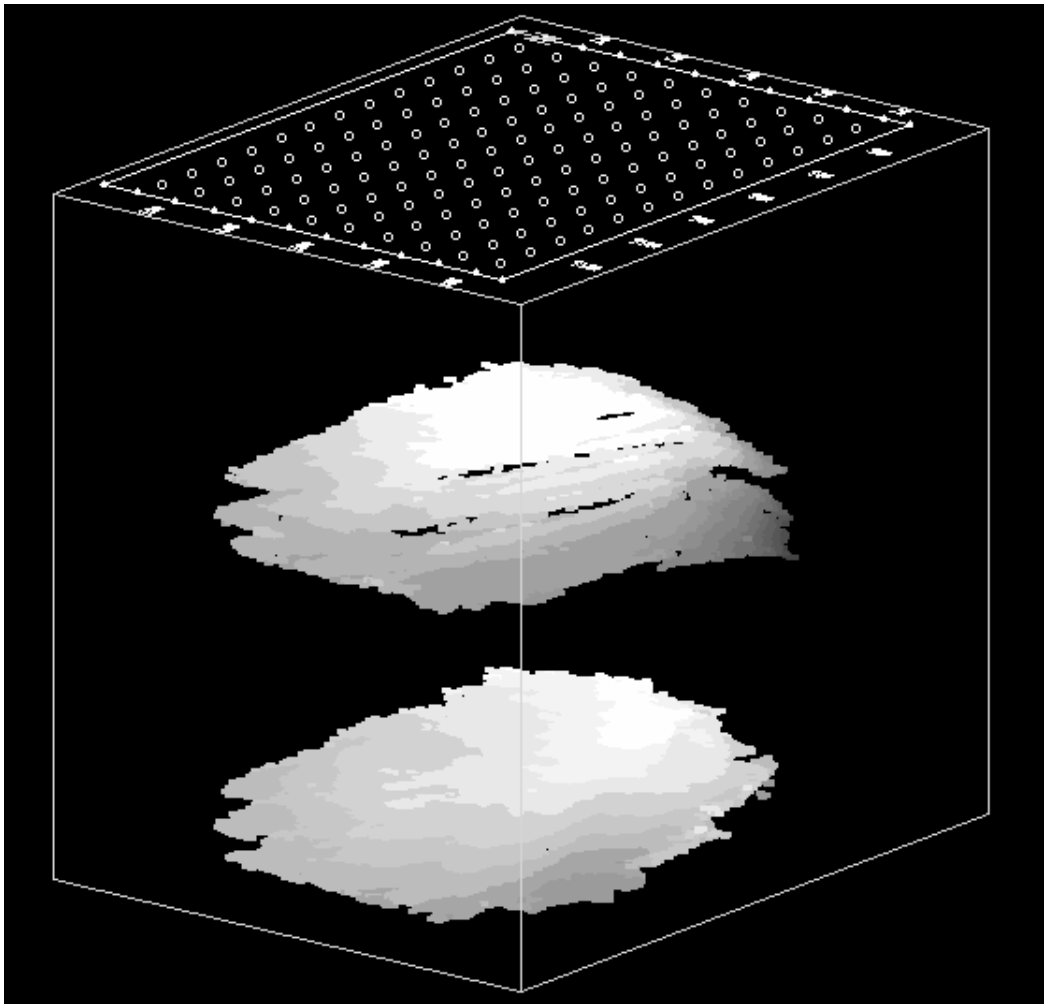

- Different software applications have different capabilities. This “perspective view” (from Landmark) shows a simple representation of the structure at two different stratigraphic levels. Compare the image of the upper level here with the following slide.

Viewing 3-D Seismic Data – Visualizing Your Interpretations

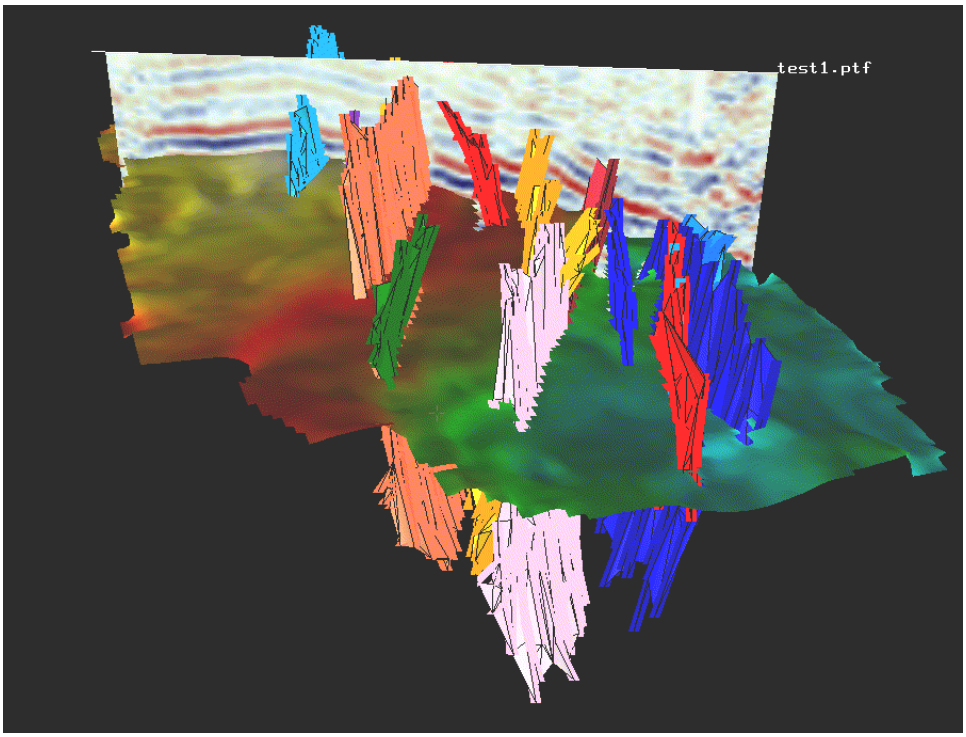

- This display shows the upper horizon from the previous slide with faults and a slice through the 3-D volume. Which image helps you to understand the structure better?
- This type of view is very useful for:
  - Performing QC on structural interpretations (e.g., do faults do physically impossible things?)
  - Presenting results to co-workers, partners or management (i.e., people who may not have been involved in the interpretation but need to quickly grasp the results of the interpretation).

Viewing 3-D Seismic Data – Cube/Voxel Displays

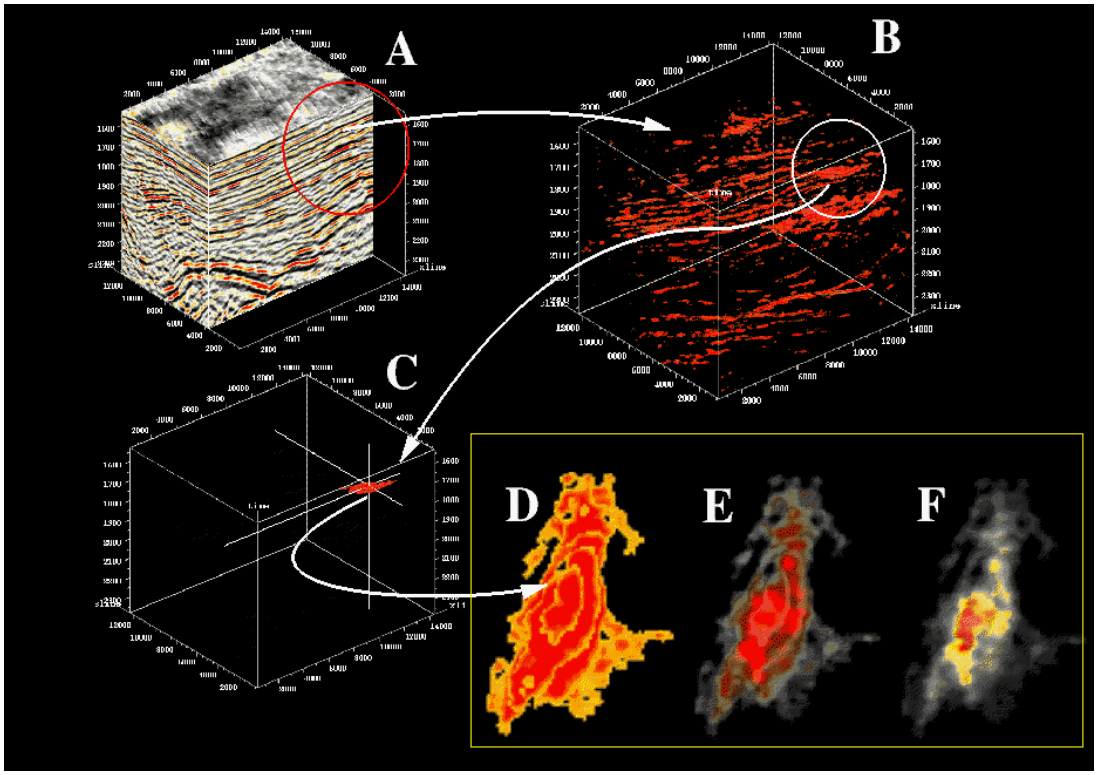

Paradigm Geophysical

- Scrolling through a 3-D seismic cube can be a very useful exercise, especially in the early stages of an interpretation.
- In some areas, we might be interested in looking at the 3-D distribution of amplitudes and, in this case, the cube visualization becomes a problem – we can only see three faces of the cube.
- Volume rendering allows the interpreter to preferentially turn on/off voxels containing selected amplitude ranges (by varying their opacity). This allows him/her to directly see the 3-D distribution of those areas.

Viewing 3-D Seismic Data – Voxel Displays

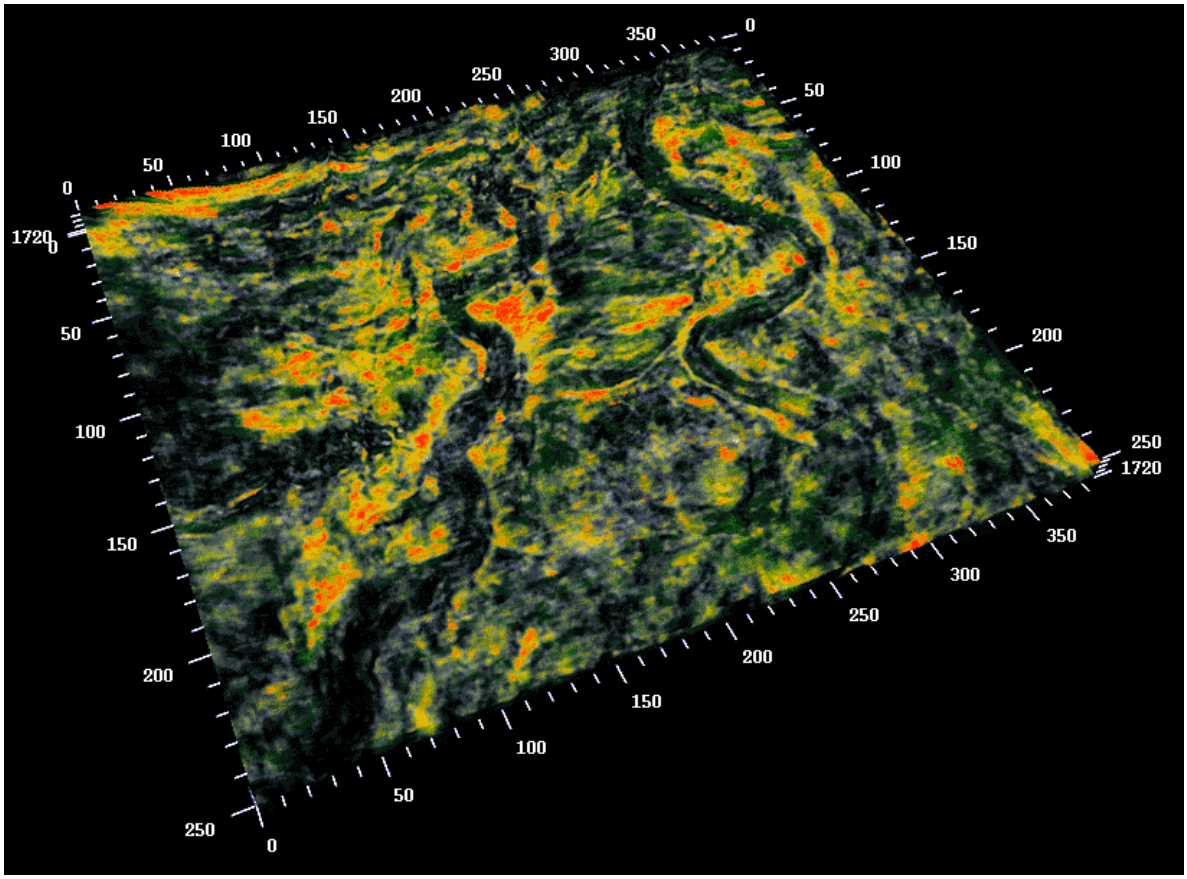

Paradigm Geophysical

- Volume rendering can help to bring out important stratigraphic and structural features (if they exist!).
- This image shows two, probably mud-filled, meandering channel systems.
- It takes a good deal of skill (color bar manipulation, volume rendering, etc.) to extract these types of images from seismic data (if they exist in the data!).

Viewing 3-D Seismic Data – Voxel Displays

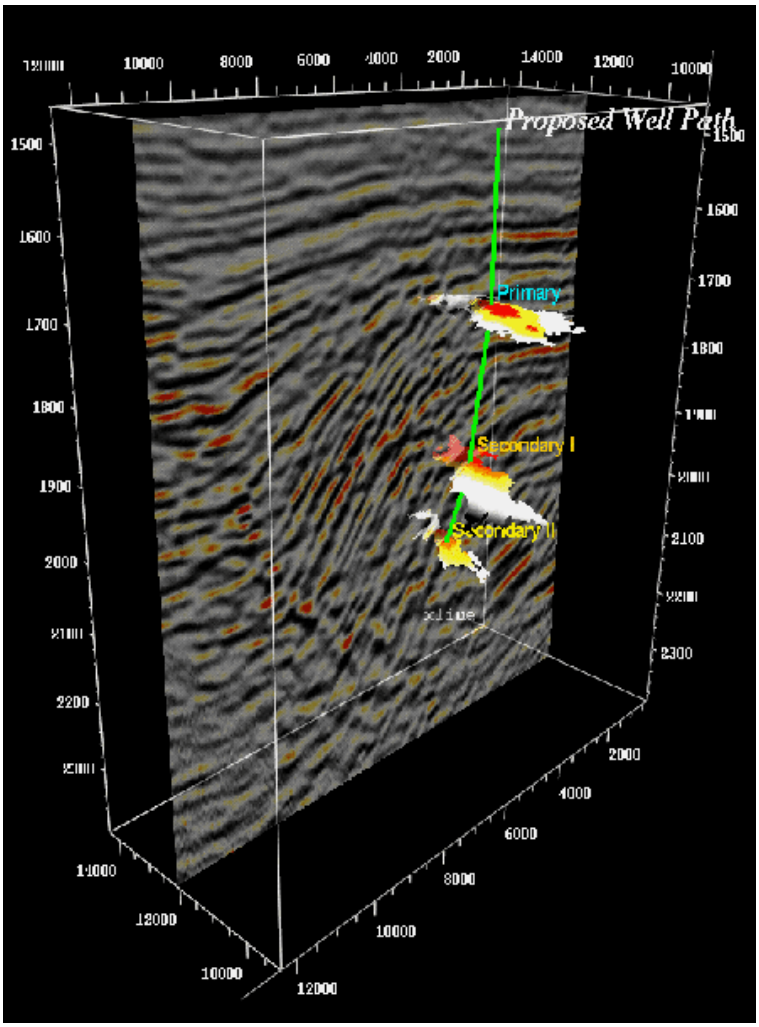

Landmark Graphics Corporation

- Voxel displays may be used to help plan wellbore trajectories.
- This image shows how a proposed well will target three high-amplitude regions at different stratigraphic levels.

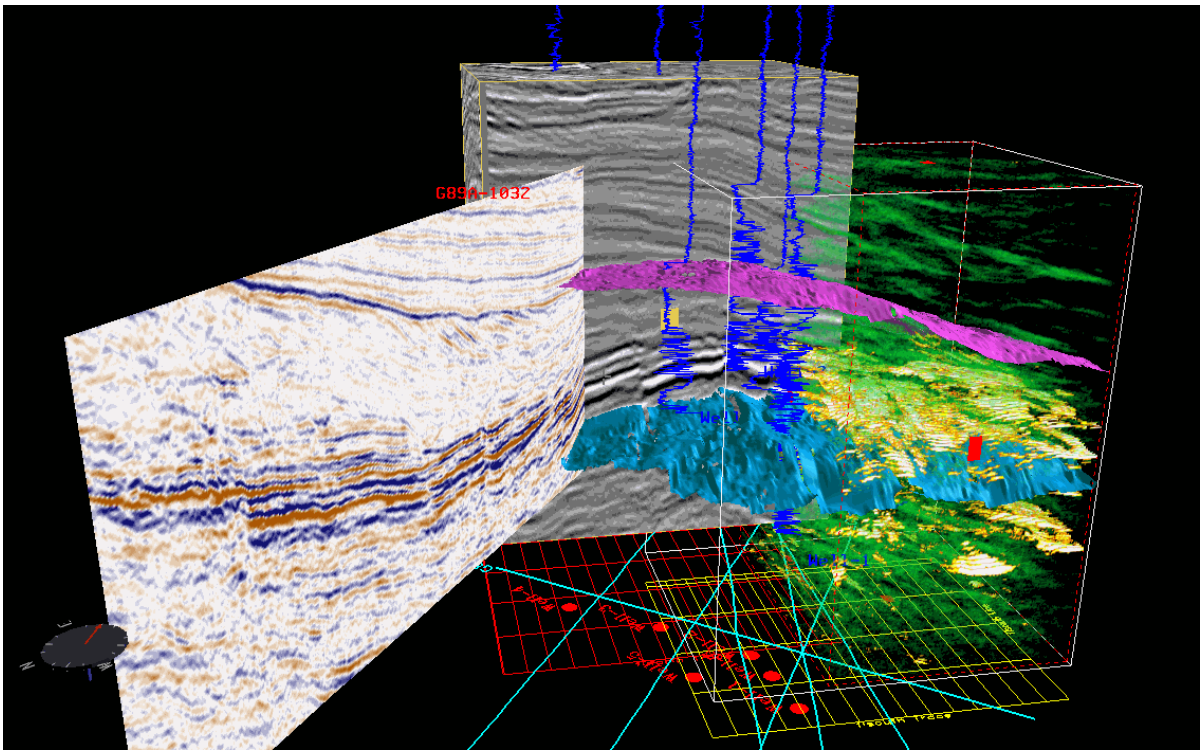

- Advanced seismic interpretation packages allow multiple volumes, 2-D seismic lines and wireline logs to be examined at once.
- Co-rendering, below, allows multiple versions of seismic data to be viewed together. The example below shows a coherency version (greytones) and reflection strength (color) version of the same data volume co-rendered.

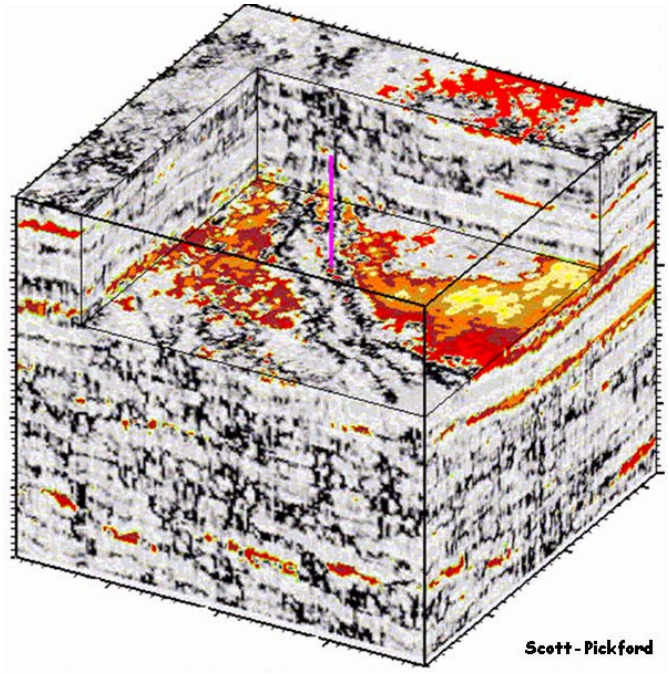

Use of Color

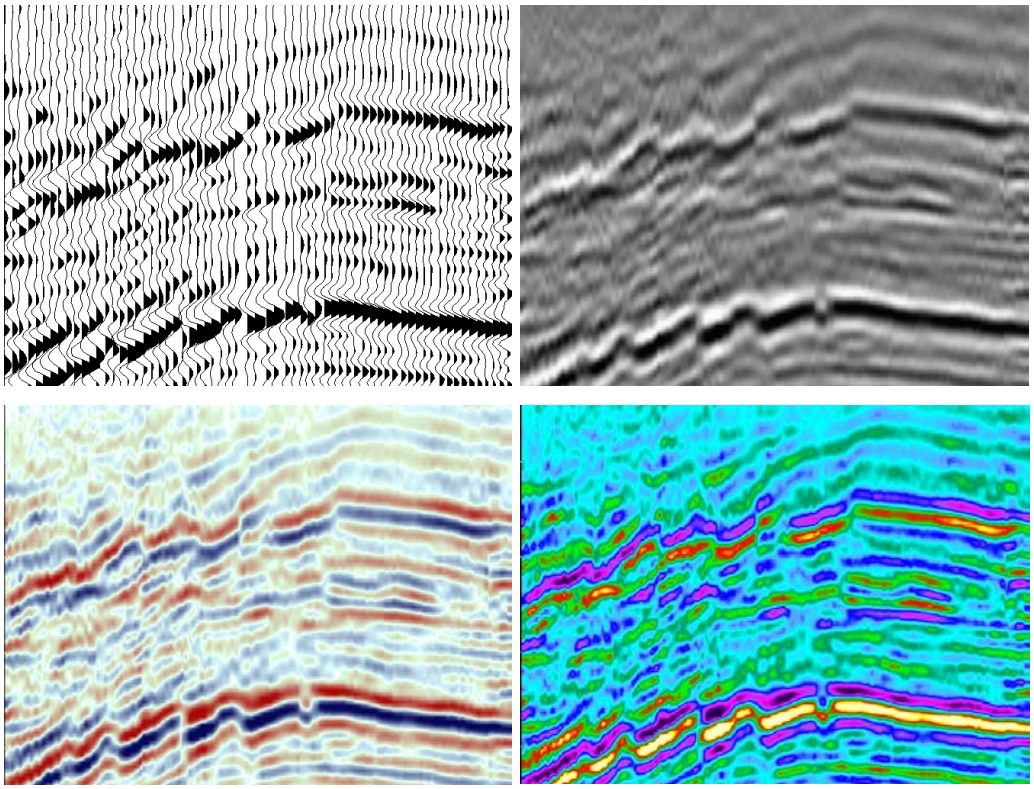

- Learn how to use color as an interpretive tool. Different color displays are better for different things. Interpreters need to learn to judiciously select, modify, and create their own color palettes.
- Image at upper left shows the traditional variable area wiggle display. Peaks are filled in black. The other three displays are variable density displays. The blue-white-red display is a “traditional” color bar, chosen to give approximately equal weight to peaks and troughs. The greytone color bar is best for picking faults. The rainbow (“spectrum”) color bar highlights amplitude changes.

Polarity

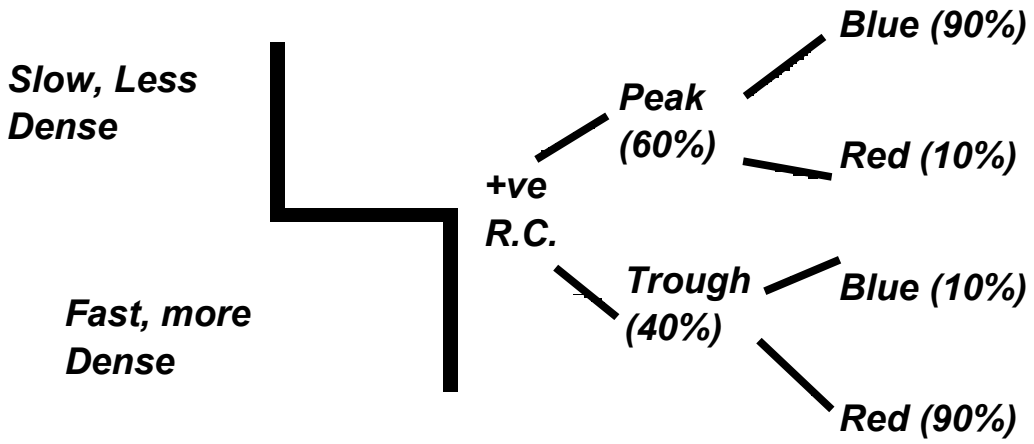

- Different interpreters use different polarity displays. This figure, from Brown, shows polarity conventions. Most interpreters, at least in North America, wish to have a positive reflection coefficient displayed as a peak in the seismic data. They call this “normal” polarity. Other interpreters call “normal” polarity showing positive reflection coefficients as troughs. As such, the term “normal polarity” can be ambiguous. To remove the ambiguity, simply ask whether a positive reflection coefficient will be displayed as a peak or a trough in the data.
- Peaks are typically shown as blue and troughs as red in the traditional blue-white-red color bar.

Color - Maps

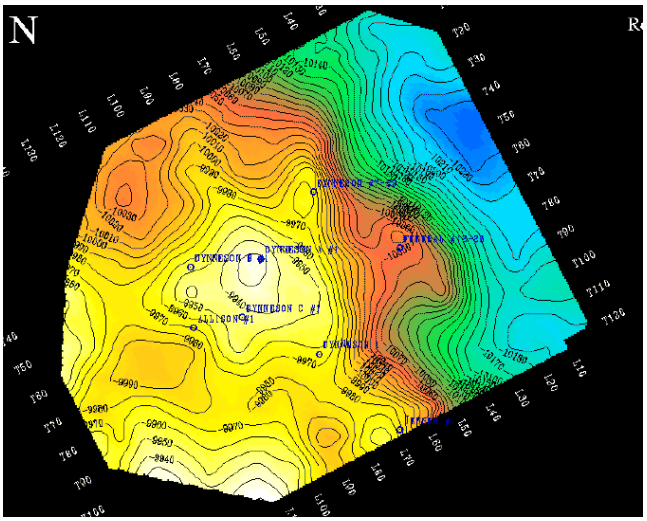

- Learn how to use color judiciously when working with map displays as well. As is the case when working with seismic transects, “bimodal” color bars may be useful for conveying some types of information, whereas gradational color bars are useful for other purposes.
- When working with structure maps, make the structurally high areas “hot” colors (white, yellow, red)
- The map above shows a small carbonate buildup with structurally high areas in yellow/white; they stand out.
- The map below shows structurally low areas in hot colors. These areas are not where the hydrocarbons will be!

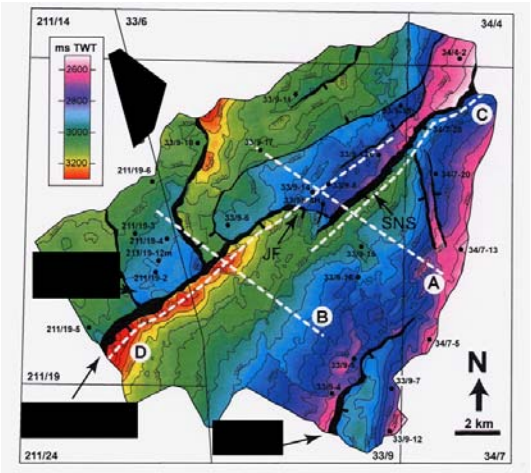

Project Preparation

If you don't know where you're going, chances are that you won't get there

- Several basic preparatory steps need to be undertaken before embarking on a seismic interpretation project:
  - Define the purpose of the project
  - Define the products – what will they be and who will use them (format?)
  - Build project database
    - What is needed?
    - What is available?
  - Understand acquisition and processing parameters – how might they affect the interpretability of the data?

Understand Your Purpose

- One of key ingredients for success when interpreting seismic data is having a clear understanding of the purpose of the interpretation
- Purpose is likely to change from project to project, or may change with time within any given project area
- Things to consider:
  - Regional study *vs* field-scale project
  - Play type (structural, stratigraphic)
  - Exploration or development (or mix?)
- Establishing a clear purpose up front will help to define:
  - How much time and effort to devote to specific aspects of the interpretation
  - What sorts of data and/or outside expertise should be brought in
  - What final products are expected

Structural & Stratigraphic Plays

- Distinction between structural and stratigraphic plays may simplistically be based on how laterally continuous potential reservoir rocks are
  - Structural: laterally continuous porosity and permeability, need structures to create traps
  - Stratigraphic: laterally discontinuous reservoirs due to primary depositional features (channels, etc.)
- Reality – most reservoirs have both stratigraphic and structural components
- Diagenesis may complicate things, needs consideration
  - Diagenetic plays (e.g., hydrothermal dolomites)
- Try to get a clear image of what potential targets should look like before interpreting
  - Published examples
  - Seismic modeling
  - Aerial photographs
  - Etc.

Structural Plays

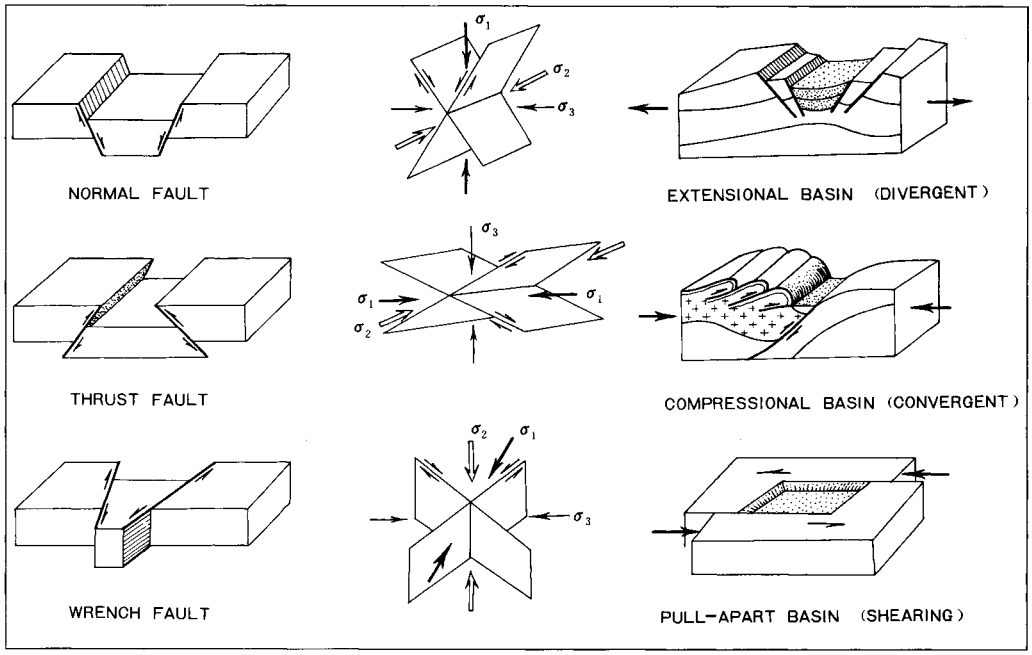

- What is broad-scale structural setting?
  - Extension
  - Compression
  - Wrench
- "Big picture" view helps to put constraints on the type of structures that are likely to have developed. This can guide the interpretation, including sub-seismically resolvable structures
  - Caveat: did structural setting change with time?
- Importance:
  - Juxtaposition of reservoir, barriers and baffles to flow
  - Migration pathways
  - Fractures in low permeability reservoirs

Stratigraphic Traps

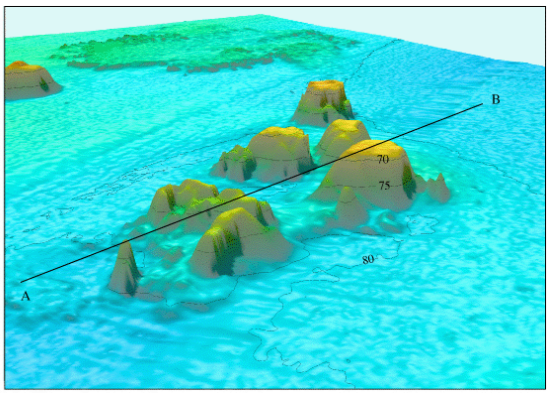

- Carbonate, clastic or mixed setting
- Hierarchy of scales:
  - Sedimentary structures to depositional sequences
  - Compartmentalization/heterogeneity may occur at all scales, not all scales may be resolvable seismically
- Some common elements include channels (fluvial, slope and basin-floor), clinoforms, reefs, etc.
- Knowledge gained through studying modern depositional environments is extremely useful
  - Image at left shows “modern” drowned pinnacle reefs at the edge of the Mississippi-Alabama continental shelf margin)
  - Image at right shows a small estuary in South Africa

Diagenetic Plays

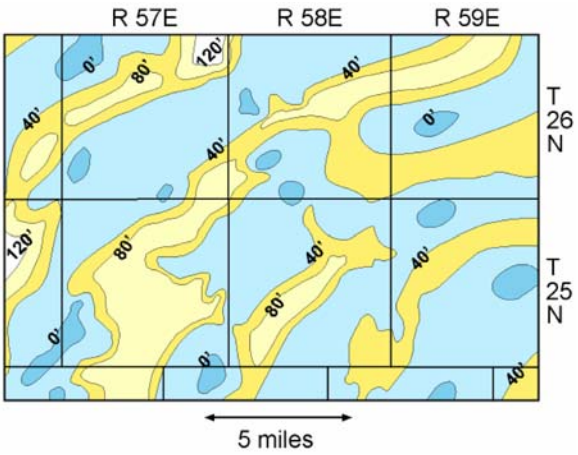

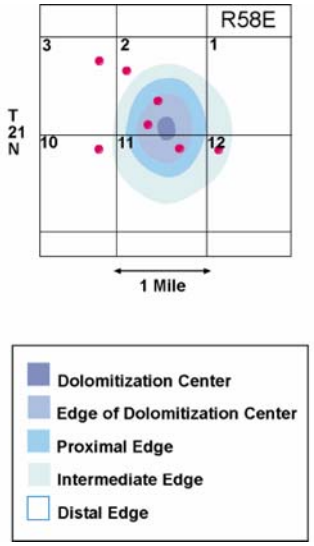

- You can identify undrilled structures or sedimentary features, but what makes you think that they have adequate porosity and permeability?
- Diagenesis may be strongly influenced by structural or stratigraphic elements
- Diagenesis may enhance structural or stratigraphic plays
- Some plays defined by diagenesis
  - e.g., Trenton/Black River hydrothermal dolomites of Appalachian basin
- Not as “sexy” as sequence stratigraphy, facies modeling, structural analysis, etc. Also, may involve more petrographic and geochemical work. Therefore commonly neglected or under-studied
- Images at top show two different models for porosity development in the Ordovician Red River Formation of the Williston Basin. Both are derived from examining data from the same area. Interpretation on left suggests porosity trends follow long, linear NE-SW trends. Interpretation on right suggests porosity is associated with localized, more-or-less circular dolomitization centers. How would each affect your exploration/development strategies? How would you decide which model provides the best predictive capabilities? Could you make a decision based on seismic interpretation?

Common Products

- Before starting an interpretation it is a good idea to think about what the deliverables will be and who will use them. Are the primary deliverables likely to be reports, maps, derived volumes (e.g., for input to simulators) or other? Should the deliverables be in paper or (preferably) in digital format? If the latter, what types of files are needed?
- Some common mapping products include:
  - Structure maps. These may be in time (time-structure maps) or depth (structure maps). The latter are needed for drilling, reservoir simulation and other purposes. You will need velocity information to depth convert.
  - Thickness. Again, these may be in time (isochron maps) or depth (isopach maps). You will need velocity information to depth convert.
  - Porosity. Different maps are sometimes used, including average porosity, thickness above some arbitrary cut-off value, or phi*h (the thickness of the porous interval multiplied by decimal porosity at every 0.5' log sample and integrated over the thickness of the interval of interest)
  - Net sandstone. The amount of a formation that is comprised of (potentially reservoir quality) sandstone rather than mudstone. Sometimes also expressed as a net-to-gross ratio
- The porosity and net sandstone maps have traditionally be log-derived, however new techniques are being developed that allows interpreters to derive these measures by integrating 3-D seismic volumes and digital logs
- Reports should document the work that was done (and why), including any assumptions that were made. They should make specific recommendations.
  - Tendency towards digital reporting: e.g., OpenJournal, PowerPoint, hypertext documents

Building a Project Database

- Seismic data should always be integrated with any available well data. To do so, or to be able to view seismic data in their proper geographic location, it is necessary to have accurate location information. Furthermore, when building the project database, it is important to check whether your project has *all* available wells in the study area. Well information should include (as appropriate):
  - Directional data for deviated wells
  - Perforated zones and production data
  - Digital logs (more on this one later)
  - Velocity data (checkshot surveys, etc.)
  - Log picks (tops)
- This information may be obtained from a variety of sources, including scout tickets (see above) and vendors
- Make basemaps showing locations of wells with any digital logs, locations of wells with sonic and density logs, locations of wells with velocity information, production bubbles, and location of seismic lines/surveys.
- Building a complete and accurate project database can be a daunting task. However, time spent on this task in the early stages of the project will pay out in spades later during the interpretation.

Building a Project Database: Well & Cultural Data

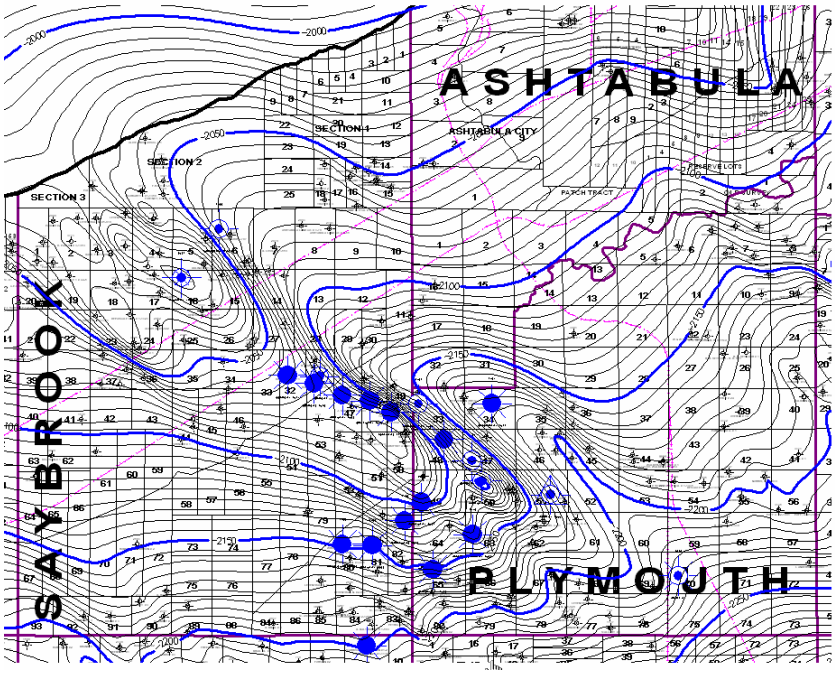

- It is also important to have “cultural” data (Township and Section lines, rivers, towns, etc.) so that well and seismic locations may be georeferenced to surface features whose positions are known (see figure).
- While setting up the project, be sure to understand which coordinate/projection system is being used for the seismic data (e.g., UTM) and make sure that all data (seismic, well, etc.) are in the same format. This may be difficult, but is vital, for international projects.

Building a Project Database: Log Data

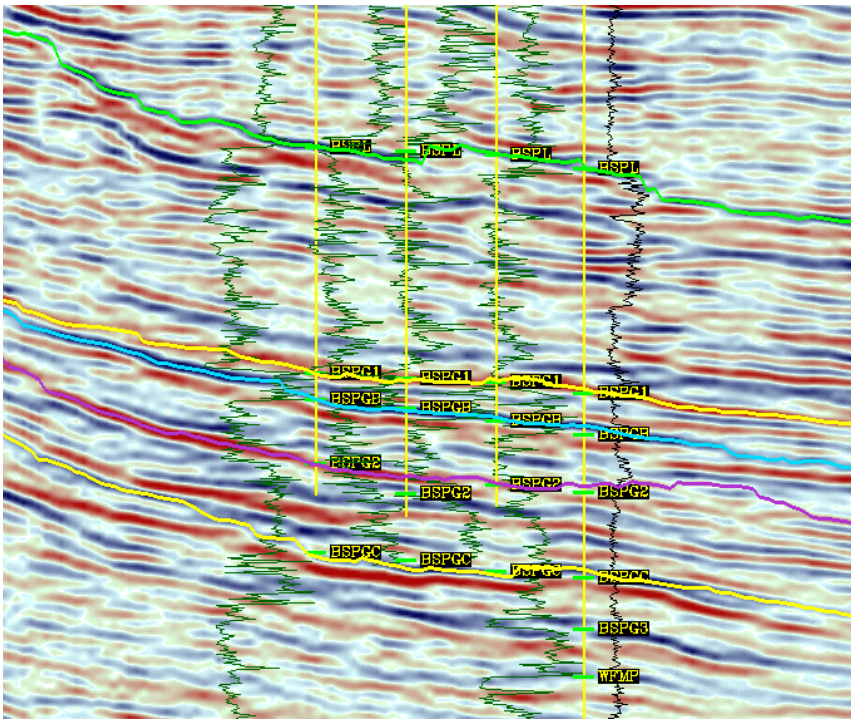

- One of the principal pieces of information you will need from wells is log data - preferably in digital format. This information will help you to make the tie between log and seismic data in at least two ways:
  - Through the generation of synthetic seismograms using sonic and density logs
  - By overlaying other types of logs on seismic data to identify lithologies (e.g., using photoelectric factor logs), fluid contacts (from resistivity logs), depositional environments (from gamma ray log shape), etc. For example, the display above shows gamma ray (green) and a photoelectric factor (PEF; blue) log (for one well on the right) overlain on some seismic data from the Permian Basin. The PEF log shows a change from limestone to dolomite between the green and yellow horizons. Discrete sandstone intervals are also apparent from the photoelectric factor log.

Checkshot Surveys

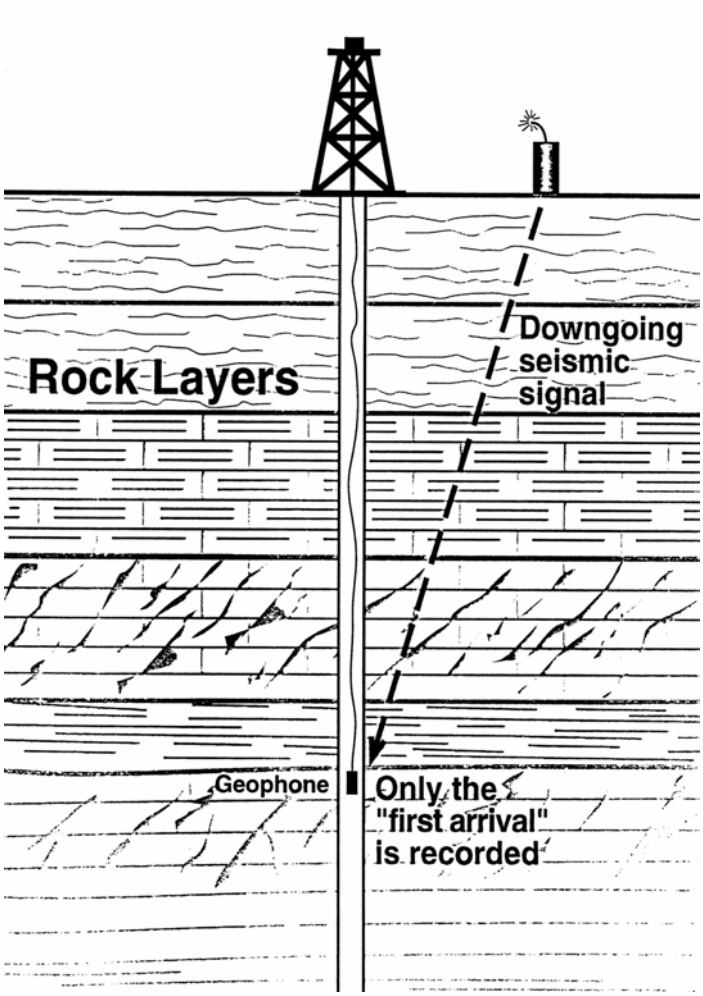

- Velocity information is needed to tie seismic data to log data. Checkshot surveys are the traditional way of collecting subsurface velocity data (since ’30s)
- Measure direct arrival time from source to receiver placed “downhole

Checkshot Surveys

BEG Stratton 3----Time/Depth Information										
Well ID	Datum	Survey Type	Survey #	Survey Point #	2-way time (ms)	1-way time (ms)	Measured Depth (ft)	True Vertical Depth (ft)	Average Velocity (ft/s)	Interval Velocity (ft/s)
422730009903	100	Checkshot	1	1	1265	632.5	4696	4696	7425	7425
422730009903	100	Checkshot	1	2	1341	670.5	5081	5081	7578	10132
422730009903	100	Checkshot	1	3	1588	794	6326	6326	7967	10081
422730009903	100	Checkshot	1	4	1649	824.5	6632	6632	8044	10033
422730009903	100	Checkshot	1	5	2500	1250	11313	11313	9050	11001

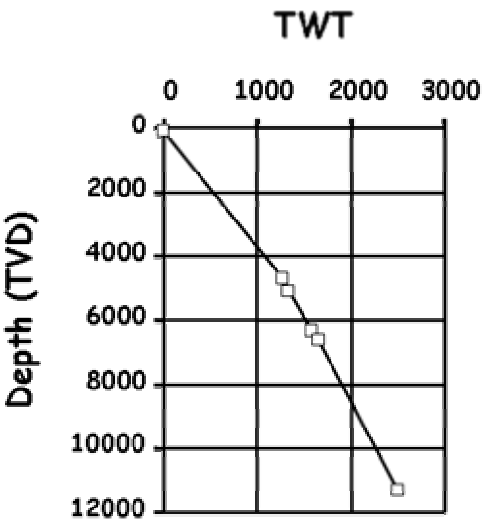

- Checkshot data are collected at formation tops and/or at regular depths downhole. They allow well data and seismic data to be calibrated, and may be used for determining average and interval velocities.
- The checkshot survey shown above shows just five data points for clarity. Most checkshot surveys are more densely sampled.
- The number of checkshot surveys needed for an interpretation is variable. It depends on how variable the velocity structure is, a function of
    - Lithologic changes
    - Pressure regime changes
    - Structural complexity
    - Etc
- Checkshots may not even be collected if it is felt that the tie between the seismic and well data is sufficiently well understood (i.e., mature basins)

Synthetic Seismograms

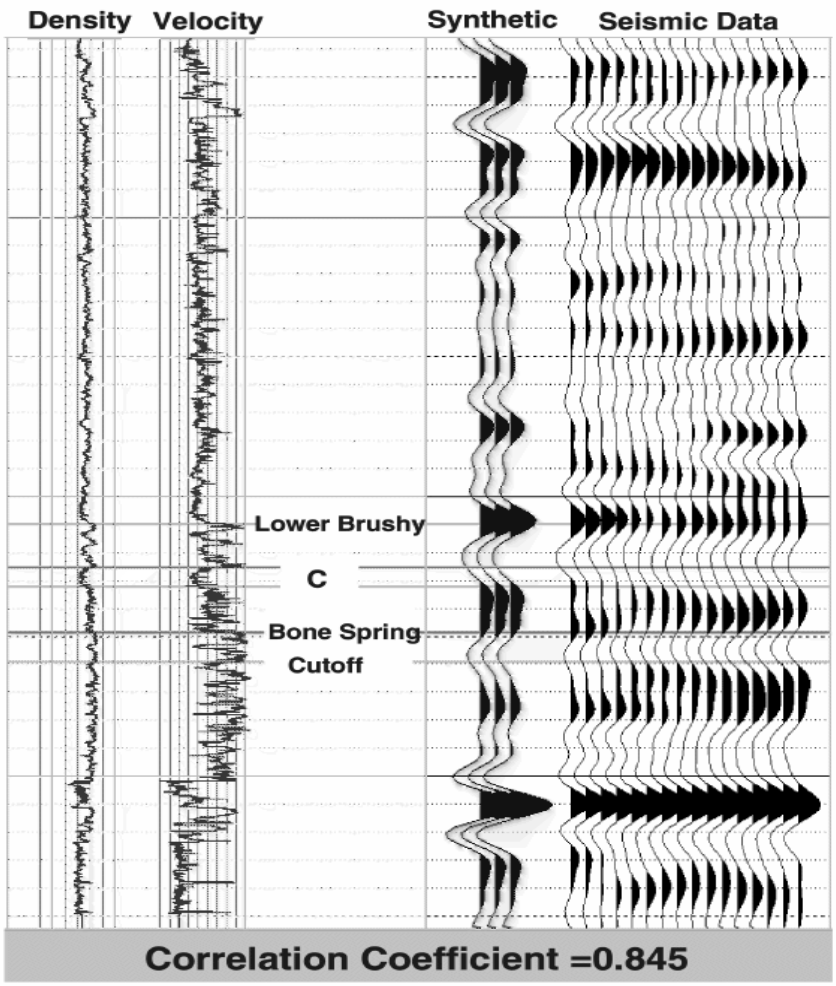

- The most common way of tying log and seismic data is through the generation of synthetic seismograms ("synthetics"). In theory, a synthetic should show what the seismic data should look like at the location of a well.
  - Use digital sonic and density logs to generate acoustic impedance log
  - Use velocity data (e.g., checkshot surveys)
  - Use acoustic impedance log to derive reflection coefficients (stick diagram)
  - Convolve reflection coefficients with a wavelet that approximates wavelet in the seismic data (phase, frequency content)
  - Compare synthetic with seismic data

Synthetic Seismograms
Software Capabilities

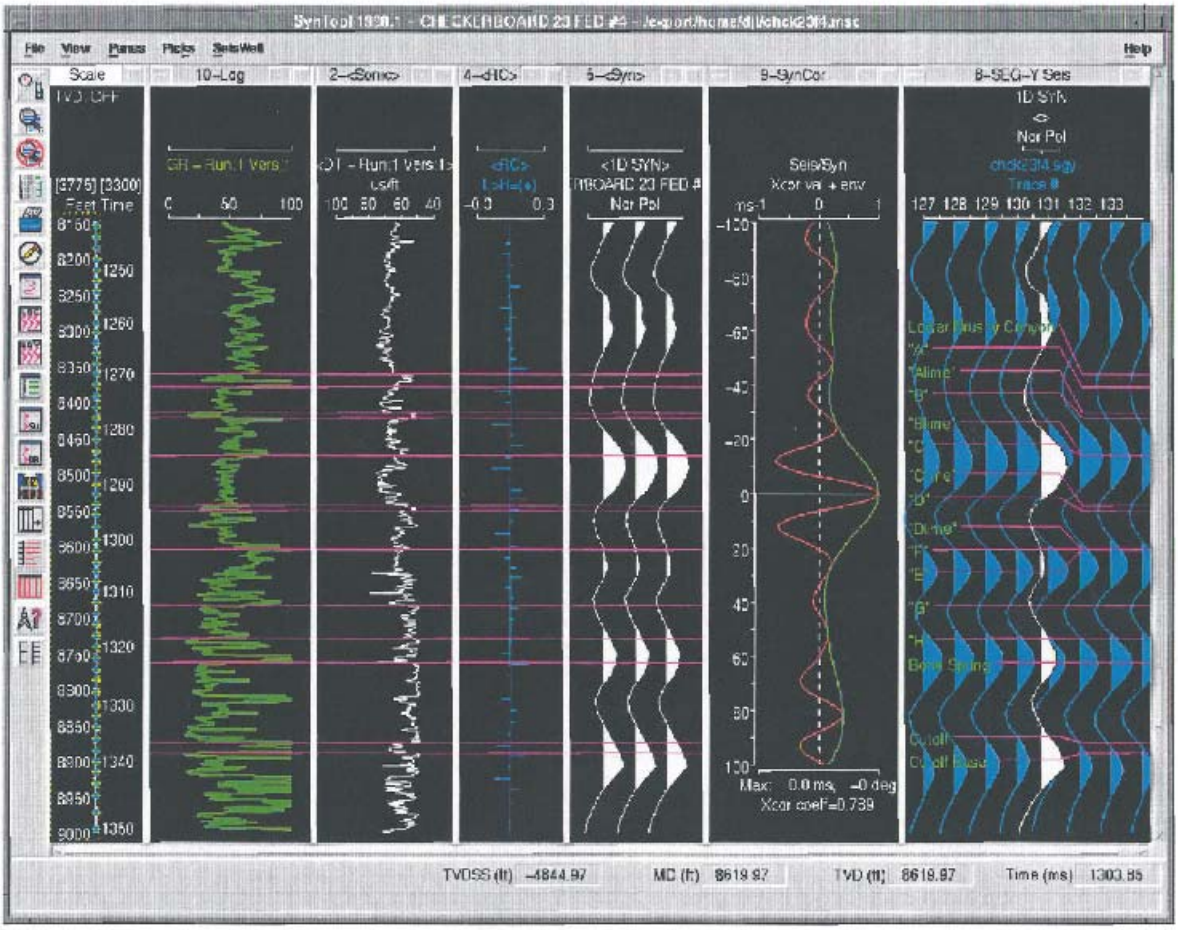

- Software (e.g., Syntool, GMA) generally has capabilities allow user to improve correlation between synthetic and seismic data
  - Wavelet extraction
  - Stretching synthetic
  - Variable wavelet over length of synthetic
  - Graphic correlation of synthetic and seismic

Synthetics - Pitfalls

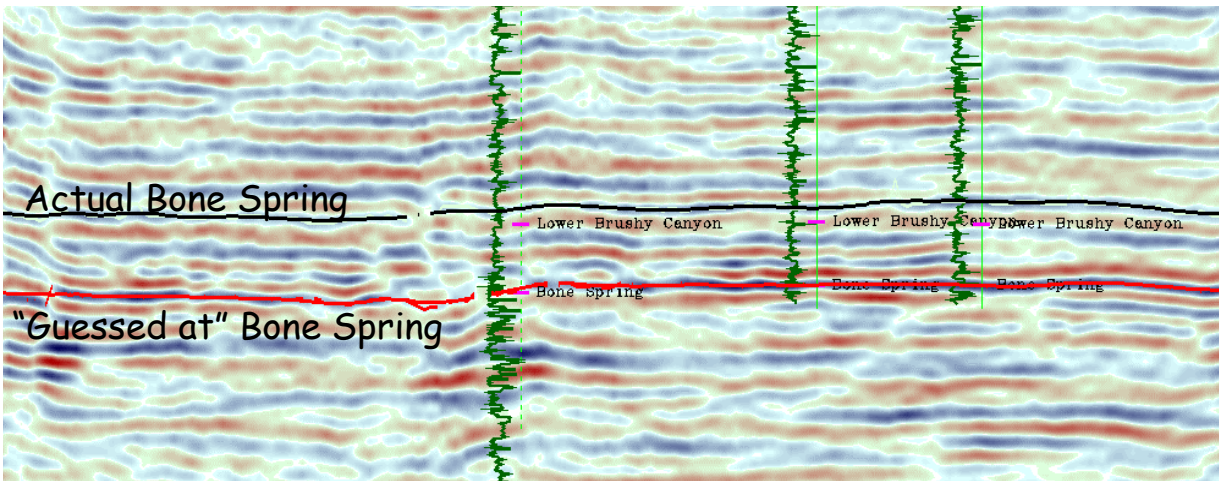

- Problem: synthetic in previous slide has a "pretty good" correlation (0.79) but is off by about 30 ms. Transect above shows Bone Spring pick based on synthetic ("Guessed at" Bone Spring) and true ("Actual") Bone Spring pick.
  - No checkshot data were available. Initial tie based on guess at where tie should be. Extracted wavelet gave high correlation.
- Conclusion: wavelet extraction, stretching of synthetics and other capabilities can make a synthetic tie to the seismic nicely when it shouldn't
- Some other problems:
  - Sonic & density logs image a limited amount of rock, seismic images larger area
  - Borehole conditions may affect log values
  - Sonic log uses much higher frequencies than seismic
  - Convolutional theorem that is the basis of generating synthetic seismograms is an *approximation* of what happens when collecting seismic data

Synthetics – Without a Sonic

Gardner:

$V_p = (\rho/a)^b$

a – constant (4)

ρ – density

b – constant (.23)

Faust:

$V_p = c(zR')^d$

c, d – constants

z – depth

R' - resistivity

- Don't have a sonic or density log? You have some options:
  - Use density log to derive sonic log (or vice versa) using Gardner equation
  - Use resistivity log to derive a sonic log using Faust equation
  - Use neural networks to derive sonic log from other logs
- When in doubt – call in an expert: Use your local petrophysicist

Velocity Data – Vertical Seismic Profiles (VSPs)

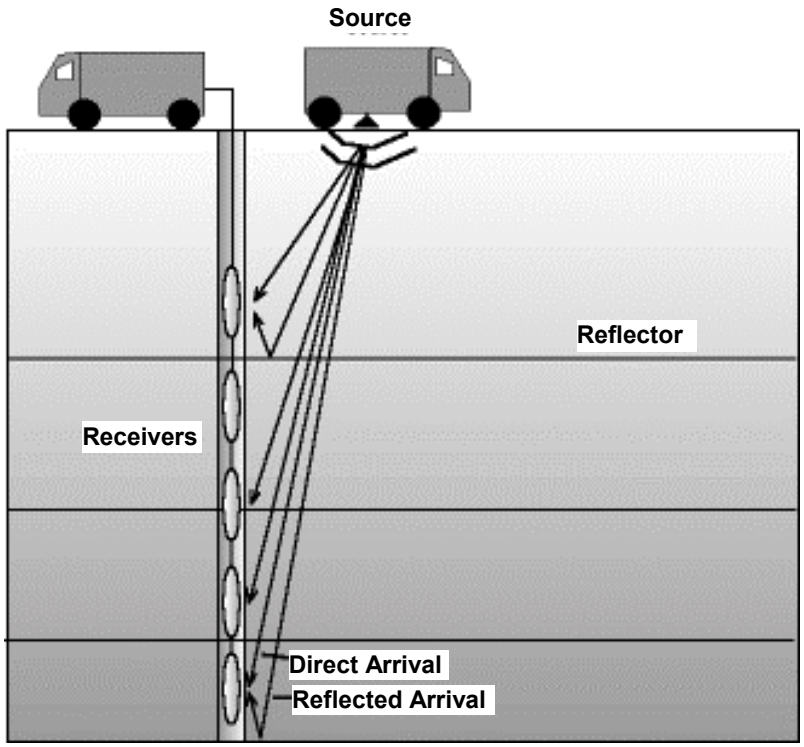

- It is possible to obtain even better velocity information using a similar set-up as a checkshot survey, but spacing receiver locations more closely (e.g., every 50'). Additionally, the focus is on recording reflected arrivals rather than direct arrivals. After processing, the result will be a vertical seismic profile (VSP) that shows the seismic response of the earth at the borehole location. Because the depths to the receivers and the traveltimes are known exactly, it is possible to derive highly accurate correlations between formation tops (derived from logs) and seismic events. In fact, the VSP may be processed to show the vertical axis in time or depth.
- Because the sound does not travel as far through the earth as when collecting surface seismic data, VSPs tend to have higher frequency content (i.e., better resolution).
- Ideally, the same source and similar processing are used to collect VSP and surface seismic data.

Velocity Data – Vertical Seismic Profiles (VSPs)

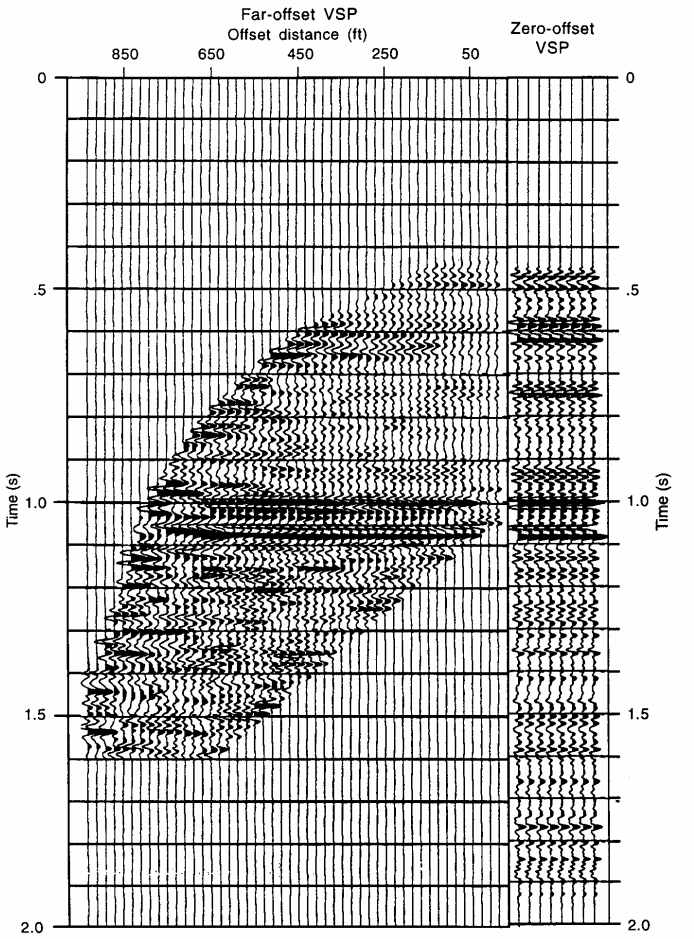

- Two sample VSPs. Vertical axis is shown here in time, but could be shown in depth.
- On the right, the zero-offset VSP was collected with the source immediately adjacent to the borehole. The result is a single trace that, like a synthetic seismogram, is shown repeated several times.
- On the left, the far-offset VSP was collected with the source at some distance from the borehole. The result is a 2-D image of the stratigraphy between the source and borehole locations.

Velocity Data – Other Sources

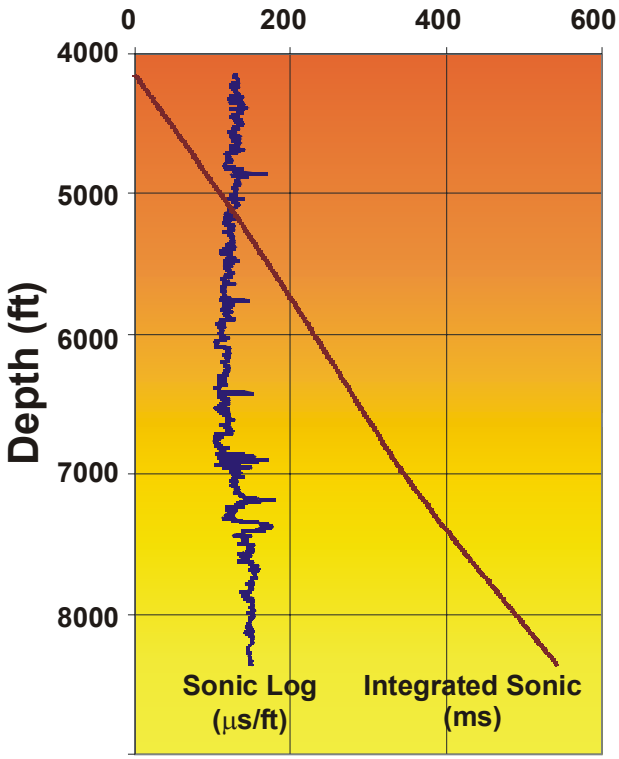

- When checkshot or VSP data are unavailable, it may be necessary to obtain velocity data from other sources.

- Integrated sonic logs. Sonic logs are measured in microseconds per foot/meter. By integrating over the length of the log, it is possible to derive a velocity function (see figure).
  - Potential problems include: a) frequency effects (sonic log vs seismic), b) borehole conditions affecting the log, and c) lack of information for the uppermost part of the section (sonic logs are seldom run all the way up to the surface).

- Stacking velocities. Velocity analysis during NMO correction provides information. Interval velocities may be derived using Dix equation.

Velocities – Sources of Information

Type	Source	Comments
Stacking	Determined through NMO velocity analyses	•Best-fit hyperbola to data that are not perfectly hyperbolic •+/- 10% true velocities
Average	Distance traveled divided by the time required to travel the path	•Depends on raypath •Derived from sonic logs, log-seismic ties, etc.
RMS	Square root of the sum of the squares of the velocity values divided by the number of values	•Gives added weight to extreme/high values •Typically a few percent higher than corresponding average velocities •Approximately equal to stacking velocity (for normal incidence & horizontal layers)
Interval	Average velocity over some interval of the travel path	•Derived from sonic logs, log-seismic ties, raytrace modeling, etc
Dix	Average velocity between reflections, derived from rms (stacking) velocity	
Reflection Tomography	2-D or 3-D definition of velocity field based on reflection measurements	•Iterative. Final model is the one whose velocities and reflectivities best describe the data
Refraction Tomography	2-D or 3-D definition of velocity field based on refraction measurements	•Typically shallow velocity definition for static corrections
Migration Post-Stack time and depth	NMO velocity analysis	•+/- 5% of stacking velocities. Selected to provide “best” image
Migration Pre-Stack time and depth	Flattened events in the pre-stack gather after migration	•Model-based. Can include effects of anisotropy

Pitfalls

- The seismic interpreter can run into various pitfalls/problems when interpreting seismic data. Some of these are listed here.
  - Bad well ties:
    - Phase incorrect
    - Lack of checkshots
    - Etc.
  - Different vintages of data have different seismic reference datums, different replacement velocities
  - Velocity problems
    - Statics
    - Pull up/push down
  - Geometric pitfalls – flattening, isochrons, etc.
- Interpreters need to know when and why these pitfalls might be expected, and be on the lookout for them.

Pitfalls

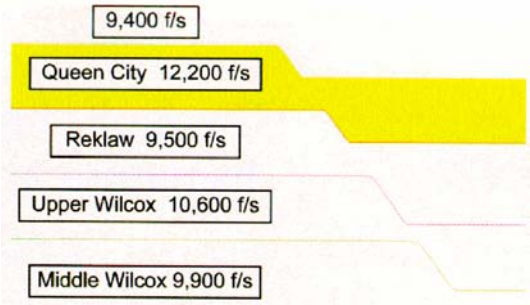

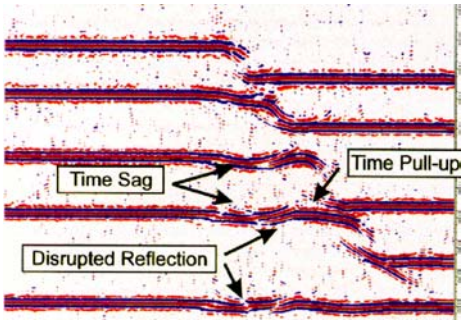

- Fault shadows are areas below faults that are poorly imaged because rocks of different velocities are thickened or thinned across a fault. This causes pull-up or push-down (sag) below the fault. At times these problems might lead the interpreter to suggest that structures are present in the footwall below the fault

- Pre-stack depth migration can help eliminate this problem. The image at lower left shows a post-stack time migrated version of a seismic line. The image at lower right shows a pre-stack depth migrated version. Note the differences below the fault.

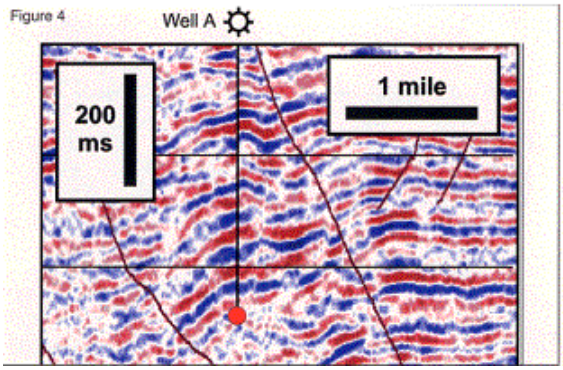

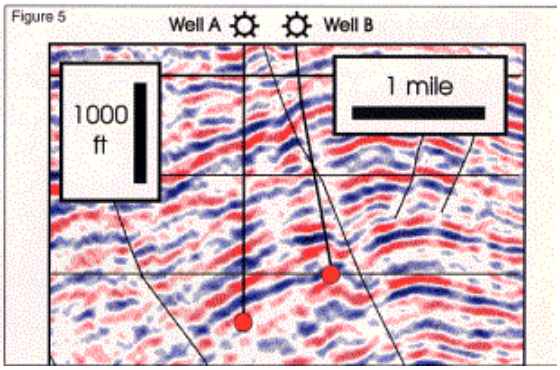

Pitfalls

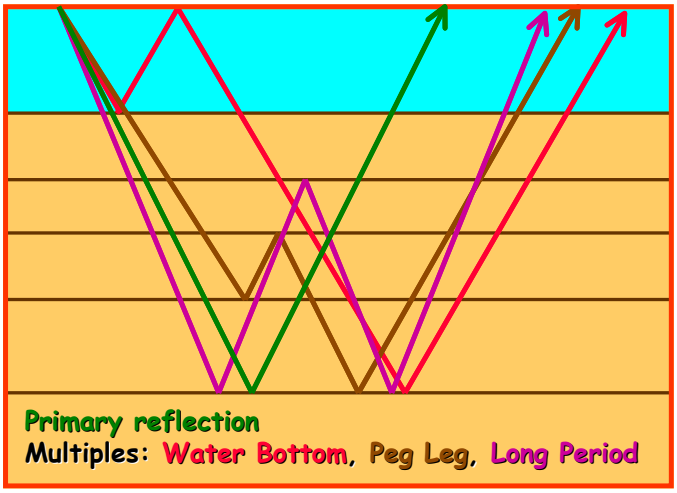

- Rapaths do not always take straight paths from source-reflector-receiver – these are the primary reflections that we are interested in.
- Multiples take more complicated paths through the Earth. They are recorded, but they obscure the geology.

- The image below shows some multiples in some offshore data. Reflection “A” is the seafloor. “B” is a water-bottom multiple of the seafloor. “C” is the base of an incised channel (strike view). “D” is a water-bottom multiple of “C”.

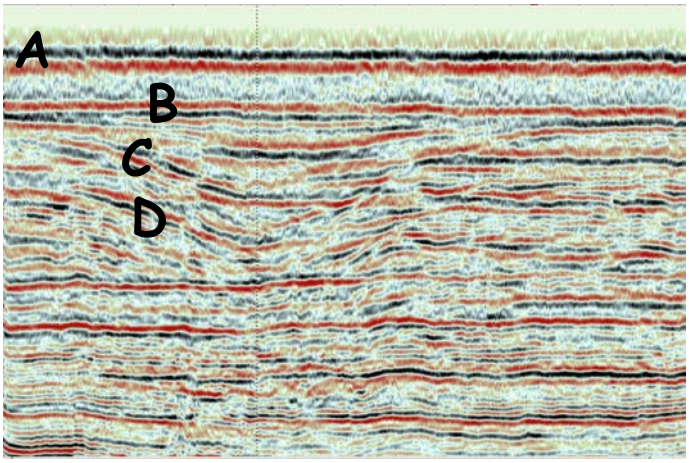

Structural Interpretation

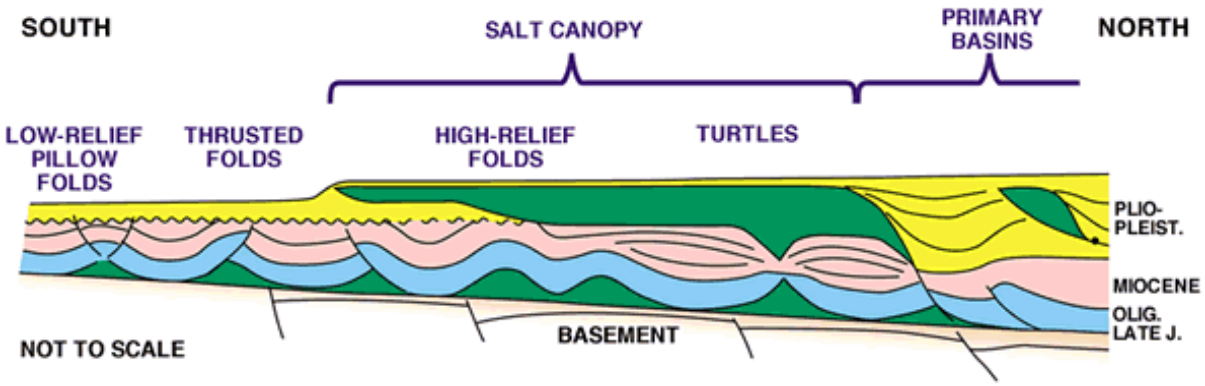

- One of the most common uses of seismic data is for definition of structural features.
- When undertaking a structural interpretation, it is important to let the regional tectonic framework guide your interpretation. How severely tectonized is your study area? Should you be seeing extensional, compressional or wrench-related tectonic features? Did more than 1 tectonic episode affect the area?
  - Image above shows some of the features that might be expected in an area, such as the Gulf of Mexico, where salt tectonics have played an important role.

Faults

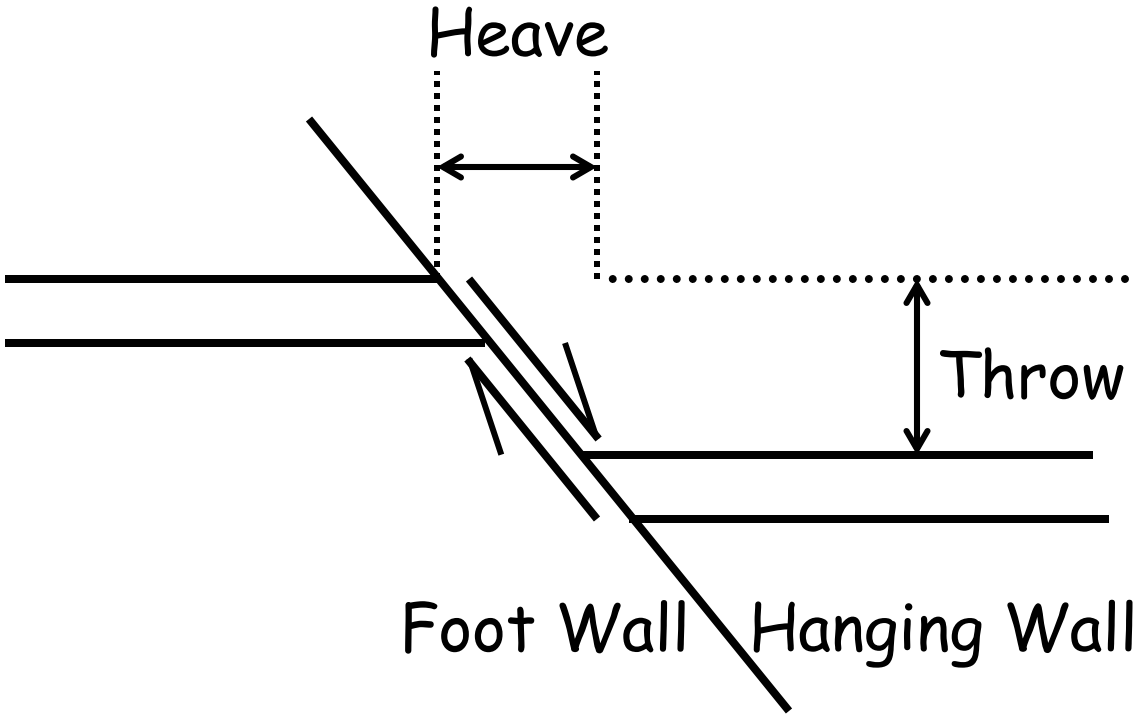

- Some simple definitions for normal faults:
  - Throw – the vertical displacement on a fault (dip-slip motion)
  - Heave – the horizontal displacement along a fault
  - Hanging wall – the fault block above the fault
  - Foot wall – the fault block below the fault

Faults – Map View

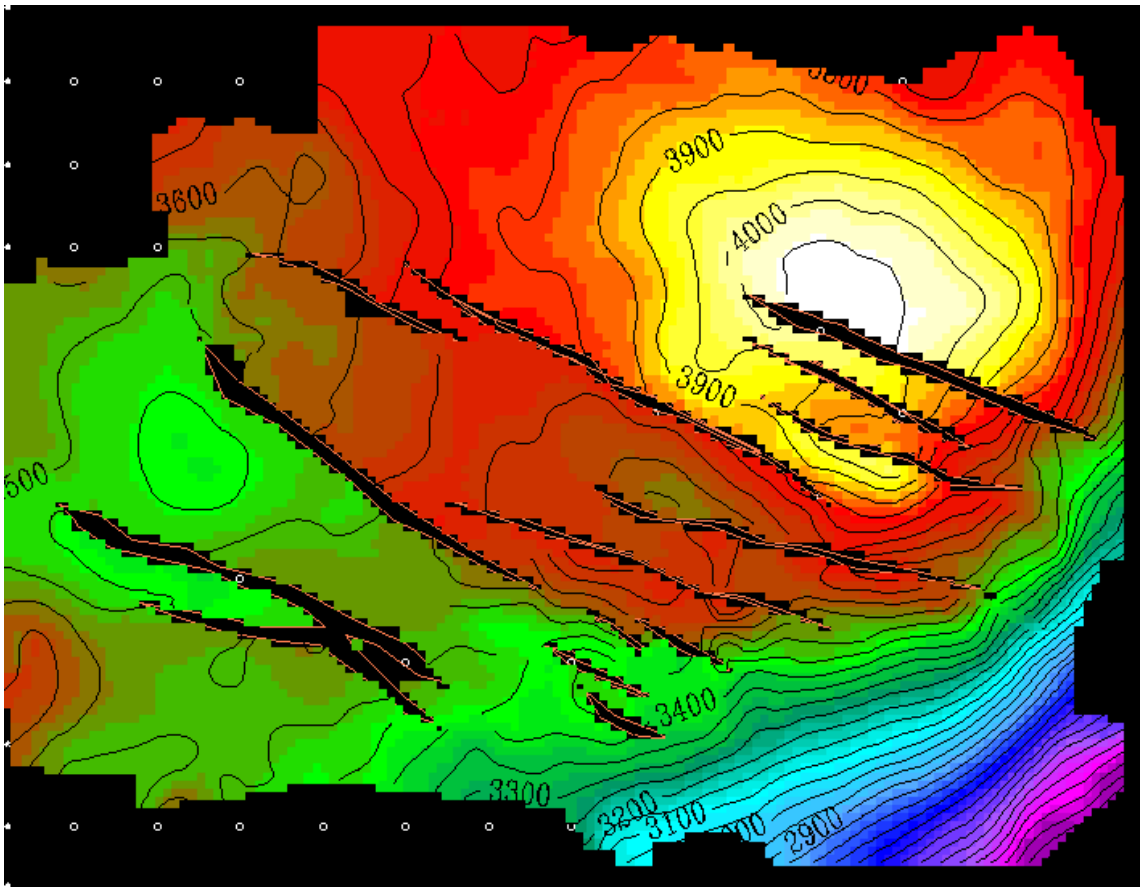

- In map view, heave on individual transects is used to define “fault heave polygons”
- Image above shows depth-converted structure map with fault heave polygons.

Faults – Variability Along Strike, Up/Down Section

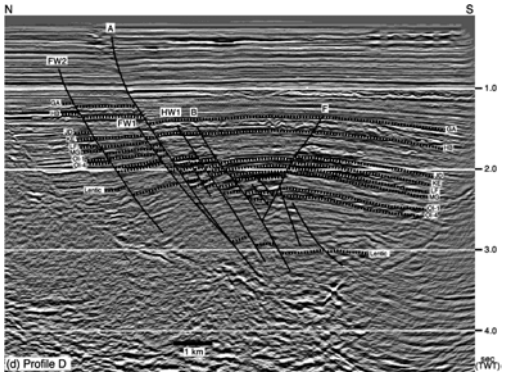

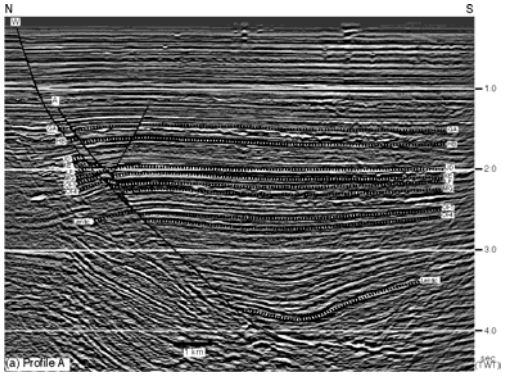

(a) HB horizon

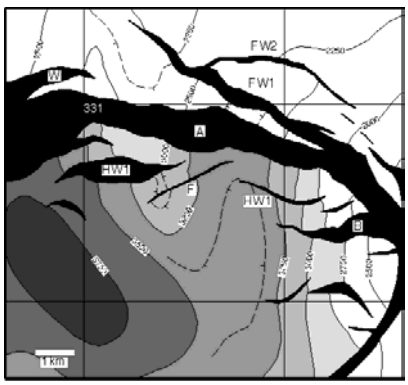

(e) Lentic horizon

- Faults have finite dimensions – they die out along strike, up/down section. As such the throw may change from one stratigraphic level to another, and heave may change along strike.
- Example shows variability in faulting as expressed in two vertical transects and two time-structure maps from the offshore Gulf of Mexico.

Faults – Questions for Interpreters

- Interpreters should keep several questions in mind when picking faults. These include:
  - Are faults soling out with depth or “hanging in space”?
  - Are fault picks consistent with regional tectonic framework?
  - What is timing on the faults?
    - Young or old?
    - How far up-section do they cut?
  - What (if any) is relationship to basement structures?
  - What is relationship to salt or shale diapirs?

Interpreting Faults
Use of Arbitrary Lines

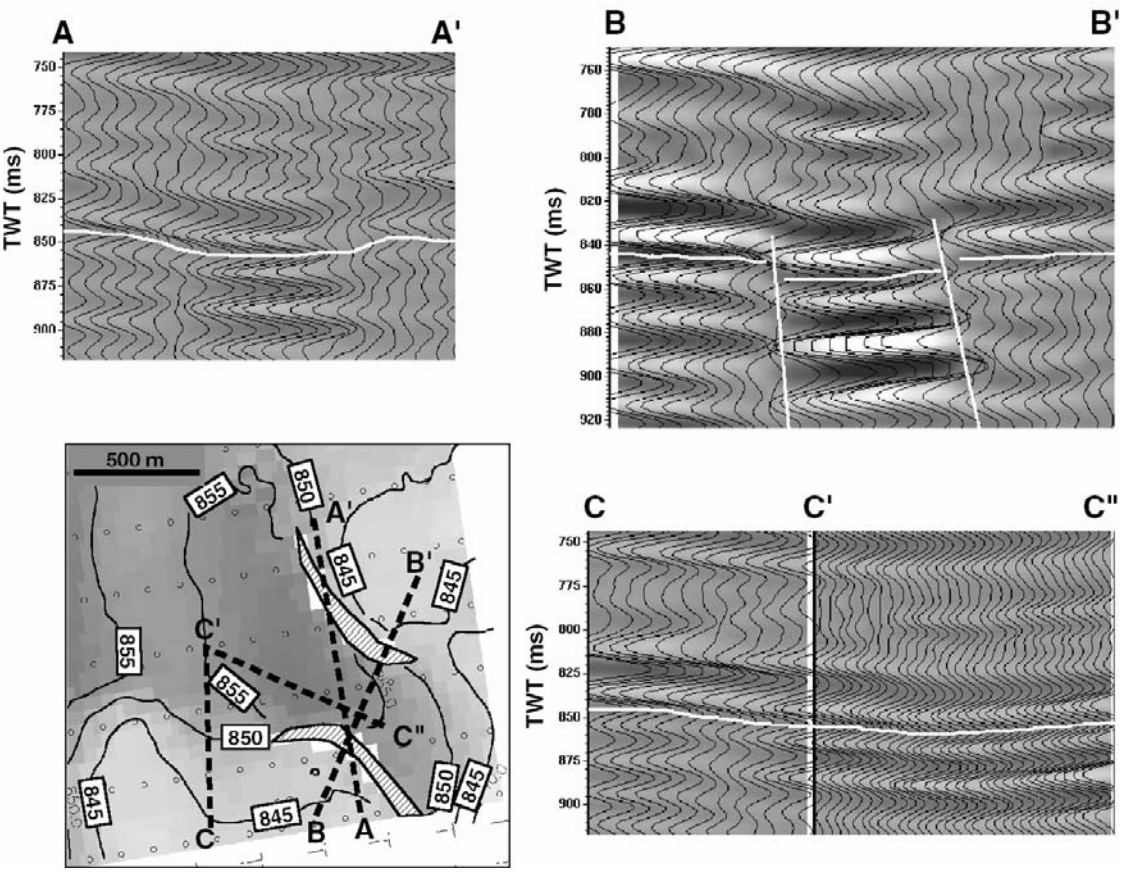

- Use arbitrary lines from 3-D volumes to view the true geometries of faults and to correlate from one fault block to another
- Example shows a time-structure map in lower left. Note the small graben in the center.
- Crossline (trace) in upper left (A-A') crosses faults obliquely, and they may be hard to recognize.
- Arbitrary line in upper right (B-B') crosses faults at almost right angles – they are very clear (one is a normal fault, the other is a reverse fault).
- Arbitrary line in lower right (C-C'-C'') correlates white horizon around fault tip from one fault block to the next. Correlation of horizon from inside to outside of graben (shown at upper right) is confirmed.

Interpreting Faults – Use of Timeslices

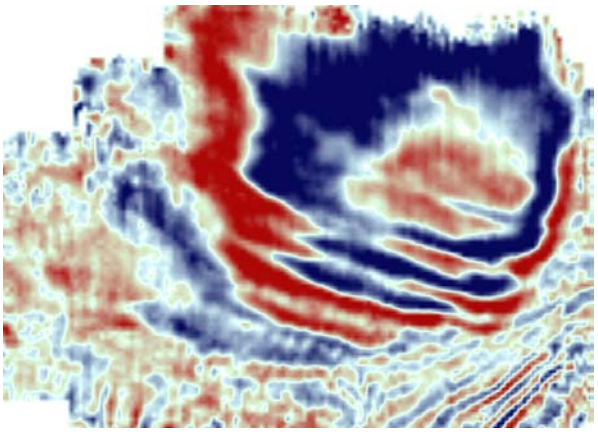

←Amplitude timeslice showing faults

Coherency timeslice showing faults ->

- Timeslices through amplitude volumes are often used to pick faults. Coherency timeslices are better.
- Image shows amplitude and coherency timeslices through a Laramide dome in the Rocky Mountain area.
  - Coherency timeslice shows faults and data quality issues.

Interpreting Faults – Timeslices & Vertical Transects Together

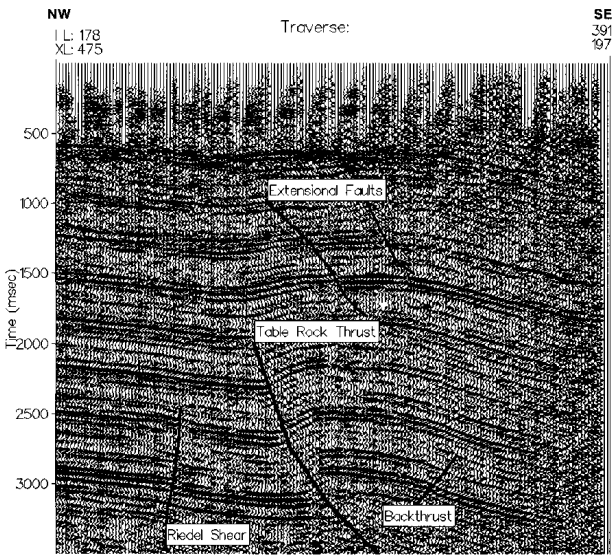

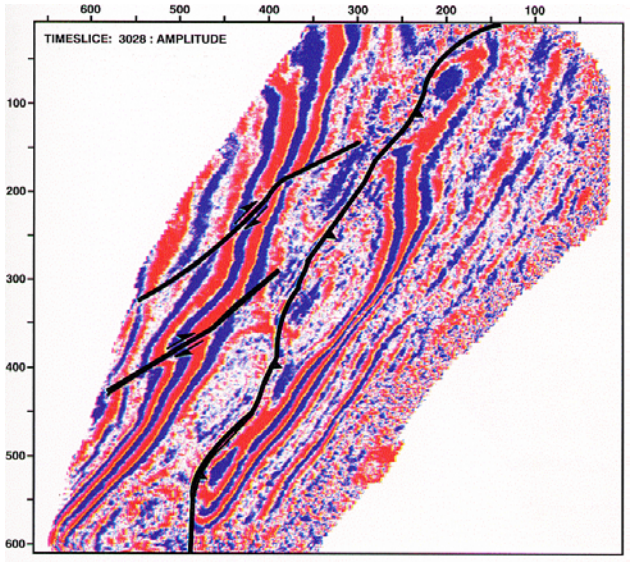

- Timeslices and vertical transects should be viewed together when interpreting structural features.
- Image at left shows an arbitrary transect across a Rocky Mountain structure. A significant thrust fault and associated other faults are visible. The vertical transect shows another structure (“Reidel Shear”) to the northwest of the reverse fault. This appears to be a subtle structure in cross-section.
- Image at right shows a timeslice from low down in the section. The Reidel Shears have a significant strike-slip component, something that was not obvious from the vertical transect. The trace of the thrust is also readily apparent.

Structural Interpretation of Horizons – Carry Multiple Horizons

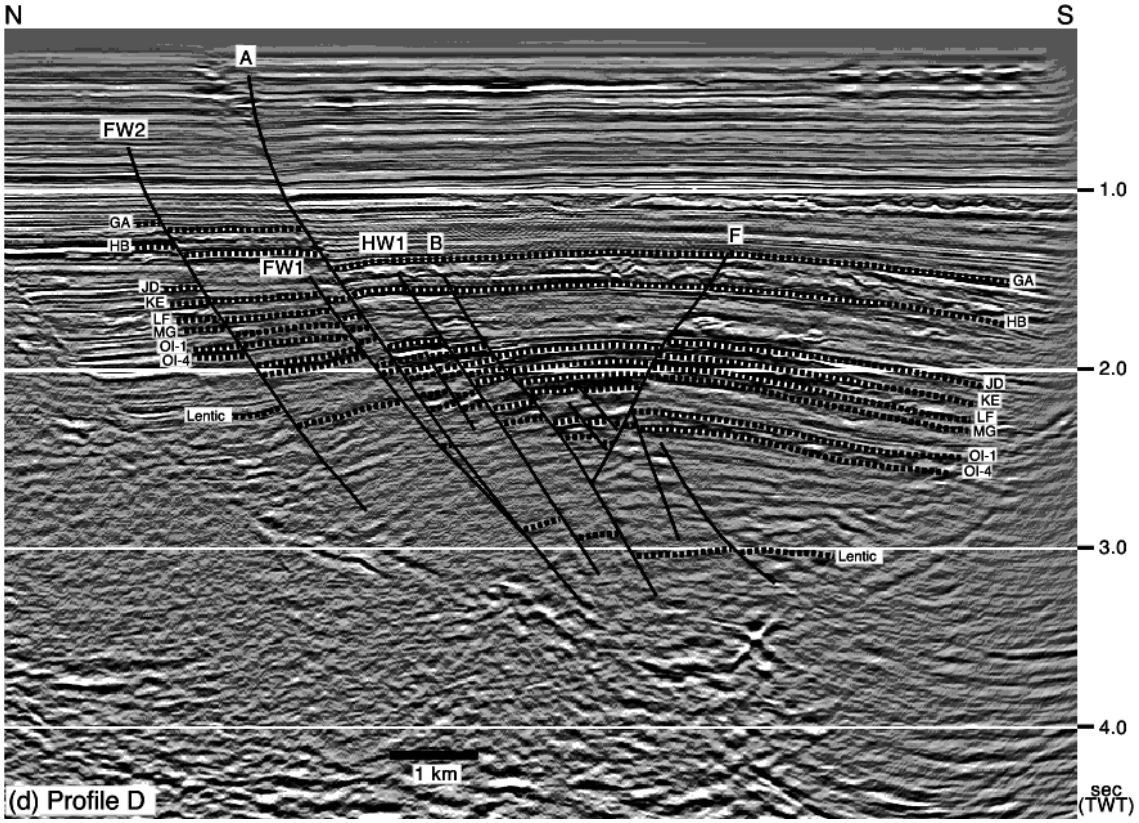

- Although you might be interested in only one stratigraphic level, it is important to map more than one horizon in a faulted area.
  - Aids in determining timing/history of structural development
  - Maintains consistency

Faults – Quantifying Fault Throw

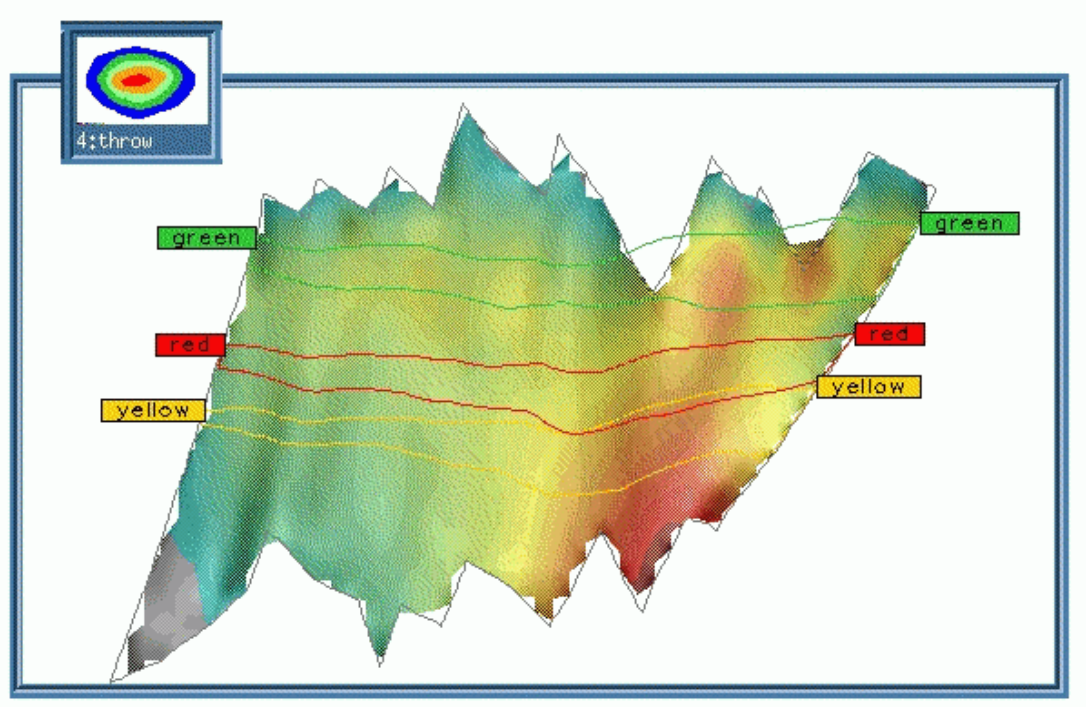

- Integration of stratigraphic picks and faults allows interpreter to quantify fault throw.

Faults – Allen diagrams

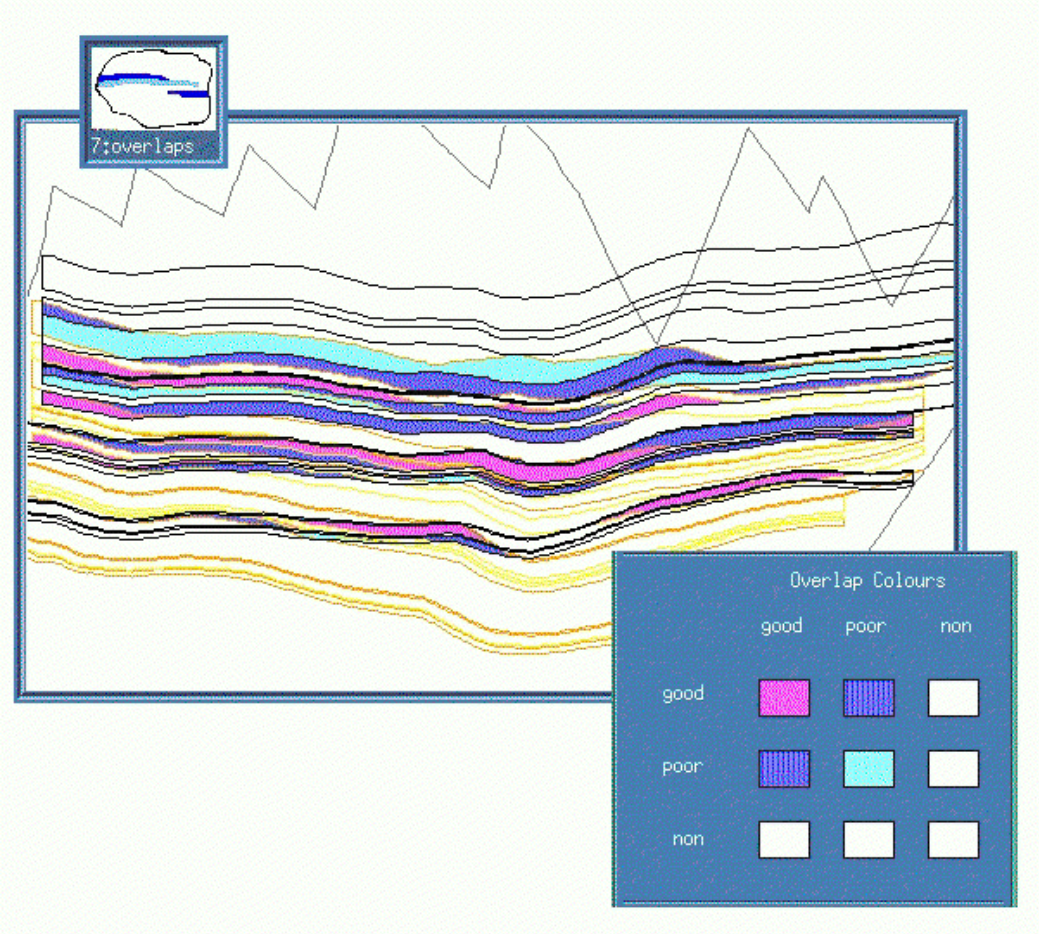

- Allen diagrams show how different reservoir quality rocks are juxtaposed from one side of a fault to the other. Structure and horizon thickness are derived from seismic mapping.
- In this image, pink means that there is good quality reservoir on both sides of the fault, dark blue means that there is good quality reservoir on one side but poor quality reservoir on the other, light blue means that there is poor quality reservoir on both sides of the fault, and white means that there is non-reservoir quality rock on one or both sides of the fault.

Faults – Allen Diagrams & Spillpoints

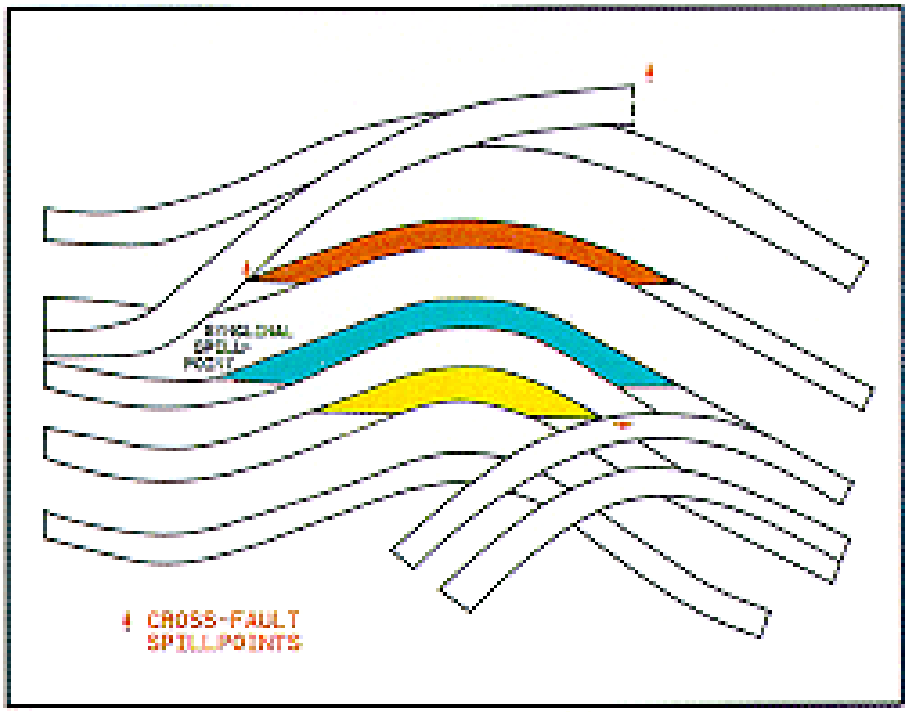

- Allen diagrams may be used to help define spillpoints and trap size.
- Example above shows fault-plane section with three separate reservoir levels.
  - Lower (yellow) interval has cross-fault spilpoint to right
  - Middle (blue) has synclinal spillpoint (faults not involved) to left
  - Upper (brown) unit has cross-fault spillpoint to left
- Use spillpoint elevation and structure map to define trap size.

Faults –
Process Flow: Extensional

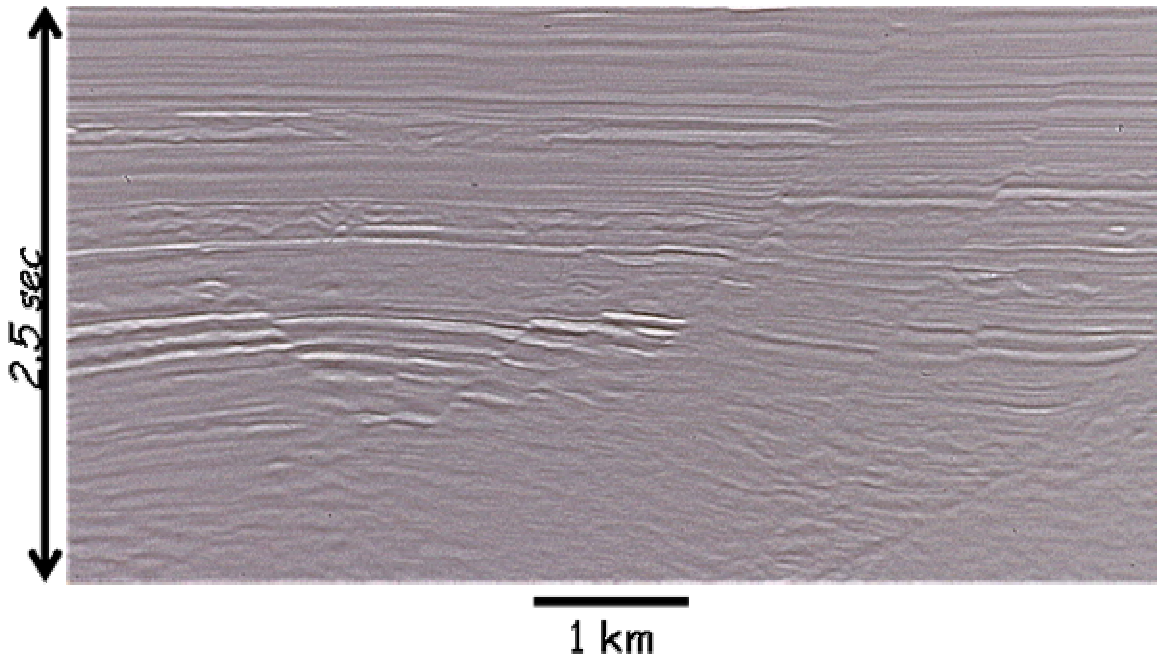

- Reconnaissance
  - Visualization helpful (cube displays, etc.)
- Interpret dip-oriented lines first
  - Use arbitrary lines if necessary (save them)
  - Use timeslices
- Map major faults first
  - Create a framework
- First pass at horizon interpretation
- Identify and map smaller faults
  - Refinement
  - Use visualization to Q.C. your picks

Develop you own flow with time

Faults –
Process Flow: Compressional

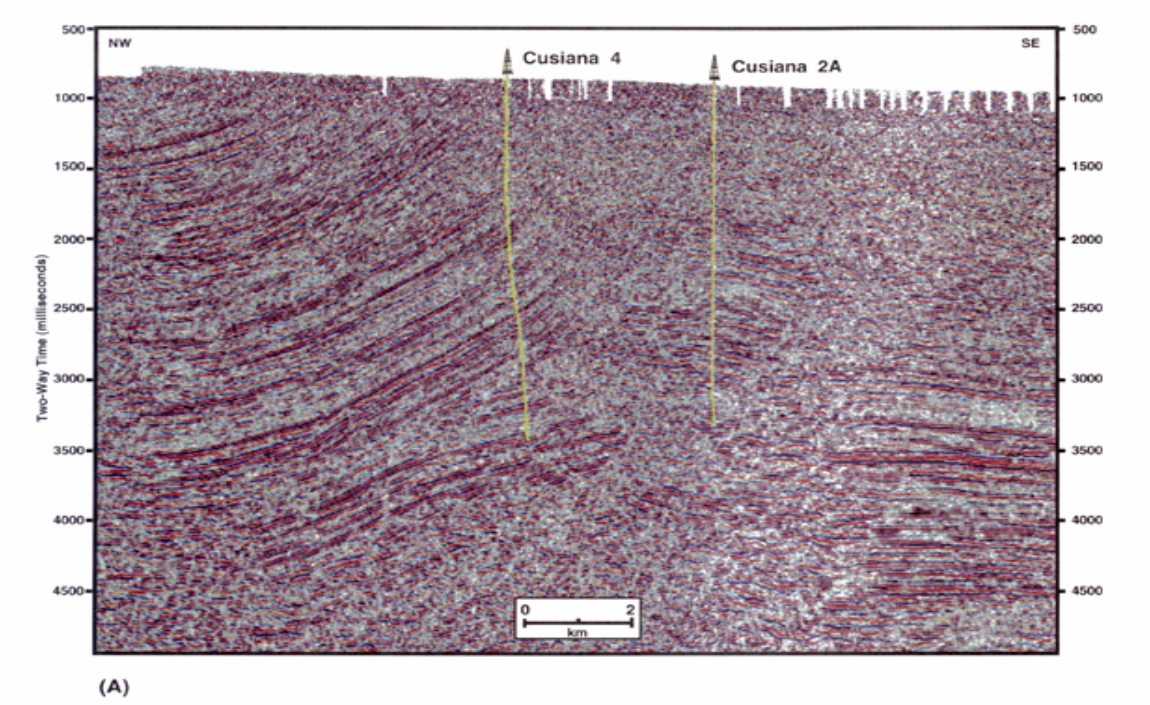

- Reconnaissance
  - Visualization helpful (cube displays, etc.)
- First pass at horizon interpretation
  - Regional stratigraphic framework
- Interpret dip-oriented lines first
  - Use arbitrary lines if necessary (save them)
  - Use timeslices
- Map major faults first
  - Create a framework
- Identify and map smaller faults
  - Refinement
- Use visualization to Q.C. your picks

Develop you own flow with time

Structural Validation – Balancing/Restoring Sections

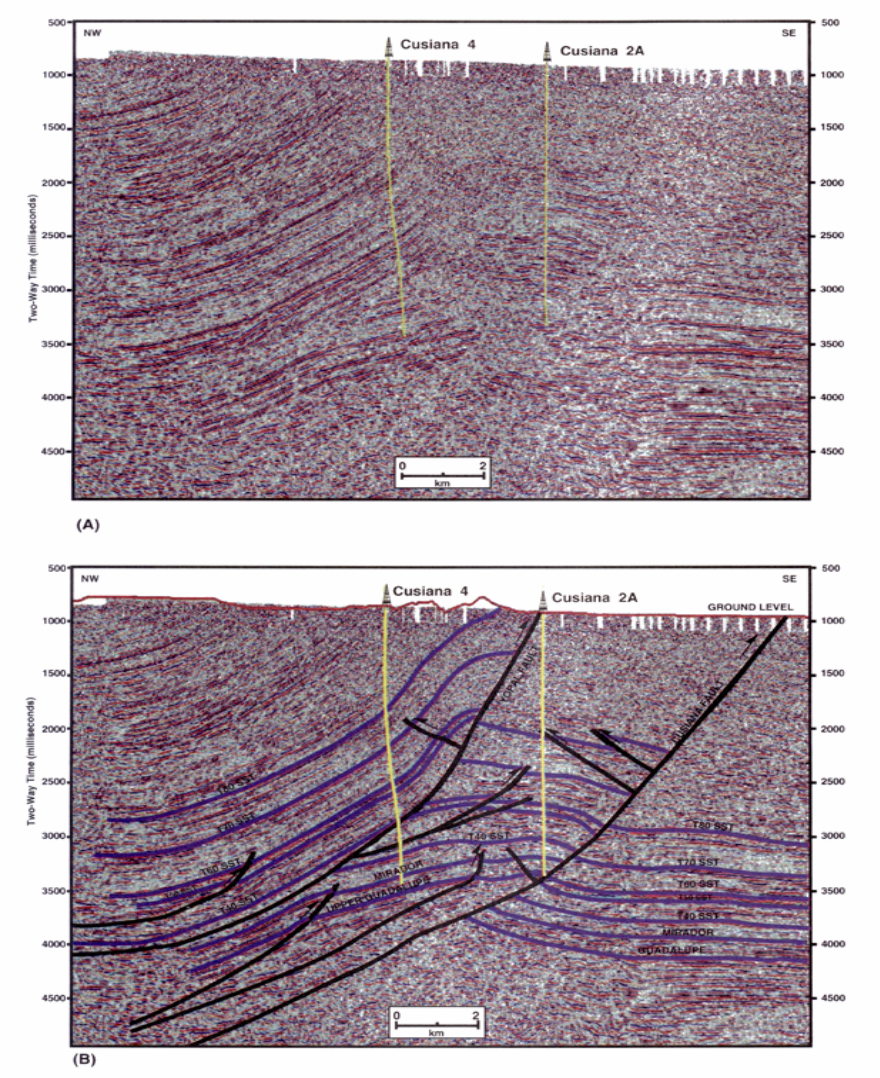

- Cross-section balancing restores stratigraphic horizons to their pre-fault locations. If faults are “reasonable” there should be no overlapping stratigraphy or missing section.
- Example above shows uninterpreted (top) and interpreted (below) versions of a seismic transect from Columbia.

Structural Validation – Balancing/Restoring Sections

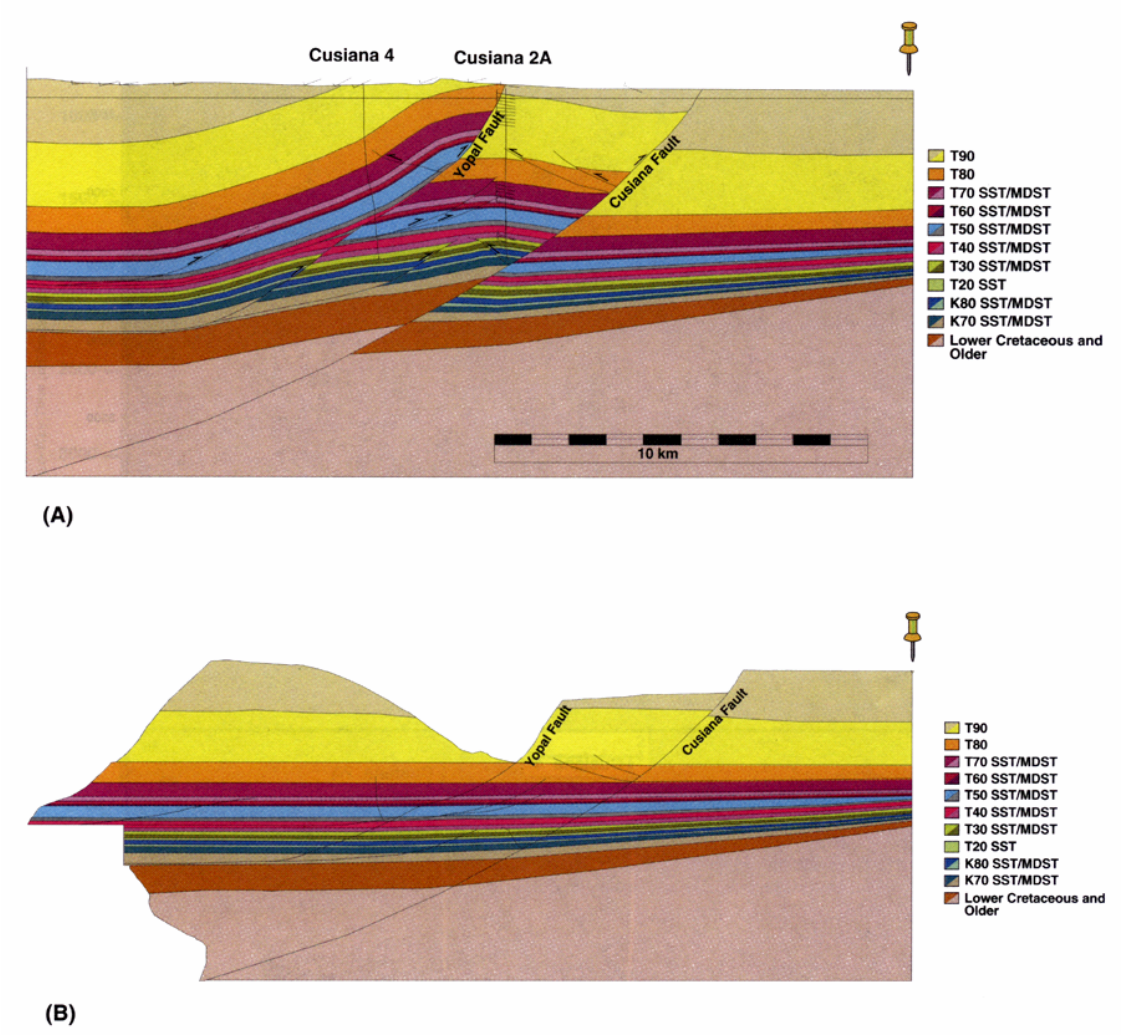

- Image above shows stratigraphy/faults as interpreted from seismic data shown on previous page.
- Image below shows restored section. There are no gaps/overlap, helping to confirm the validity of the seismic fault picks.

Structural Validation – Fault Restoration/Visualization

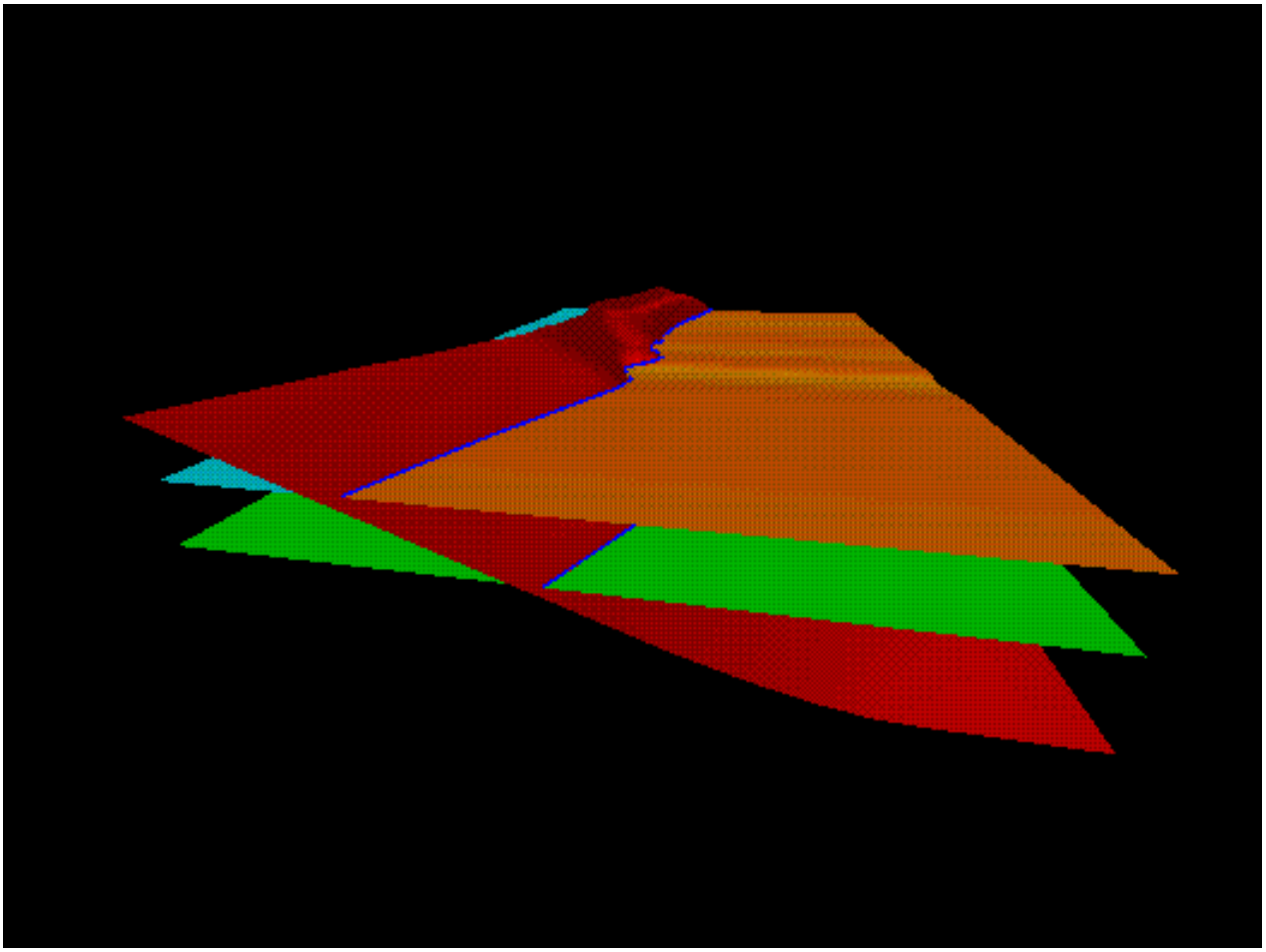

- Various software packages may be used to help in fault restoration exercises.

Faults – Validation using Pressure Data

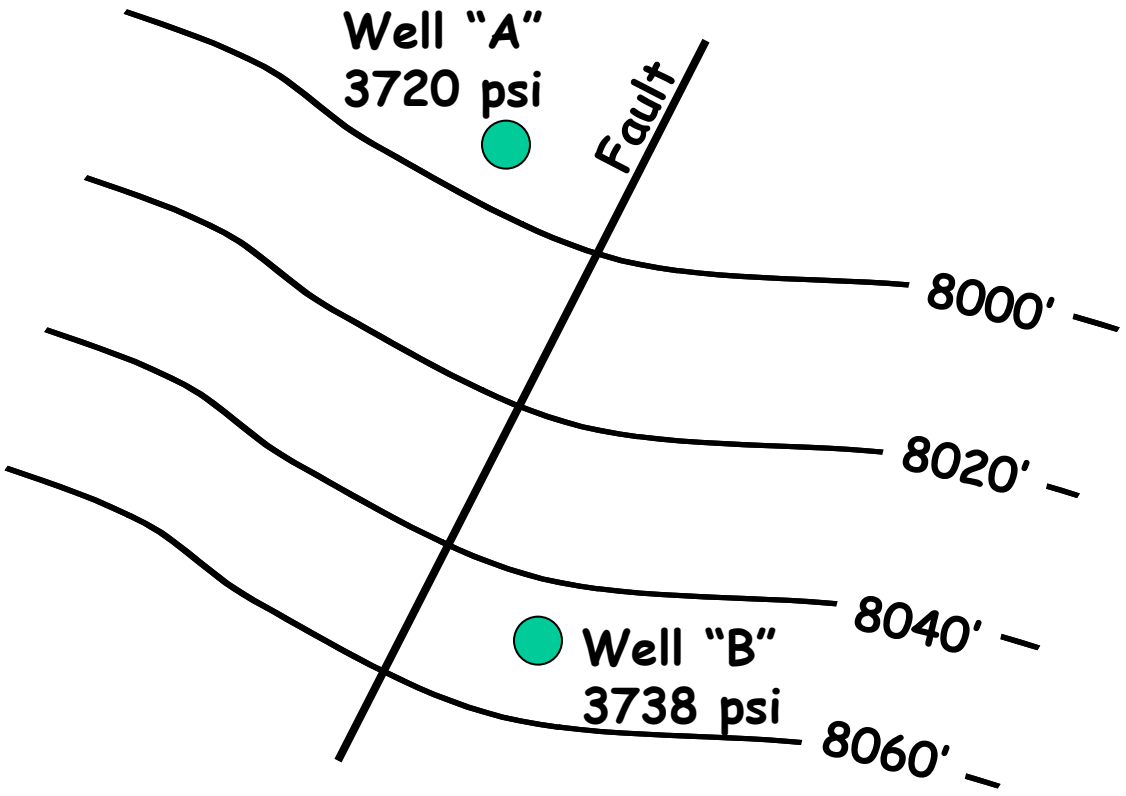

- Pressure data may be used to help determine whether seismically defined faults are acting as seals to compartmentalize the reservoir.
- Two wells that are in fluid communication with each other should have equivalent pressures – once differences in elevation and fluid composition are taken into account.
  - Use pressure gradient data
- Wells "A" and "B" are both in the oil leg of a reservoir, but are separated by a seismically defined fault. Assume oil pressure gradient of 0.33 psi/ft – are they in separate pressure compartments?
- Other engineering data (fluid contacts, fluid composition, etc.) also useful

Structural Interpretation of Horizons – Tying it in with Synthetics

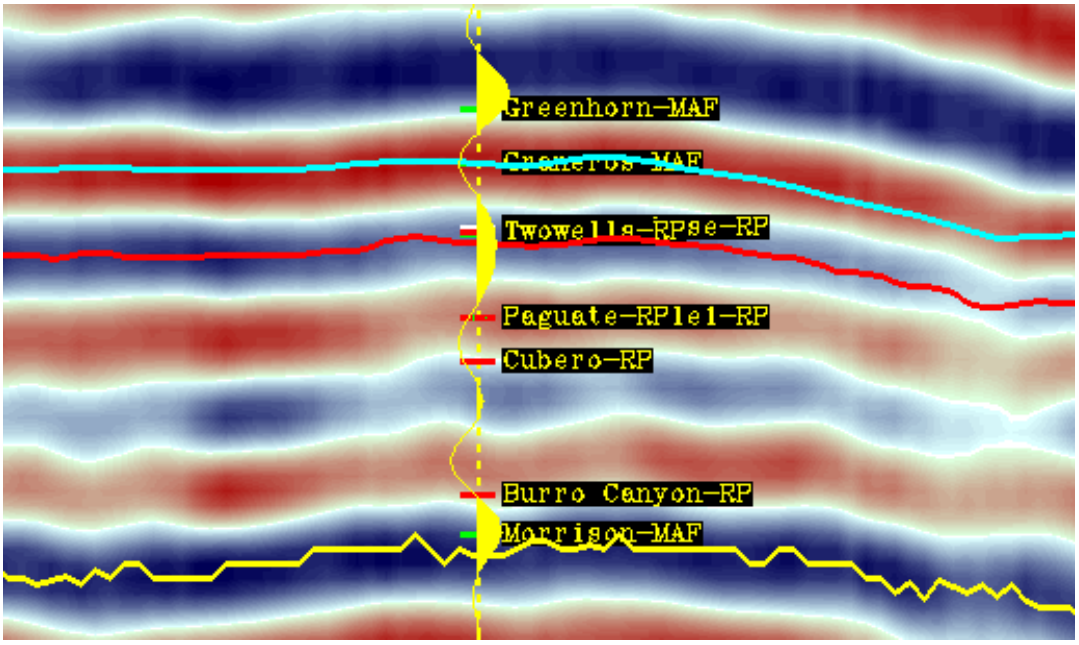

- Make sure you can tie your wells to the seismic data with synthetic seismograms.
- Just because data are nominally zero phase, doesn't mean that acoustic impedance/formation contacts will be directly in middle of peaks or troughs. For seismic thin beds, interference from adjacent reflections may cause pick to be somewhere in between.

Structural Interpretation of Horizons – Visualization

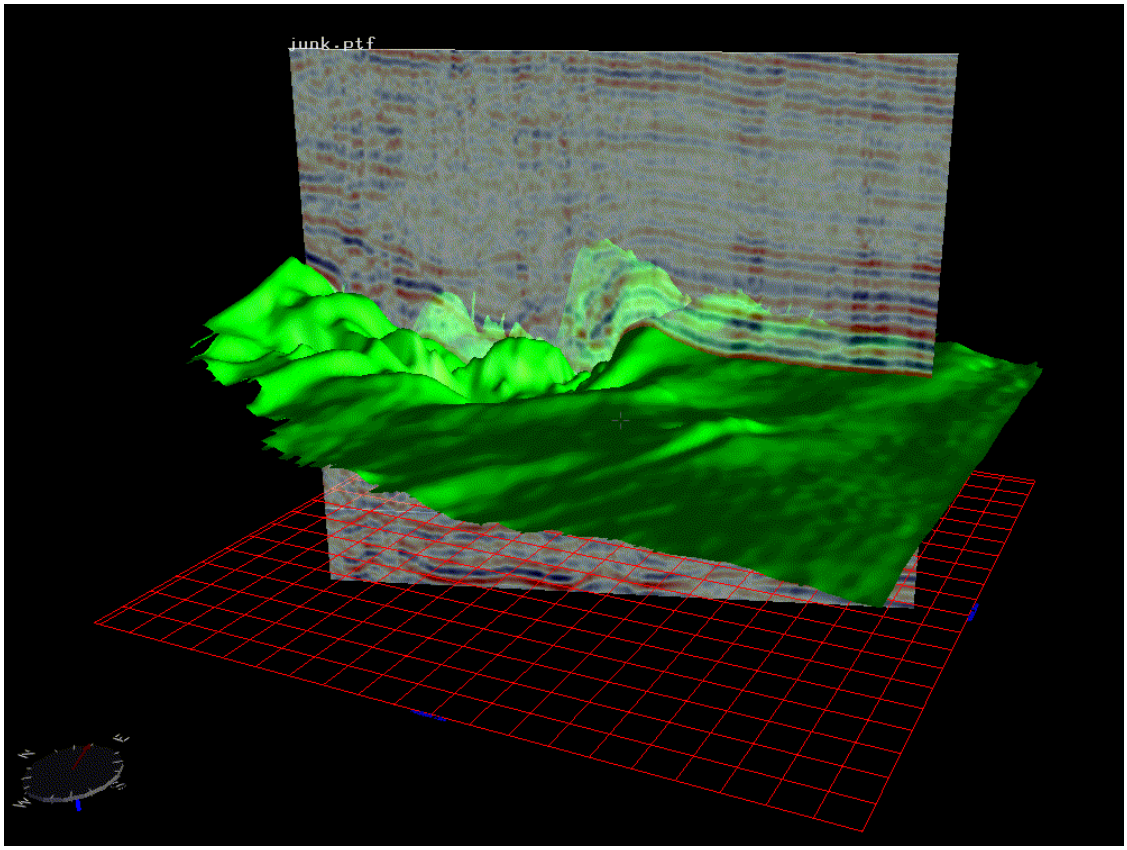

- Maps are useful tools for conveying structural information, but visualization of surfaces may help the interpreter to understand structural relationships (subtle or not-so-subtle)
- Image above shows a “top of salt” horizon picked in an area of salt tectonics. Surface has been illuminated so that shadows highlight structural features. Partly transparent seismic line helps interpreter to understand relationships between horizon and seismic data.

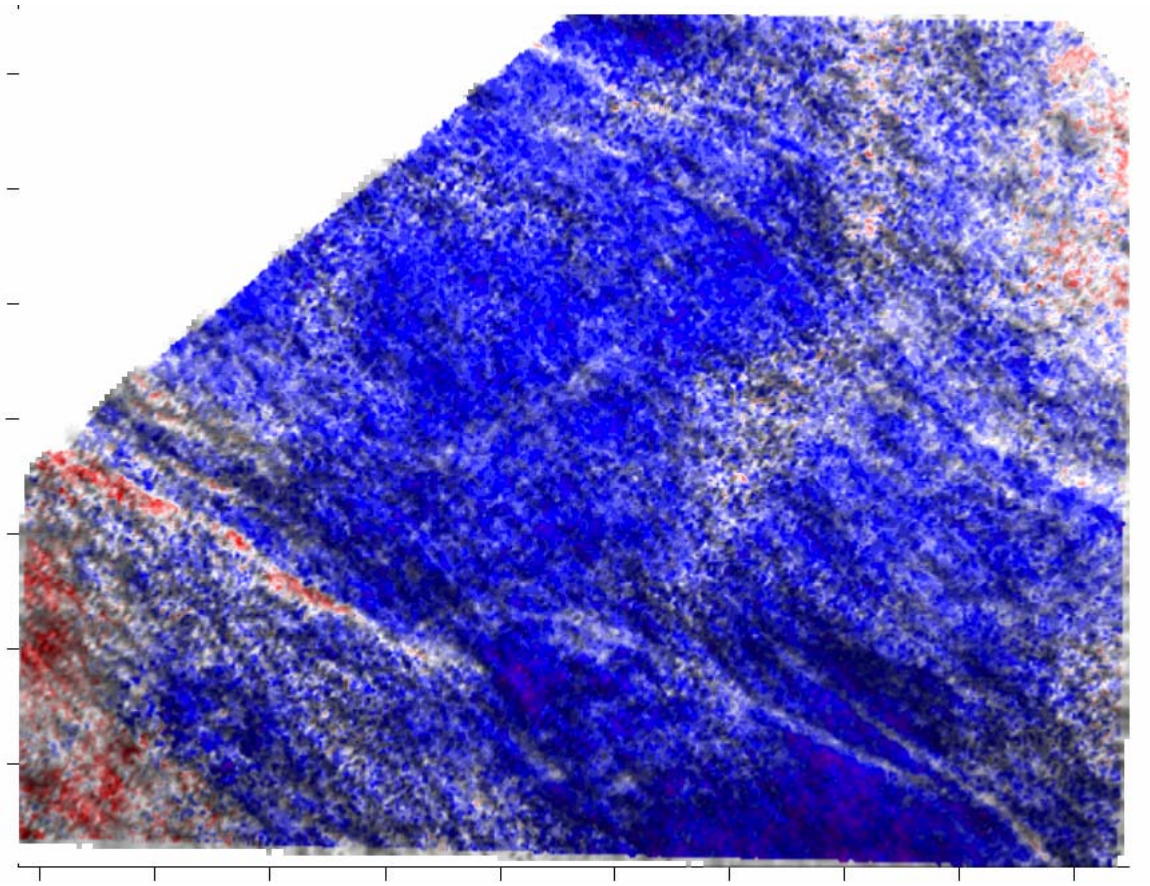

The image above shows the use of surface-associated attributes to define subtle faults in a foreland basin fill. The image shows seismic amplitude map (low amplitudes in red, high amplitudes in blue) draped over a surface visualization that incorporates shaded relief (lighting from upper right). Note how this display highlights the NW-SE trending structures. Area is approximately 100 square miles (256 square km).

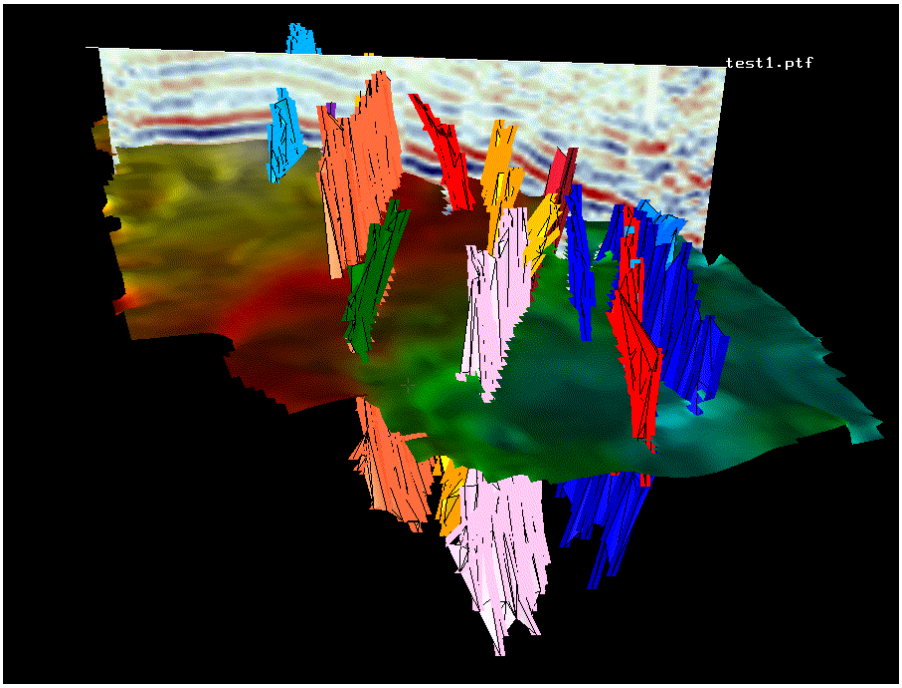

- Use visualization to Q.C. your picks
  - Are they crossing in physically impossible ways?
  - Are they correlated properly?

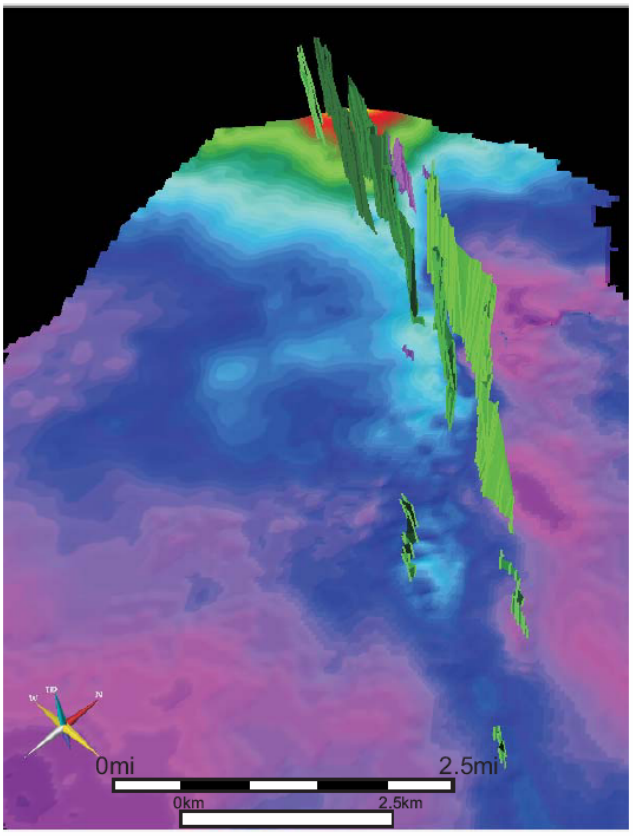

Structural Interpretation – Before and After 3-D Seismic

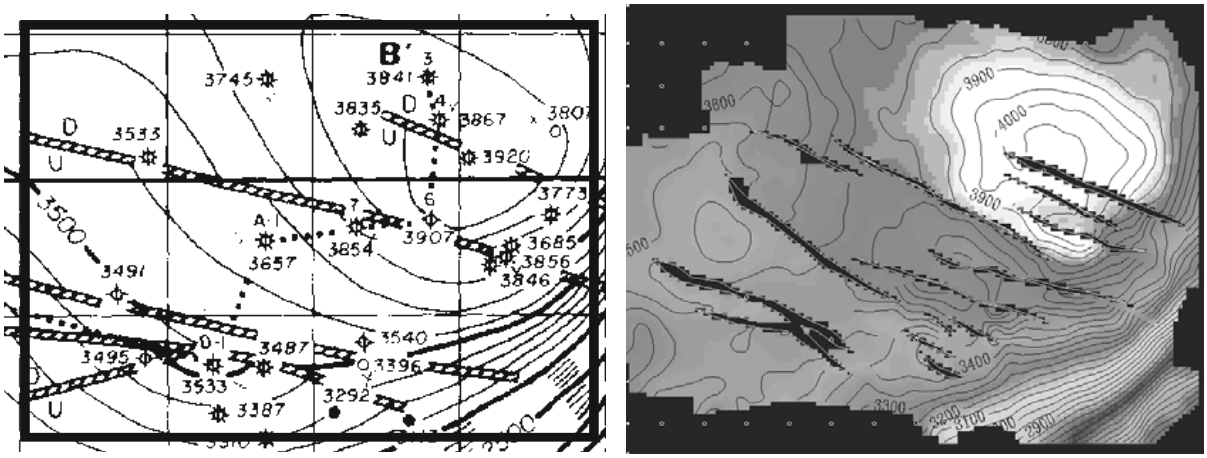

- After 3-D seismic interpretation, many fields are revealed to be more structurally complex than originally thought.
- Image at left above shows a 1979 interpretation of the structure of the Upper Cretaceous Dakota Formation at Ute Dome Dakota Field in northwestern New Mexico based on wells and (possibly) 2-D seismic data. Five faults are apparent. Image at right shows the same formation based on 3-D seismic mapping. Note the dramatic increase in the number of faults that could be mapped.

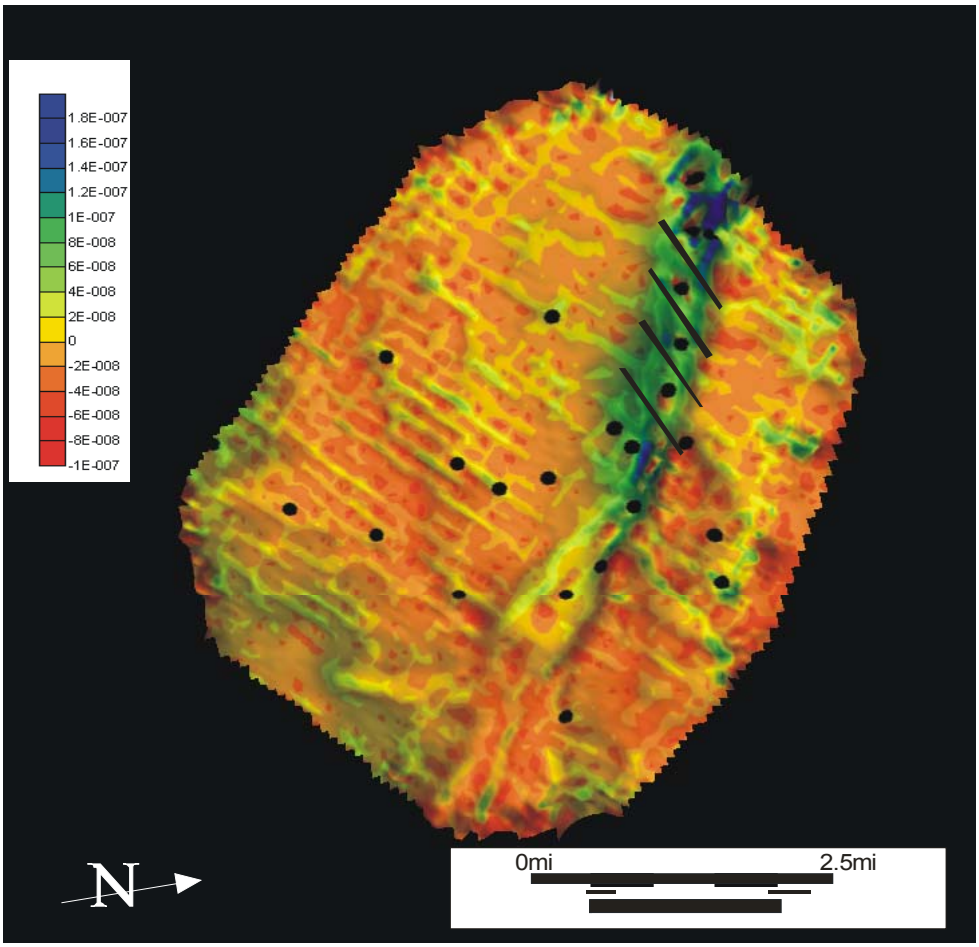

The first pass at the structural interpretation may have identified major faults and folds that can act as traps or conduits for subsurface fluids. However, subtle structures that are at or near the limit of seismic resolution may play an important role in influencing reservoir behavior. These subtle structures are likely to have been missed using conventional interpretation techniques. Like the more easily detectable large faults, subtle faults can act as barriers to fluid flow, conduits for fluid flow (including the breaching of seals) or may be associated with high fracture density ("damage zones" around faults). Subtle folds may also be associated with high fracture density. Fracture zones may be either barriers or baffles to fluid flow (if the fractures have been mineralized) or high-permeability "fairways" (in low permeability reservoirs). In any of these cases, understanding the nature, location, orientation and magnitude of the structures can be important. In this section we will examine a variety of ways for detecting subtle structures, paying particular attention to the role of fractures. Naturally fractured reservoirs, sometimes also referred to as "tight" reservoirs or "basin-centered" reservoir s are a type of unconventional reservoir that is receiving increased attention. Two case studies illustrate the role that fractures can play in determining reservoir behavior.

The image above shows maximum curvature draped over a 3-D representation of a hydrothermal dolomite reservoir. A left-lateral wrench fault system is present. Synthetic shear faults are highlighted by black lines. Dots indicate well locations (not all of which are producers).

Map View

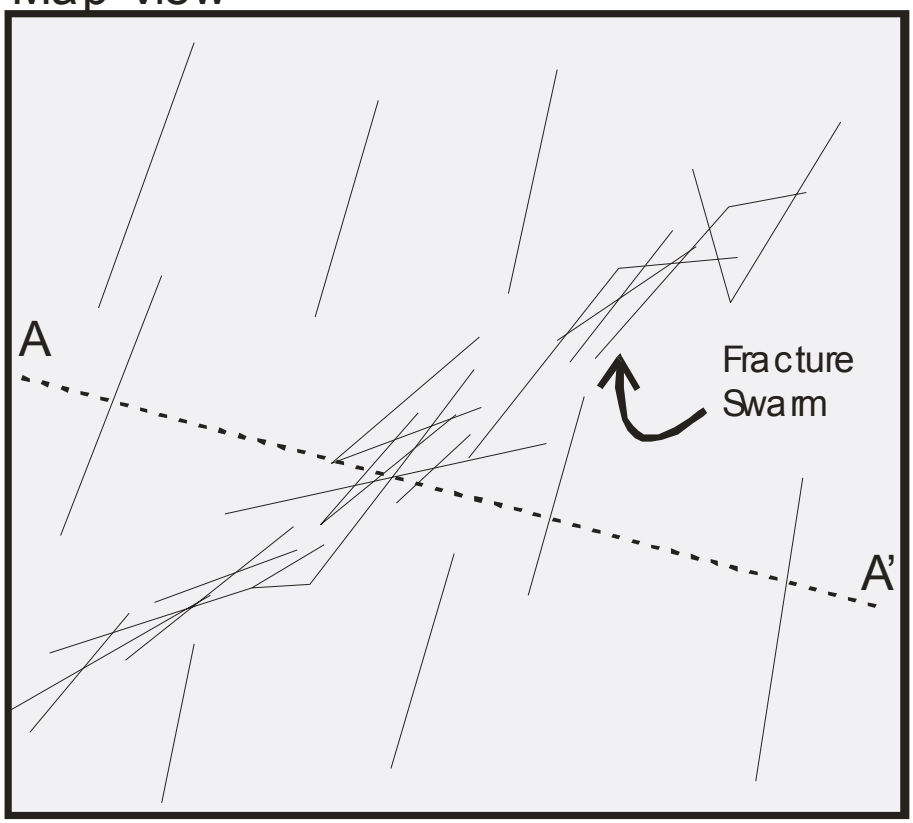

Cross-Section View

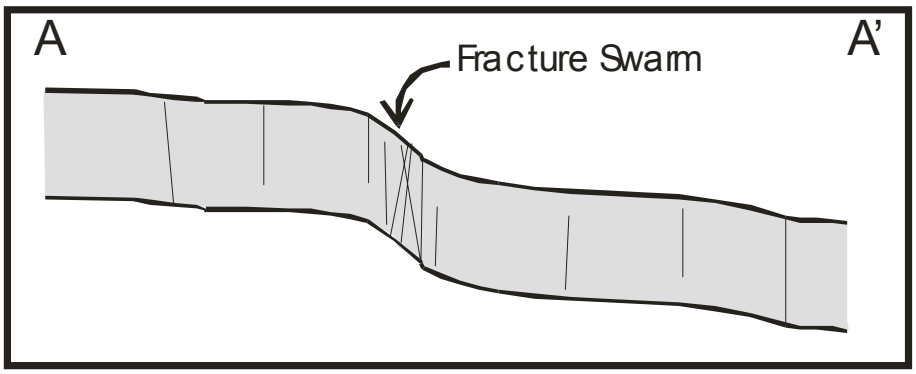

Hart et al., 2001

Fractures can have an important impact on reservoir behavior. Open fractures can act as enhanced permeability conduits in low-permeability reservoirs, whereas mineralized fractures can act as barriers or baffles. For our purposes, we will define two different types of fractures. “Regional fractures” have more-or-less the same orientation, spacing and length, and are found throughout broad areas. They form in response to forces acting over large areas, for example some extension fractures form parallel to far-field compressive stresses found adjacent to convergent tectonic settings. The NNE striking fractures in the upper image might be a regional fracture set formed by NNE-SSW compression. “Tectonic fractures”, such as the fracture swarm indicated above, form in response to localized deformation, such as faulting and folding. The orientation of the tectonic fractures need not be the same as the regional fractures.

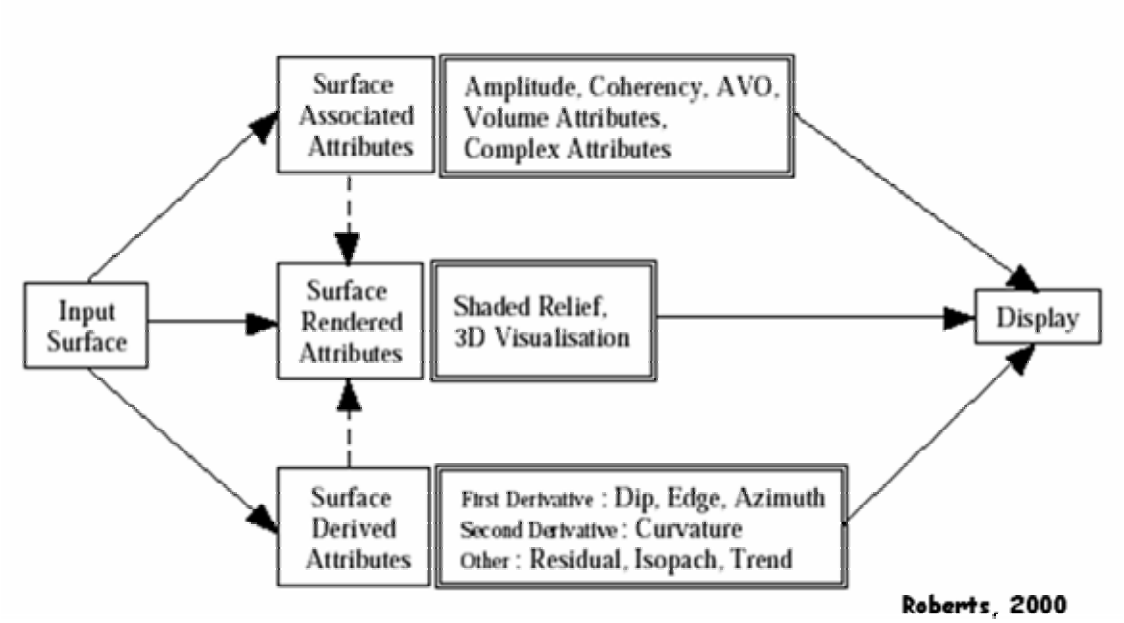

Roberts, 2001

We will focus on subtle structures that are detectable using surface-related attributes, i.e., attributes associated with or derived from horizons that we have mapped in 3-D seismic volumes. The image above, adapted from Roberts (2001), shows three main categories of attributes associated with surfaces. All of these attributes are defined on a bin-by-bin basis. *Surface associated attributes* are those that might be extracted from a 3-D volume along a horizon; they are effectively horizon slices. *Surface rendered attributes* are associated with visualization technologies. *Surface derived attributes* will be the primary focus of this chapter. They are based on mathematical manipulations of the surface to define how it deviates from a planar surface, which way the surface points, etc. Ideally, different types of attributes (e.g., curvature and shaded relief) may be viewed together in a single display by exploiting visualization technologies.

Surface derived attributes are also known as “horizon attributes’.

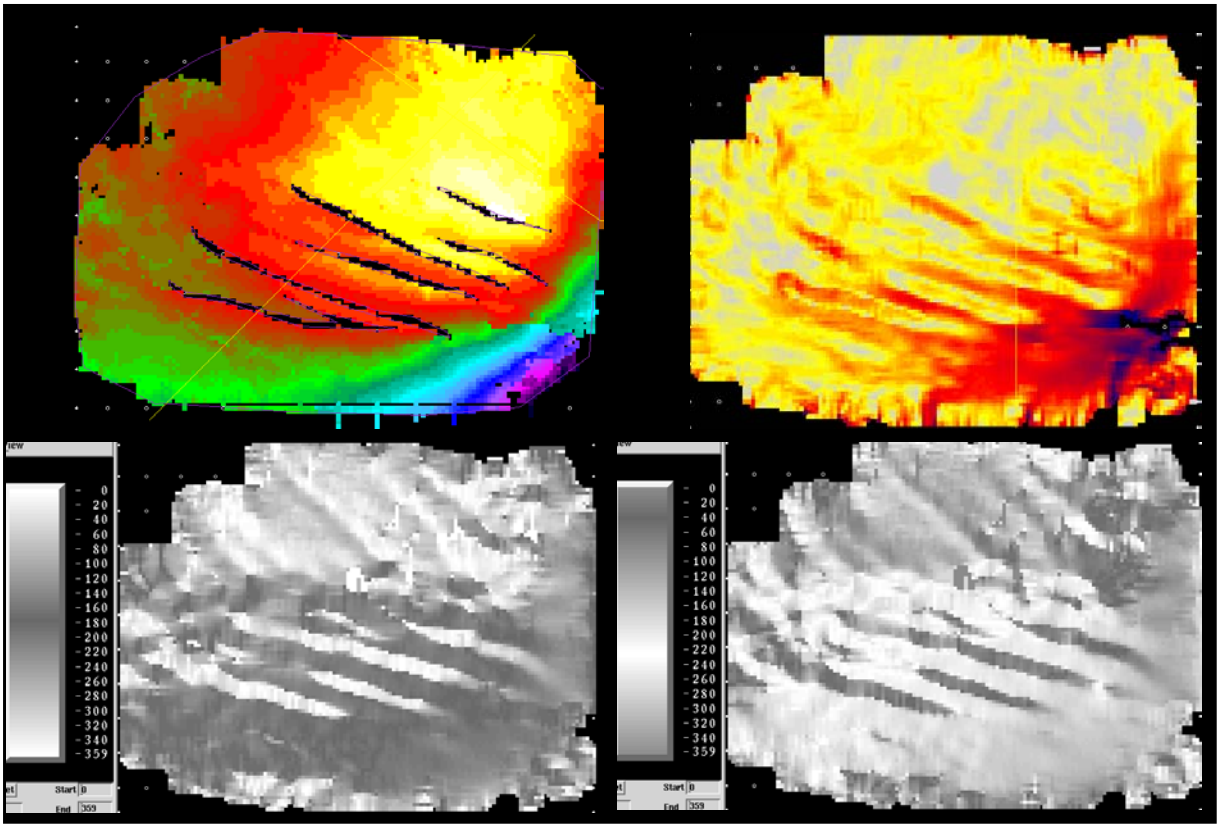

Dip and azimuth are the most widely known horizon attributes. Both attributes are derived by comparing the two-way traveltime (TWT) at a bin with the TWT at neighboring bins. Both are derived at every bin location along a horizon. Dip measures the deviation from the horizontal. Azimuth measures the orientation of the surface (e.g., north, southeast, north northwest – expressed as a compass orientation between 0 and 360).

The images above show dip and azimuth displays for the surface shown at upper left. The surface has fault polygons that were removed during the dip and azimuth calculations.

The dip display is shown at upper right. Flat-lying areas are in white and steepest dips are in red and purple. Comparison of this display and the original time-structure map shows similar trends but some differences that should prompt the interpreter to fine-tune the original fault interpretation.

The lower images are azimuth displays. The color bar has been constructed to mimic the effects of surface illumination. For example, at lower left parts of the surface dipping north will be light, whereas south-facing parts of the surface will be dark (“shadows”). At lower right, parts of the surface pointing southwest will be light and parts of the surface pointing northeast will be dark. The main faults are visible in these displays, but they also bring out some subtle NW-SE structures near the top of the survey.

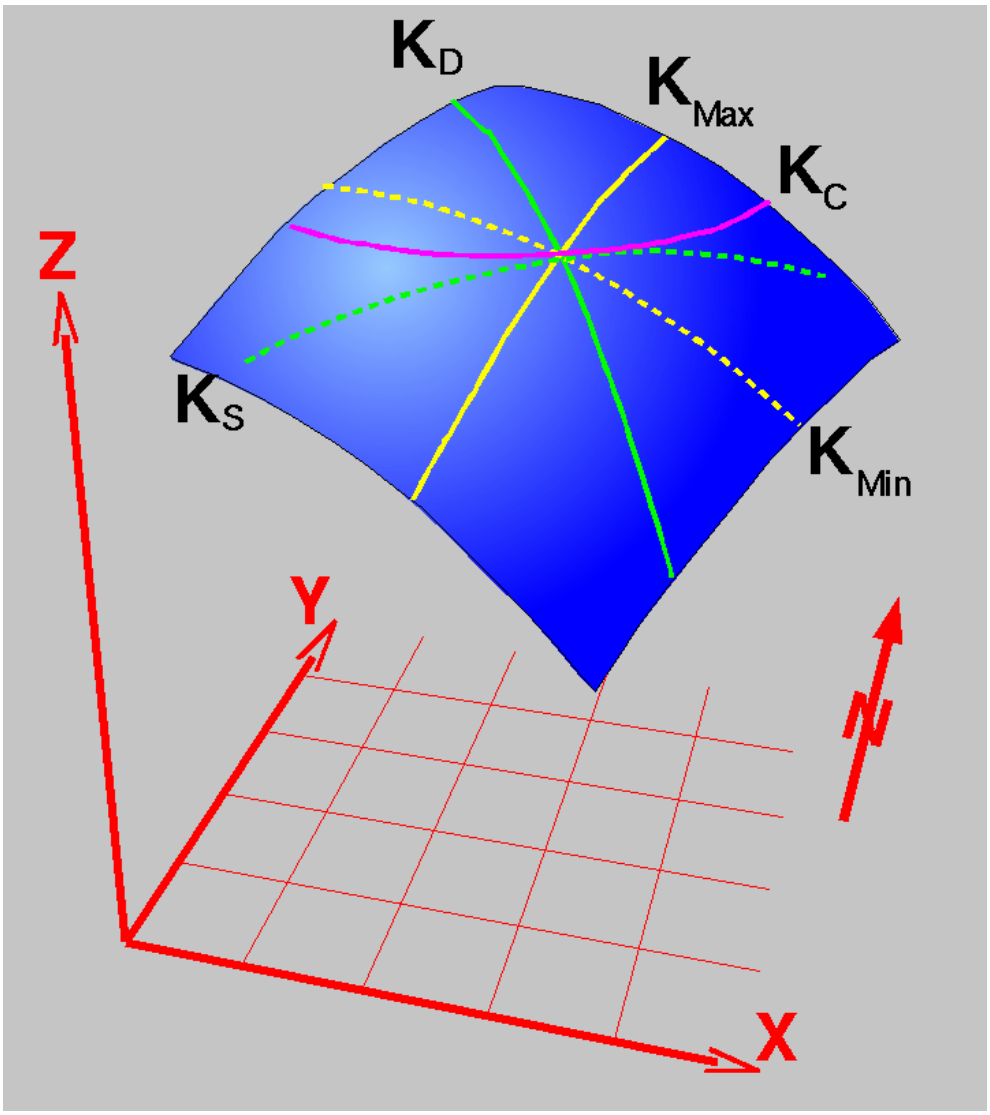

Curvature is a two-dimensional property that describes the deviation of a horizon from a planar surface. An infinite number of curvatures may be derived at any point on a surface, although not all are of interest. Some curvatures are shown above, including:

K_D – Dip curvature (curvature in the dip direction)
K_s – Strike curvature (curvature in the strike direction, at 90 degrees to K_D)
K_{Max} – Maximum curvature (the maximum curvature of the surface)
K_{Min} – Minimum curvature (the minimum curvature of the surface, at 90 degrees to K_{Max})
K_C – Contour curvature (curvature along structural contours)

Roberts (2001) described these and other types of curvature.

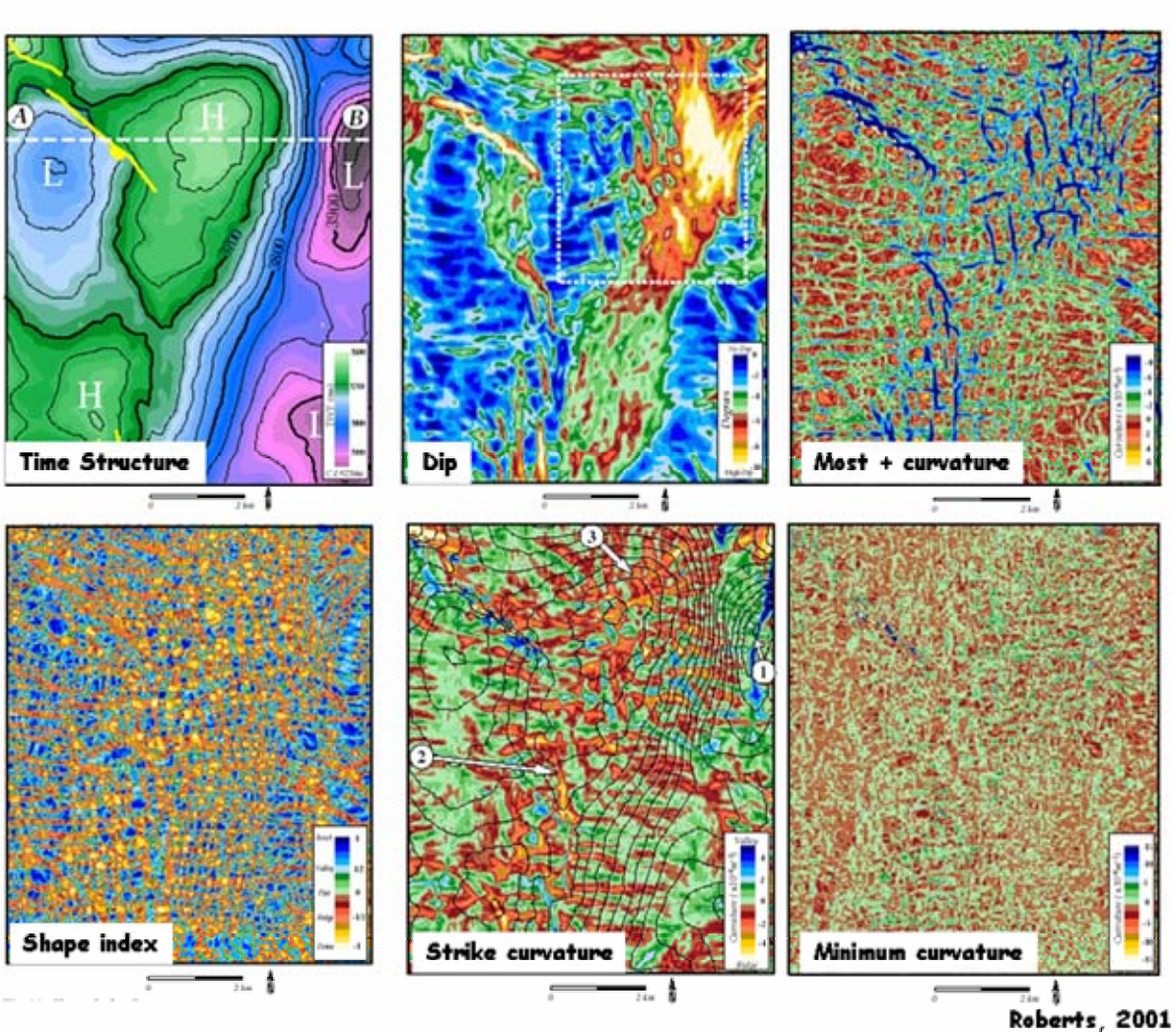

These images, from Roberts (2001), show various curvature attributes derived from a surface mapped in the North Sea. Time-structure shown in upper left. The dip map shows high dips, some of which are associated with faulting (e.g., upper left of image). At upper right in the dip map, steep dips obscure other structures, a problem known as "dip saturation". Note the appearance of structure in this area in the most positive curvature map (upper right). Other curvature maps (lower row) do not necessarily show useable features. In any case, software allows the user to quickly generate and evaluate various types of curvature maps. It is prudent to generate them all, and discard those that are not useful.

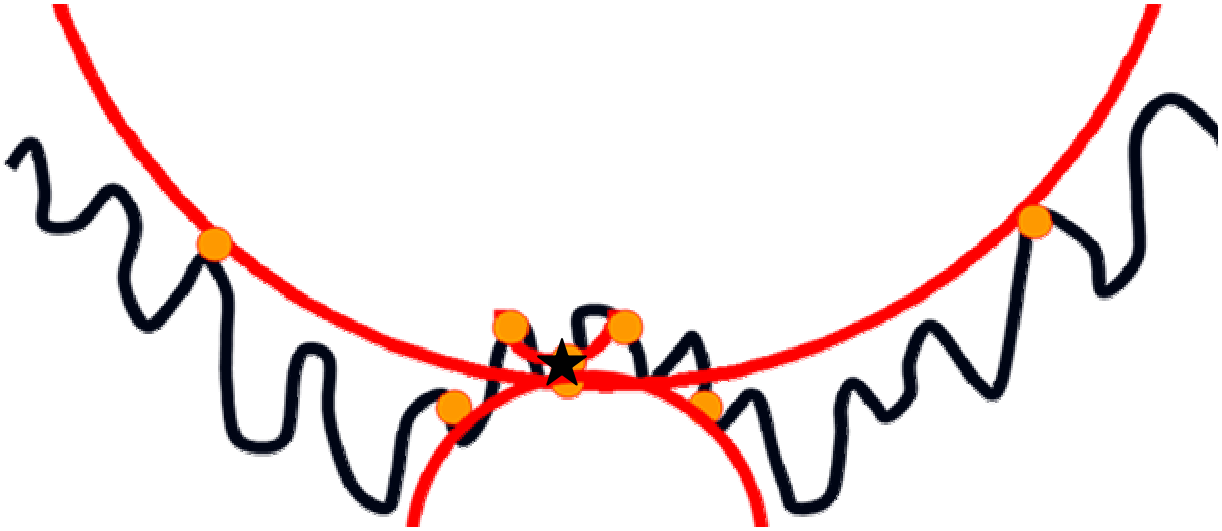

Stewart and Wynn (2000) pointed out that it may be necessary to examine curvature at various scales to account for different wavelengths. With surfaces derived from 3-D seismic interpretations, this involves using bins at various distances (aperture) from the bin for which the calculation is being derived.

The example above illustrates the importance of different apertures. Several different wavelengths of feature are superimposed on the surface (black line). We seek to derive curvature at the bin in the middle of the image (star). If we use the adjacent bins, we derive a curvature that detects the small-scale syncline. If we use bins that are located a few traces away, we might define a medium-scale anticline. If we look at bins that are far away from the center trace, we detect the large-scale syncline.

Which scale of curvature is the most important? Small-scale features are commonly associated with noise in the seismic data, but can also be associated with real structures. Knowledge of the scale of expected geologic features and, perhaps, linking curvature aperture with production data can be useful. More than one scale of curvature might be important.

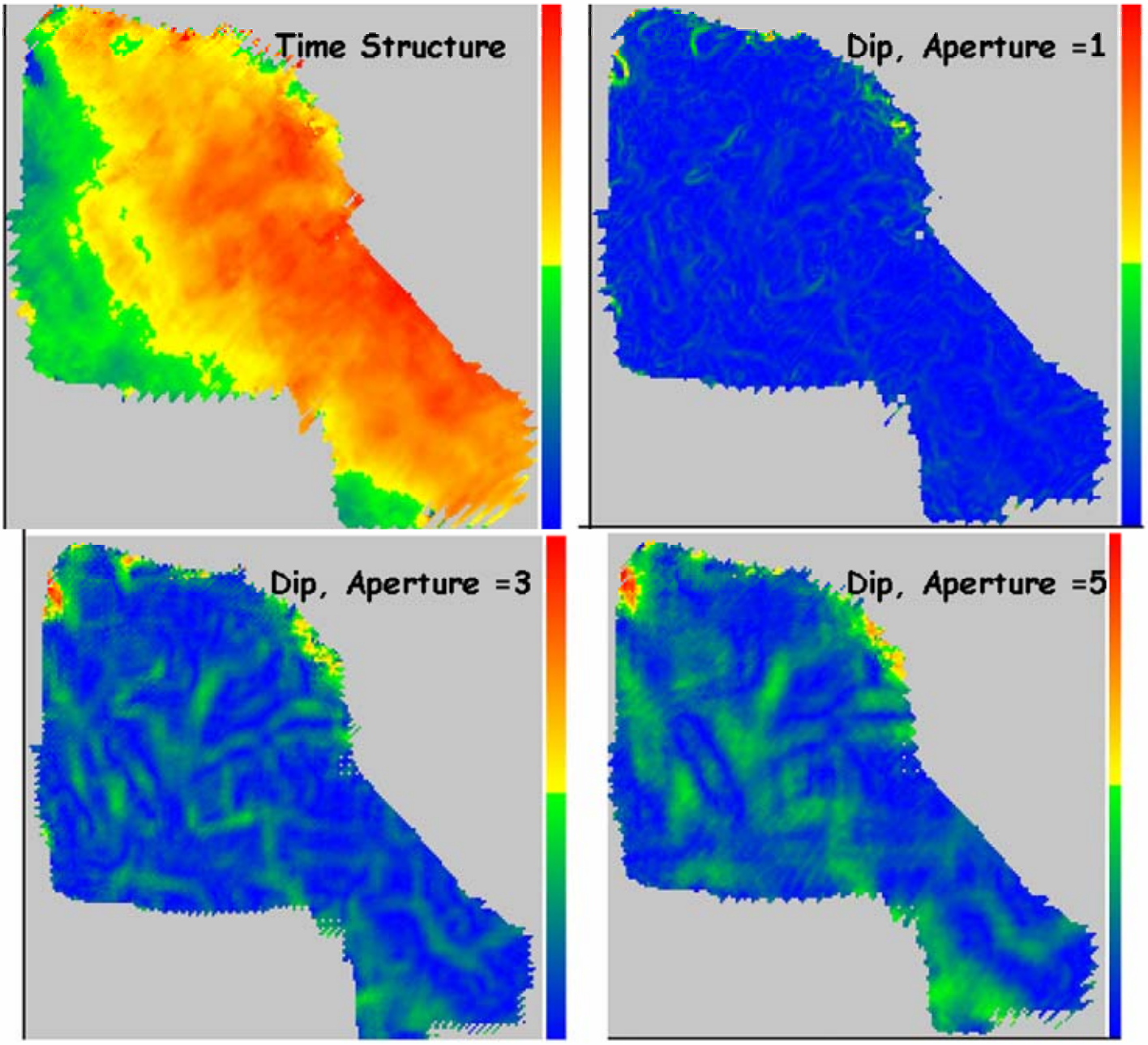

These images show the effect of changing the aperture when calculating curvature using the *Curvz* application (available at: http://www.eps.mcgill.ca/~hart/CURVZ_website.htm). Upper left shows a time-structure map (structural lows in orange). The other three images show horizon dip derived using apertures of 1, 3 and 5 bins. The image derived using an aperture of 1 bin shows short-wavelength features that are associated with noise around the margins of the survey. As the aperture is widened, real structures become apparent.

Case Study: Tight Sandstones

The following material is drawn from a paper, in preparation, that describes some of the analyses associated with the characterization of a low-permeability Cretaceous tight-gas reservoir. Tight-gas reservoirs are sometimes also referred to as “naturally fractured” or “basin-center gas” reservoirs although there is currently debate about the nomenclature. In North America, production from “unconventional” gas reservoirs, such as tight-gas sandstones and coalbed methane, is becoming widespread, with some estimates suggesting that tight-gas sandstones may eventually account for up to ½ of domestic US production.

The study area is the San Juan Basin of the southwestern USA. Two Upper Cretaceous units, the Mesaverde Group and the Dakota Formation, produce from low matrix-permeability sandstones that were deposited in shelf, shoreline and coastal plain settings as second-, third- and higher-order cycles prograded to the northeast and were pushed landward (SW) during transgressions. Drilling depths are approximately 1500 m (~5000’) for the Mesaverde Group and 2500 m (~7000’) for the Dakota Formation. The Mesaverde had produced approximately 8.5 TCF by the end of 1997, and the Dakota had produced approximately 5 TCF by the end of 1997. Matrix permeability is variable, but generally < 0.1 md. These permeability values cannot be reconciled with production rates and so natural fractures are thought to contribute significantly to production. Natural fractures have been observed in core, borehole image logs and outcrops of equivalent strata.

Wells drilled in this area generally produce < 1 BCF although occasionally much higher production is encountered in “sweet spots”. 3-D seismic data is not used extensively to guide drilling, and so the origin of the enhanced production remains enigmatic.

Four “sweet-spot wells” are present in the area of a ~ 260 km^2 (~100 square mile) 3-D seismic survey. Three of these wells are located on curvature-defined subtle structures thought to be associated with trans-tensional wrench faulting. Drainage interference is present between two of the wells, separated by ~3 km, that both lie on one of the fault trends. High fracture density, responsible for the enhanced production and drainage interference, is associated with faults. The fourth sweet-spot well is located on the flank of a half graben, another area of suspected high fracture density.

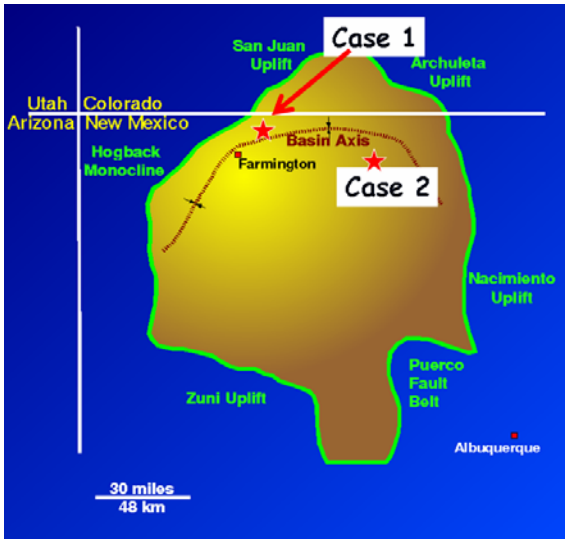

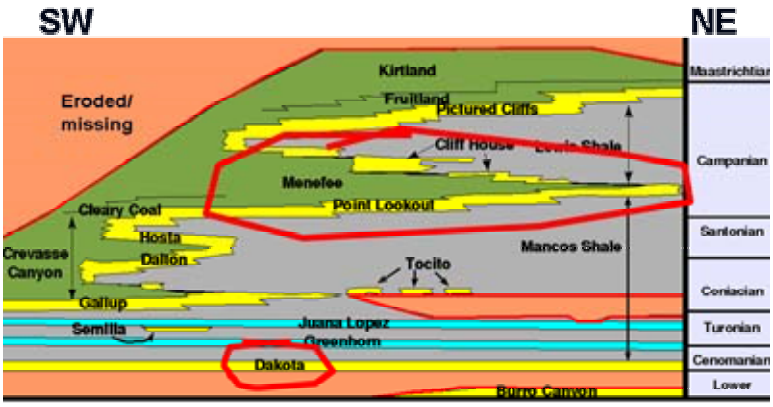

San Juan Basin – New Mexico

Location map (left) showing the San Juan Basin and the location of the Mesaverde ("Case 1") and Dakota ("Case 2") examples presented here. The image at right shows a schematic cross-section through the basin showing the relative stratigraphic positions of the Mesaverde Group and Dakota Formation.

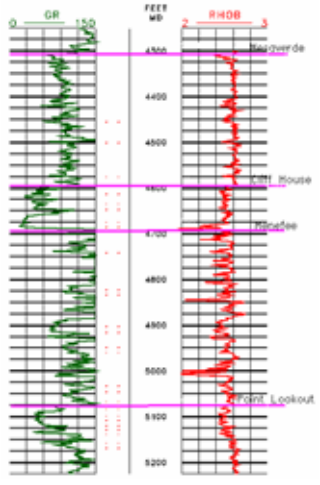

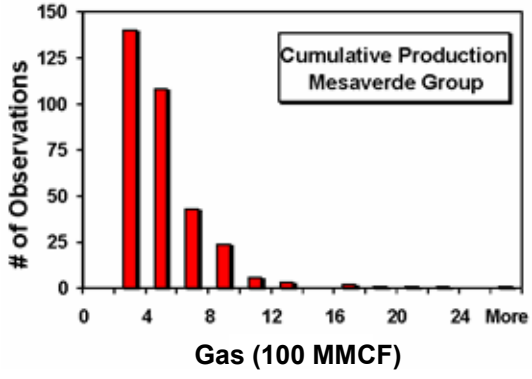

Sample logs through the Mesaverde Group in the Case 1 study area showing the log expression of the Point Lookout, Menefee and Cliff House formations (left). Histogram at right shows cumulative production for wells in the area of the 3-D seismic survey. A few wells have produced much better than the others.

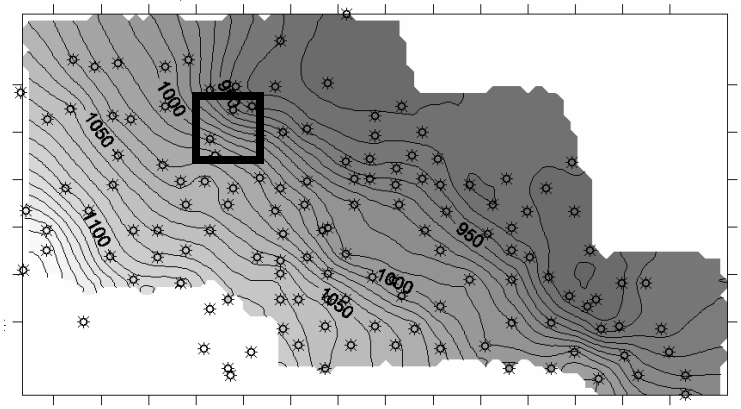

Structure map of the top of the Point Lookout Formation generated by integrating 3-D seismic and wireline log data. The area of the subtle structures shown on the next page is indicated by the square. These structures are not apparent on this map.

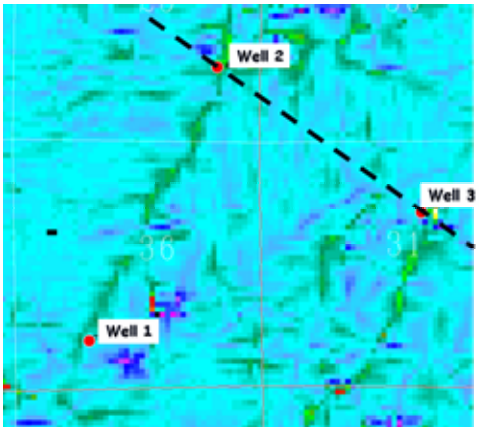

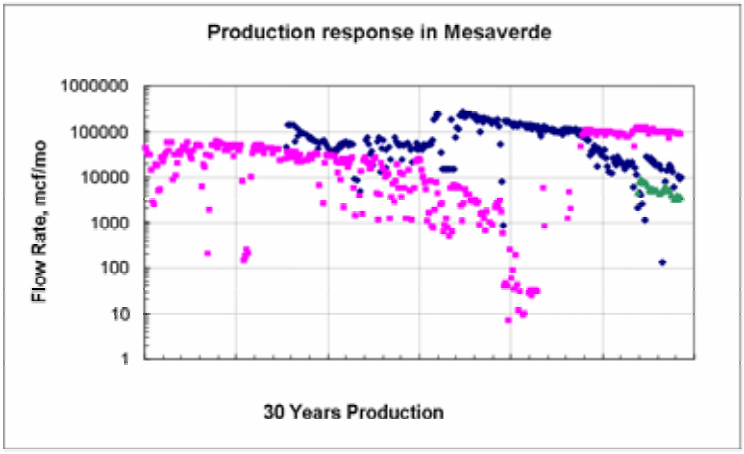

Strike-curvature map (left) shows the location of three sweet-spot wells on NE-SW striking structures. In this display, green areas are concave up (structural troughs) and blue are convex up (ridges). Rate versus time plot for Well 1 and Well 2, both located on the same curvature-defined structure, shows drainage interference between the wells. Other producing wells between these two wells (not shown on the map at left) show no signs of drainage interference.

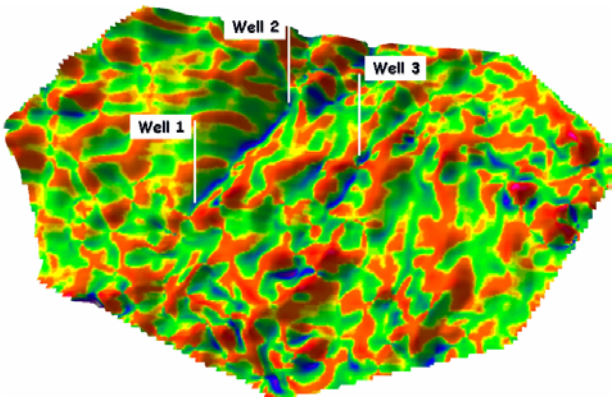

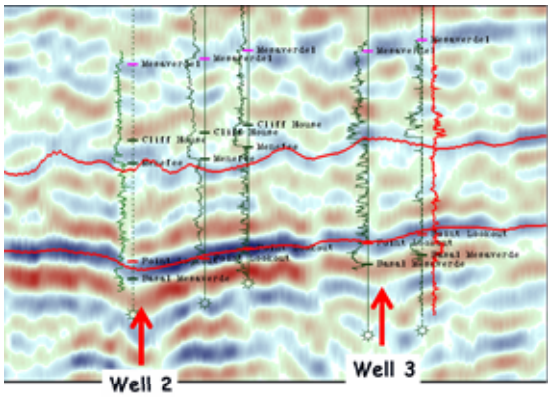

Visualization of curvature attribute showing the location of sweet spot wells in small trans-tensional grabens. The seismic transect at right, location shown in map at top left of this page, shows the very subtle seismic expression of the structures.

The Dakota Formation likewise has subtle, but production-enhancing, structures that may be defined using curvature analysis of 3-D seismic data. This is illustrated using a 3-D seismic dataset that comes from an area approximately 50 km to the southeast of the Mesaverde example. Wireline logs commonly show evidence of borehole washouts in the sandstones; the sandstones are commonly heavily fractured (as seen in outcrop) and brittle.

A single Dakota sweet-spot well is present in the 3-D survey area. It lies on a curvature-defined structure. Drainage interference cannot be used to prove the existence of a dense fracture network associated with the structure, but the structure overlies and is parallel to a Paleozoic normal fault that may have been reactivated during the Late Cretaceous or Early Tertiary as a wrench fault. Thus, there is geologic support for the fracture interpretation.

The Mesaverde and Dakota examples illustrate the importance of fracture swarms in enhancing production from low-permeability reservoirs. Integration of 3-D seismic and other data types (log, core, outcrop analogs, engineering) plays an important role in the characterization of these reservoirs.

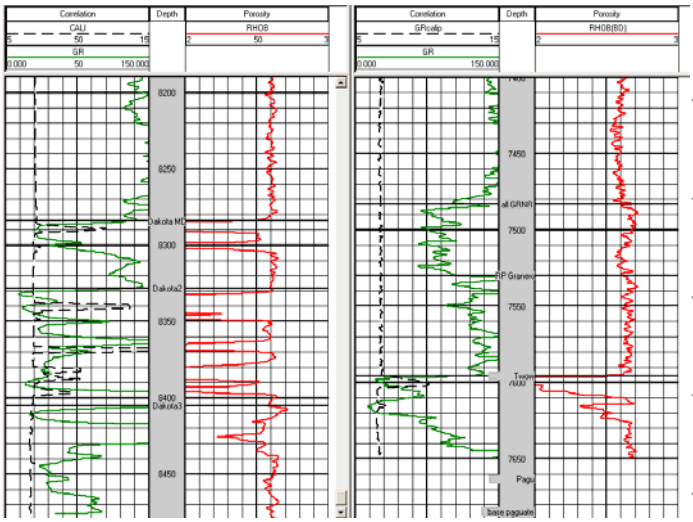

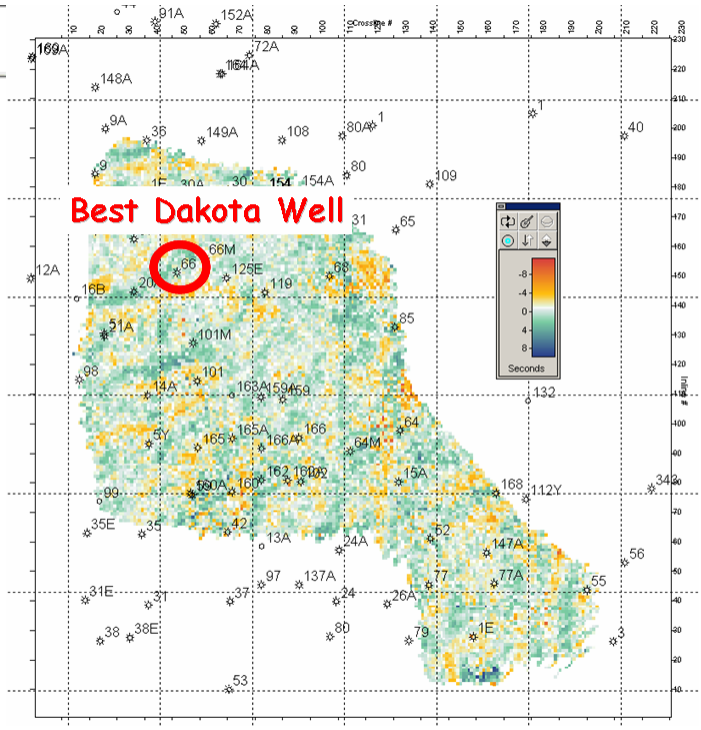

Sample wireline logs through the Dakota Formation (left). Borehole enlargement and anomalous low density values in the sandstones indicate caving zones associated with fractures. Map at right shows the location of the best-producing Dakota well on a strike-curvature anomaly.

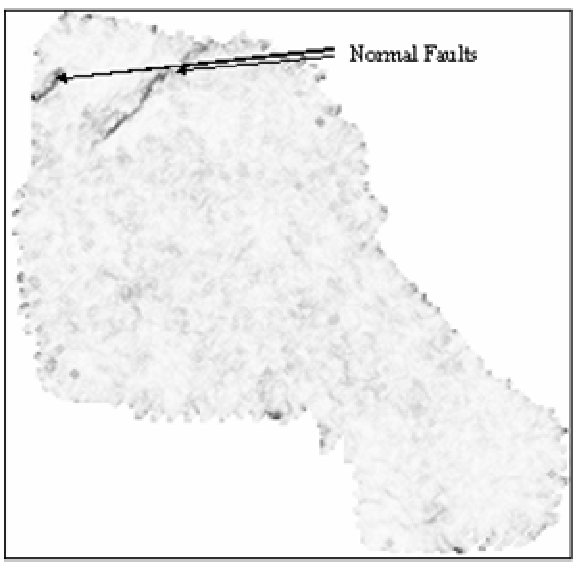

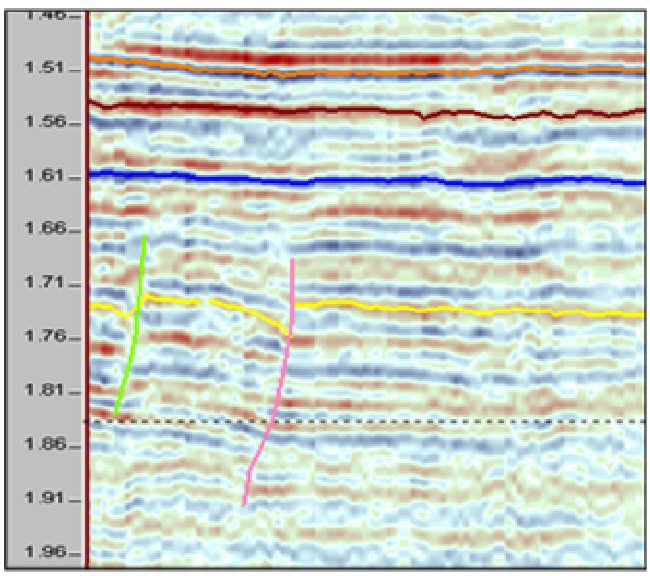

Dip map on a Paleozoic horizon, high dips in black, shows the location of two normal faults (left). The arbitrary line at right shows the seismic expression of the faults. They were probably reactivated as strike-slip faults during the Late Cretaceous/Early Tertiary Laramide Orogeny.

Depth Conversion

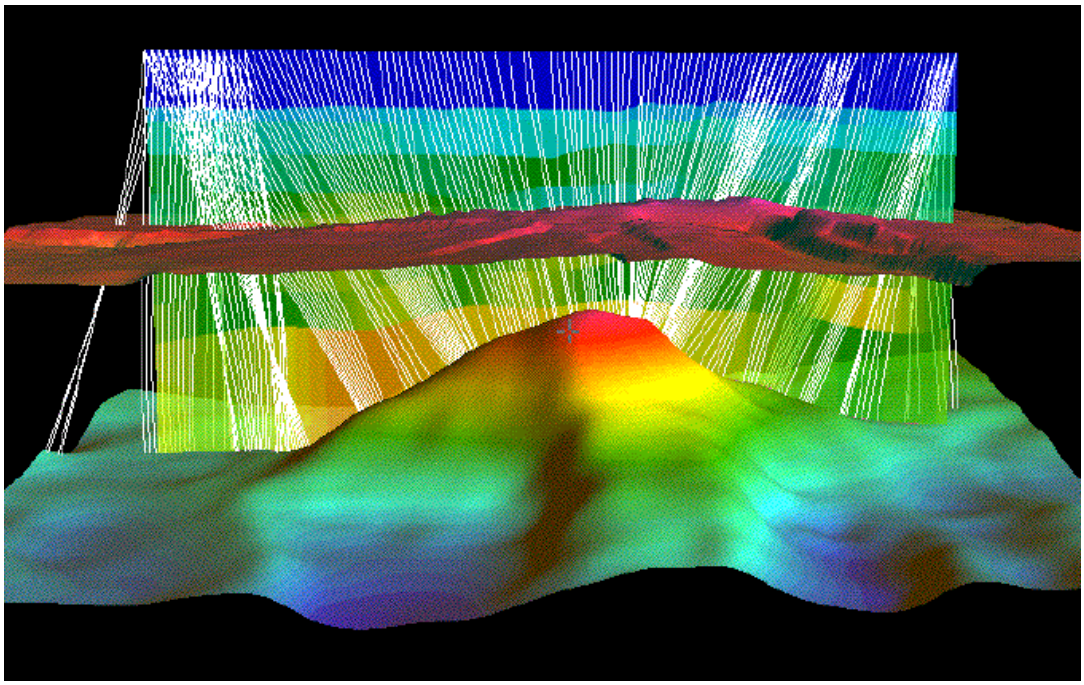

- Seismic data measure depths (“distances”) in time (TWT). Drilling must be done in depth. Furthermore, velocity problems may distort true structural relationships in time sections/maps. As such, there is a need to depth convert seismic data/horizons/faults. The seismic data themselves may be converted to a depth volume.

- Various methods used for depth conversion, although all are based on simple relationship:

  Distance = Velocity x Time

- Degree of sophistication of the depth conversion method depends on variability (lateral, vertical) of velocity field. In this chapter we focus on some of the simpler methods.

Depth Conversion – Simple Average Velocity

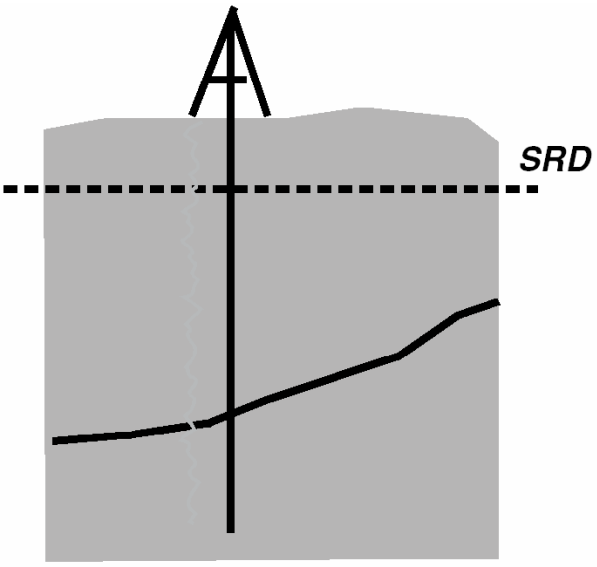

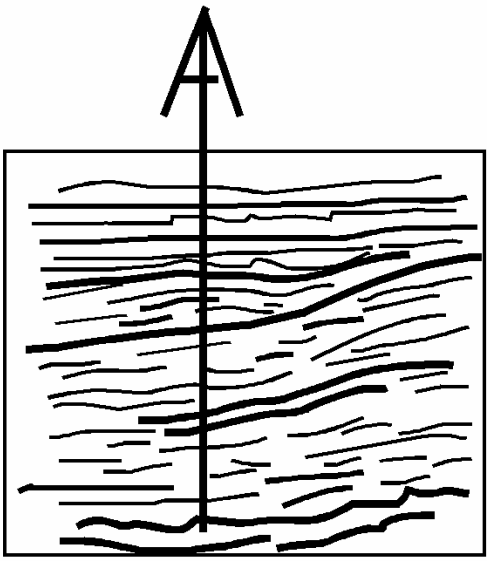

Measured depth (m) ***Measured TWT (s)***

Velocity = Distance/Time
= (Depth below SRD)/(1WT)

- Integrated 3-D interpretations provide two pieces of structural information:
  - Depth to top of a formation from well logs, converted to a depth (distance) (above, left)
  - Two-way traveltime to associated seismic horizon at the well location (above, right)
- Convert depth to depth below seismic reference datum, and convert TWT to a one-way time.
- Average velocity from seismic reference datum to top of formation (at the well location) is then equal to the depth below the seismic reference datum divided by the 1WT

Depth Conversion – Simple Average Velocity

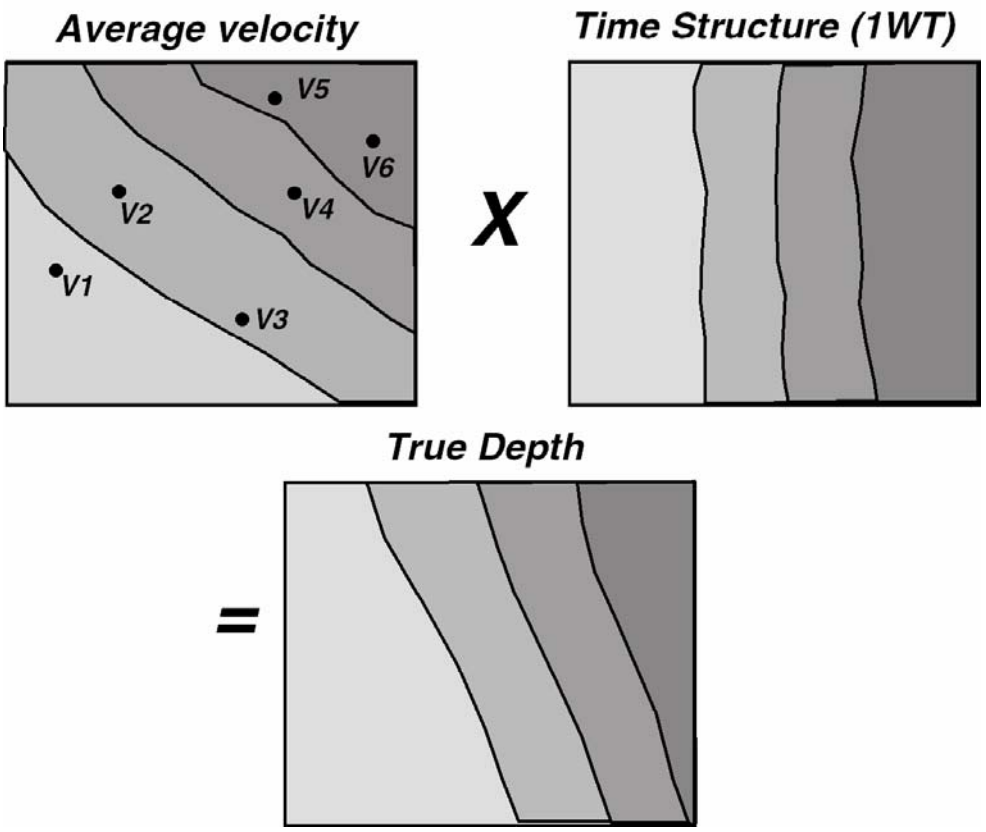

- Repeat procedure from previous slide for each well. It should then be possible to contour the data to produce a velocity map (upper left)
  - Wells should cover area of 3-D survey
- Multiply velocity map by a 1WT structure map (upper right). Result is a depth map (bottom)
  - Need to account for difference (if any) between seismic reference datum and sea level to convert to true depth/elevation with respect to sea level

Depth Conversion – Simple Average Velocity

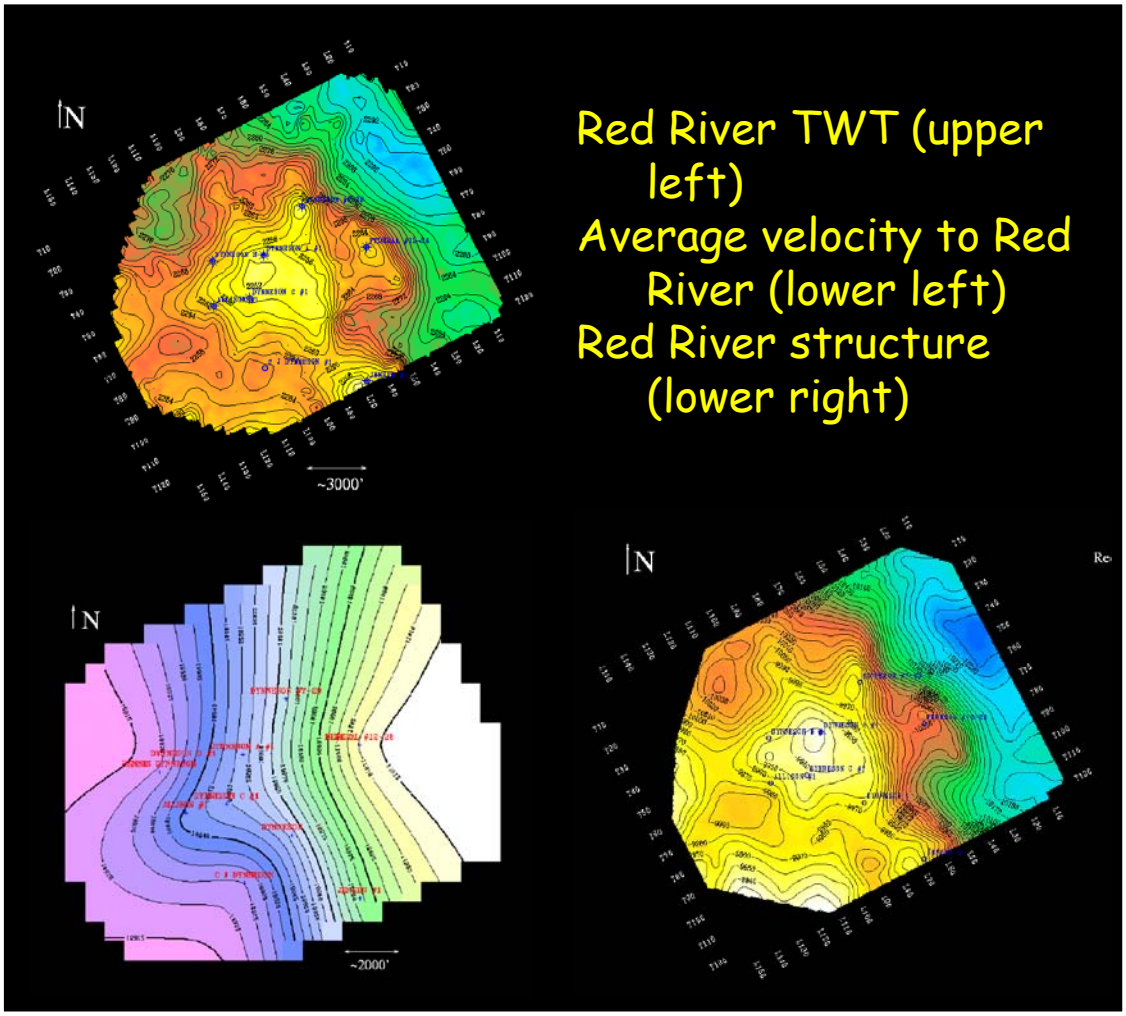

- Example of simple average velocity method
  - Image at upper left shows time-structure map of an Ordovician carbonate buildup in the Williston Basin
  - Image at lower left shows velocity map produced using ten wells. Note the non-uniform velocity gradient
  - Image at lower right shows depth-converted structure map. There are some subtle differences between it and the time-structure map but generally the two are quite similar. This is not always the case.

Depth Conversion – Simple Average Velocity

Nisku TWT

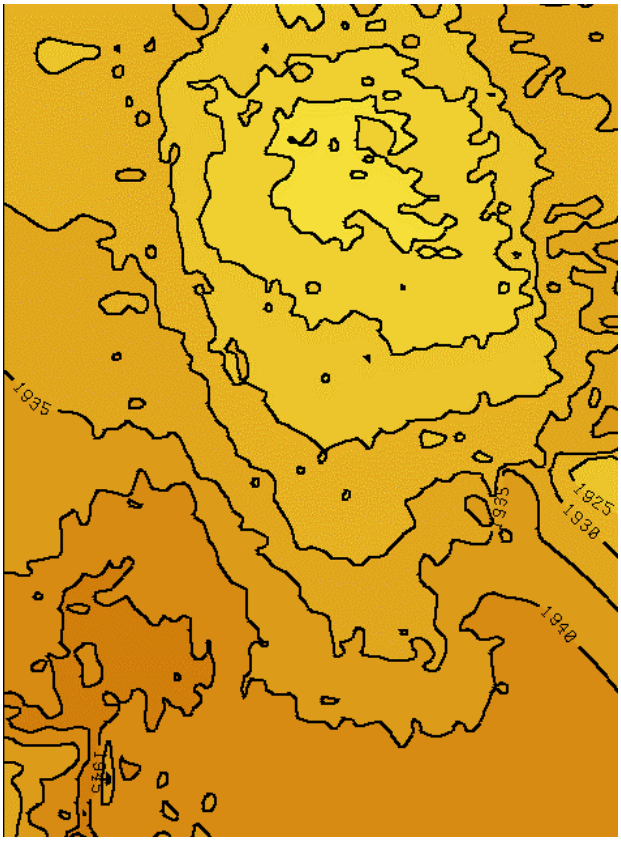

Nisku Depth

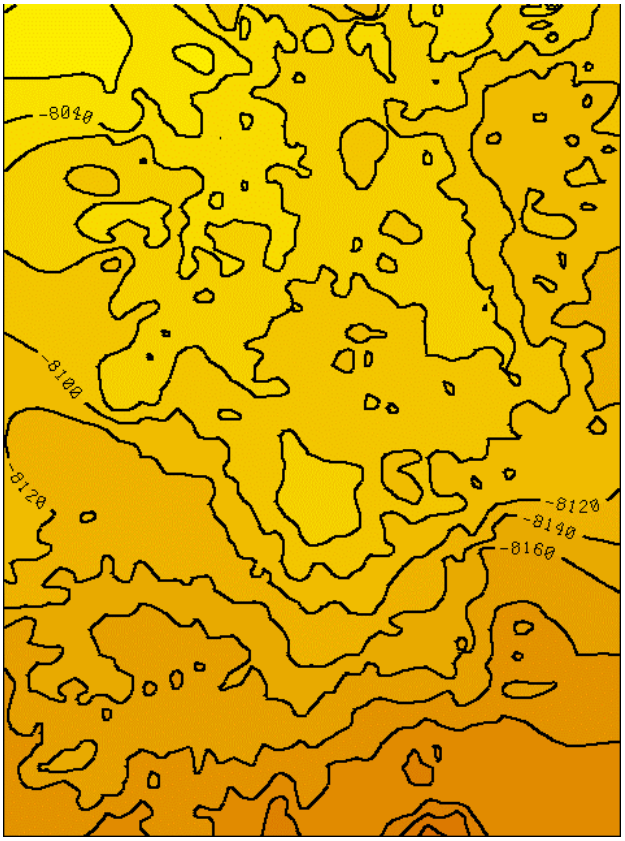

- Sometimes the differences between the time-structure map and the depth-converted map aren't subtle.
- Images above show time-structure map for a Devonian horizon in eastern Montana (left) and corresponding structure map (right) that was depth-converted using a simple average velocity model.
  - Subsequent drilling showed map on right to be accurate to within a couple feet.

Depth Conversion – Simple Average Velocity

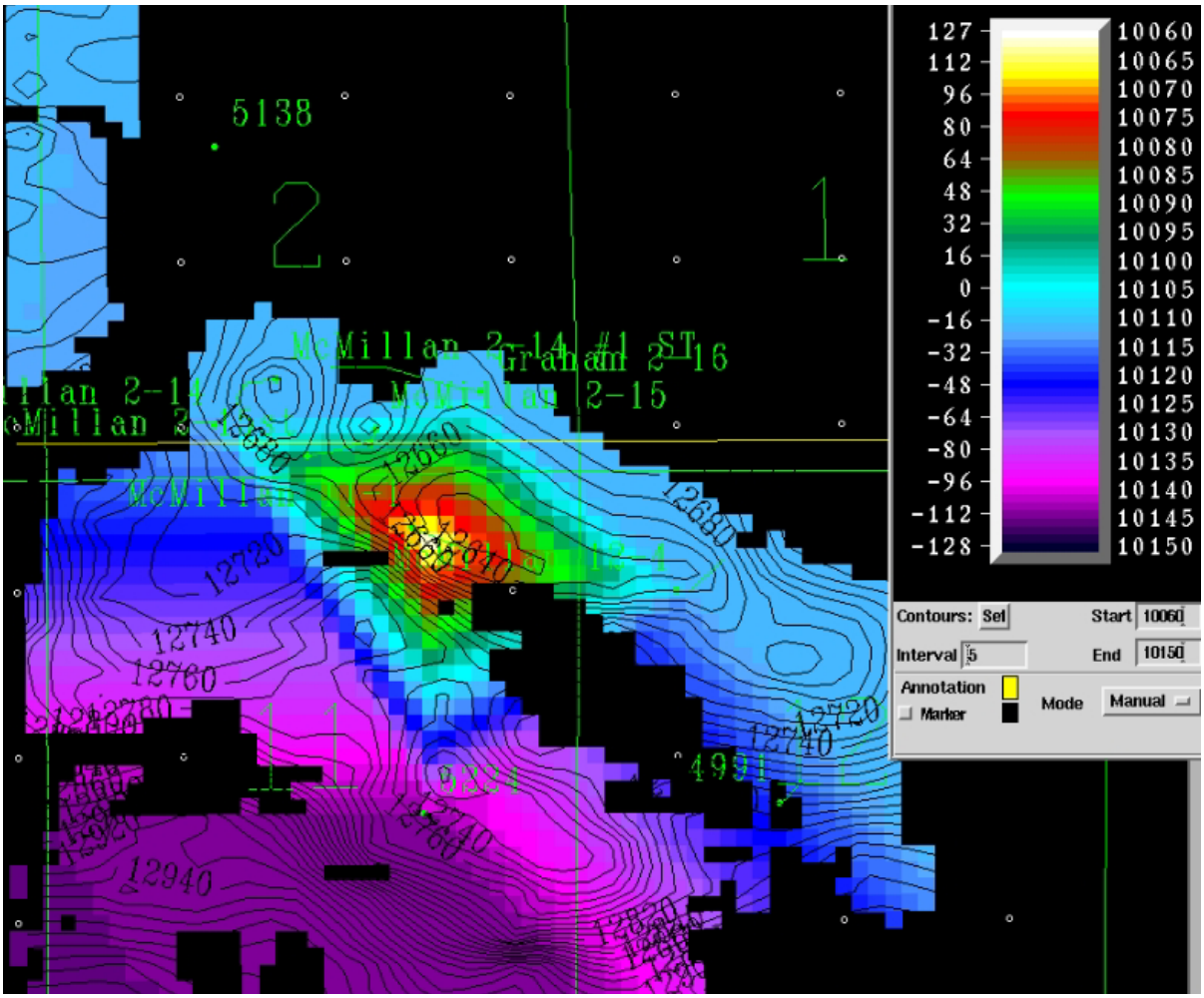

- A problem with the simple average velocity map is that the interpreter can force-fit an answer, getting a result even when there may be bad input data. QC your velocity and structure maps carefully to help avoid this problem.
- Image above shows a big velocity anomaly around a well in the center of the image. Unfortunately the wrong deviation survey had been loaded for this well.

Depth Conversion – Simple Average Velocity

- Pros
  - Simple
  - Can be very accurate
    - Need representative coverage throughout survey area
    - Need accurate picks (logs, seismic)
    - Need accurate database (KB, deviation surveys, etc.)
- Cons
  - Can obtain a solution even when it isn't correct
  - Solution limited to a single horizon
- QC
  - Re-evaluate picks (seismic, log) and well data
  - Look for bulls eyes
  - Use smoothed average velocity map and look for differences
  - Assess geological meaning of velocity maps

Depth Conversion – Downward Layer Building

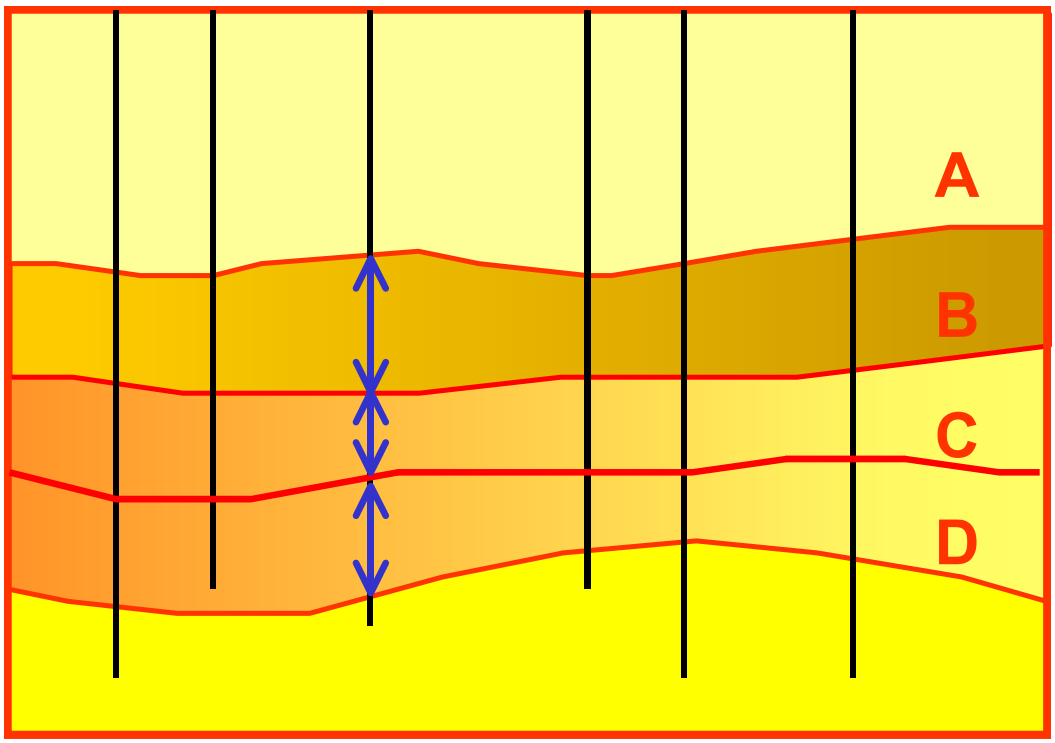

- Once a horizon (A) has been depth converted, it is possible to depth convert lower horizons through a downward layer building approach.
  - Start with depth-converted layer A
  - Derive isopach A-B using A-B isochron and velocities derived from well picks and isochron
  - Add A-B isopach to depth-converted horizon A to get structure of B
  - Continue working down to lower horizons
- Pros
  - Consistency, simplicity
- Cons
  - Errors are cumulative

Depth Conversion – Hybrid

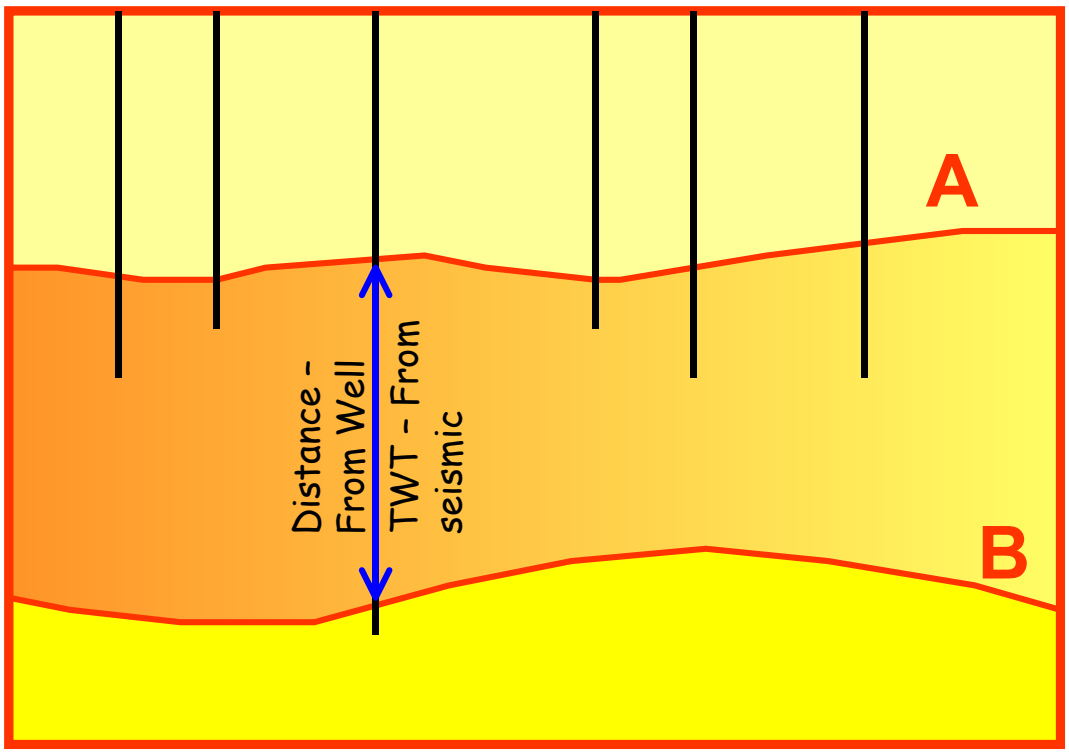

- Depth convert shallow horizon “A”
- Calculate average velocity for interval A-B
  - Use distance from wells, time from seismic
- Calculate thickness for A-B
  - Multiply velocity x isochron
- Add thickness of A-B to depth-converted A
- Helps account for velocity variations above A, but assumes no lateral velocity variations between A and B

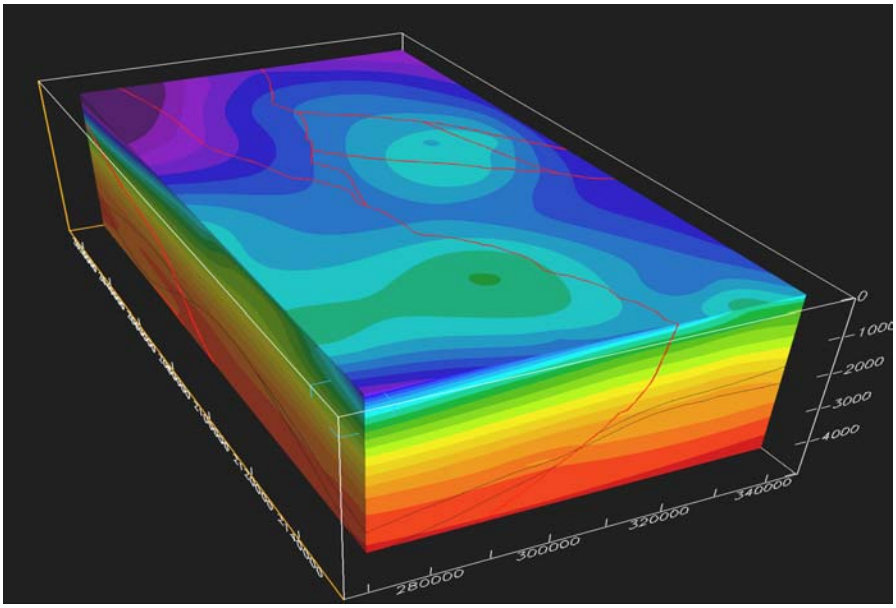

- It is possible to create velocity cubes using data from a variety of sources:
  - Multiple depth-converted horizons (downward layer building)
  - Stacking velocities (need to be calibrated, good spatial control)
  - Checkshot surveys, VSPs
  - Etc.
- Horizons/faults may be depth-converted by inserting them into the cube.
- Complexity of velocity model will be a function of structural complexity, complexity of velocity field, availability of data, cost/benefit analysis
- As shown below, it is possible to insert faults into velocity cubes, and have velocity fields vary from one fault block to another
- It is possible to use velocity cubes to depth convert an entire seismic volume

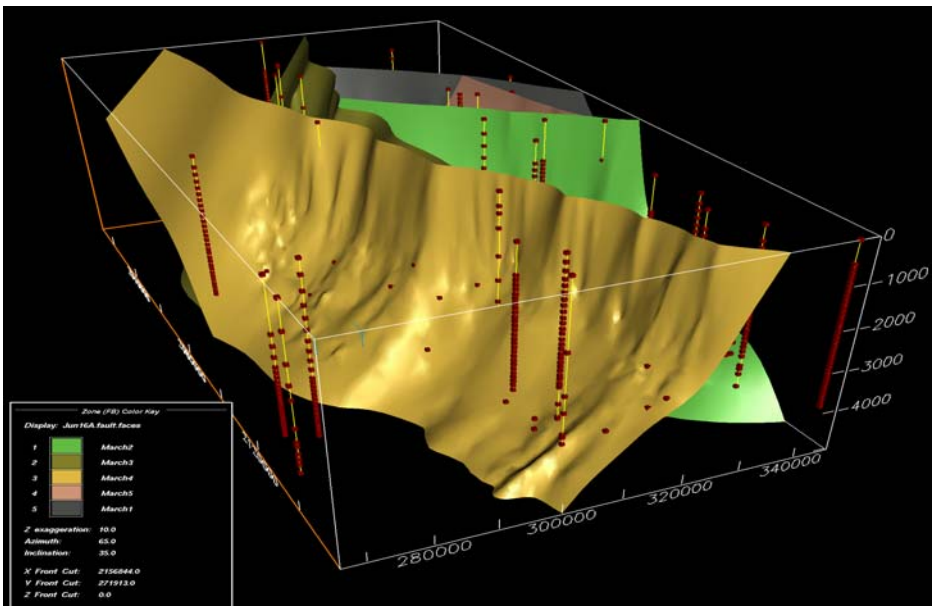

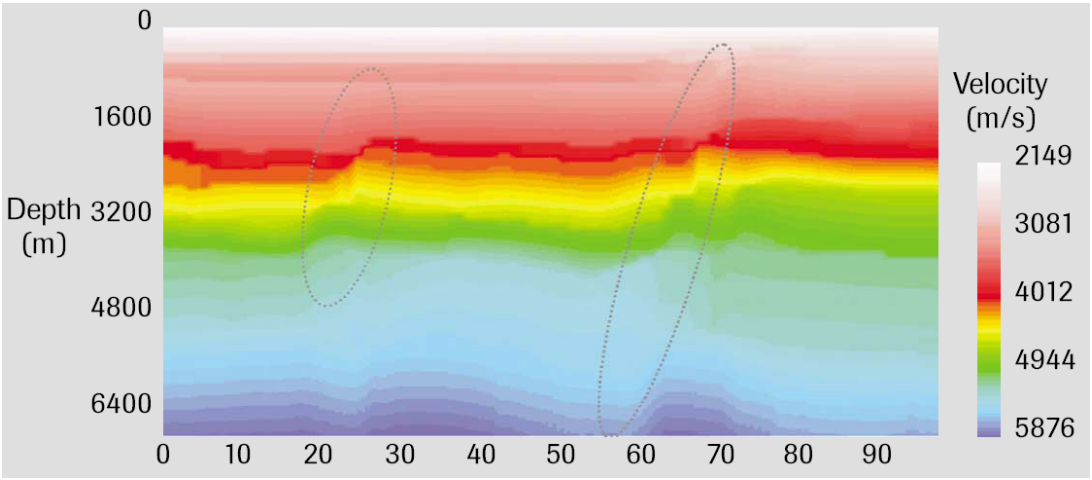

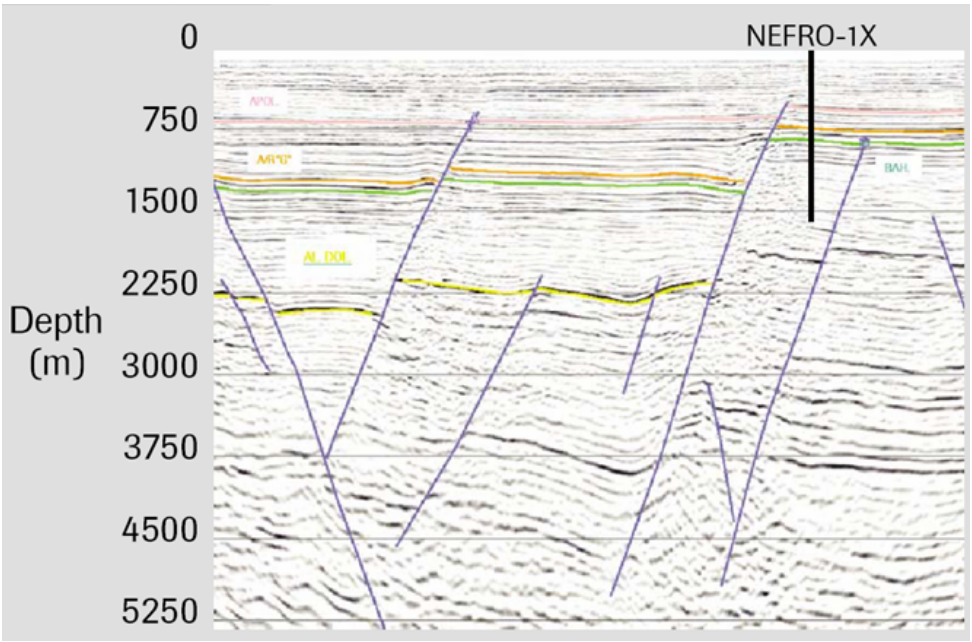

Courtesy WesternGeco

- In the chapter on acquisition and processing we discussed the use of depth migration to improve structural imaging.
- With depth migration, it is possible to produce a volume that has depth as the vertical axis rather than two-way traveltime. Horizons that are interpreted in these volumes do not need to be depth converted because the seismic data are already in the depth domain
- Remember that the accuracy of the depth migration is only as good as the velocity model used to construct it. If the model is wrong, or too coarse, the depths in the data will not be correct

The example above shows a velocity model used for Kirchoff prestack depth migration and a portion of the final result. It is from the Western Desert of Egypt.

Exercise

1. The image below shows a time-structure map (in ms TWT) for a horizon. Well locations are shown by numbered dots, and the table on the next page shows SSTVD measured from the wells for the horizon of interest. Calculate the average velocity at each well location, then contour the results. Assume the seismic reference depth is sea level.

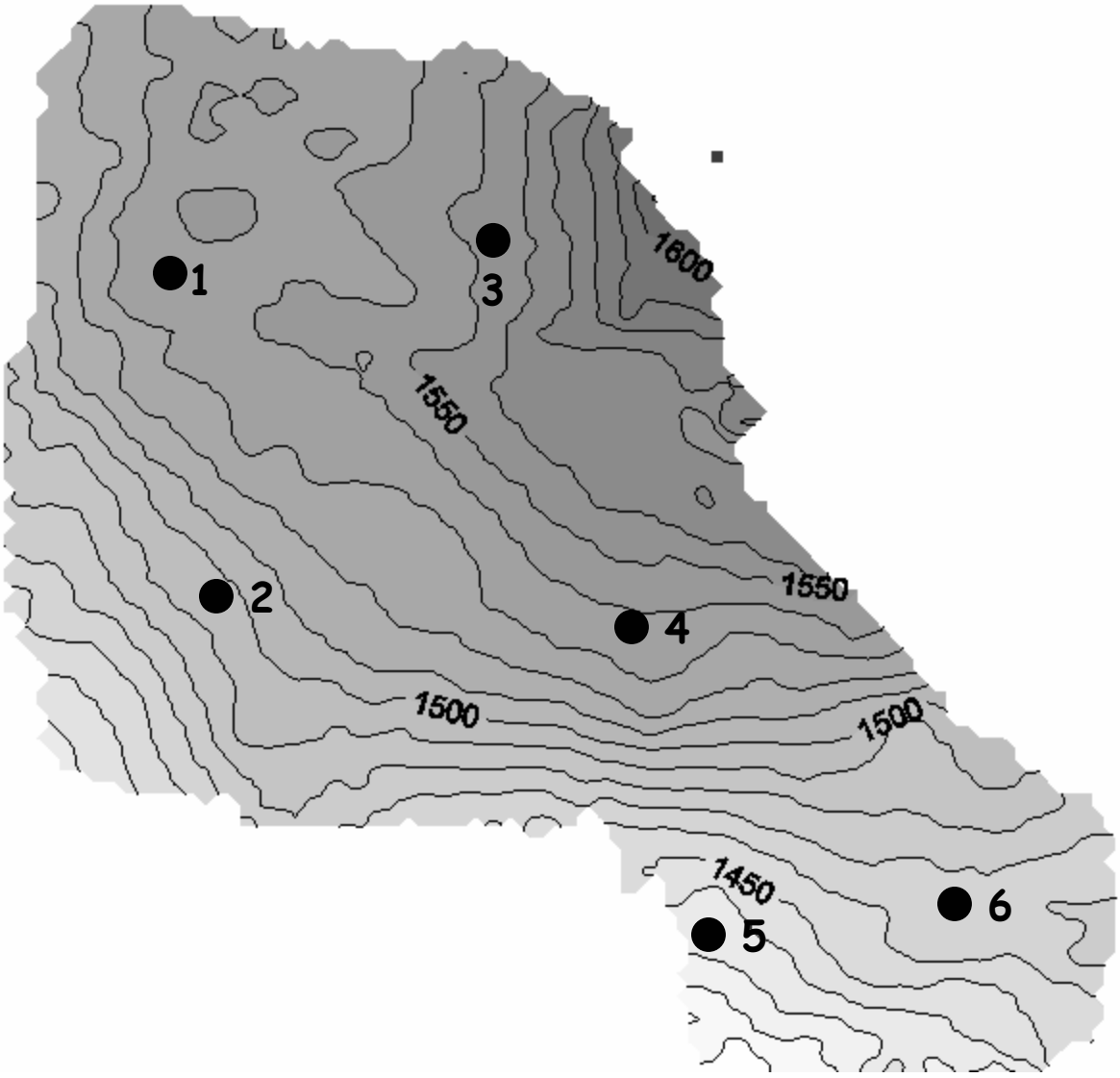

Well Number	TWT	1WT	Depth (SSTVD - m)	Velocity
1			2590	
2			2513	
3			2633	
4			2595	
5			2407	
6			2484	

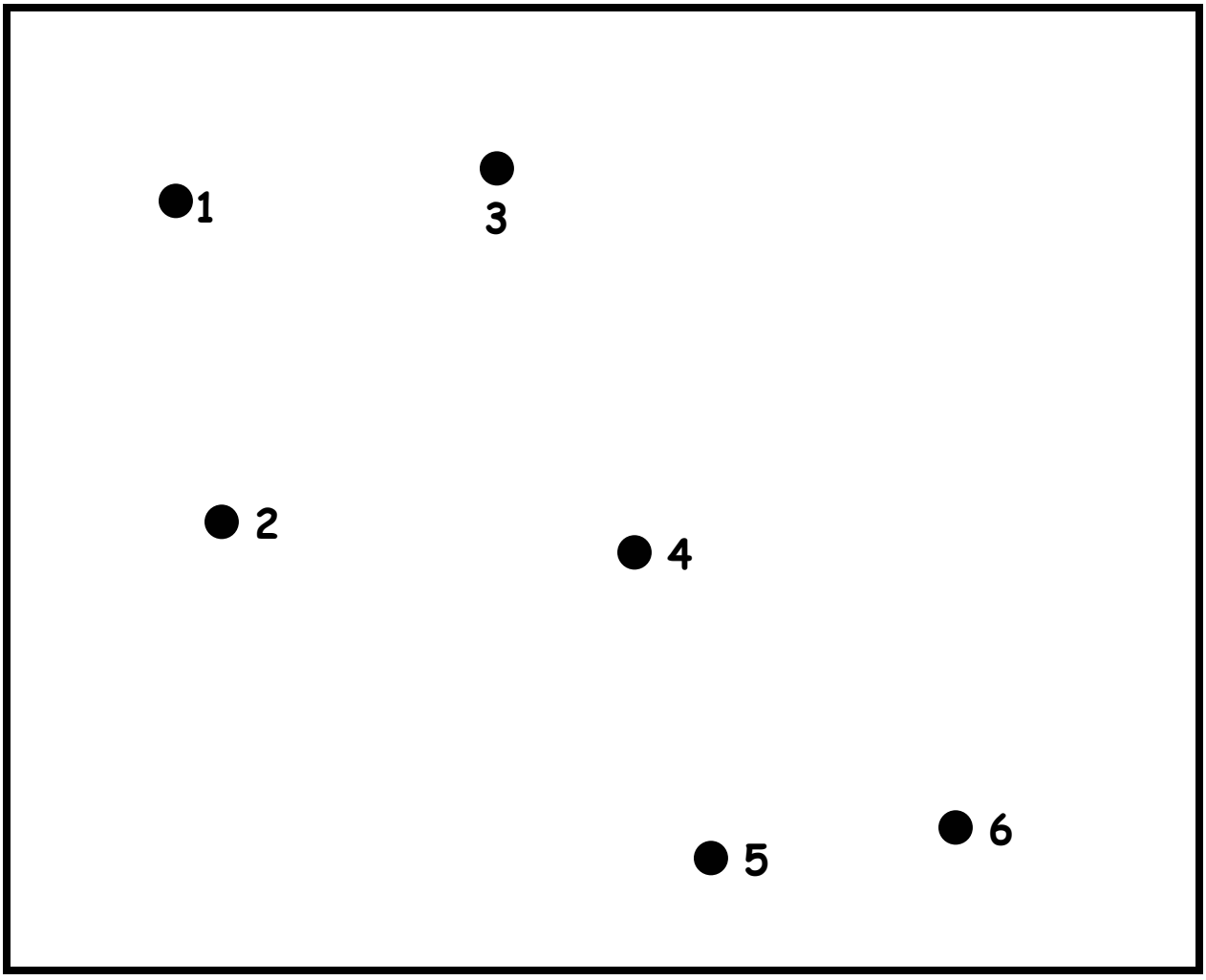

Stratigraphic Interpretation

- A structural interpretation of the data is likely to only be a partial interpretation of the data.
- Stratigraphic features may compartmentalize reservoirs, define hydrocarbon migration pathways, etc.
- Application of seismic/sequence stratigraphic concepts may help interpreter to define basin evolution, and predict lithologies.
- Approach used will vary on the scale of the project (regional, prospect, reservoir scales) and the objectives (exploration -> development)

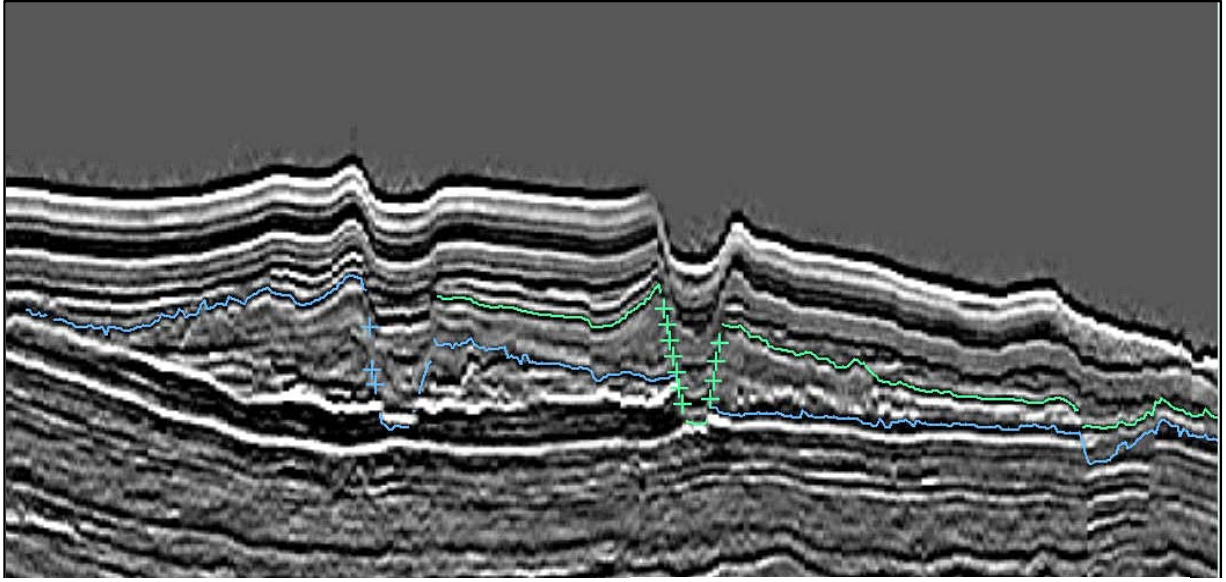

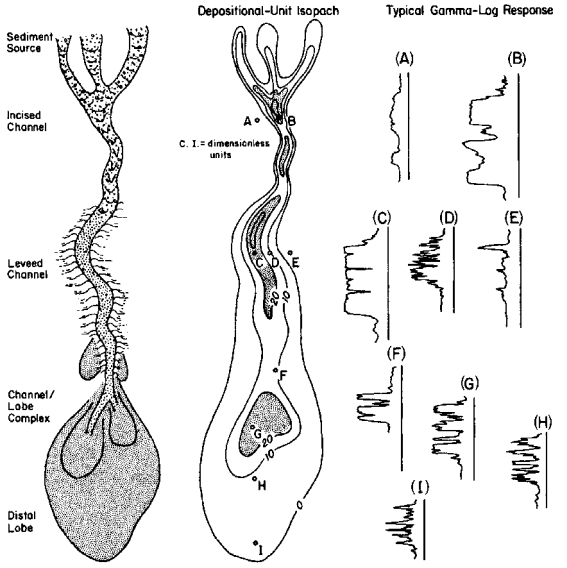

Galloway

There are significant differences in scale between the features that may be detected in seismic data (top), the features that are detectable with well logs (lower right), and the outcrop-scale features (lower left) that can compartmentalize reservoirs. Seismic interpreters need to be aware of these differences. Depending on the depositional facies involved, knowledge of stratigraphic architecture may be gained through studies of outcrop analogs, modern depositional environments, modeling, etc.

These three images show different views of submarine fan depositional settings. The 3-D seismic data volume (top) shows two shingled Tertiary submarine channel systems. We can see and map the large-scale features such as seismic facies, external form (e.g., isochron maps), internal architecture (channel-levee systems), etc. but we need to infer stratigraphic continuity, sand/shale ratio, etc. Exceptional outcrops (lower left) allow us to examine these features in detail, but the 3-D linkage of facies is unclear. Log (and perhaps core)-based facies interpretations require more speculation than 3-D volumes and are less clear about lateral continuity, exact margins of channels, etc.

Sequence Stratigraphy

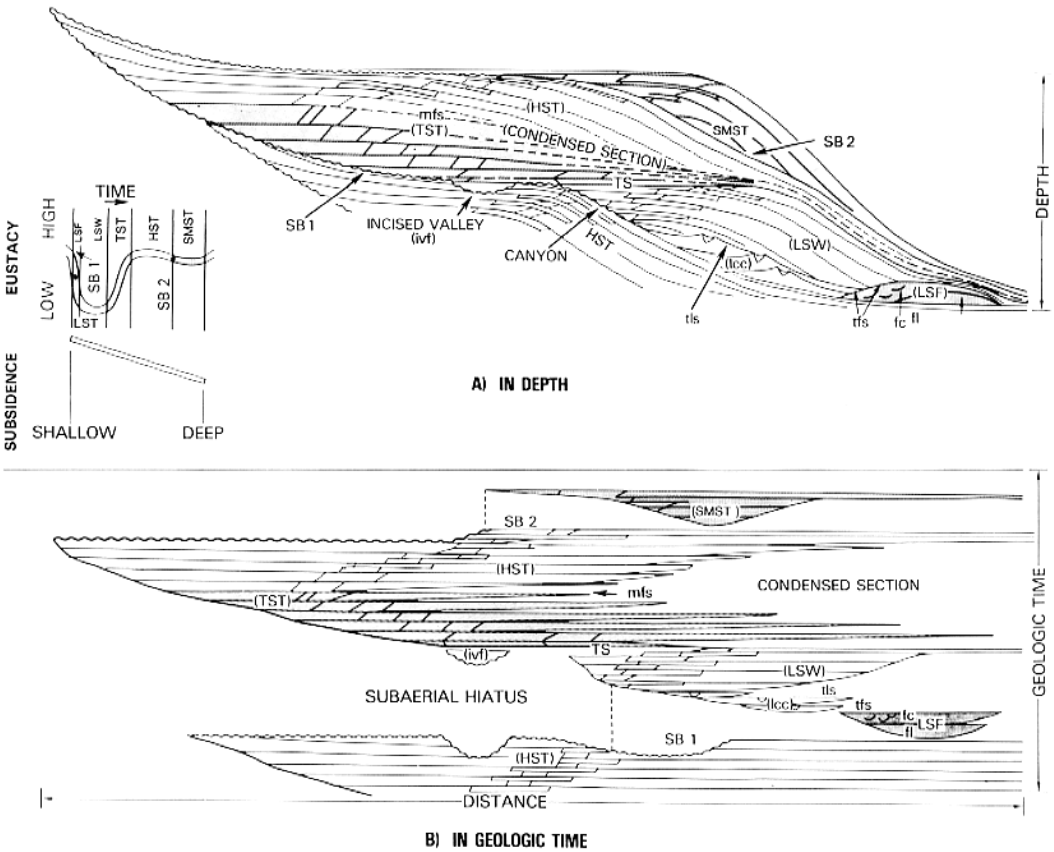

- Concepts of sequence stratigraphy were originally based on analysis of seismic data.
- Reflection terminations and other information used to define depositional sequences and systems tracts that might be associated with changes in global sea level, local/regional subsidence/uplift and/or sediment supply.
- Control of global sea level has been downplayed through time.

Seismic Stratigraphy – Reflections as Timelines (Regional Scale)

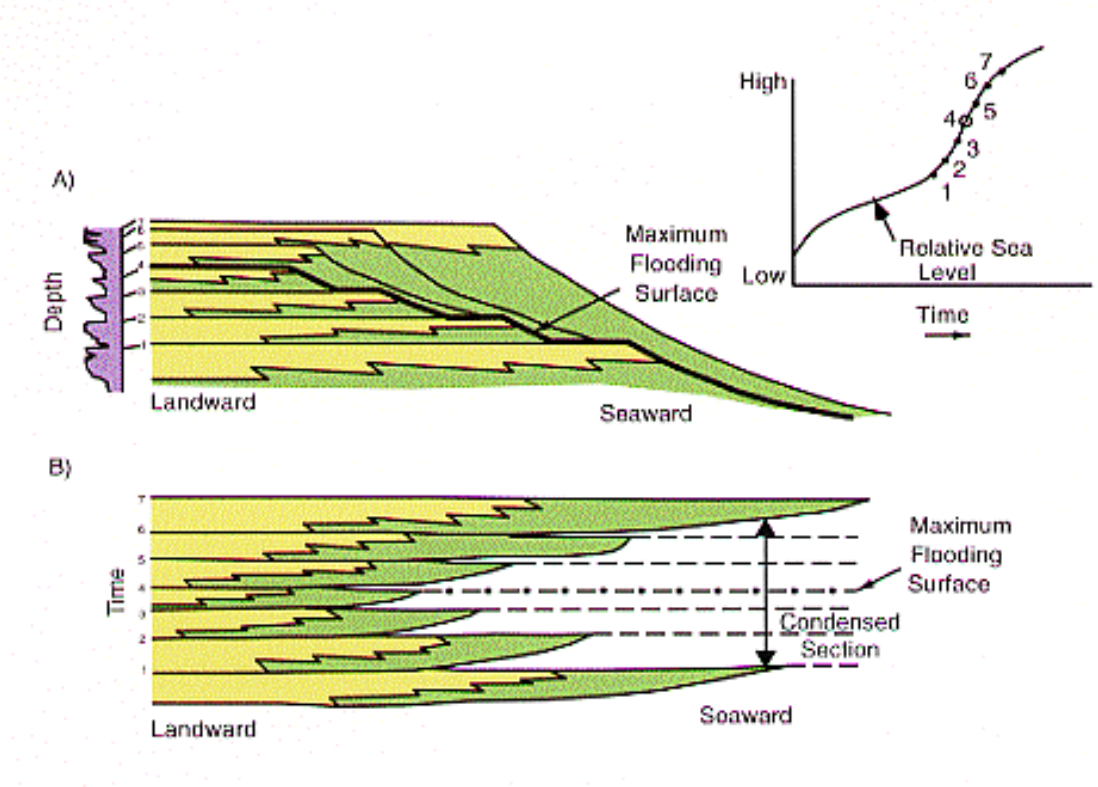

- Sequence stratigraphers attempt to define “timelines” (such as flooding surfaces that bound parasequences) that may be traced from onshore to offshore, etc.
- Timelines cross lithologic boundaries (e.g., top image)
- Timelines represent change in physical properties along (most of?) their length
- *On a regional scale*, seismic reflections will approximate timelines – separating older from younger rocks/sediments.
- *On a local/field scale*, seismic reflections will generally represent lithologic boundaries.

Seismic Stratigraphy – Terminations

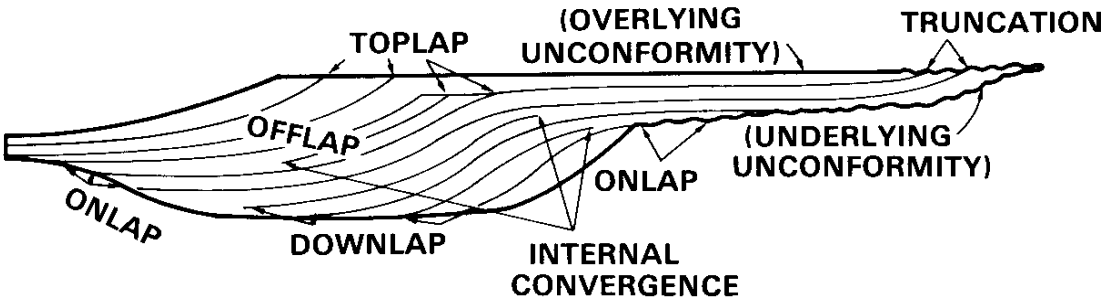

- Different types of reflection terminations may be identified on seismic sections. They provide clues that may be used to define depositional histories.
- As shown below, reflection/stratal terminations are defined on seismic lines and used to define seismic stratigraphic units

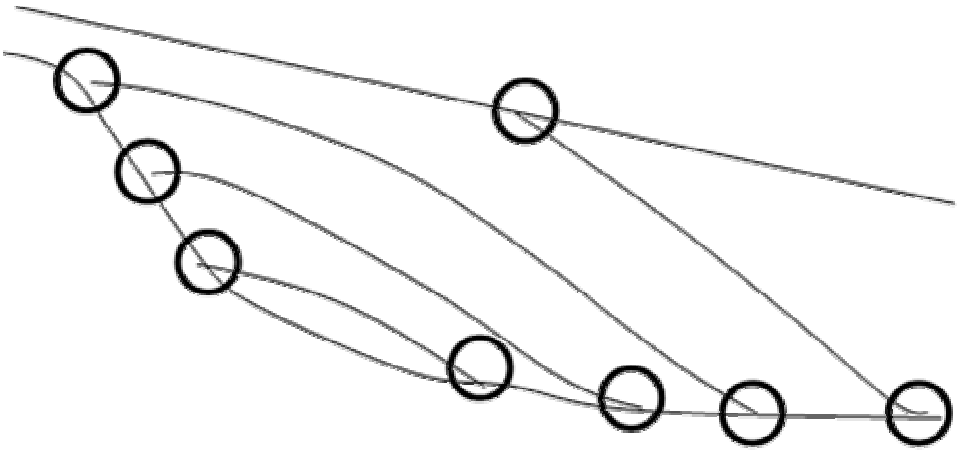

Seismic Stratigraphy

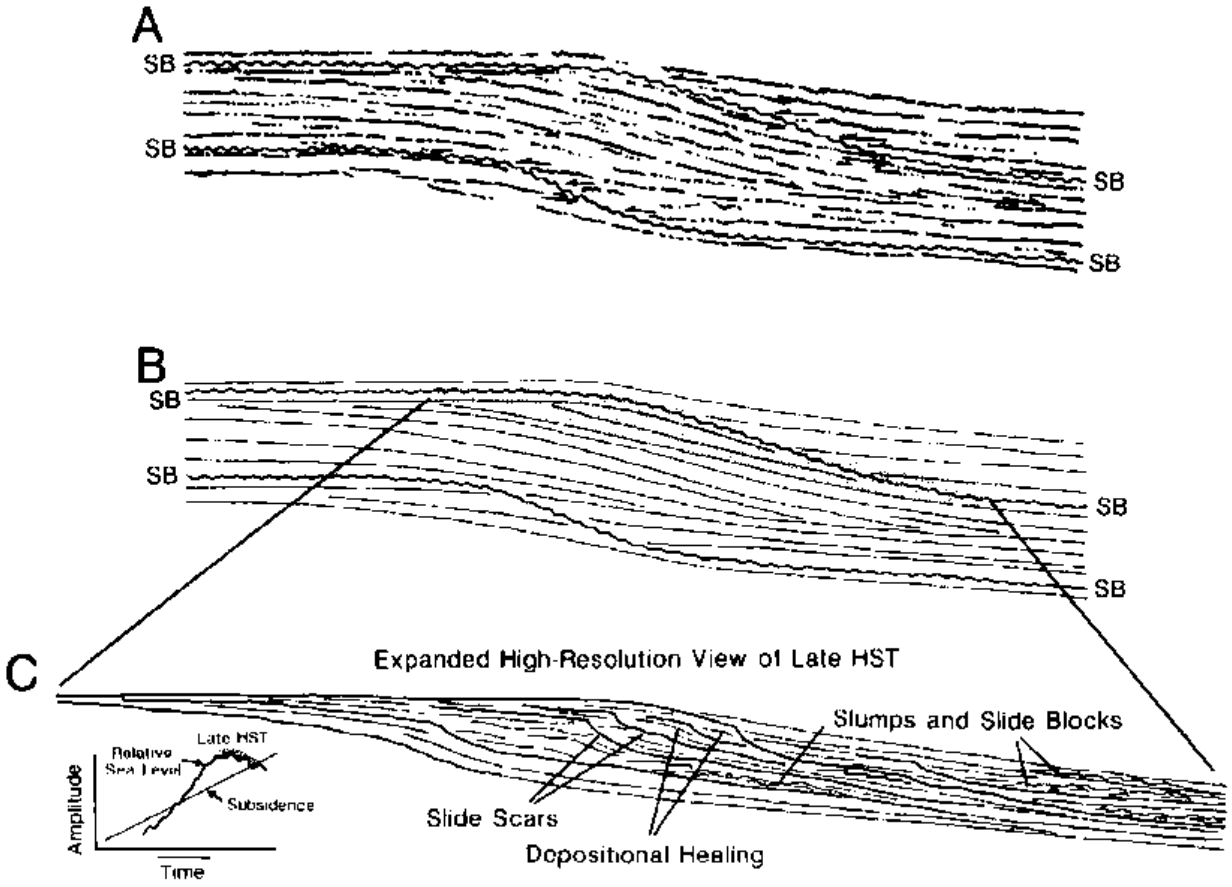

- From a procedural perspective, stratal terminations observed on a seismic line (top) may be simplified (B) for use in seismic stratigraphic studies. Remember that, depending upon the frequency content of the seismic data, reflection geometries visible on seismic records may not truly represent stratigraphic relationships (C).

Seismic Stratigraphy – Stratal Patterns

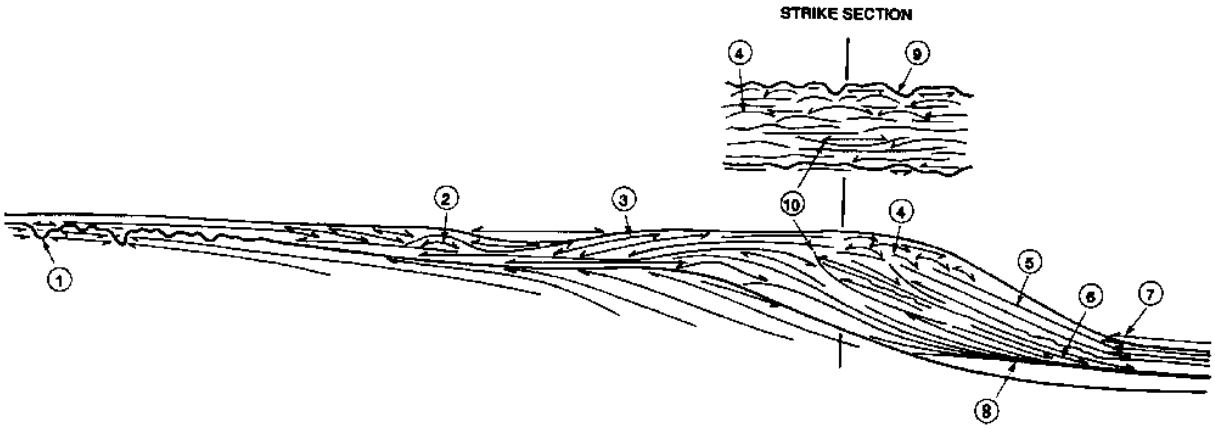

- Common stratal termination patterns of carbonate platforms that may be visible on seismic transects:
  1. Karst-related truncations
  2. Shelf mounds
  3. Landward migrating clinoforms (rimmed shelves)
  4. Bioherms (rimmed shelves)
  5. Steep depositional slopes (> angle of repose)
  6. Downlapping clinoforms at toe-of-slope
  7. Alternating downlap/onlap
  8. Convergence of clinoform reflections
  9. Shelf edge incision
  10. Incision within sequences

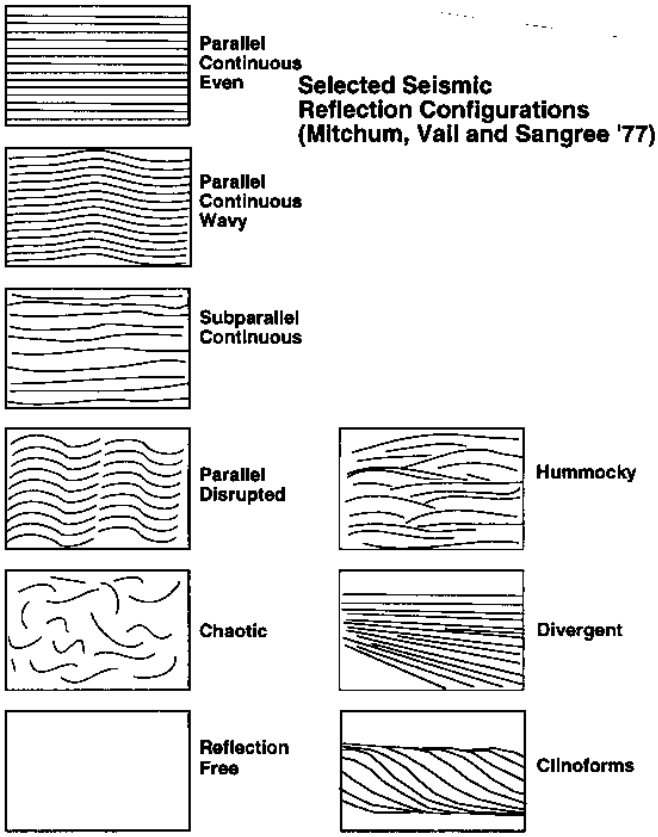

It is important to define not only stratal terminations and key surfaces, but the nature of the reflections within seismically defined “packages” as well. Seismic reflection configurations (selected types shown above) can provide information about depositional environments, lithology, lateral continuity of lithology, etc.).

Most seismic interpretation packages are not particularly useful for mapping out the distribution of various reflection configurations. One approach is to map their distribution on paper using techniques shown below.

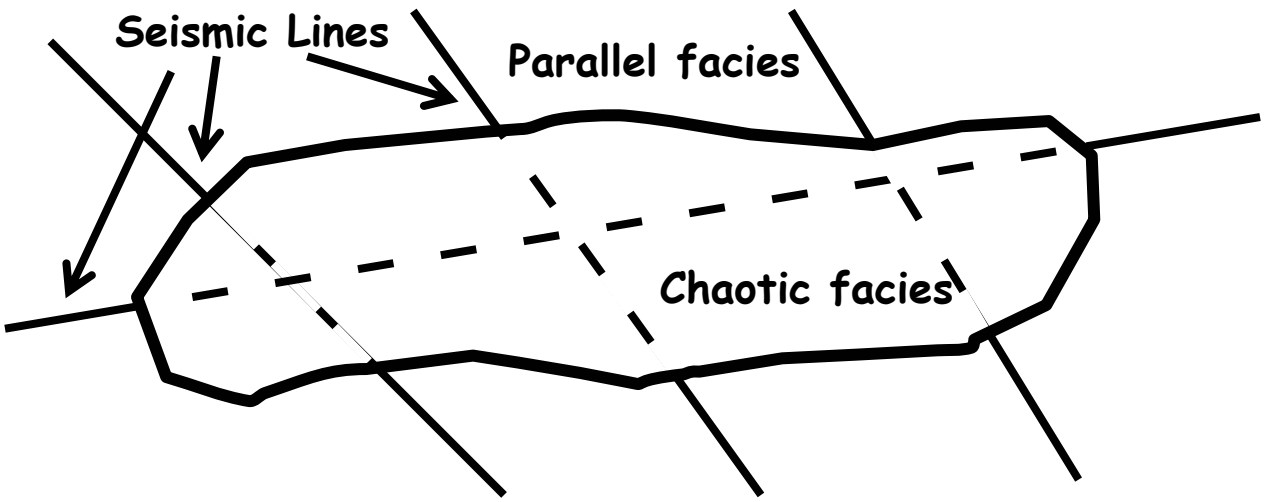

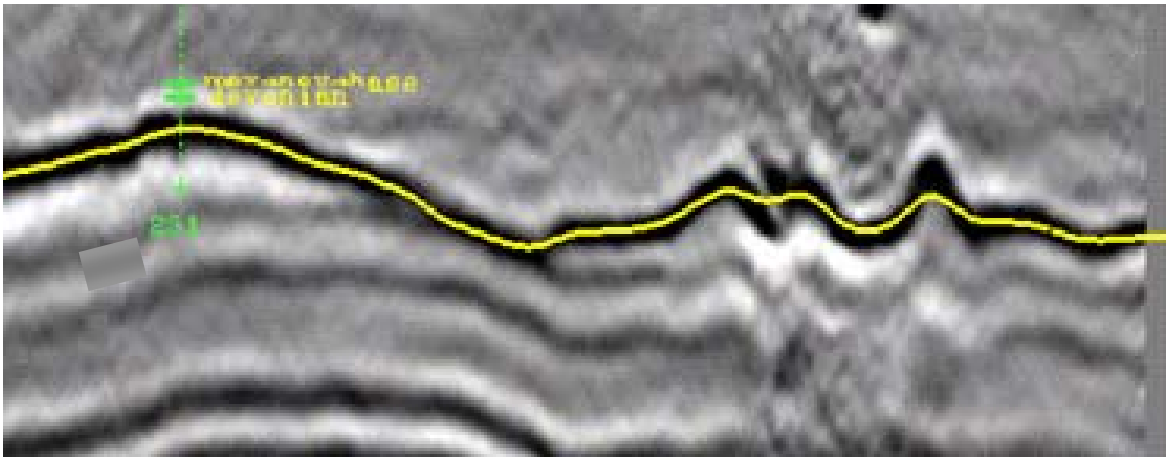

Unconformities are produced by subaerial erosion associated with a drop of relative sea level. Different amounts of time may be associated with these surfaces. On seismic images they are recognized by erosional truncation of underlying stratigraphy.

The image above shows a significant unconformity (yellow line) between Devonian carbonates and Lower Cretaceous clastics for an area of western North America. Approximately 250 million years is missing at the unconformity. Note the reflection truncations below the unconformity.

The image below shows two “nested” unconformities in a Lower Cretaceous offshore section. Each unconformity is probably associated with a fourth-order sequence superimposed on a third-order fall of relative sea level. The section has been flattened on an underlying horizon for clarity.

Unconformities can cut through shale layers that otherwise may have formed vertical compartment boundaries.

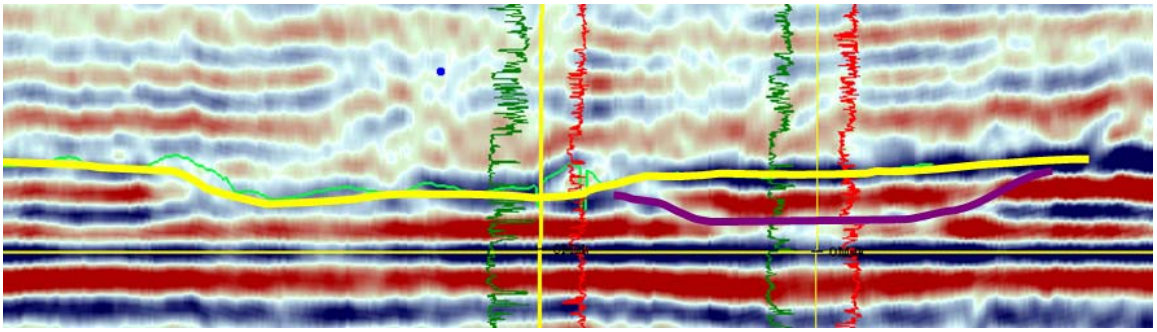

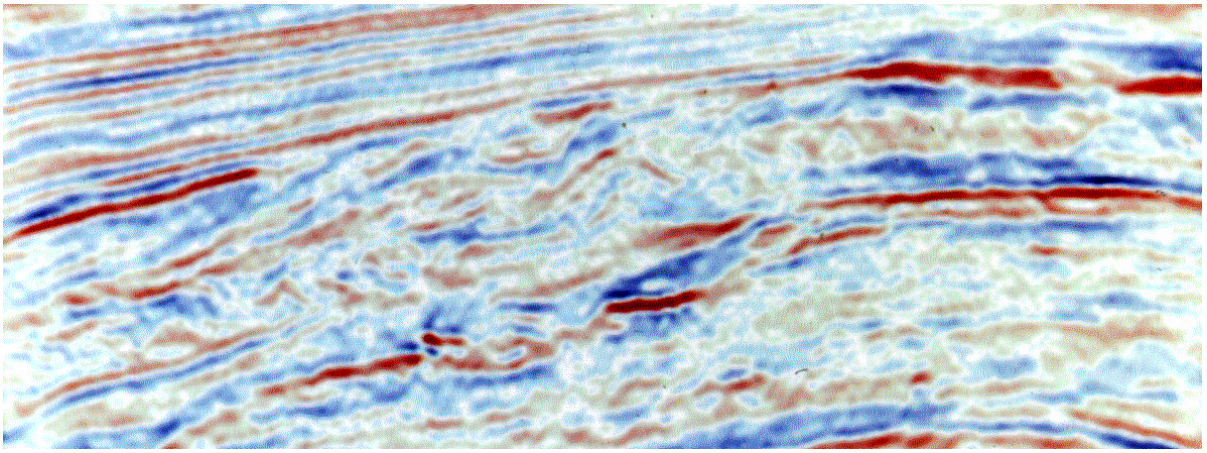

Downlap surfaces are present at the base of prograding packages. They are commonly associated with maximum flooding surfaces produced by a rise in relative sea level, but may be present in deltaic settings where they separate packages generated by allocyclic lobe switching. The image above shows a downlap surface separating two different deltaic lobes in a young lowstand deltaic setting.

Downlap surfaces may be associated with shale accumulations, and so may represent source beds (on large-scale images) associated with condensed sections. In the image above, a shale horizon at the downlap surface acts as a vertical barrier to fluid flow, separating two stacked reservoir intervals.

A downlap surface is present in the image below near the bottom of the image. It is present at the bottom of a submarine slope fan, defining the base of the basin-floor fan (BFF). The application of sequence stratigraphic terminology to such settings remains controversial – is the sequence boundary at the base of the slope fan or at the top?

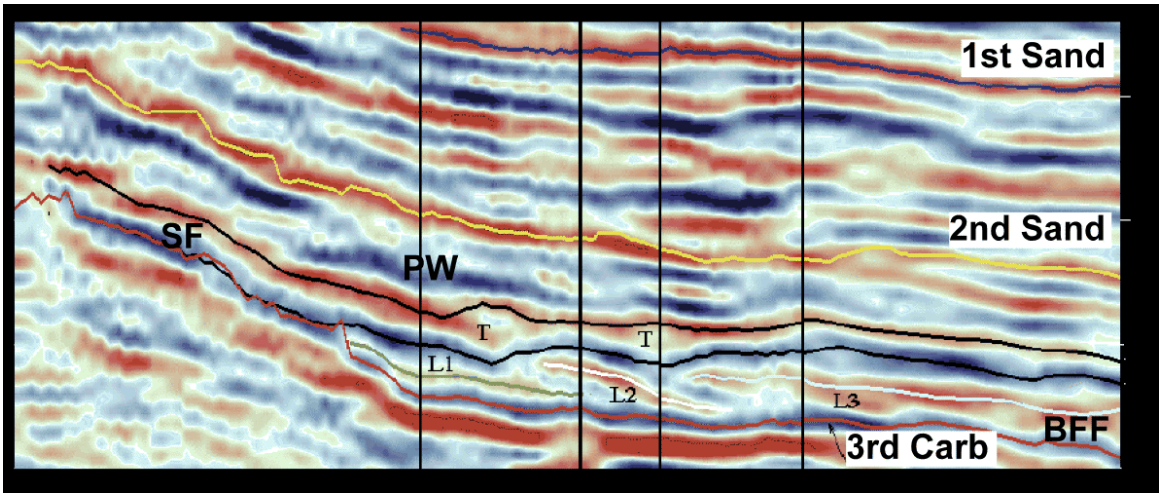

Seismic Facies

Facies Parameters	Geologic Interpretation
Reflection Configuration	Bedding patterns Depositional processes Fluid contacts
Reflection Continuity	Bedding continuity Depositional processes
Reflection Amplitude	AI contrast Bed thickness (tuning) Fluid content
Reflection Frequency	Bed thickness Fluid content
Interval Velocity	Lithology estimation Porosity estimation Fluid content Pressure
External Form and Linkages of Facies Units	Depositional environment Sediment source Geologic Setting

- Physical properties that an interpreter might try to qualitatively evaluate from seismic characteristics. Modified from Mitchum et al. (1977)

Seismic Facies - Example

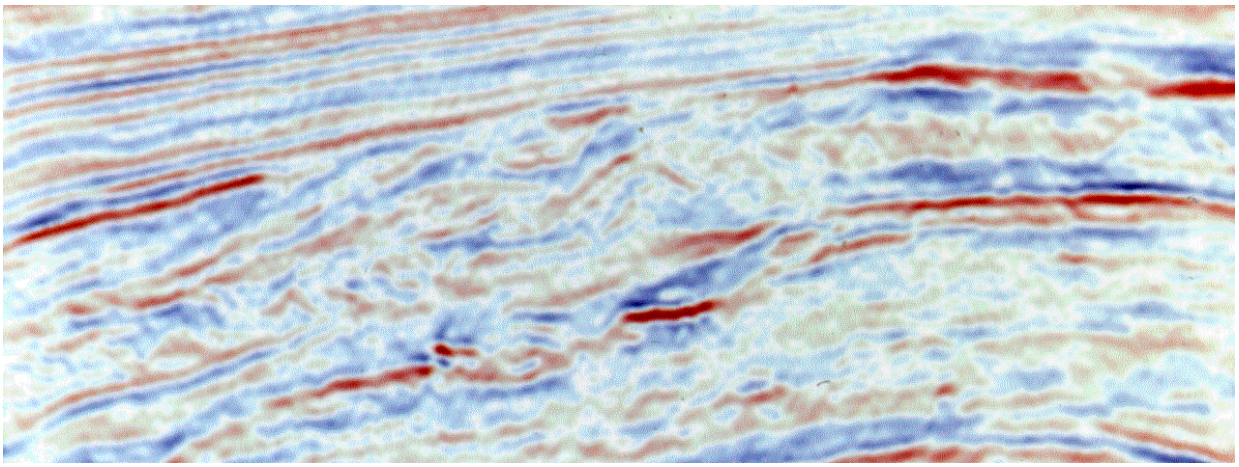

- Describe the principle seismic facies/reflection geometries.
- What type of depositional environment might be represented?

Seismic Facies - Example

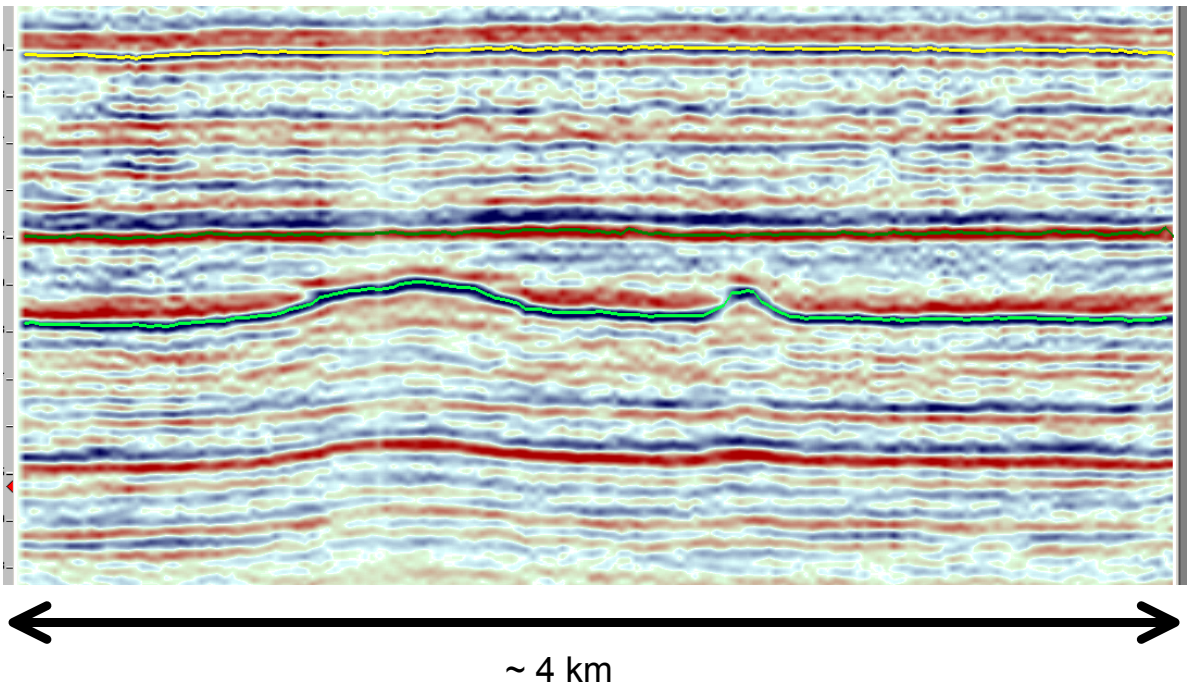

- Describe the principle seismic facies/reflection geometries.
- What type of depositional environment might be represented?

Seismic Facies - Example

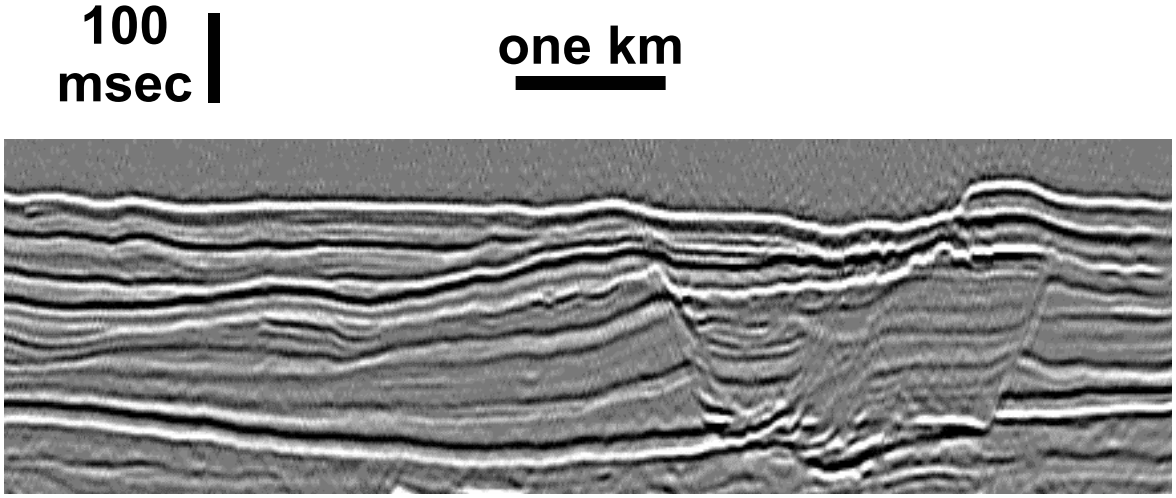

- Describe the principle seismic facies/reflection geometries.
- What type of depositional environment might be represented?

Seismic Stratigraphy – 3-D Capabilities

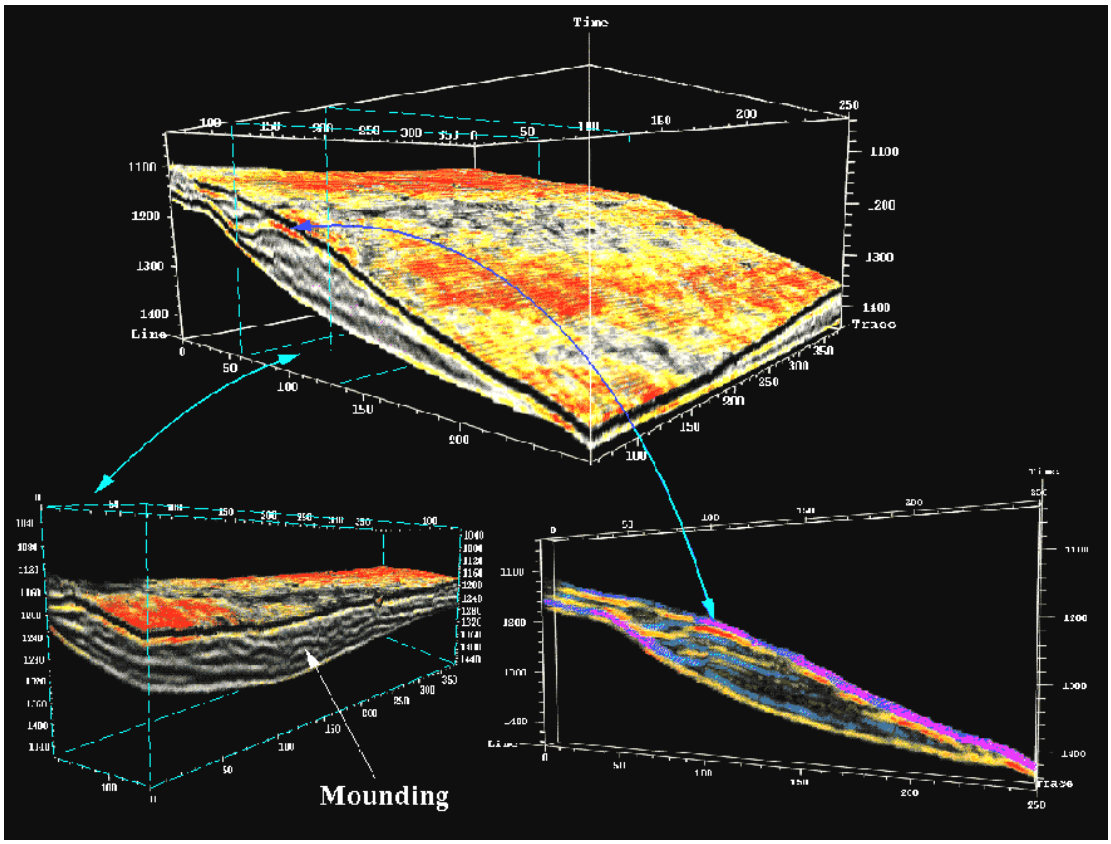

- 3-D seismic data may be clipped at key surfaces to isolate depositional sequences or systems tracts
- Use volume visualization to look for relationships between thickness, structure, seismic facies, etc.

Isochrons

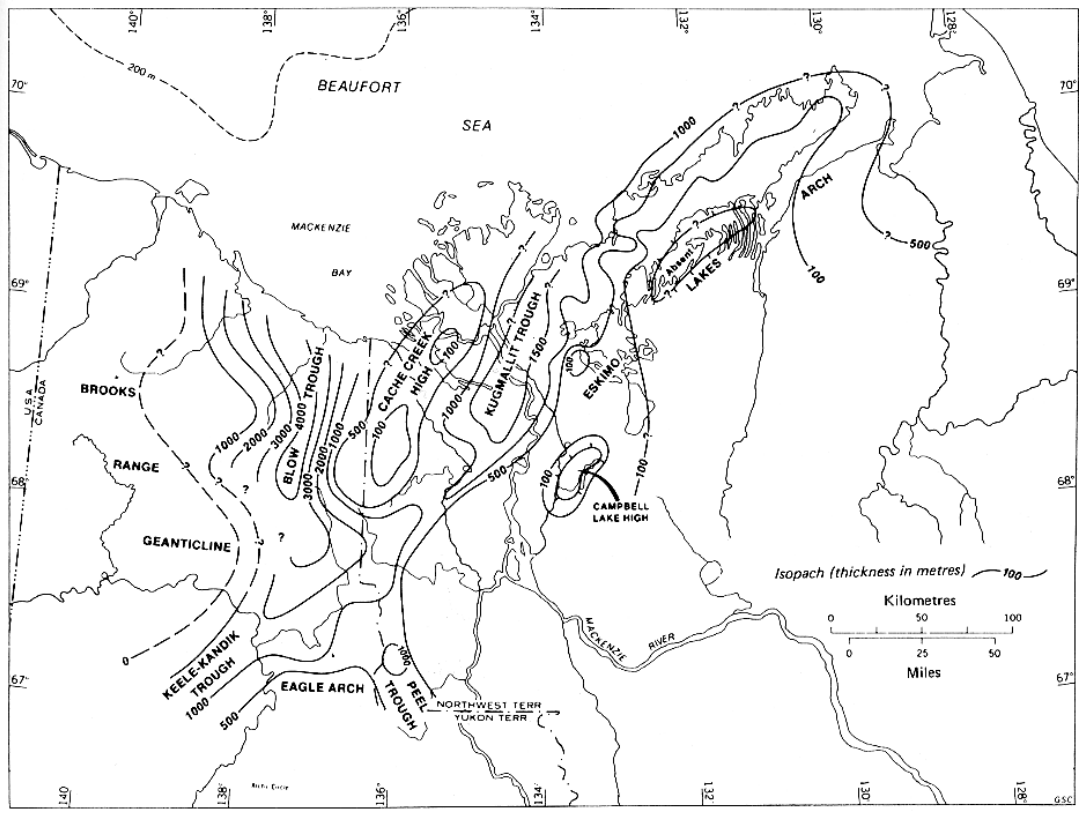

- Large-scale isochron/isopach (if depth converted) patterns may be used to help define depocenters, syndepositional structural elements, etc.
- Image above shows isopachs (depth converted from seismic data) of Barremian-Albian (Lower Cretaceous) strata showing thickness trends in the Mackenzie Delta region of Canada.

Isochrons

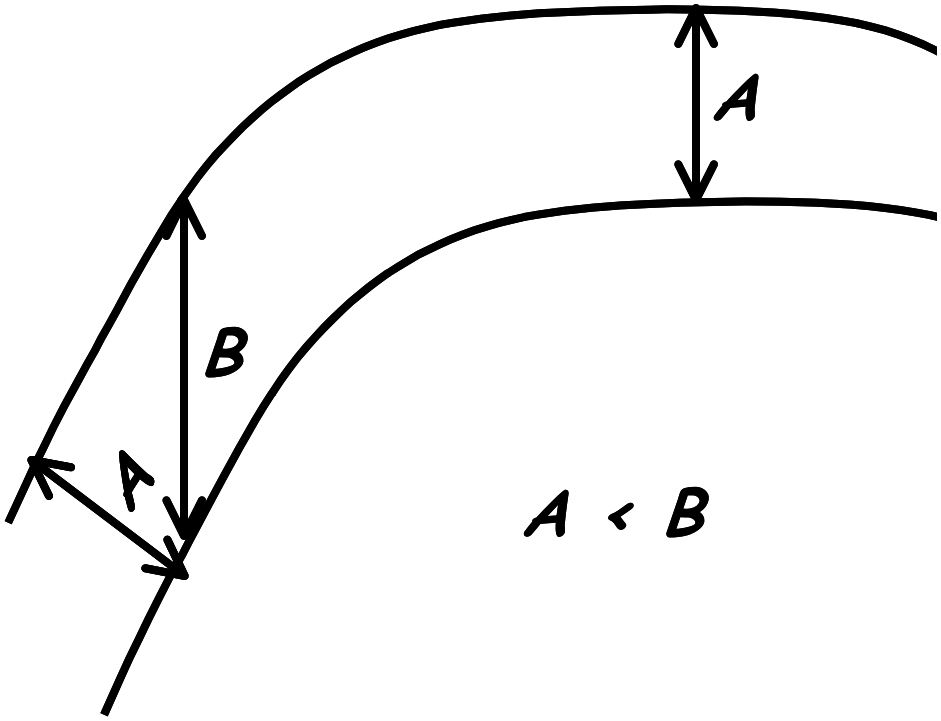

- Be careful, when interpreting isocrhon maps, to watch out for geometric pitfalls.
- Image above shows a fold. Bed maintains constant thickness (“A”) but isochron will show the bed as being thicker on the steeply dipping limb.

Flattening

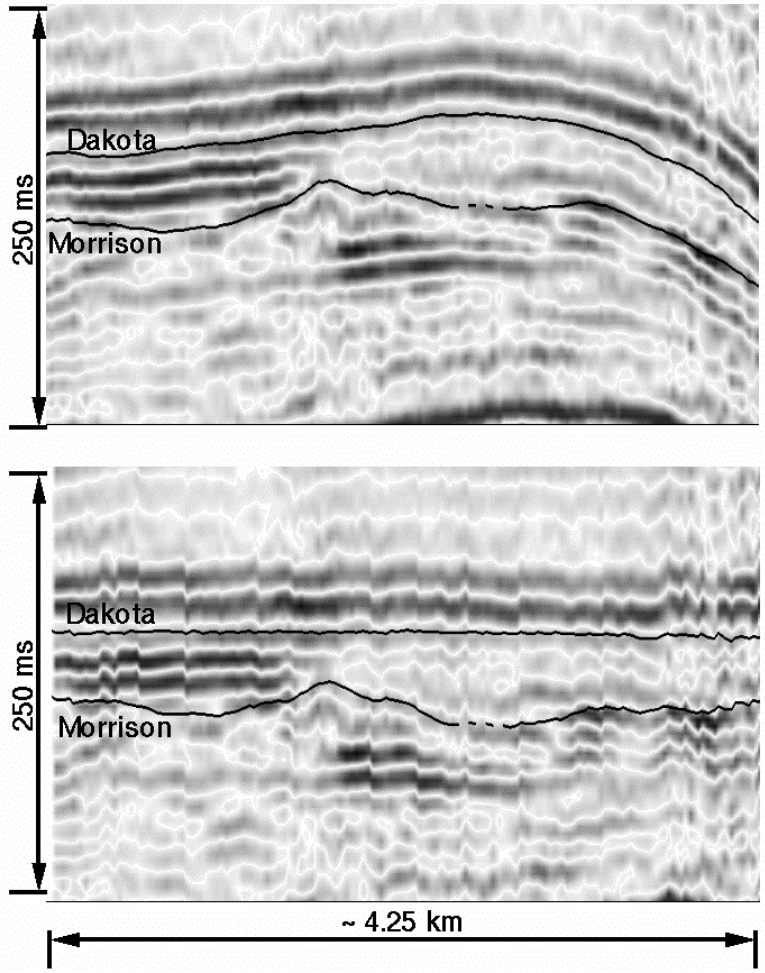

- Flattening can help the interpreter to better visualize structural relationships in deformed areas.
- Images above show original view (top) and top view of an arbitrary transect through a 3-D volume.
  - Top of Dakota is a flooding surface
  - Base of Dakota is a regional unconformity
- Make sure that the surface you flatten on was originally a horizontal surface.

Timeslices, Horizon Slices, Stratal Slices

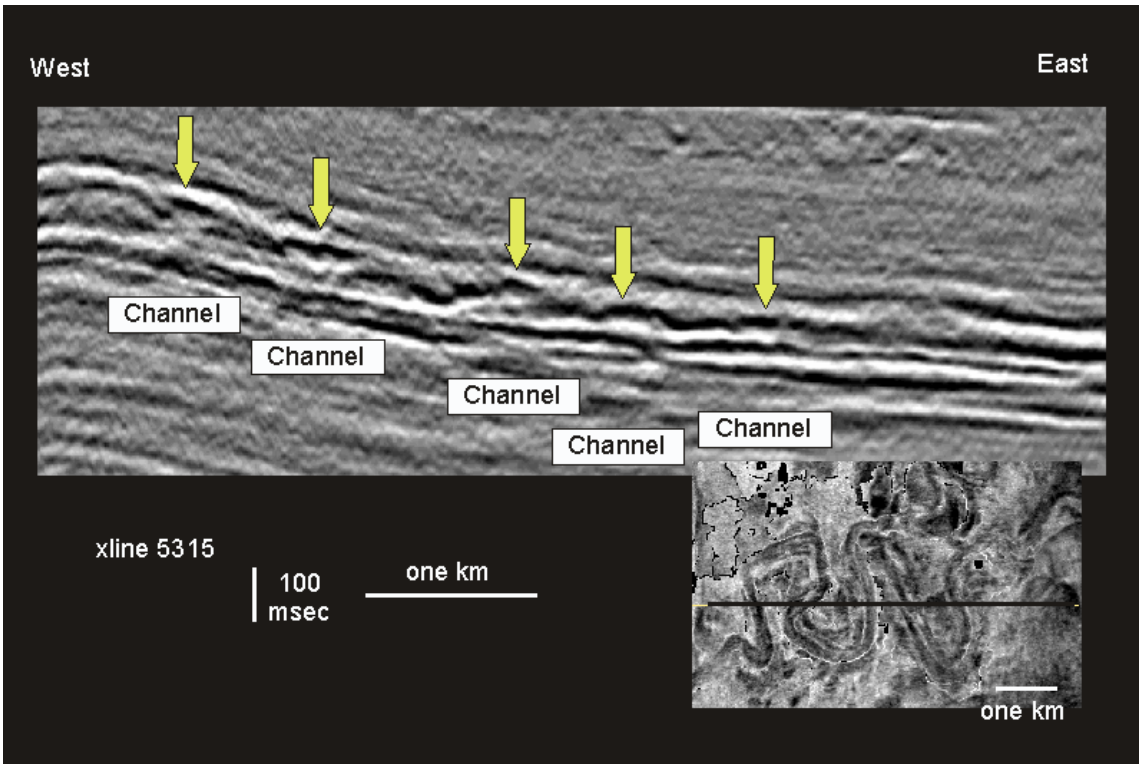

- Use different types of slices in conjunction with vertical transects to identify depositional elements

Stratigraphic Interpretation – Coherency Timeslices

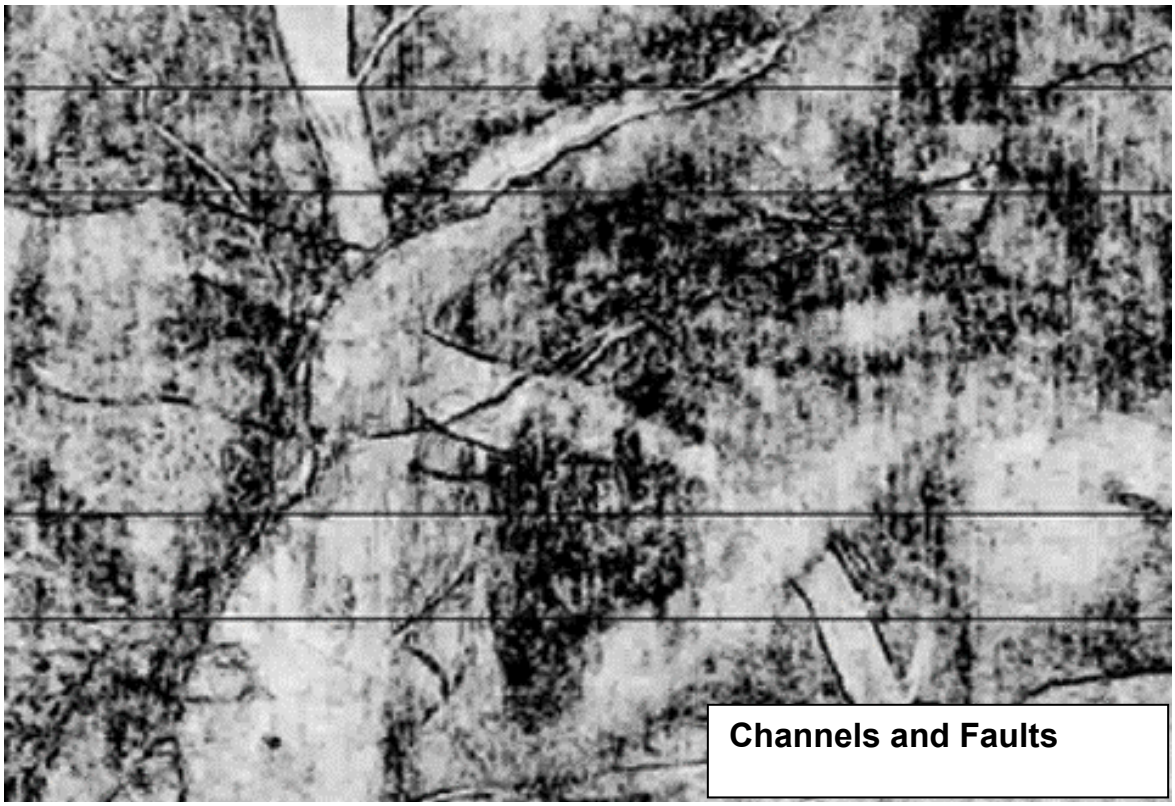

- Coherency volumes can be helpful for definition of channels and other stratigraphic features (e.g., reefs)

Stratigraphic Interpretation – Visualization

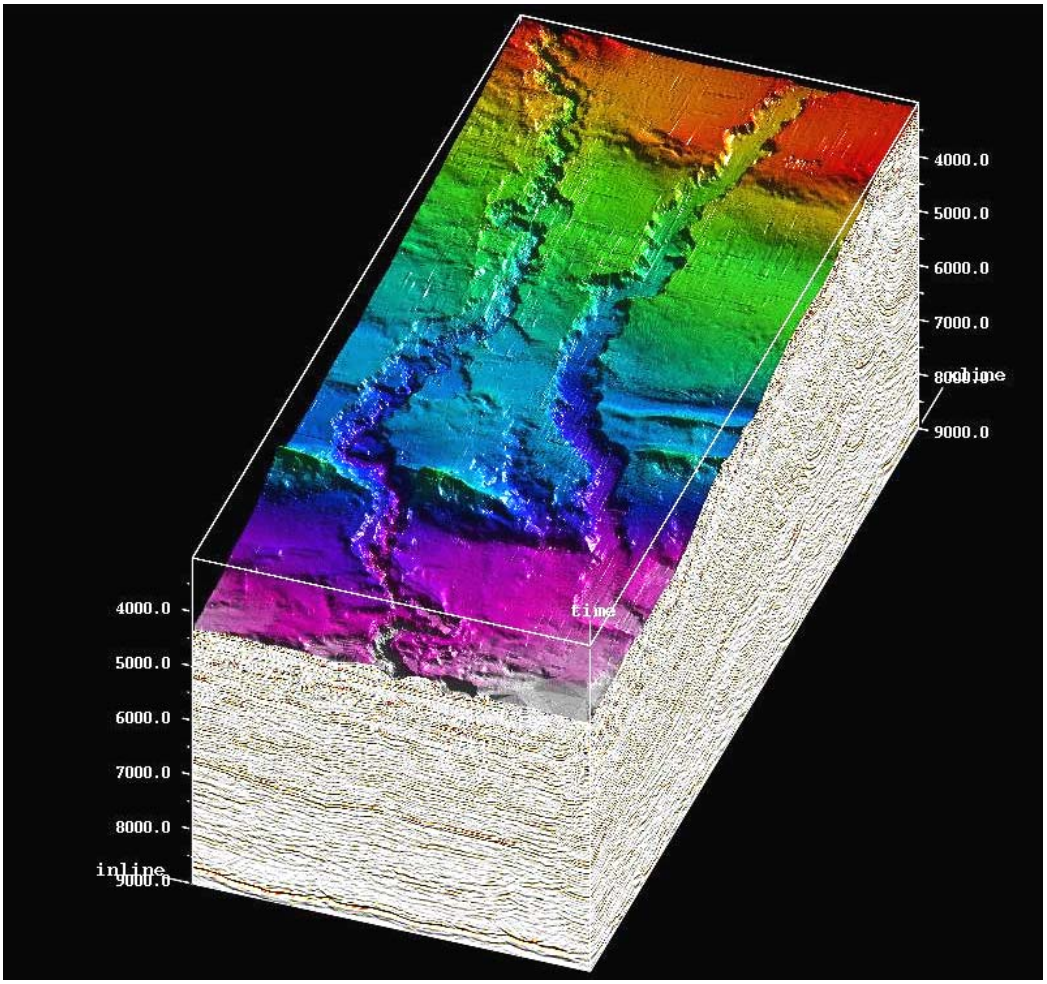

- Use visualization to identify depositional systems in large 3-D volumes (e.g., spec surveys, offshore areas).
- Image above shows a seismic horizon (seafloor) over an area of approximately 20 x 40 km from offshore west Africa.

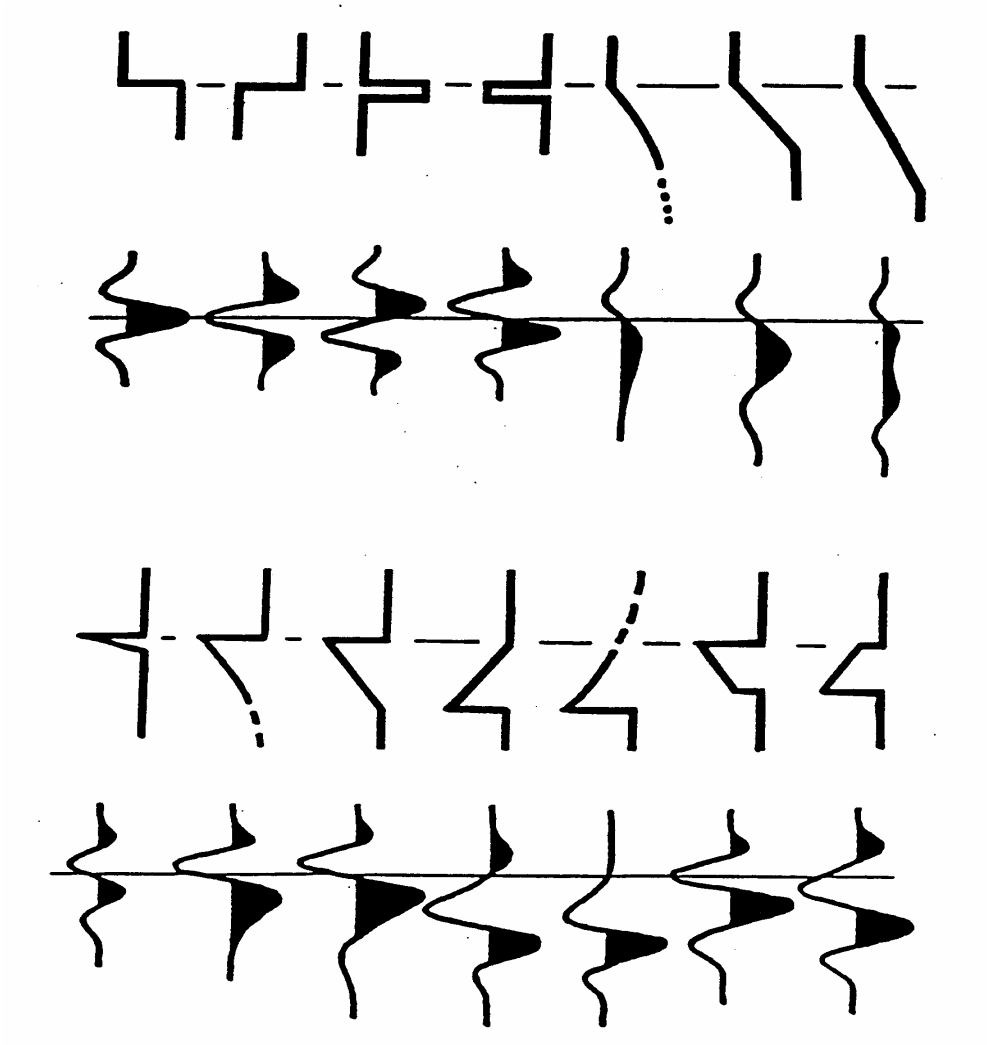

- Changes in wavelet shape along a seismic horizon can be indicative of changes in lithology, porosity, thickness, etc. Detailed analysis of wavelet shape can sometimes be useful for identifying these changes.

- The images above show how selected acoustic impedance profiles might express themselves seismically. The acoustic impedance profiles might be associated with gamma ray profiles (fining-upward packages, thin beds, blocky sands, etc.).

- Note that the actual seismic response is non-unique. Several possible acoustic impedance profiles could give the same seismic response. Seismic modeling is a useful tool for narrowing the range of possible options.

- Changes in seismic amplitude, for example with changing bed thickness, are discussed in the chapter on seismic attributes.

Prospect Scale Analysis

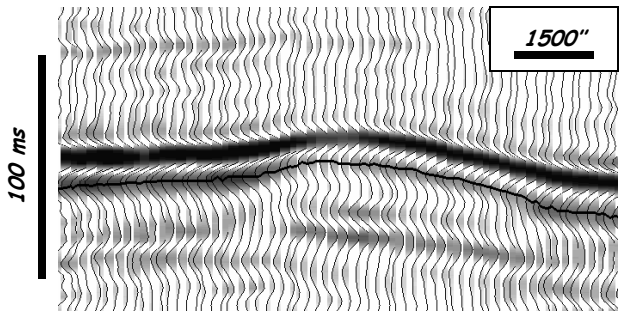

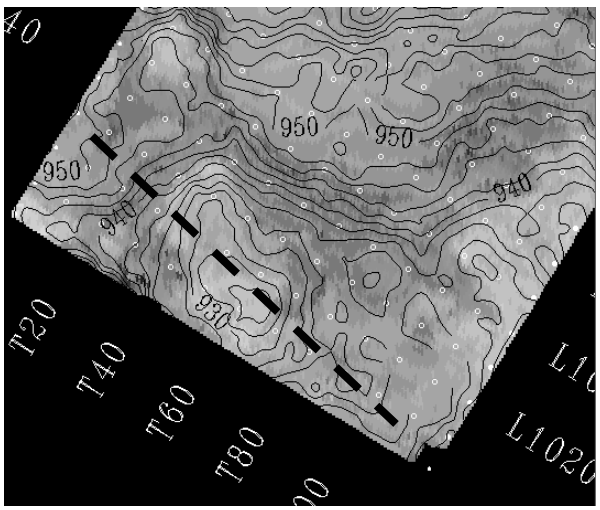

- Use reflection character analysis, horizon slices and other approaches together when interpreting. Use several lines of evidence, not just one.
- Images show arbitrary transect (top) through an potentially prospective Jurassic eolian unit (Entrada) in NW New Mexico and horizon slice (below) along the overlying lacustrine carbonate (Todilto). Lower amplitudes are in lighter greys in the horizon slice, contours show time-structure on Entrada pick.
  - Seismic modeling suggests that prospective dunes should be associated with three characteristics: 1) time structural bump, 2) dimming of Todilto amplitudes, 3) Entrada peak splits into doublet. Do you drill?

Automated Tools

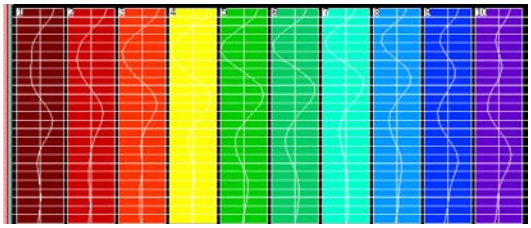

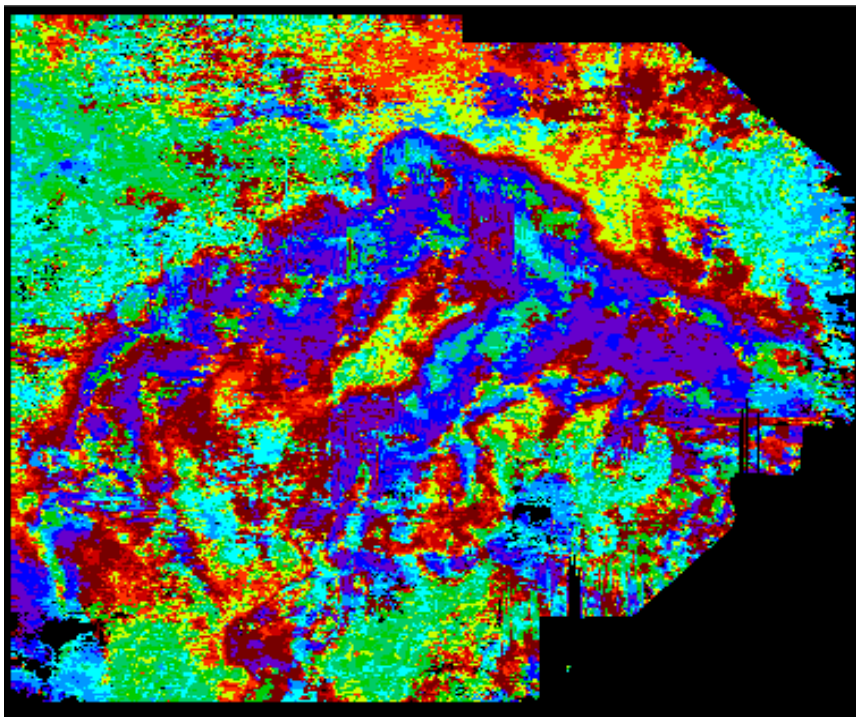

- *Stratimagic* and similar packages use artificial intelligence to identify differences in reflection character.
  - Need to pick an analysis window
  - Software analyzes data to establish different “end-member” trace types, then color codes them (top)
  - Mapping software shows the distribution of the different trace types (below)

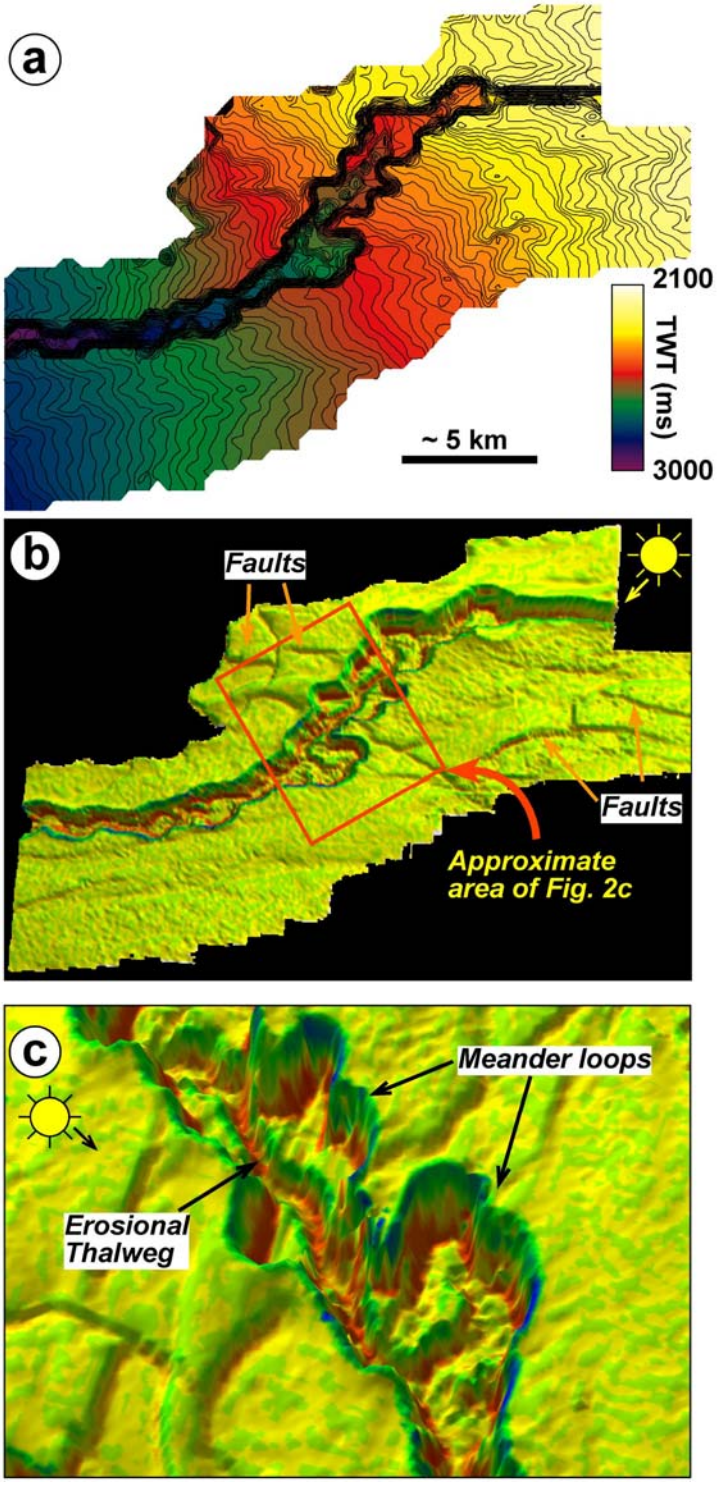

As described in the chapter on subtle structures, horizon curvature is a useful measure for defining subtle structures. Curvature attributes, derived from horizons interpreted in the seismic data, are also useful for defining stratigraphic features as well.

The image at top shows a time-structure map of the top of a Tertiary channel-levee complex. The two images below show dip curvature overlain on a 3-D representation of the horizon with shaded relief to enhance features. Note the improved definition of stratigraphic and structural features compared to the time-structure map.

Case Study – Offshore Gulf of Mexico

The data for this study come from the Eugene Island Block 330 area in the offshore Gulf of Mexico. The field consists of two rollover anticlines, bounded to the north and east by a large arcuate, down-to-the-basin growth fault system. More than 25 Pleistocene sandstones are productive at depths of 701 to 3658 m (2300 to 12,000 ft). Faulting and permeability barriers separate these sands into more than 100 oil and gas reservoirs. Ultimate recoverable reserves are estimated at 307 million bbl of hydrocarbon liquids and 1.65 tcf of gas. Production started and peaked in the early 1970s. By the late 1980s production had declined significantly. The 3-D seismic data used in this project were collected in an effort to help reverse that decline.

The work presented here was published by Hart, Sibley and Flemings in the AAPG Bulletin in 1997. The work focused on the uppermost reservoir level in the field, the “GA” sand, deposited in a shelf-margin deltaic setting. At the time, the issues were: 1) Reservoir compartmentalization. Were there undrilled stratigraphic and/or structural compartments? 2) Overproduction. Some of the reservoir intervals in the field had produced more oil than original recoverable reserve estimates had predicted. Where was the oil coming from?

The logs were tied to the seismic data by generating synthetic seismograms. The results suggested that hydrocarbons should show up as bright spots in the seismic data, and indeed bright spots are present at the crest of structures. Mapping showed the presence of an anticline with four-way closure in the middle of the study area. The anticline is bounded by a NW-SE striking growth fault to the north and antithetic normal fault to the southeast. A small graben, associated with the antithetic fault, is present in the southeast part of the area. Production at the GA level is from the crest of the anticline and from within the graben.

Seismic stratigraphic principals were used to define seismic facies and stratigraphic subdivisions of the GA Sand. At least two stacked prograding parasequences are present in the unit. They are thought to be associated with lobe switching in a deltaic setting and are separated by a flooding surface imaged as a downlap surface (named the “Green Surface” in the figures) in the seismic data. The upper prograding lobe has good development of clinoforms whereas the lower lobe appears to have suffered from mass failures and clinoforms are less well developed. The combination of seismic transects and log cross-sections on the following page shows how seismic interpretations may be used to guide log interpretations and vice versa.

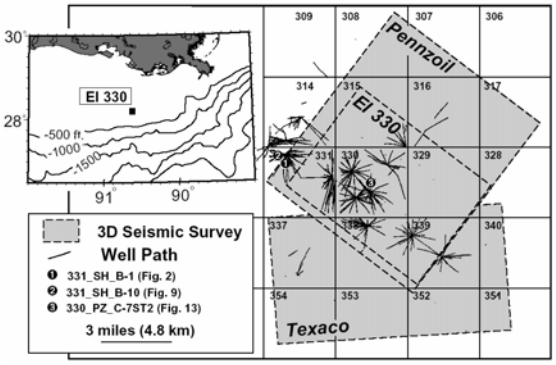

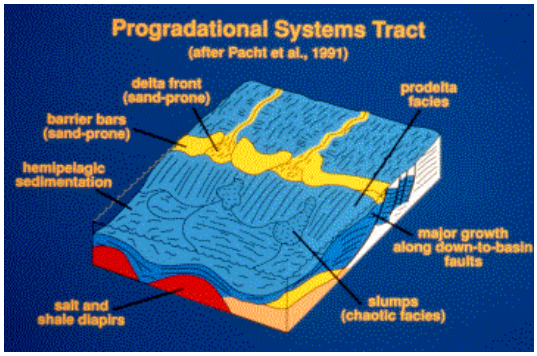

Left – Location map, showing 3-D seismic and well control. Right – Depositional model for a shelf margin delta as part of a "progradational" (i.e., "highstand") systems tract.

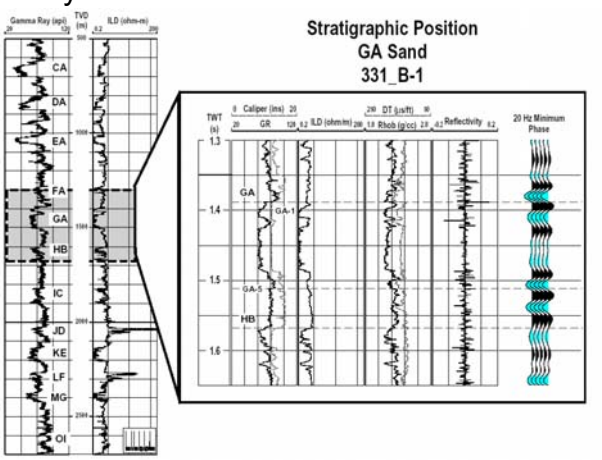

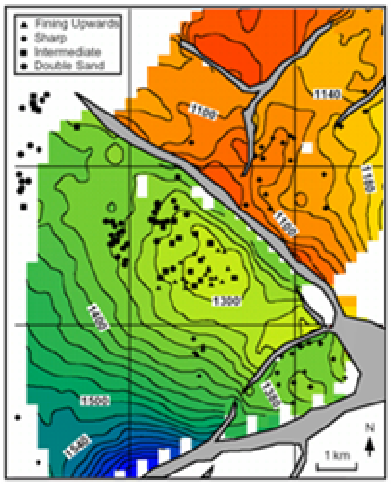

Type log at left showing the stratigraphic position of the GA Sand and a synthetic seismogram. The unit is wet at the location of this well. Right – structure map on top of the GA Sand.

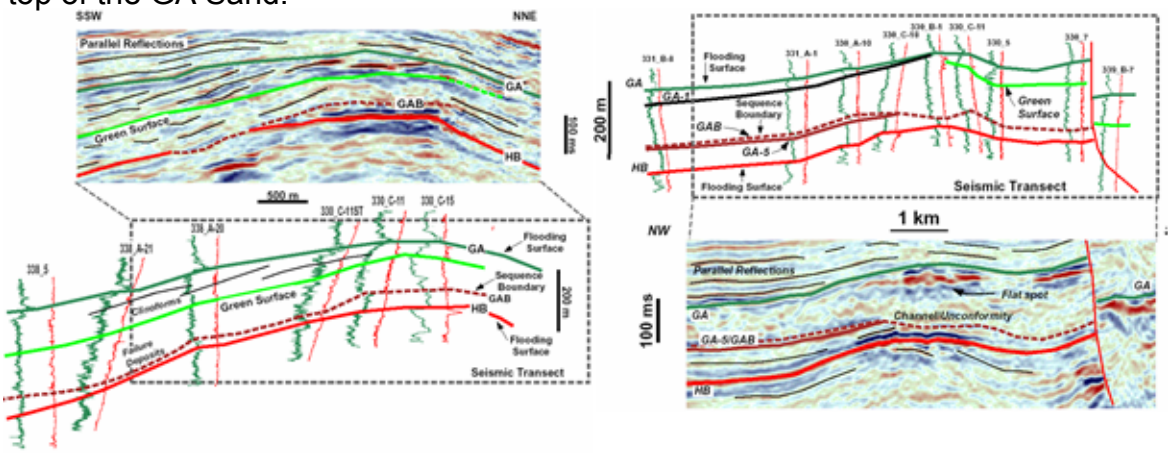

The image at left shows a stratigraphic dip section through the 3-D seismic volume and a corresponding log cross-section. The GA Sand is composed of at least two stacked progradational packages separated by a flooding surface. The image at left shows a strike section through the seismic data and corresponding log cross-section. Note the flat spot and evidence of erosion at the base of the package.

Case Study – Offshore Gulf of Mexico

Dip-oriented seismic transects through the crest of the anticline show bright spots that are somewhat discontinuous. The frequency content of the seismic data is not high enough to resolve these features properly, although they can be traced down-dip (to the south) into the clinoform package of the upper deltaic lobe. A log cross-section at this location shows that the discontinuous seismic bright spots correspond to a series of thin, shingled sands that are hydrocarbon charged. The sands have a progradational geometry. Conceivably, each of these small-scale sandy parasequences could be its own reservoir compartment.

In map view, the amplitudes have a “patchy” distribution on the crest of the anticline; they do not follow structural contours. Using the knowledge that the amplitudes are associated with charged sands at the up-dip limit of a prograding deltaic lobe, we can interpret the patchy amplitudes to be imaging lobe-like mouth bars deposited in a delta front setting. Core plug and production data, integrated with the seismic image, show that the best production is from high-amplitude patches (thick, porous and permeable clean sands) near the crest of the anticline. An area of reduced amplitudes right at the crest is shalier and has poorer production. High-amplitude areas lower on the structure watered out early in the production history.

In the graben area, the amplitude anomalies form ~ E-W striking linear trends that represent prograding inter-distributary delta front sands. A strike-oriented log cross-section through this area shows good clinoform geometries in the upper deltaic lobe, although these are not apparent in seismic transects. The flooding surface between the upper and lower deltaic lobe acts as a barrier to vertical fluid flow – some oil is trapped in the lower lobe. A fault compartmentalized one of the linear delta-front sands.

Based on evidence for stratigraphic and structural compartments, operators in the anticline and graben areas began an aggressive drilling program in the early 1990s The production decline was reversed and by the middle of the 1990s was better than it ever had been.

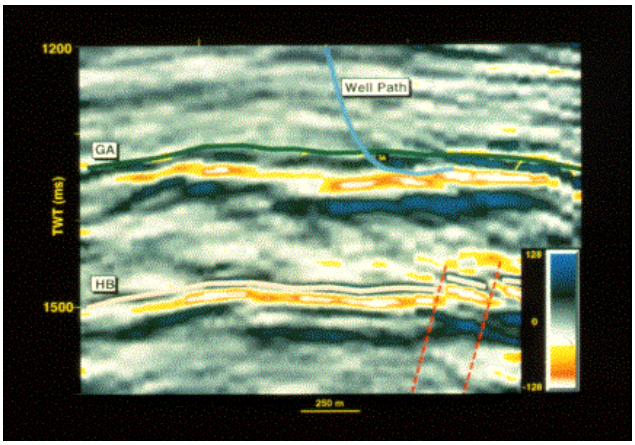

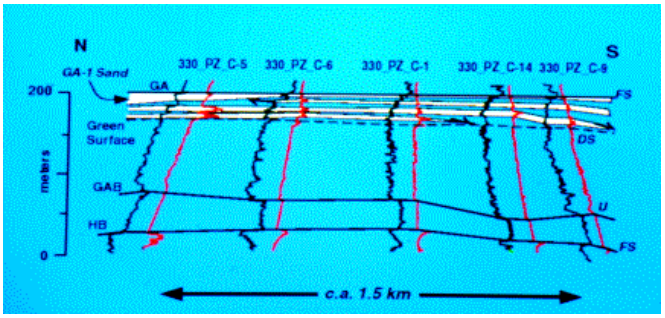

The seismic transect at left is a dip section through the GA Sand on the crest of the main anticline. The bright spots are discontinuous, but the reasons for this are not immediately apparent. The log cross-section at right (note that the orientation has been reversed) is datumed on a flooding surface at the top of the GA Sand. Several downlapping sandy parasequences may be defined. These discontinuous sands are responsible for the amplitude trends seen in the seismic data.

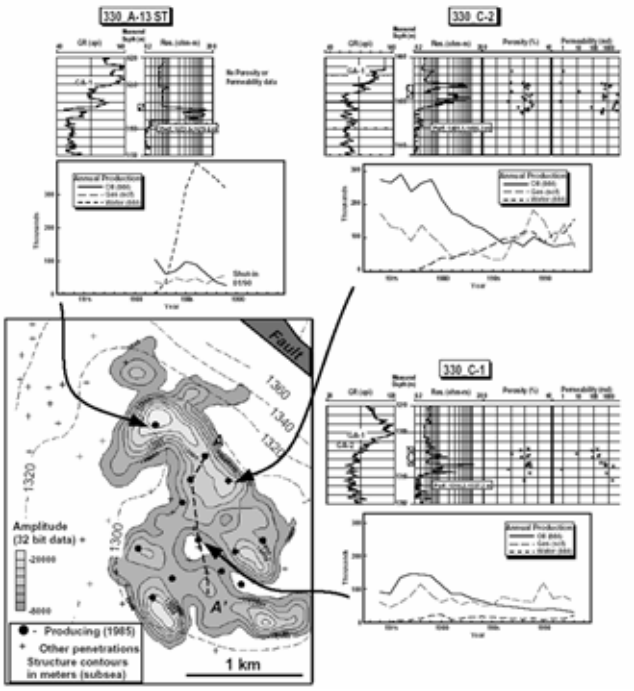

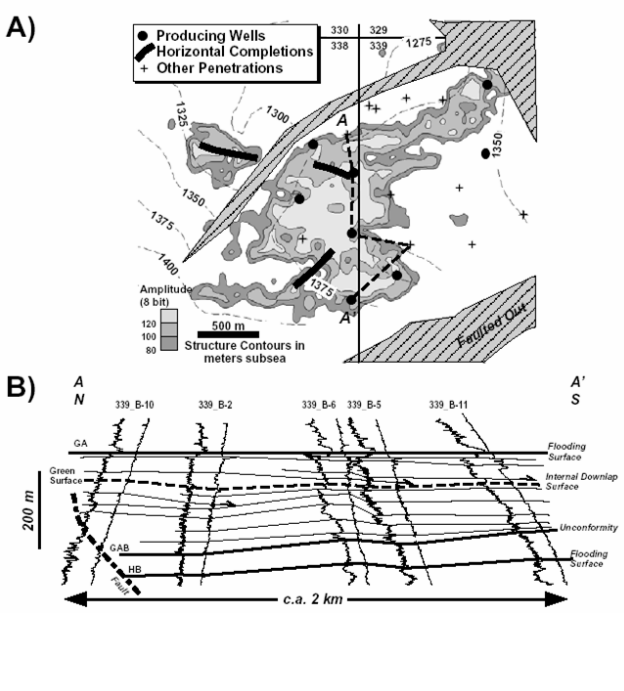

In map view, the amplitude anomalies at the crest of the anticline form “patches” that do not correspond to structural contours (left). This is because of the highly compartmentalized nature of these delta mouth-bar sands. Core and production data show that the best production is from high amplitude areas near the crest of the anticline. Undrilled patches are drilling targets. In the graben area (right) linear amplitude trends and clinoforms in log cross-sections indicate deposition in an interdistributary delta front setting. Deviated wells were drilled to target undrilled amplitude patches.

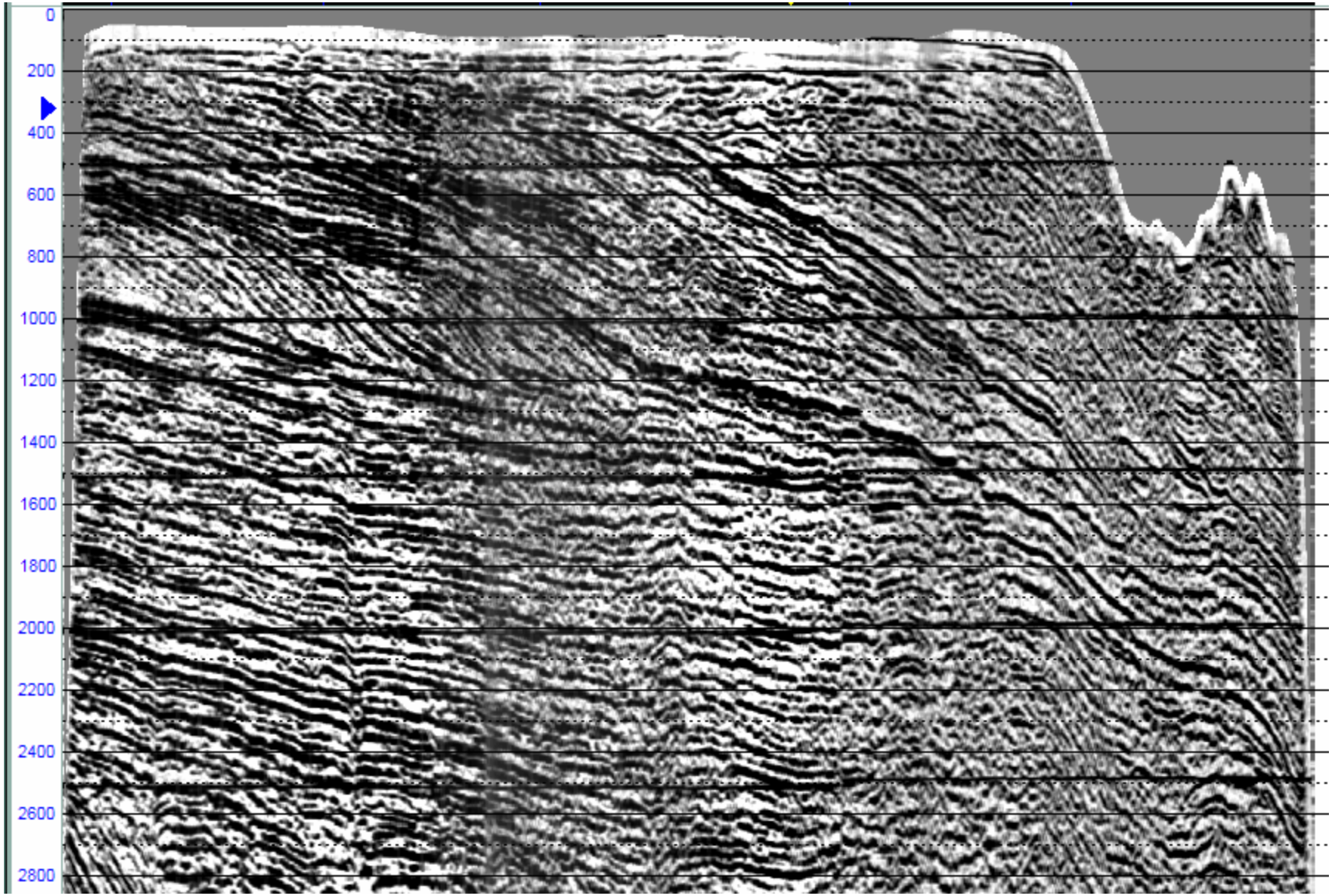

Identify stratal terminations and reflection configurations.

Advanced Topics

- Seismic technology is a rapidly evolving discipline. It can be hard for interpreters to keep up-to-date on all aspects.
- This chapter briefly explores some advanced topics in seismic technology that you may come in contact with:
  - Amplitude variation with offset (AVO)
  - Seismic attributes
  - Time-lapse (“4-D”) seismic
  - Multicomponent seismic
  - Inversion

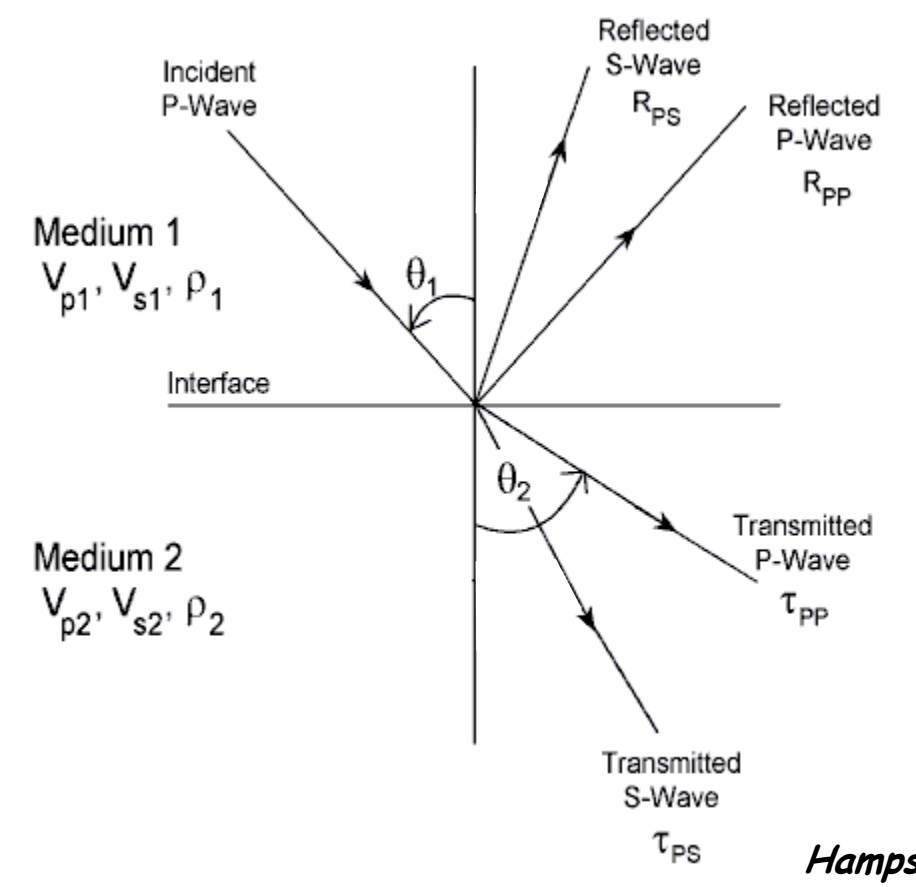

•The Schlumberger Oilfield Glossary (http://www.glossary.oilfield.slb.com/) defines amplitude variation with offset (AVO) as "*Variation in seismic reflection amplitude with change in distance between shotpoint and receiver that indicates differences in lithology and fluid content in rocks above and below the reflector*". It is a technique that may allow us to determine lithology and fluid content of rocks or sediments.

•When a downgoing p-wave hits a reflective interface, four waves are produced: transmitted and reflected p-waves, and transmitted and reflected s-waves. In other words, mode conversion occurs at the interface. The distribution of energy amongst the reflected and transmitted waves depends on the angle of incidence (theta) and physical properties of the layers above and below the interface.

•The media above and below the reflective interface each have characteristic p-wave velocities (V_p), s-wave velocities (V_s), and densities (ρ). Before we continue with AVO analyses, we need to examine the controls on these rock properties.

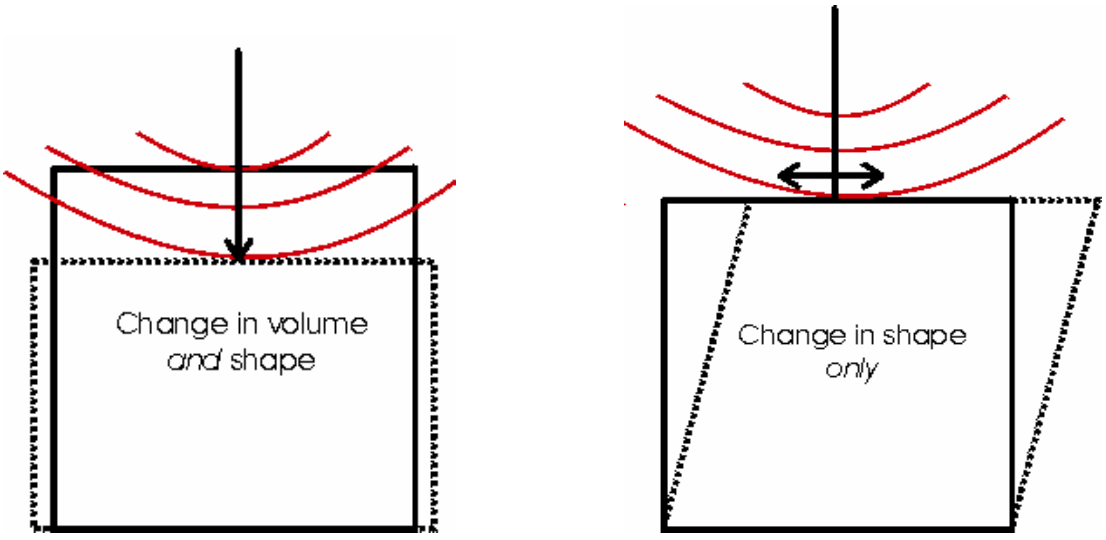

Scott-Pickford

•When a compressional wave (p-wave) travels through a body (left), the body undergoes changes in both volume and shape. When a shear wave (s-wave) travels through a body (right), the body undergoes a change in shape only.

•The p-wave velocity through a body is given by:

$$v_p = \sqrt{(\kappa + 4(\mu/3))/\rho}$$

•The s-wave velocity through a body is given by:

$$v_s = \sqrt{\mu/\rho}$$

•Where κ is the bulk modulus, μ is the shear modulus and ρ is the density.

•The bulk modulus, is a measure of the compressibility of a body (e.g., rocks or fluids). It is the stress-strain ratio under simple hydrostatic pressure, and measures the body's propensity to change volume (it is sometimes called the "incompressibility"). The shear modulus ("rigidity") is the stress-strain ratio for simple shear, and measures a body's reluctance to change shape. It provides information about the rock matrix.

•Importantly, from an AVO perspective, The shear modulus of a rock does not change when the fluid is changed. However, the bulk modulus changes significantly when the fluid changes. As such, the p-wave velocity of a rock will change as hydrocarbon saturation changes whereas the s-wave velocity will change relatively little (there is a slight density effect). Therefore, if we look at the V_p/V_s ratio of rocks we should be able to predict pore fill.

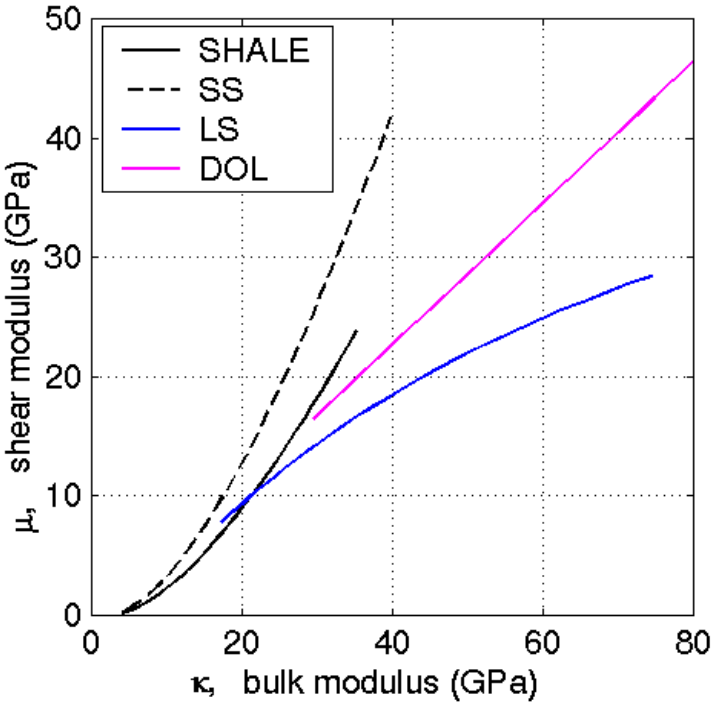

With increasing:	Compressional velocity	Shear velocity	Density	Incompressibility	Rigidity
Temperature	↓	↓	—	↓	↓
Pressure	↑	↑	↑	↑	↑
Pore Pressure	↓	↓	—	↑	↓
Porosity	↓	↓	↓	↓	↓
Clay content	↓	↓	—	↓	↓
Gas Saturation	↓	↑	↓	↓	—

•These two images, courtesy of Scott Pickford, illustrate relationships between bulk and shear moduli for different rock types (top), and how they, density and p- and s-wave velocities change as a function of various variables (bottom).

•The cross-plot at top shows how different lithologies may be distiinguished on the basis of their elastic moduli. The values are for brine-filled rocks/sediments. Unconsolidated materials (e.g., mud, unconsolidated sand) 0plot in the lower left, and highly consolidated materials plot in the upper right. The presence of gas in pore space will decrease the bulk modulus but not the shear modulus. Therefore the curves will be shifted to the left as gas saturation increases.

•The chart shows how changes in temperature, overburden pressure, pore pressure, porosity, clay content and gas saturation will affect elastic moduli (incompressibility – bulk modulus, rigidity – shear modulus), density and hence p- and s-wave velocity. Note that changes in gas saturation do not affect rigidity and only have a slight effect on the shear wave velocity.

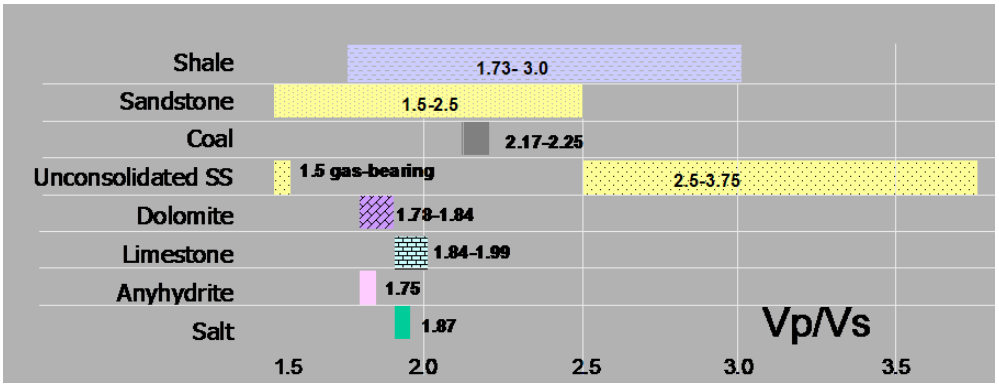

•The images on the previous page suggested that compressional- and shear-wave velocities are a function of several variables, including lithology and pore-filling fluids. This leads to the possibility of using the ratio of those two velocities to define lithology and gas content. This figure shows V_p/V_s ratios for various lithologies. There is some overlap between rock types, but each has its own characteristic range. Note the large change in V_p/V_s ratio for unconsolidated sand when the pore fill contains gas.

•Poisson's ratio (σ), a measure of the compressibility of a material perpendicular to applied stress, can be defined as:

$$\sigma = \frac{1 - 2\gamma^2}{2(1-\gamma^2)}$$

•where:

$$\gamma = \frac{V_S}{V_P}$$

•The images below show Poisson's Ratio versus Vp and versus porosity for different rock types. Note the difference between clastic and carbonate behaviour, and gas effect.

•All images on this page courtesy of Scott Pickford.

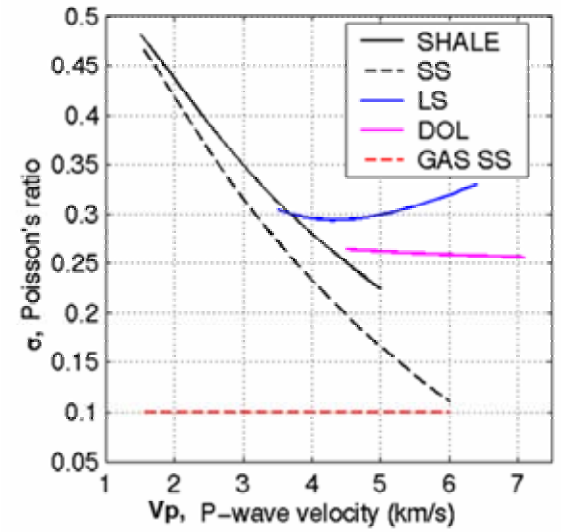

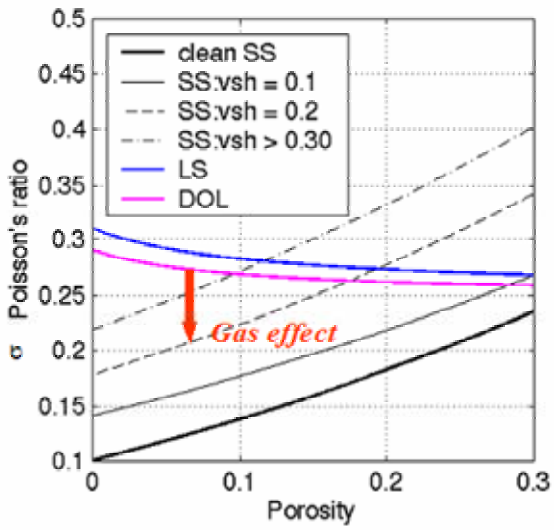

$$RC(\theta) \cong NI_P + \left[A_O\, NI_P + \frac{\Delta\sigma}{(1-\sigma)^2} \right] \sin^2\phi + \frac{1}{2}\frac{\Delta\alpha}{\alpha} \left(\tan^2\phi - \sin^2\phi\right)$$

$RC(\theta)$ = reflection amplitude for incident angle θ
NI_P = Normal incidence p-wave reflection
$A_O = B - 2(1 + B)\left[(1 - 2\sigma)/(1-\sigma) \right]$
$B = \left[(\Delta\alpha/\alpha) / (\Delta\alpha/\alpha) + \Delta\rho/\rho \right]$
α - average p-wave velocity = $(\alpha_2 + \alpha_1)/2$
$\Delta\alpha$ -difference in p-wave velocity = $\alpha_2 - \alpha_1$
σ - average Poisson's ratio = $(\sigma_2 + \sigma_1)/2$
$\Delta\sigma$ - difference in Poisson's ratio = $\sigma_2 - \sigma_1$
ρ - average density = $(\rho_2 + \rho_1)/2$
$\Delta\rho$ - difference in density = $\rho_2 - \rho_1$
ϕ - average of incident and transmitted angles

•Why the interest in Poisson's ratio? Shuey simplified the Knott-Zoepritz equations and showed that the variation in reflection coefficient as a function of angle of incidence (RC(Θ)) could be broken down into three terms, as shown above. The first term is the normal incidence p-wave reflection coefficient, it contributes at all angles. The second term starts to contribute significantly for angles of incidence over 15º (i.e., "middle" offsets"). The third term represents the far angles/offsets and can be ignored for angles < 30º. Note the importance of Poisson's ratio for the middle term.

•Further simplification led Shuey to propose the following two-term approximation:

$$RC(\theta) \cong NI_P \cos^2\theta + \frac{(\sigma_2 - \sigma_1)}{1 - \frac{(\sigma_2 + \sigma_1)}{2}} \sin^2\theta$$

•Where σ_1 and σ_2 are Poisson's ratio for the upper and lower layers respectively.

•The first term in the two-term formulation is known as the "normal incidence reflectivity" and the second term is the "Poisson reflectivity".

•Other simplified versions of the Knott-Zoepritz equations have been proposed (e.g., Aki and Richards, Gelfand). All of these methods do a fairly decent job of predicting the true response, at least up to angles of about 20 - 30º.

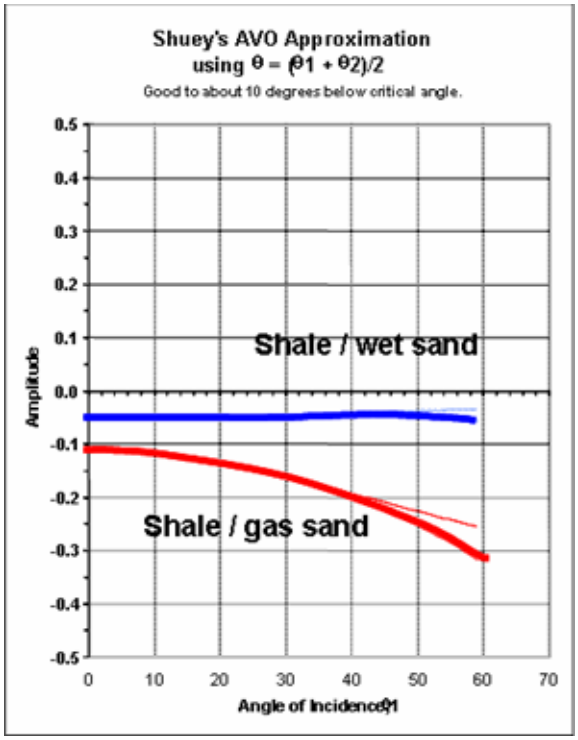

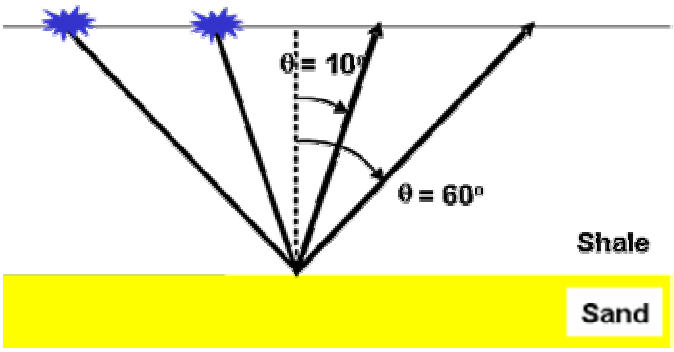

Courtesy Chroma Energy

•From the previous discussion, it should be clear that changes in gas saturation should change Poisson's ratio, causing an AVO effect (from Shuey equation). The variation in amplitude may be either a brightening with offset or a dimming. In fact, a wide range of AVO responses is possible, depending on the geologic setting of the reservoir. It is the contrast between a gas-charged reservoir and the encasing medium that matters.

•To examine AVO effects, we must work with prestack data. The images above shows a "classic" AVO response for a water filled sand overlain by a shale that has a higher acoustic impedance (i.e., a negative reflection coefficient is present at the shale/sand interface). A negative amplitude response (trough) will be generated at the interface. The blue curve shows that relatively no change in amplitude will be present when the angle of incidence increases. For a gas sand, red curve, the normal incidence amplitude is more negative (i.e., stronger) and there is a pronounced strengthening of reflection amplitude (more strongly negative) as the angle of incidence increases.

•The images below show changes in amplitude with offset for a real dataset.

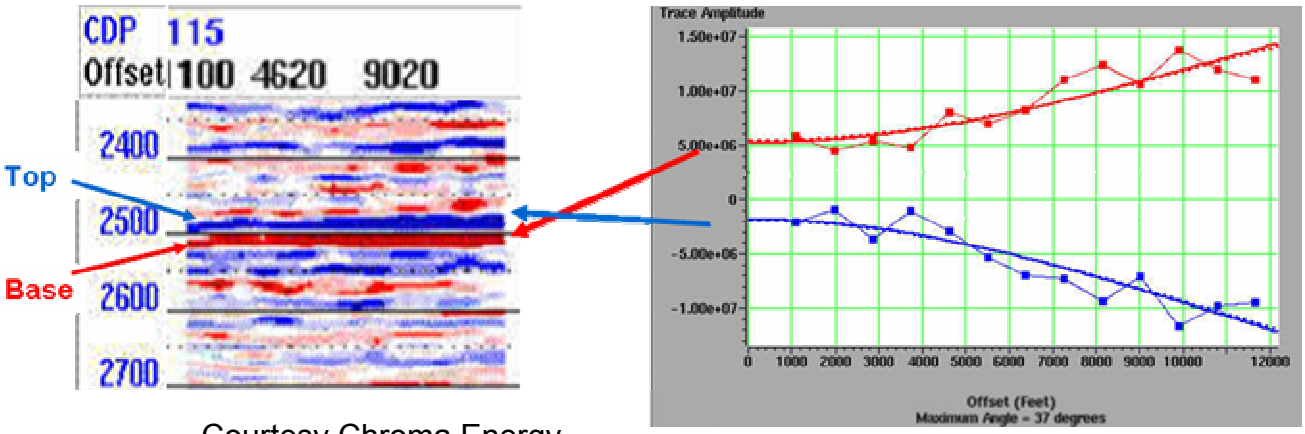

Courtesy Chroma Energy

Type of Gas-Sand Reflector (relative to overlying medium)	AVO Response	DHI Response
Class 1 – Higher impedance gas sands	Peak decreases in amplitude with offset	Dim out
Class II – Near-zero impedance contrast	Amplitude may increase or decrease with offset	Phase reversal
Class III – Lower impedance gas sands	Bright trough at near offsets, brightens with offset	Bright spots
Class IV – Lower impedance gas sands	Trough bright at near offsets, dims with offset	Bright spots (Vs gas < Vs overlying)

•The table above lists four different classes of AVO response. For each class the relative acoustic impedance contrast is given, how amplitude changes along the reflection, and the type of "direct hydrocarbon indicator" (DHI) amplitude response.

•The figure below shows model examples for each class. Class II responses may be further subdivided into two types.

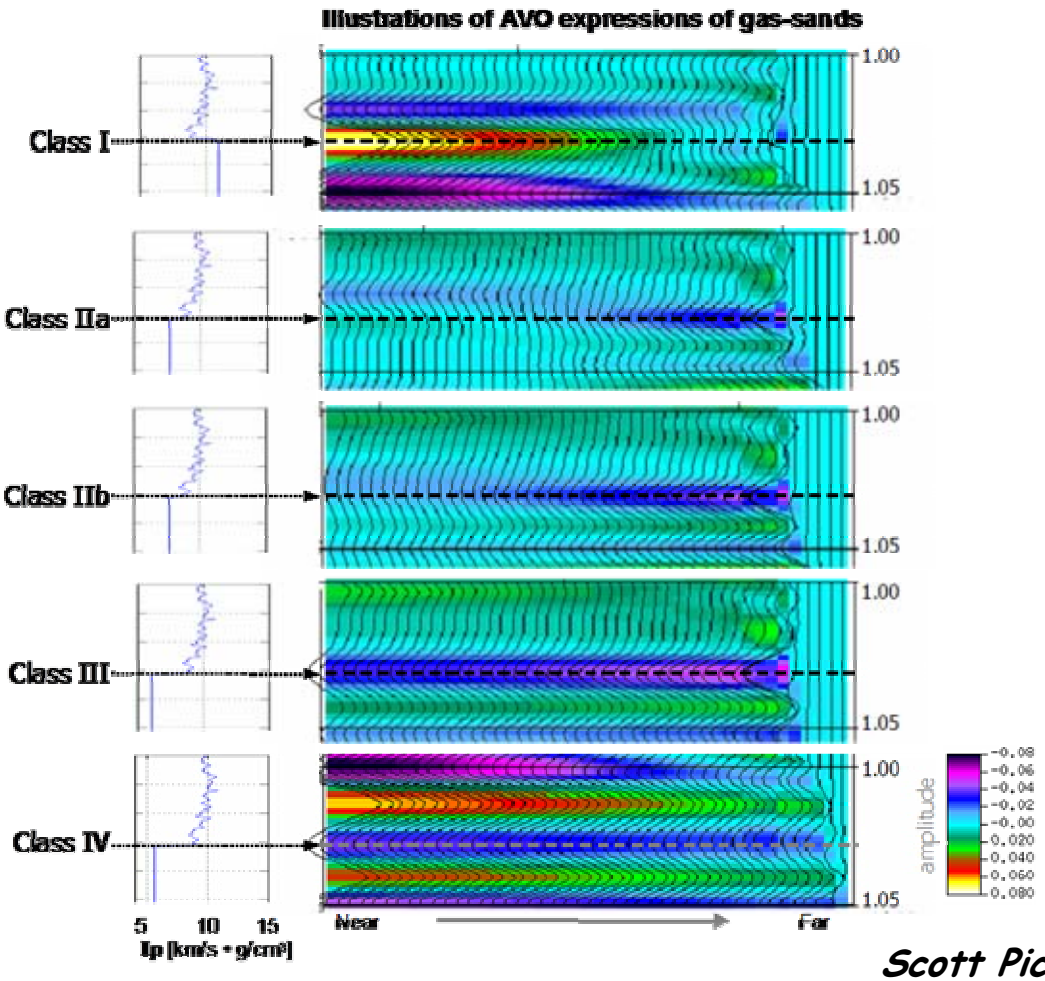

Scott Pickford

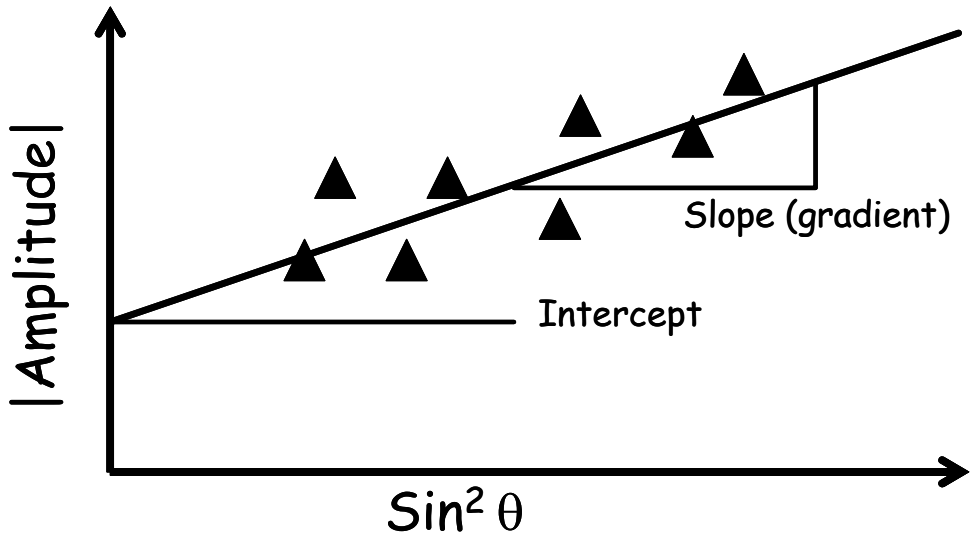

•If we plot how amplitude changes with angle of incidence for a given reflection in a gather, we might get an image like the graph shown above. The amplitude is on the y-axis and Sin^2 of the angle of incidence is shown along the x-axis. The amplitude of the reflection for each trace in the gather is shown as a triangle. Although there will be some scatter, it should be possible to fit a regression line to the data points. The regression line will have an intercept and a slope:

$$\cdot R(\Theta) = A + B\sin^2\Theta$$

•Where A is the intercept (denoted by "P" in Europe) and B is the slope (denoted by "G" in Europe). The intercept corresponds to the normal incidence reflectivity in the two-term Shuey equation. The slope corresponds to the Poisson reflectivity term.

•As shown in the image below, we can use cross-plots of A and B to distinguish the different AVO classes.

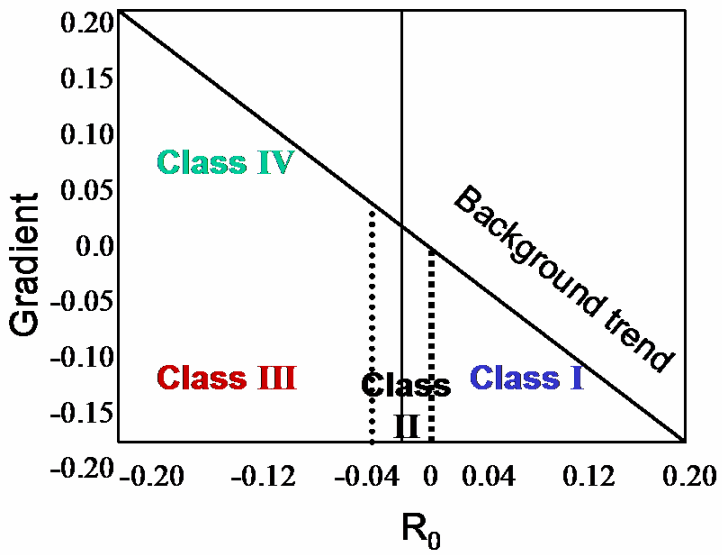

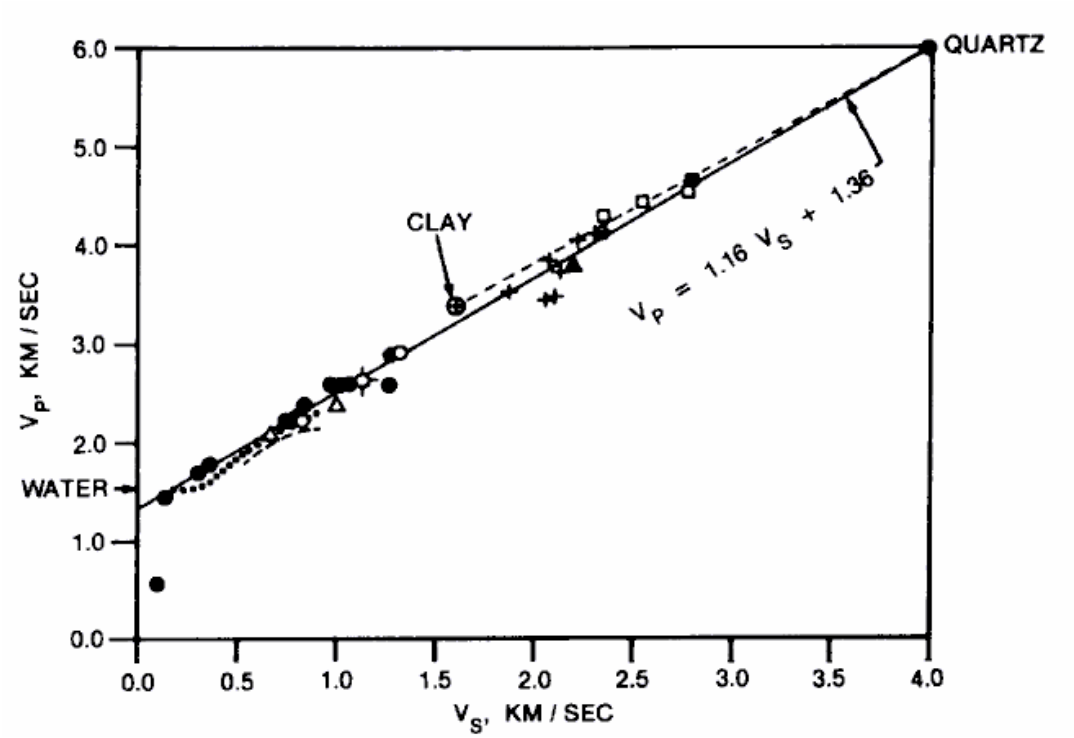

Castagna et al., 1985

•It is deviations from the "background trend" shown in the previous image, rather than the absolute values of A and B, that allow the different AVO classes to be identified. The background trend corresponds to "wet" rocks and may be estimated using Castagna et al. (1985) compiled available data and defined a "mudrock line" that empirically relates Vp to Vs (velocities in km/s) for a range of clastic rocks (water to quartz end members):

$$\bullet Vp = 1.16\ Vs + 1.36$$

•Since then the coefficients for the mudrock line have been shown to vary from basin to basin. Proper determination of these coefficients is required for accurate AVO analysis. Knowledge of V_p and V_s can be used to predict Poisson's ratio, and hence the gradient term in Shuey's equation.

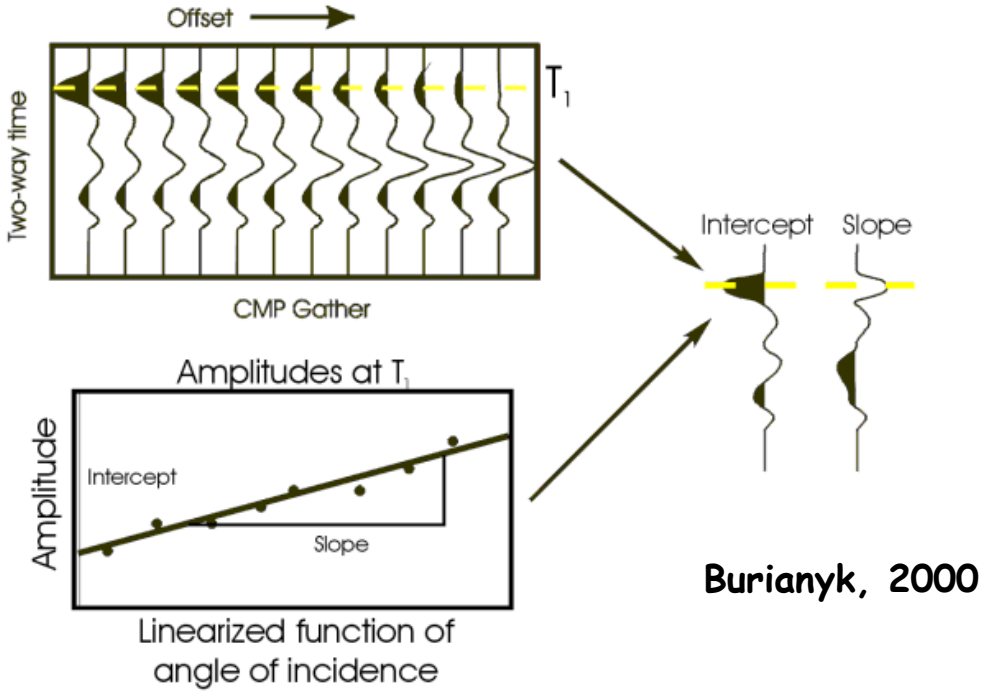

Burianyk, 2000

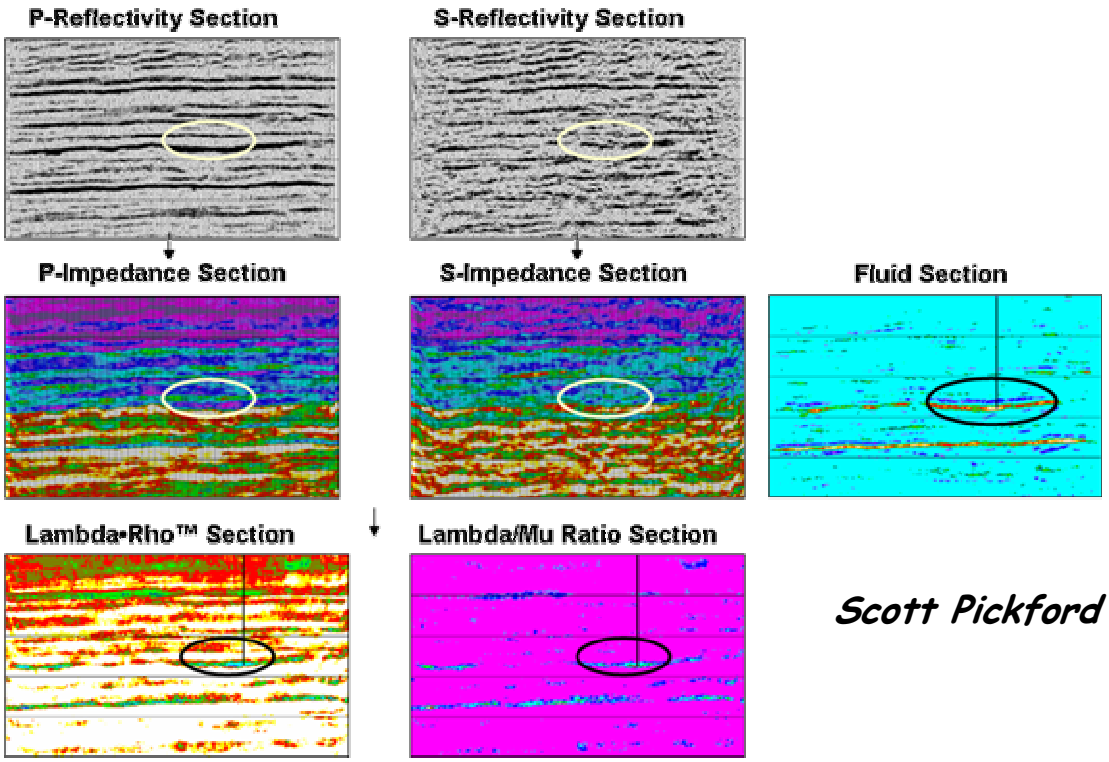

Scott Pickford

•In principle, pre-stack analyses allow intercept and gradient (A and B) to be defined for every sample on every trace in the stacked volume/line. As such, for 3-D data we can generate “intercept” and “slope” attribute volumes (2-D data will allow us to generate “intercept” and “slope” versions of those lines).

•The use of different algorithms will allow us to generate a variety of other AVO attributes (“elastic impedance” attributes), some of which are shown below.

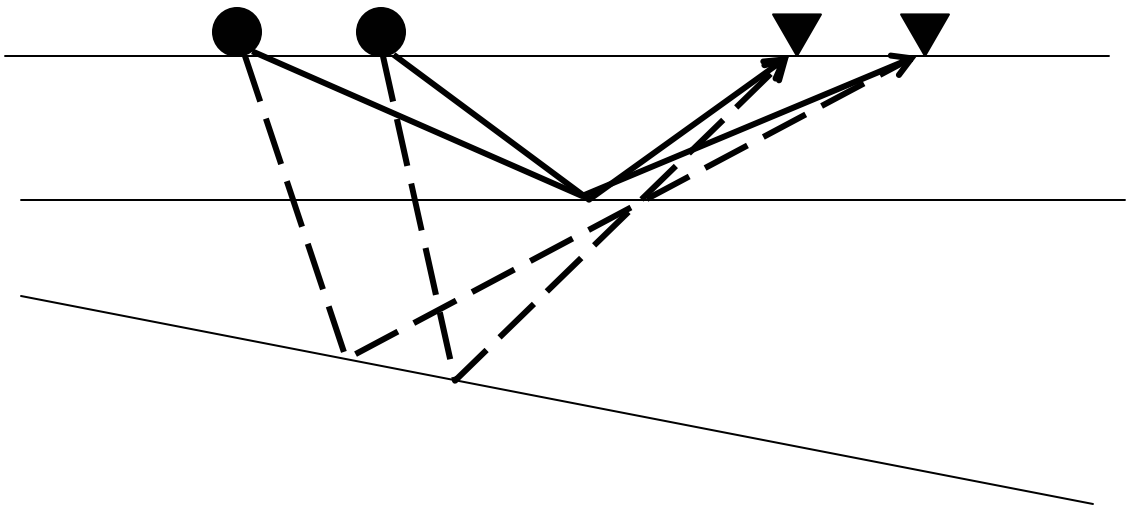

•Specialized processing needs to be undertaken in order to undertake AVO analyses.

•These include:

•Amplitude corrections

- Spreading, array effects, etc.

•Deconvolution/multiple attenuation

- Filtering

•Velocity corrections

- Non-hyperbolic moveout
- Pre-stack DMO, advanced velocity analyses, etc.

•Noise attenuation

- Filtering, muting

•Additionally, until now we have been assuming that source-receiver offset is an approximation of the angle of incidence. This will only be true if the layers are horizontal (e.g., for the upper reflector and solid raypaths in the image at top). If not (e.g., lower reflector and dashed raypaths), the data will need to be converted from common midpoint gathers to common reflection point gathers.

Case Study - AVO

•The following case study is taken, with permission, from Hampson-Russell training material. It illustrates integration of synthetic seismic modeling, fluid replacement modeling, and AVO analysis (including cross-plot techniques). Figures are shown on the following page.

•The first step is to use logs to predict whether an AVO response should be present. To do so, we need to be able to measure Poisson's ratio. The example uses a well that has a density and p-wave sonic log, but no s-wave sonic log. As such, the s-wave sonic needs to be generated artificially from the p-wave log using Castagna's empirical mudrock line equation. Note that this assumes that the pore-fill is brine, which is potentially (hopefully!) not the case for the sand we are studying. To account for this problem we need to perform fluid replacement modeling to predict the velocity (p- and s-wave) and density of the sand for a given hydrocarbon type and saturation. We also need to specify parameters such as brine salinity, sandstone matrix composition, etc. The Biot-Gassman equations are used for this purpose.

•Once the correct log parameters have been modeled, we will generate an offset-dependent synthetic seismogram for the data showing the expected AVO response. The synthetic uses the Zoeppritz equations to calculate the amplitude for given angles of incidence. For the data used in this example, we predict a strong Class III AVO response.

•Cross-plotting of the synthetic seismogram results allows us to view a plot of intercept versus gradient. The graph shows a background trend ("wet"), and two clouds of points that deviate from the trend. By drawing circles around these points, we can see where they appear in the synthetic seismogram. Note that they represent the top and bottom of the gas-charged sand. We will use this technique on a real dataset later.

At right are the offset-dependent synthetic seismogram and shear wave sonic and Poisson's ratio logs. Because a shear-wave sonic log was not run in the well, these two logs have been calculated using Castagna's relationship between Vp and Vs. As such the values are probably incorrect in the sand.

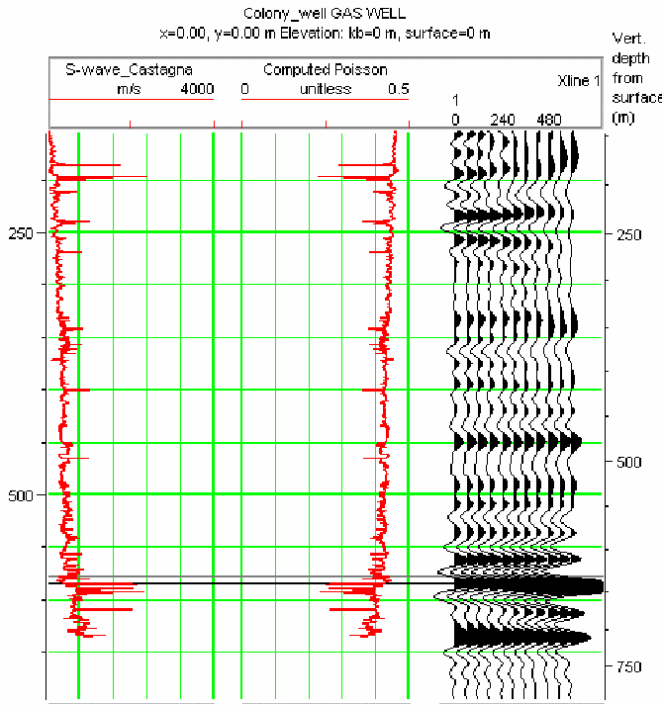

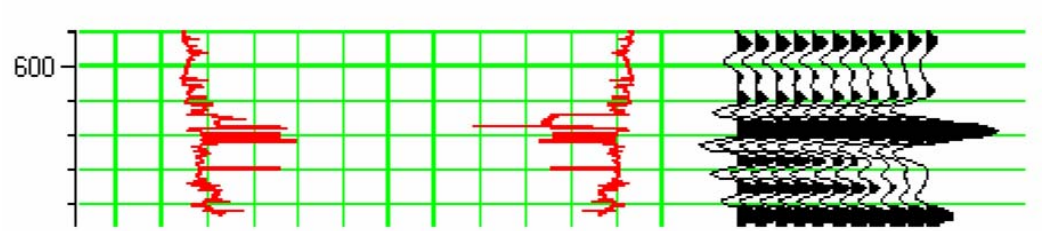

Fluid replacement modeling, based on Biot-Gassman equations, has been used to modify the shear wave sonic log, and hence Poisson's ratio log, in the sand to a value that corresponds to 50% gas saturation. The synthetic now shows a marked AVO effect.

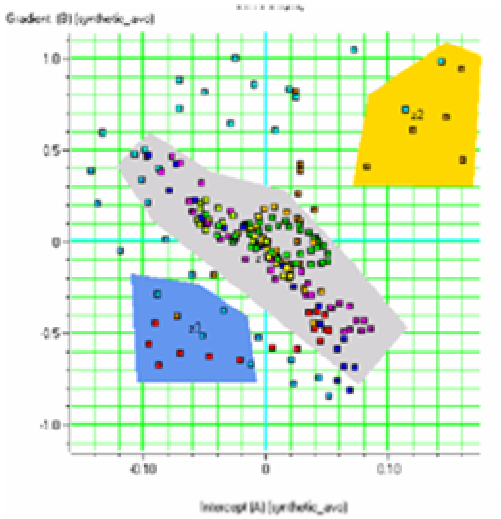

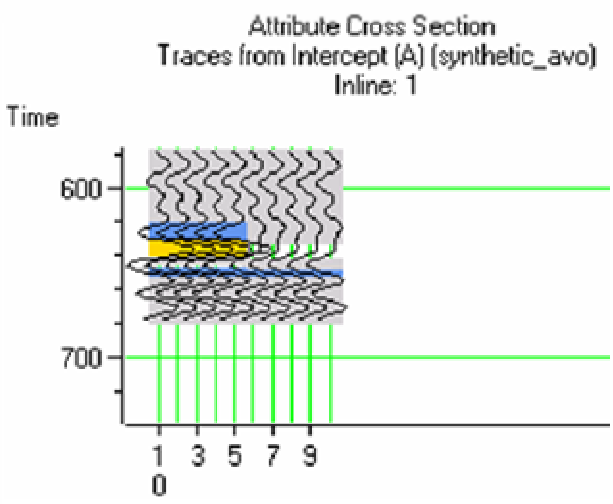

The gradient/intercept crossplot (left) shows different data clusters. The grey area in the middle corresponds to the "background trend" – wet sands and shales. Areas in the upper right (yellow) and lower left (blue) correspond to anomalies – the blue trend corresponds to a Class III anomaly. The colored zones show up on the synthetic.

Case Study - AVO

•We have used modeling to predict that we should be able to see an AVO anomaly corresponding to a gas sand. Now it is time to look for similar trends in the data.

•The well is located with respect to CDP gathers on a 2-D seismic line. We focus on the CDP that corresponds to the well location. As with the synthetic seismogram, we can make a crossplot of gradient versus intercept for the gather. This time, there is significantly more scatter in the data points than with the synthetic example. However, it is still possible to identify a background trend (grey area) and data points in the Class III anomaly field (blue) and others in the upper right (yellow) that would correspond to the base of a gas-charged sand.

•The software is able to dynamically link the CDP gathers with the corresponding data points in the stacked seismic image. As such, the grey, blue and yellow areas identified on the crossplot will show up on the stacked seismic image. This image shows the location of a Class III AVO anomaly on this 2-D seismic image. Gas is known to be present in this level at the well location. How would you adapt this technique for use in exploration areas – i.e., those without well control?

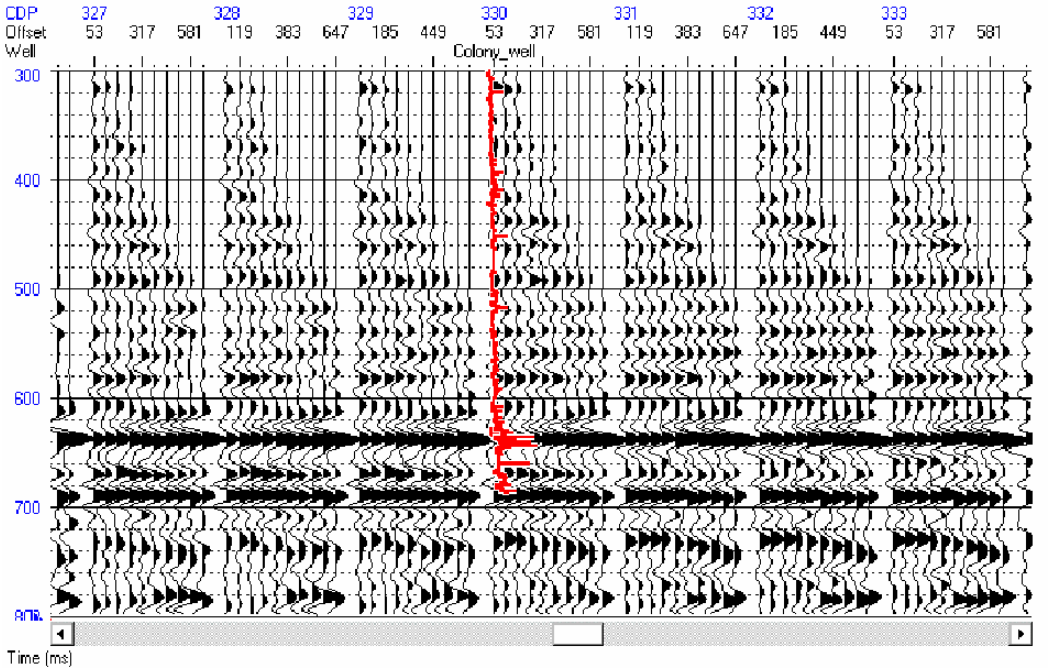

NMO-corrected CMP gathers for a 2-D seismic line. The well location corresponds to the gather in the middle of the image.

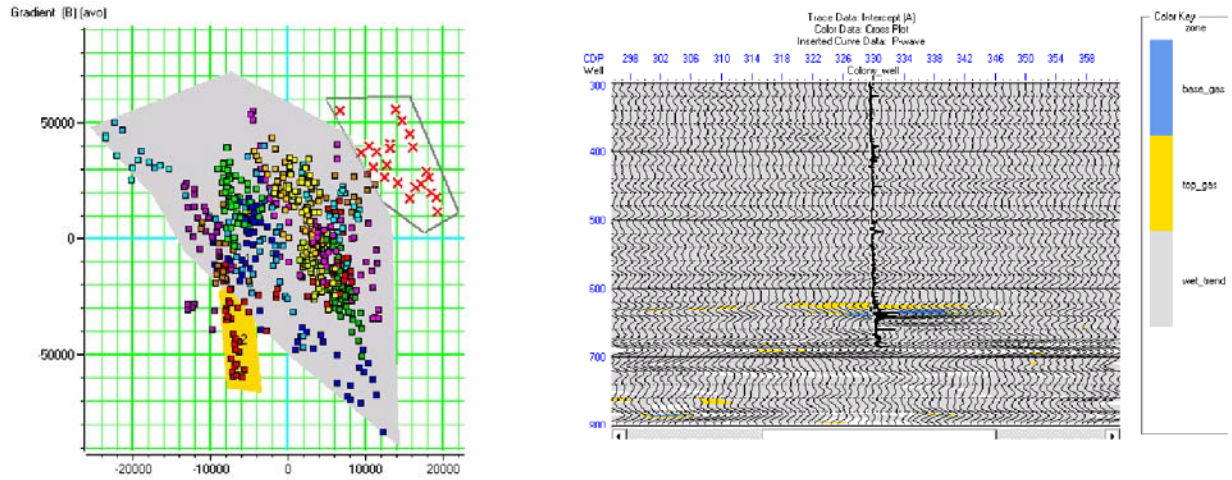

Gradient versus intercept plots (left) may be generated for the CDP gathers. A background trend, with much scatter, is identified (grey) and anomalies (yellow and upper right) are identified. Because the crossplot is dynamically linked to the seismic data, it is possible to see the distribution of the anomaly areas, even in the stacked seismic image (right). The yellow area has been identified as a Class III AVO anomaly (top of the sand) and the blue area corresponds to the base of the sand.

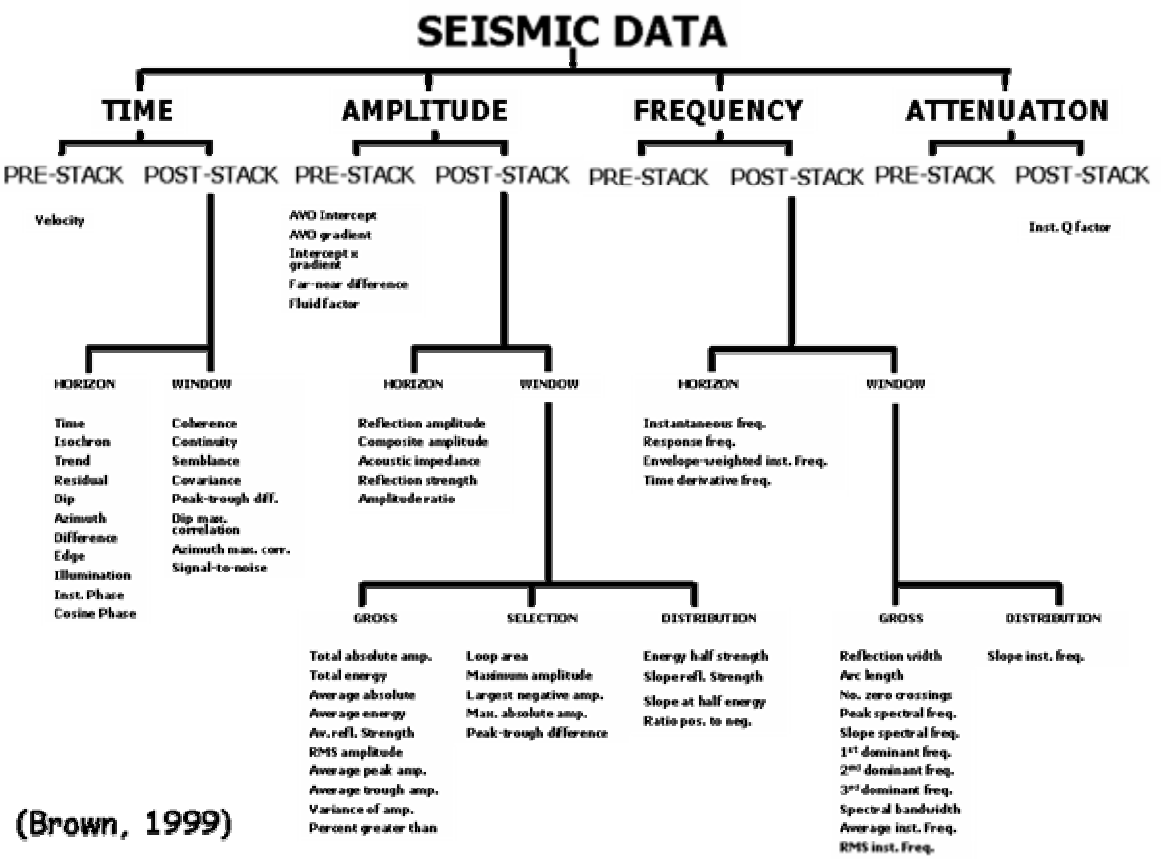

•What is a seismic attribute? Brown (1996) defined a seismic attribute as “a derivative of a basic seismic measurement”. Chen and Sydney (1997) defined an attribute as “a specific measurement of geometric, kinematic, dynamic or statistical features derived from seismic data”. Other definitions exist. Essentially, an attribute is: a) some sort of quantitative measure, b) derived from the data itself or from the interpretations (e.g., “horizon attributes” described in a previous chapter).

•Many different types of attributes have been defined, described or proposed, and it can be difficult even for specialists to keep track of them. Some attributes have been derived from the field of signal analysis and their relationships to geological features remains poorly documented. Some attributes are “proprietary”, e..g, those that have been developed by large oil companies. For example, coherency (used to identify faults and stratigraphic features) was developed and patented at Amoco.

•The table above, modified from Brown (1996) is an attempt to classify some of the more widely used seismic attributes.

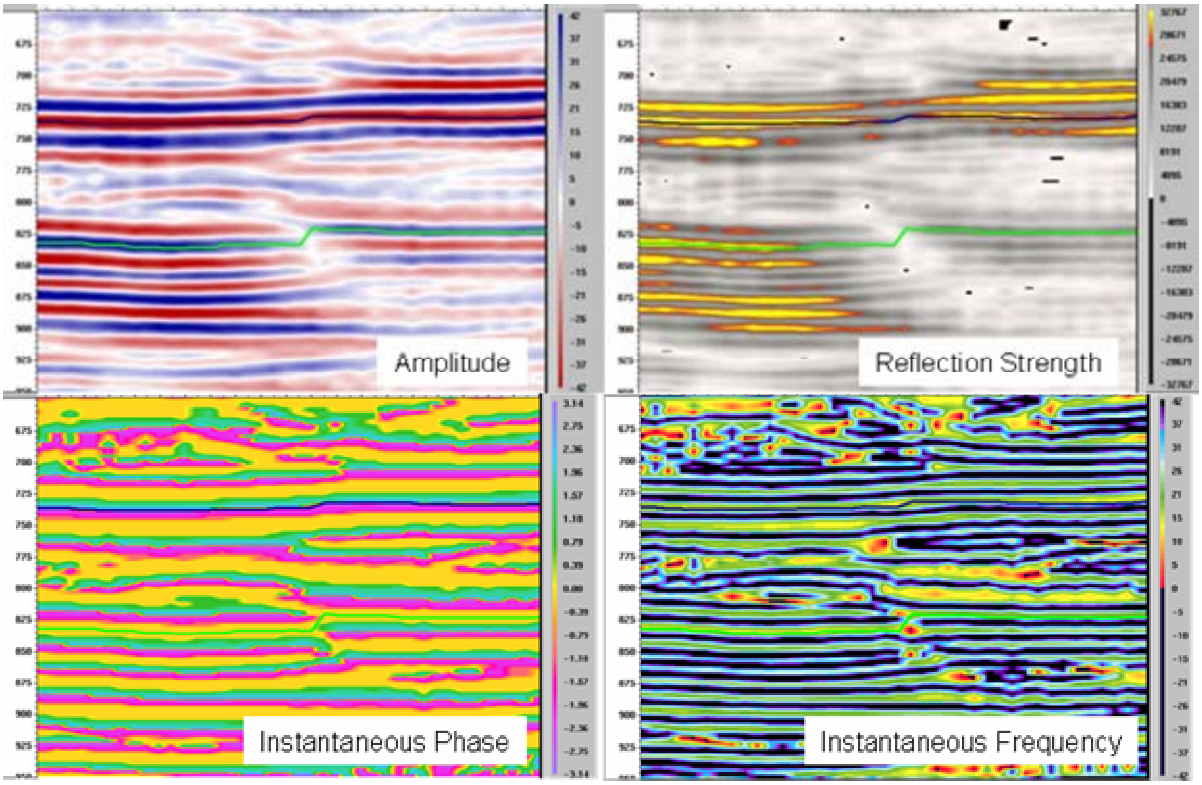

•The four principal attributes are shown above. Each image shows the same portion of a 3-D seismic survey. Seismic amplitude (top left) is the “basic measurement” of seismic data. Traces consist of a time-series of amplitude measurements. At upper right is reflection strength – amplitude independent of phase. Lower left shows instantaneous phase – phase independent of amplitude. At lower right is instantaneous frequency – the rate of change of phase. Notice how each measure changes throughout the images.

•Reflection strength, instantaneous phase and instantaneous frequency are derived using the Hilbert transform. As such, they are referred to as “complex trace attributes”.

•Each of these attributes is described in more detail in the following pages.

•In this area, a small reverse fault affects the lower part of the section. These are Lower Paleozoic carbonates and clastics.

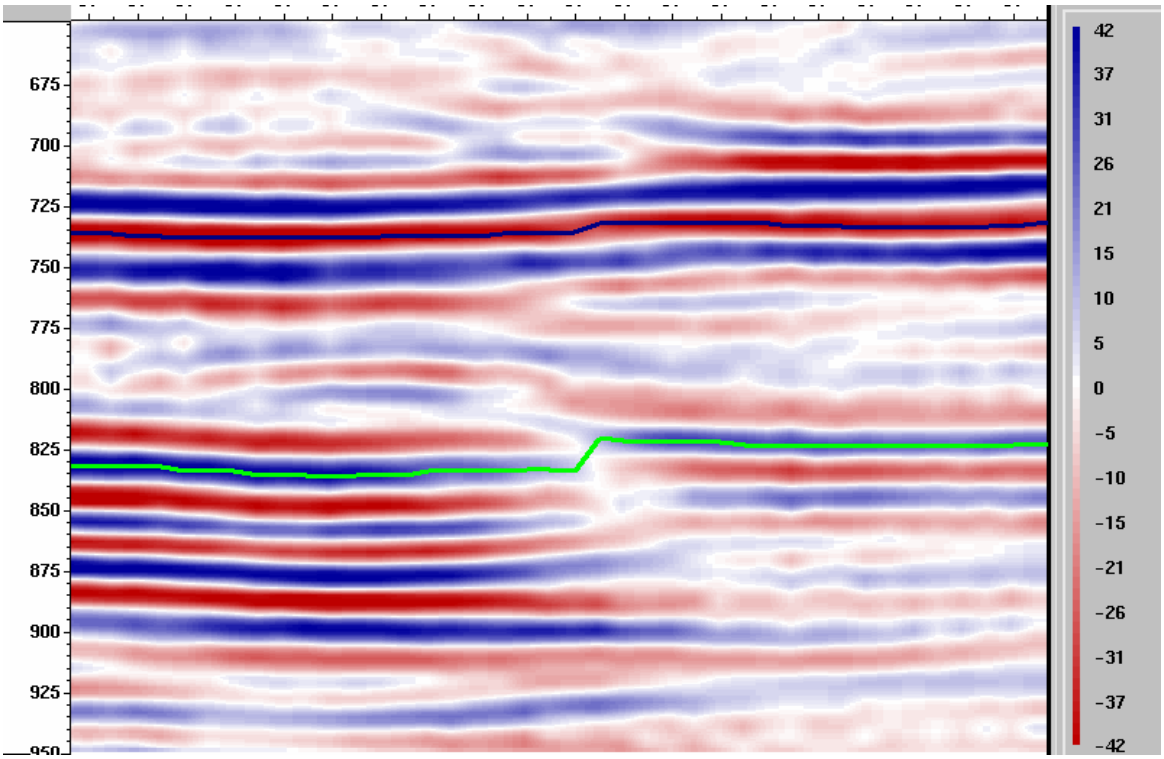

•This seismic transect shows a transect through some Lower Paleozoic carbonates and clastics. Two horizons have been interpreted (black – upper, and green – lower). A reverse fault, actually associated with some wrench faulting into the plane of the section, is present below the green horizon. This section will serve as a reference section for comparing other complex trace attributes.

•Seismic amplitude is the “basic measurement” of seismic data, each trace consists of a time series of amplitude measurements.

•The range of amplitude values in a seismic dataset depends on how the data have been stored. For 8-bit data, amplitudes theoretically range from ±128, 16-bit data theoretically range from ± 32,768 and 32-bit data range from ± 4,294,967,296. 32- and 16-bit data have more dynamic range than 8-bit data, but take up correspondingly more amounts of storage space. Most monitors are only able to display 356 colors (corresponding to 8-bit data). It is advisable to work with 16- or 32-bit data when doing quantitative attribute analyses.

•The blue-white-red color scale is a “standard” for seismic interpretation. The North American convention, positive values shown as blue, is used in this image. Other color bars are useful for other purposes.

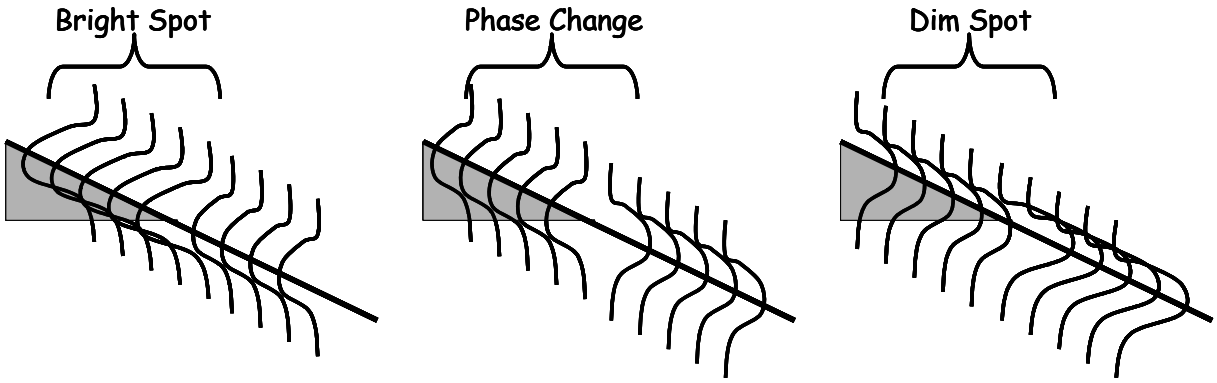

•Changes in seismic amplitude are sometimes used as a direct hydrocarbon indicator (DHI). Three different possibilities are possible.

•Bright spots occur when the acoustic impedance of a brine-filled sand is less than the acoustic impedance of the surrounding shales. This leads to a negative reflection coefficient that is displayed as a trough (at least in North America). If gas replaces at least some of the water in the pore space, the acoustic impedance of the sand becomes much less than the acoustic impedance of the surrounding shales and the trough becomes stronger ("brighter"). Bright spots are typical of young, unconsolidated sands but may also be present in older unconsolidated deposits (e.g., gas in unconsolidated Lower Cretaceous sands in the heavy oil areas of western Canada).

•When the acoustic impedance of a brine-filled sand is slightly higher than the acoustic impedance of the surrounding shales, putting gas in the pore space causes the sands to have lower acoustic impedance than the shales. The reflection at the top of the sand changes from a low-amplitude peak to a trough – i.e., a phase change.

•Finally, if the acoustic impedance of the brine-filled sand(stone) is higher than the surrounding shale (as in older, consolidated rocks), the addition of gas to the pore space causes the acoustic impedance to drop, but it still remains higher than that of the surrounding shale. The result is a dimming of the peak – a dim spot.

•Not all hydrocarbon accumulations produce detectable amplitude changes. Similarly, not all changes in seismic amplitude are associated with changes in fluid saturation. Changes in lithology, bed thickness, porosity and other factors can cause changes in seismic amplitude. Finally, it only takes a small amount of gas to generate an impressive looking bright spot; not all are associated with commercial accumulations of hydrocarbon.

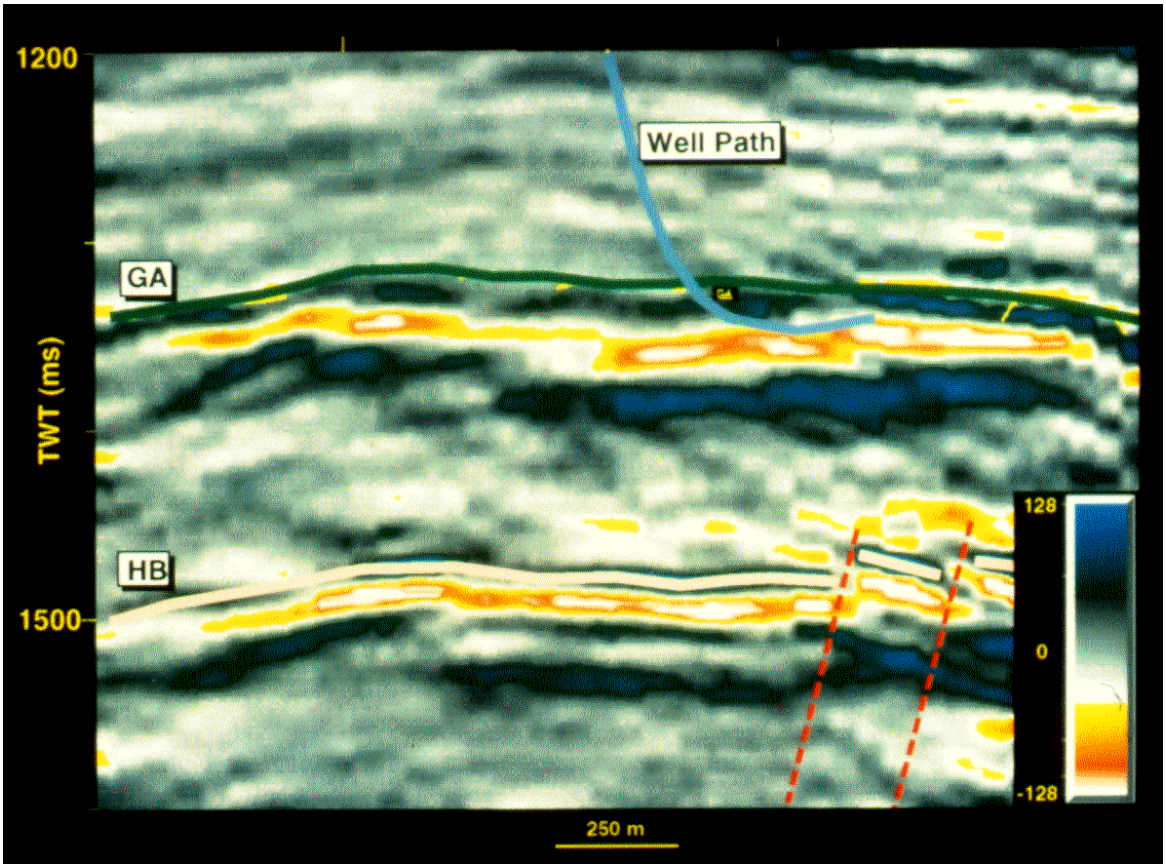

•Skillful manipulation of color bars is a useful technique for highlighting amplitude anomalies. This image shows two stacked hydrocarbon accumulations from a young (Pleistocene) deltaic succession. This is bright spot territory, and so the tops of hydrocarbon-charged sands are expected to generate a trough. The color bar shows low amplitudes in white/grey and strong peaks in black - dark blue. High-amplitude troughs (bright spots) are shown in “hot” colors – yellow/orange/white. Notice how well they stand out. The bright spots are noticeably discontinuous – at least at the GA level, due to reservoir compartmentalization in these delta front deposits.

•The well path appears to have missed the reservoir, but in fact went through it. This is an artifact of the data’s mixed-phase character.

•Notice how the HB horizon appears to sag at the crest of the anticline. This is probably a velocity artifact (“push down”) due to the relatively slow velocities in the hydrocarbon-charged sands of the overlying GA interval.

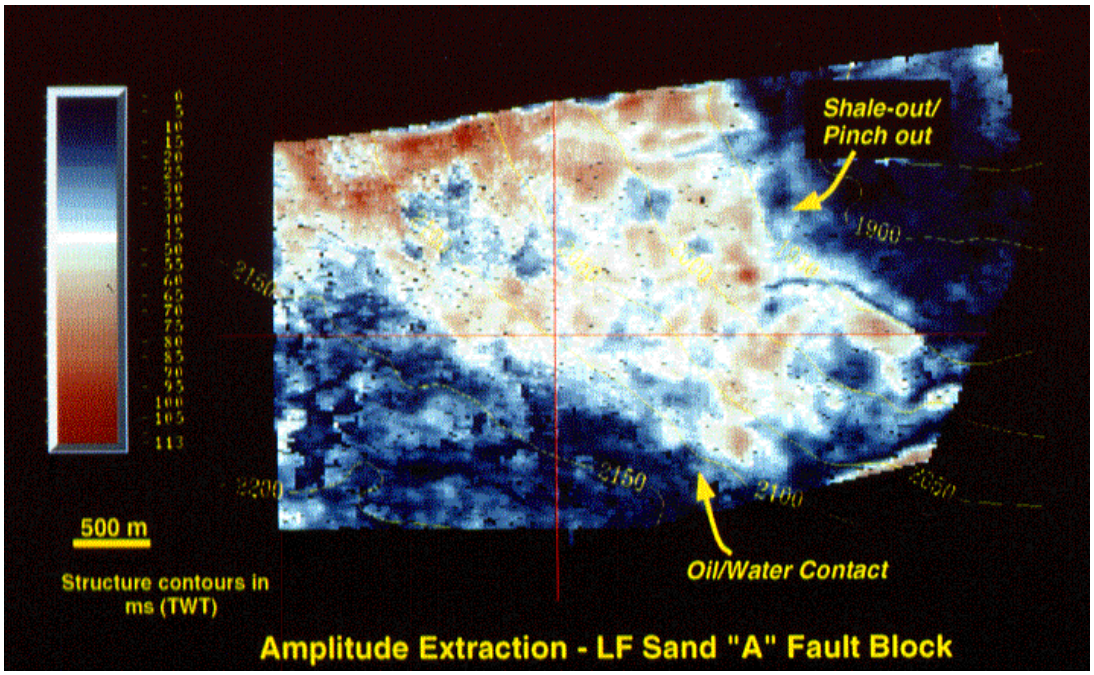

•It is often useful to examine seismic amplitude in map view. This image, a horizon slice from a young clastic region, shows a classic “bright spot”. Low amplitudes are shown in blue, high amplitudes in red. Time-structure contours are shown in yellow. The lower limit of the high amplitudes (at left) is approximately parallel to structure contours and corresponds to an oil-water contact (known from well control). The upper limit of the high amplitudes (at right) corresponds to a pinch-out of the sands onto a dome (known from well control).

•Conformity between structure contours and the limits of a high-amplitude area is often considered to be an indication that the amplitudes are related to the presence of hydrocarbons (a bright spot). However, this correspondence will only be observed if: a) the sand is continuous (not compartmentalized by stratigraphic or structural features), and b) there are no hydrodynamic factors that tilt the fluid contact.

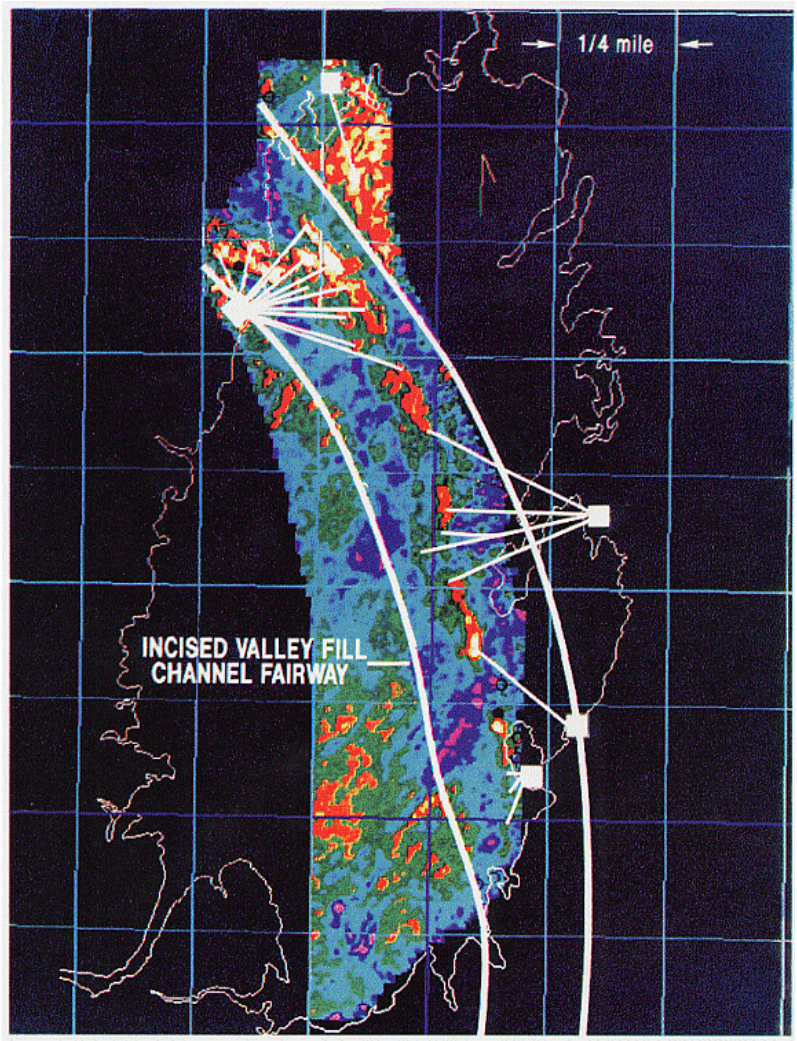

•As noted previously, not all amplitude variations are caused by changes in hydrocarbon saturation. Integration of geologic analyses, seismic modeling and petrophysical modeling may be needed to determine the controls on seismic amplitude.

•This example, from Broger and Syhlonyk (1995), shows a horizon slice through a Cretaceous clastic section. An incised valley fill (IVF) fairway could be tracked beneath a lake. From drilling north and south of the lake, it was known that clean, porous fluvial sands within the IVF were the drilling targets, and that these sands were not as wide as the valley. It was not possible to set up drilling platforms in the lake, and so all drilling needed to be done directionally from the margins of the lake. A 3-D seismic data volume was collected in an attempt to image the channel sands. The white lines show the trend of the incised valley as predicted from well control north and south of the lake. The horizon slice shows high-amplitude reflections (red/yellow/white) form elongate, but discontinuous trends within the valley. Seismic and petrophysical modeling showed that the high amplitude response was an indication of the cleanness of the sandstone, not the presence of hydrocarbons. Drilling in the neighboring areas however suggested that clean, porous sands in this area should be charged. The company used these analyses to drill directional wells from the margin of the lake and was successful on >90 % of their drilling. High amplitudes outside of the valley are due to other factors (non-porous sands stratigraphically below the IVF. Geologic recognition of the limits of the valley helps distinguish these high-amplitude anomalies from the productive channel fill sandstones.

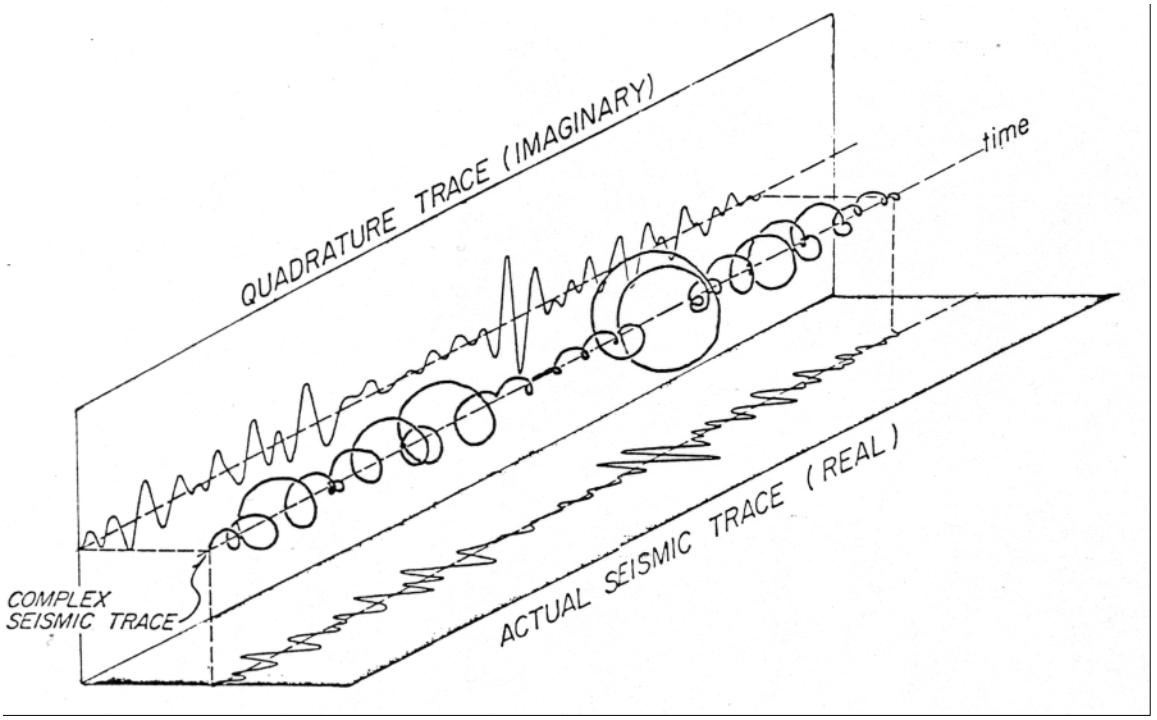

Taner & Sheriff, 1977

•The complex seismic trace consists of a real component and an imaginary component. The real component is the trace we record, g(t) and it can be decomposed into two components, reflection strength and instantaneous phase:

$$\bullet g(t) = A(t)\cos\Theta(t)$$

•Where:

•g(t) – seismic amplitude at time "t" (seismic trace)

•A(t) – reflection strength at time "t"

•Θ(t) – instantaneous phase at time "t"

•The imaginary component is the quadrature trace, h(t), which is the real component rotated by 90º. Numerically:

$$\bullet h(t) = A(t)\sin\Theta(t)$$

•The actual seismic trace and the quadrature trace are used to derive a series of seismic attributes. These attributes are known as "complex-trace attributes".

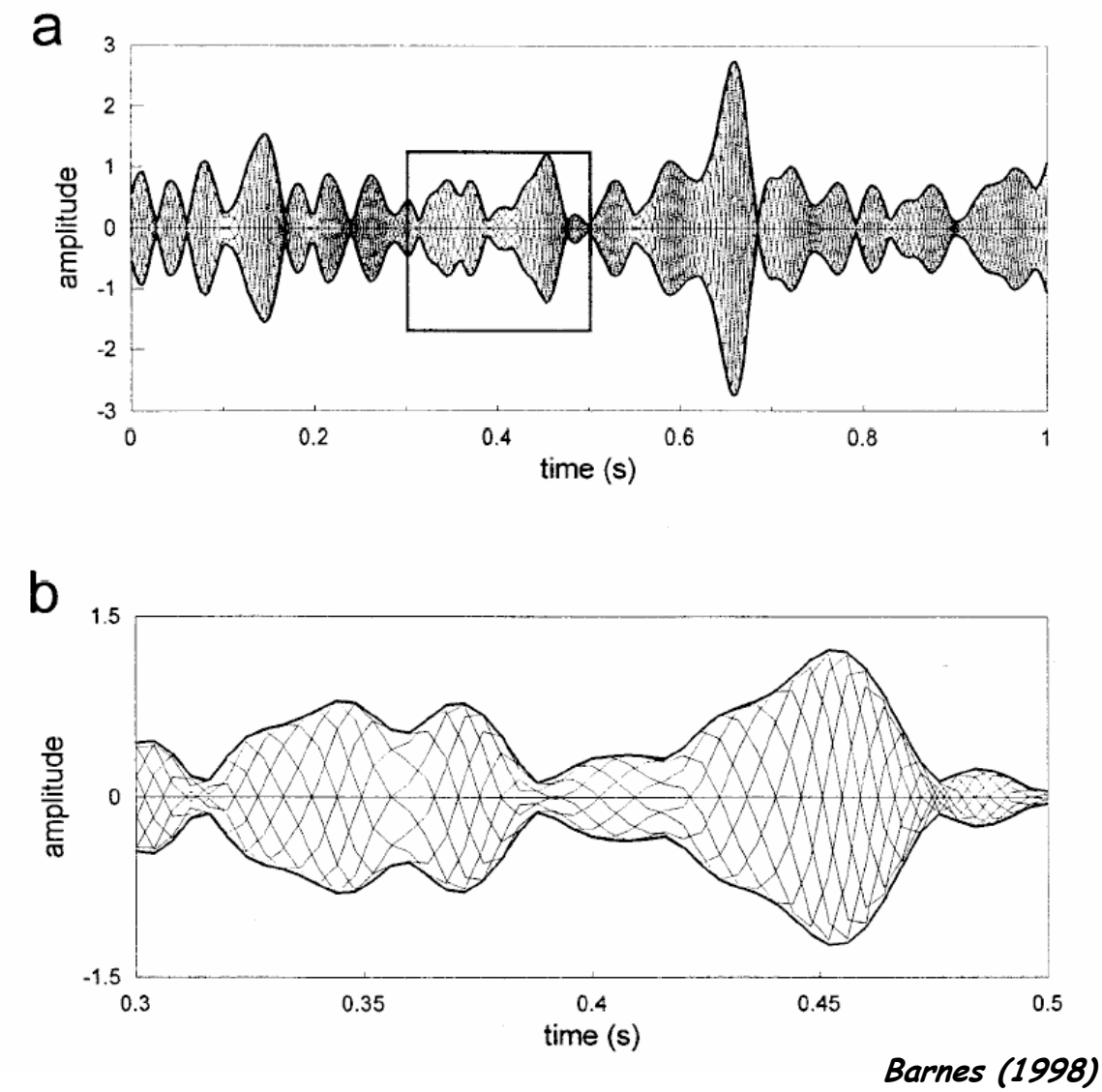

Barnes (1998)

•Reflection strength is amplitude independent of phase. It is derived using:

$$\bullet R(t) = [g(t)^2 + h(t)^2]^{1/2}$$

•These images, adapted from Barnes (1998) illustrate the derivation of reflection strength in a non-mathematical way. At top, the seismic trace is rotated through all possible phase angles and an envelope is fit to the resulting curves. The absolute value (all positives) is taken. Its values range from approximately zero to about the maximum amplitude value of the seismic amplitude.

•Reflection strength is also sometimes referred to as “instantaneous amplitude’, “amplitude envelope”, or simply “envelope”.

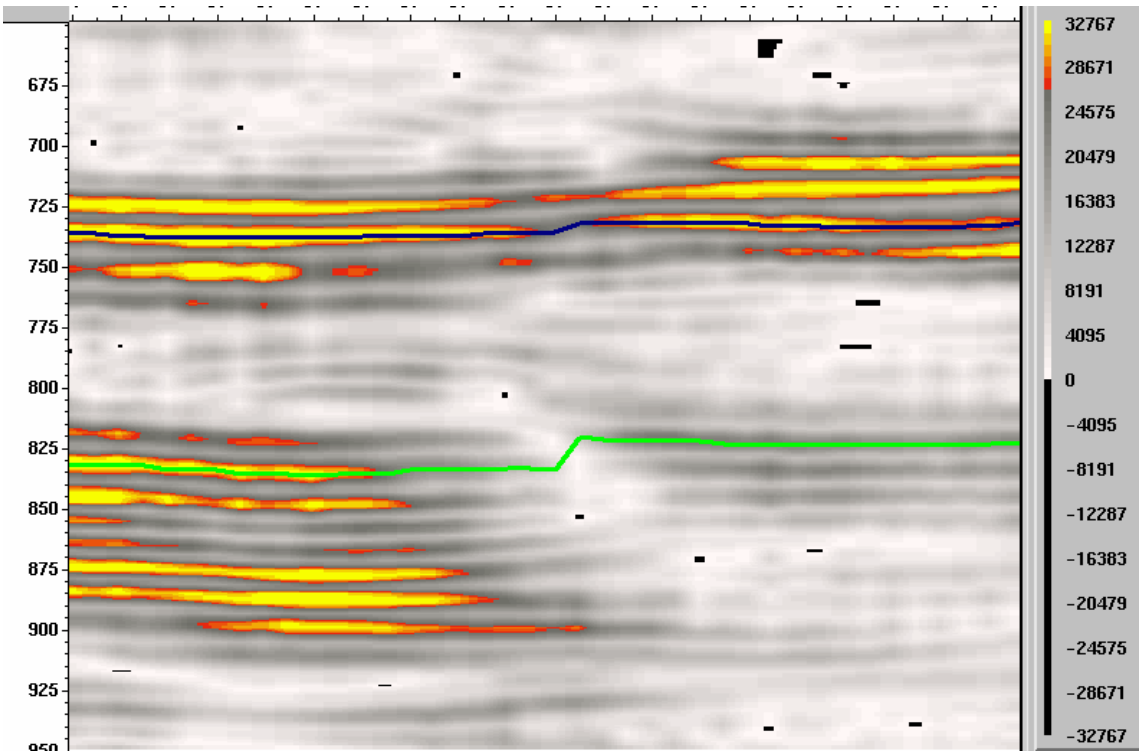

•Reflection strength, like seismic amplitude, shows acoustic impedance contrasts and so is useful for identifying bright spots, tuning effects (although the maximum reflection strength occurs at a different thickness than the tuning thickness for seismic amplitude), interference, etc.

•This view shows reflection strength for our reference seismic image. It uses the standard SEG color scale for reflection strength: low reflection strength in white/grey, and high reflection strength in yellow/red. Note the variations in reflection strength along the horizons and compare them to the changes in amplitude shown earlier.

•Other attributes that may be derived from reflection strength include the derivative of reflection strength, second derivative of reflection strength and the perigram.

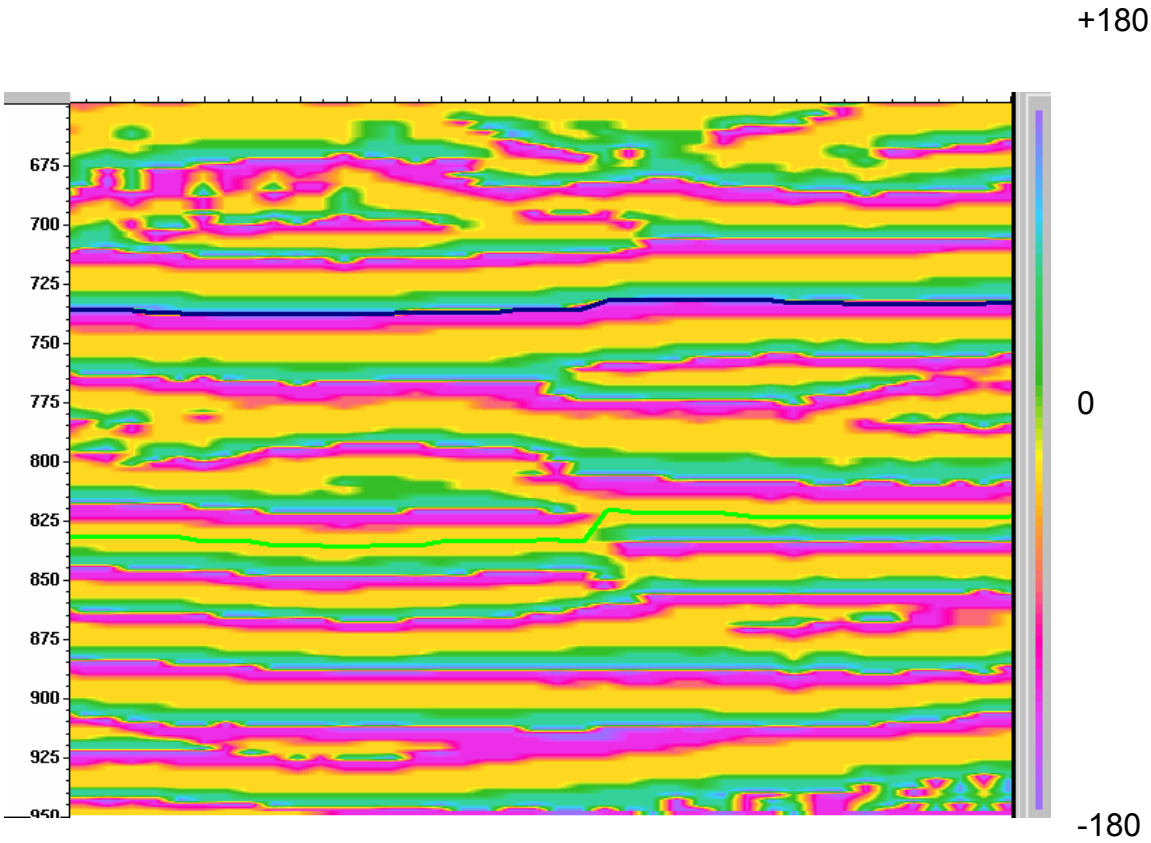

•Instantaneous phase is derived using:

$$\bullet \Theta(t) = \tan^{-1}[h(t)/g(t)]$$

•It is phase independent of amplitude, and its values are in degrees and range from +180 to -180. Because instantaneous phase contains no amplitude information, it is commonly used to examine reflection (i.e., stratigraphic) continuity; changes in amplitude along a reflection can sometimes give the impression of lateral discontinuity.

•This display shows an instantaneous phase display of our seismic image. It uses the standard SEG color scale for reflection strength. Notice how the lateral continuity of reflections, a function of stratigraphic continuity, faulting and noise, is enhanced compared to the original seismic image. The green horizon is seen tracking the zero phase position on the wavelet (i.e., a peak) and the black horizon tracks the +/- 180 position (a trough). Instantaneous phase displays are useful for detecting faulting (e.g., note the offsets associated with the reverse fault), and some interpreters prefer to pick horizons on instantaneous phase versions of the data.

•The cosine of instantaneous phase is sometimes derived because it avoids the wrap-around associated with the +/- 180^{o} position. As such, it gives an even better representation of reflection continuity than instantaneous phase.

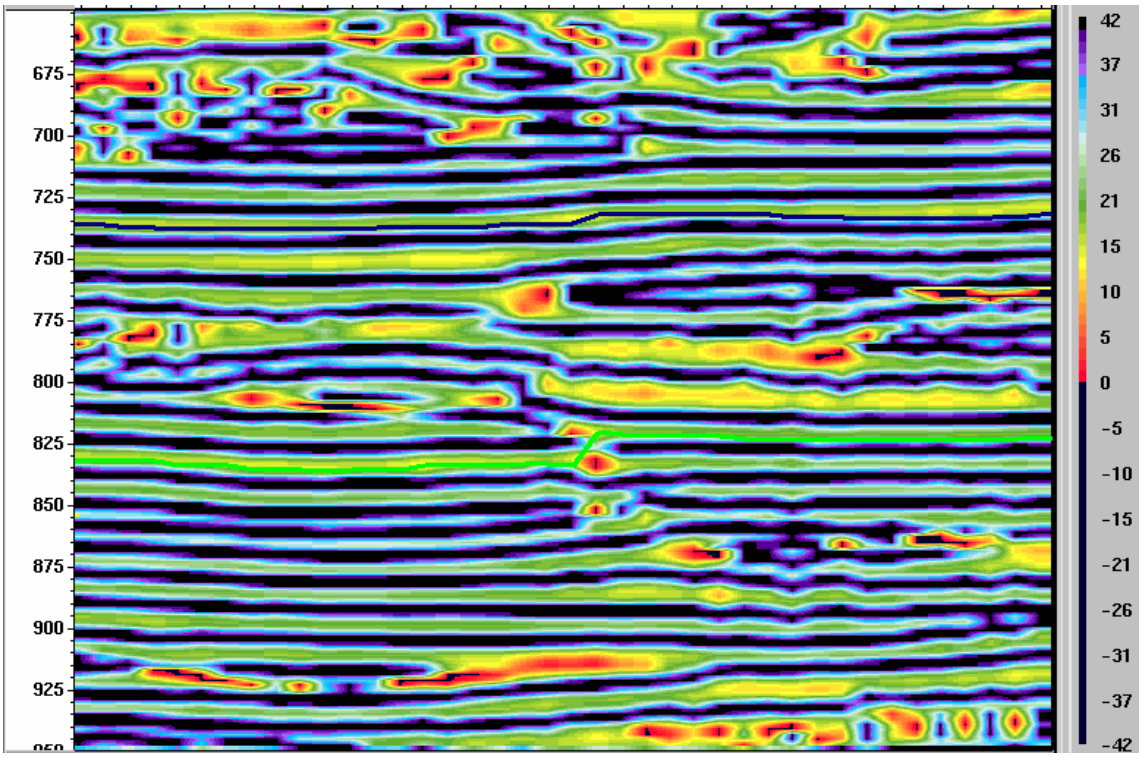

•Instantaneous frequency is the rate of change of phase. Its values are in cycles/second (Hertz).

•Instantaneous frequency is useful for detecting tuning effects (although peak frequency occurs at a different thickness than for tuning of seismic amplitude), fractures, gas (see next slide) and other features.

•This instantaneous frequency display of our reference image uses the standard SEG color scale for instantaneous frequency. High frequencies are in blue and dark purple and low frequencies are in yellow/red. The trace of the reverse fault appears as a “string of pearls” of low frequencies. Note also the relatively low frequency area (yellow) associated with the subtle flexure of the black horizon above the reverse fault. This could be an indication of fractures at this location.

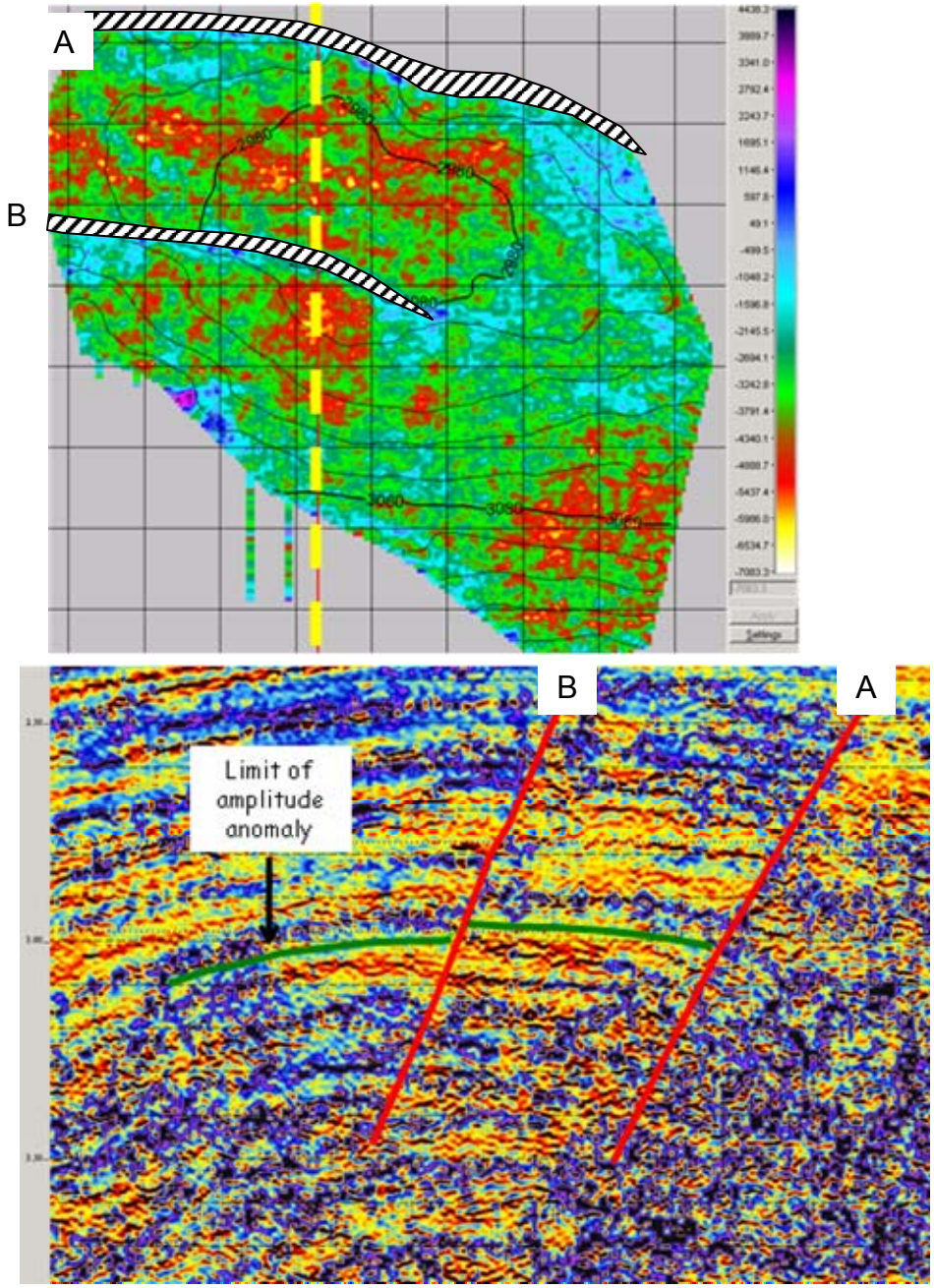

•These images, show the attribute response of a gas accumulation in a Tertiary clastic section. Two normal faults, labeled A and B are present. The map at top shows a horizon slice along the seismic pick shown in green in the lower image. High amplitudes (red, yellow) occur high on structure between the two faults and on a subtle structure in the hanging wall of the B fault. The lower image is a transect (location shown by the dashed yellow line on the map) through an instantaneous frequency volume and uses the standard SEG color scale. Low frequencies (yellow/orange) are present below the horizon in the areas corresponding to the high amplitudes. Based on this evidence, the interpreter could conclude that the amplitudes represent bright spots (hydrocarbon indicator) and the frequency display is showing a “low frequency shadow” below the gas accumulation. The presence of gas at this level is confirmed by wells (not shown).

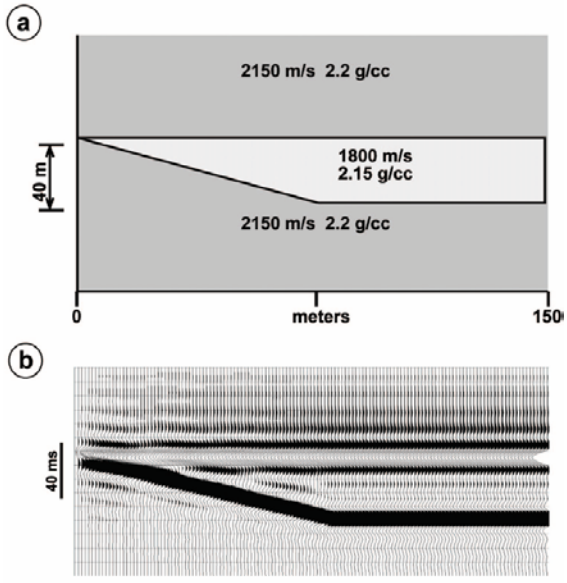

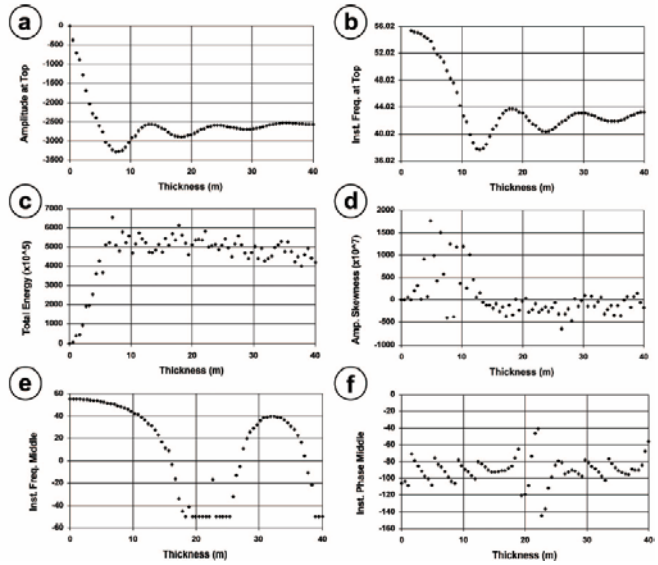

Even simple stratigraphic geometries can lead to complex seismic attribute responses. These images, from Hart and Chen (2004) show this effect for a simple wedge model. At left, a geologic model is constructed (a) and physical properties are assigned. A seismic model (b) is then produced by convolving the geologic model with a wavelet.

Seismic attributes are then extracted from the seismic model. The graphs at upper right show how various attributes change as a function of thickness of the wedge. a) amplitude at the top of the wedge shows classic tuning behavior, b) tuning effects are also visible in this plot of instantaneous frequency versus thickness, c) total energy and d) amplitude skewness are attributes that are extracted in the window bound by the top and base of the wedge in the seismic data. Both attributes show some scatter. Proportional slices down the middle of the wedge through instantaneous frequency e) and instantaneous phase f) versions of the line show more complex attribute responses.

These images help to explain why methods, such as neural networks, that can best capture non-linear relationships between attributes and physical properties, are apt to give the best results when predicting physical properties from seismic attributes. The use of seismic attributes to predict physical properties is discussed later.

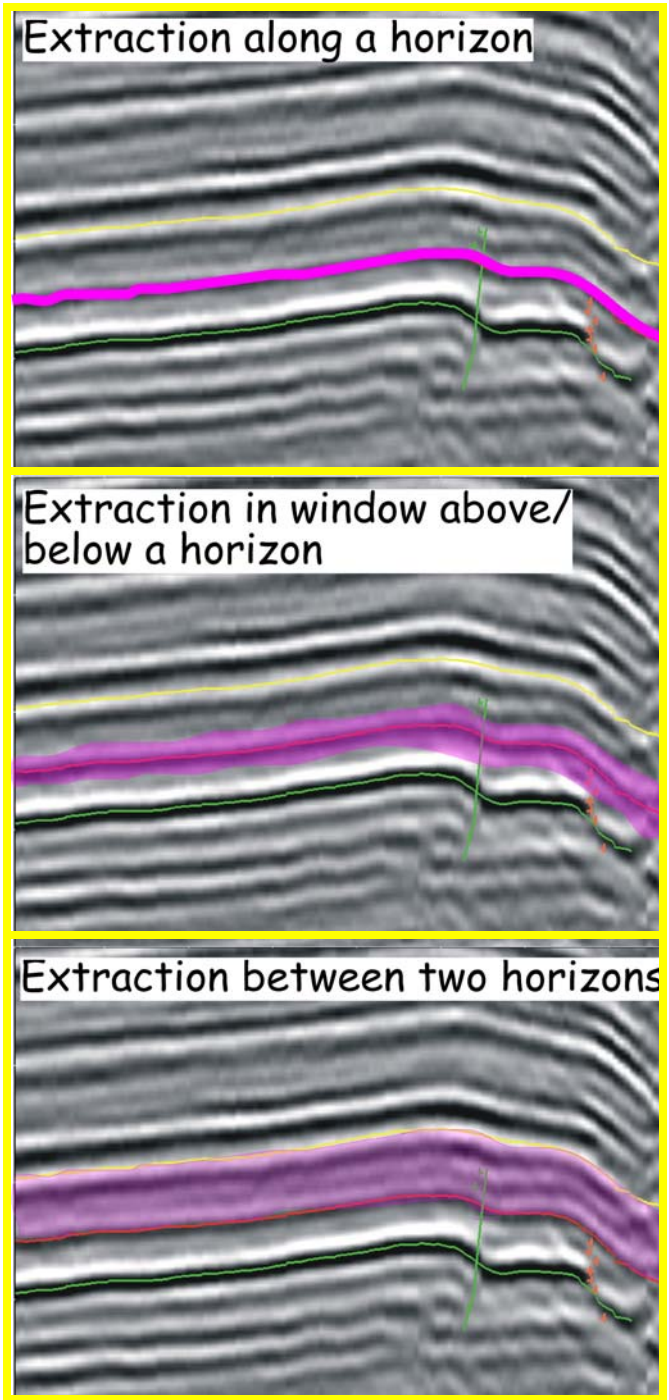

•Seismic data volumes may be converted to complex-trace or other attribute volumes (e.g., frequency volume, reflection strength volume). Using seismic horizons that we have picked, it is possible to extract attributes in a variety of ways. The top image shows attribute extraction along a horizon (i.e., a horizon slice). Some of the previous images have shown horizon slices through amplitude volumes. The middle image shows attribute extraction in a user-defined window above and/or below a horizon. The lower image shows attribute extraction between two horizons. Both of the window-based extraction methods may be used to compute statistical and other measures, such as RMS amplitude, dominant frequency, number of zero crossings, etc. The choice of attribute extraction method will depend on the interpreter's objectives.

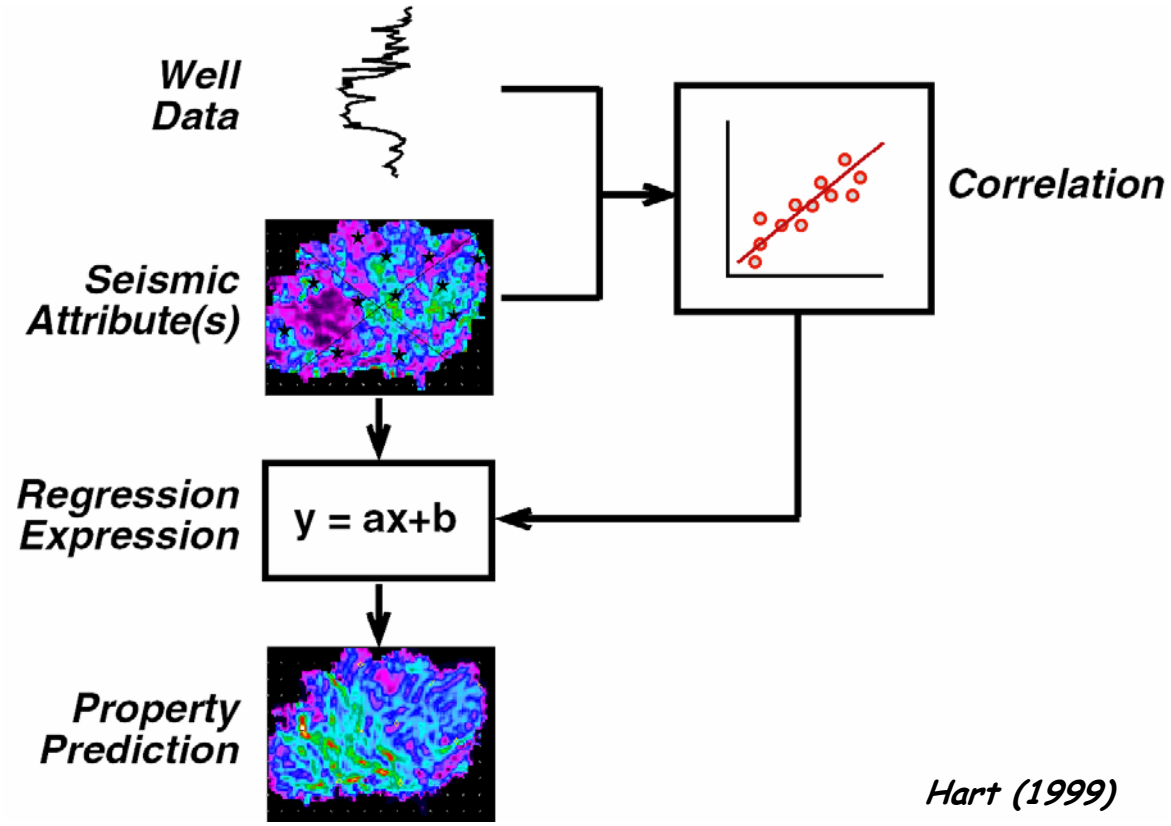

•In the mid-1990s it became apparent that empirical correlations could sometimes be found between seismic attributes and log-derived physical properties (e.g., Schultz et al., 1994), and that these correlations could be used to predict the distribution of physical properties away from well control. This figure, from Hart (1999) illustrates the methodology.

•At upper left we have well log data that provide the physical properties of interest (e.g., porosity, V_{shale}) at each well location. Using our software, we are able to derive a number of seismic attributes at locations corresponding to the wells from our 3-D seismic data. We then try to correlate the attributes and physical properties (upper right). If we find statistically significant correlation, we can use that regression expression (middle left) and the relevant seismic attributes to predict the physical property of interest everywhere within our 3-D seismic survey (lower left).

•Although simple linear correlations (like the one illustrated here) are sometimes found between a single attribute and a physical property of interest, relationships are generally non-linear (e.g., Hart and Chen, 2004) and more than one attribute is needed predict the physical property of interest, either through the use of multivariate linear regression (MLR), artificial neural networks, (ANN), geostatistics, etc..

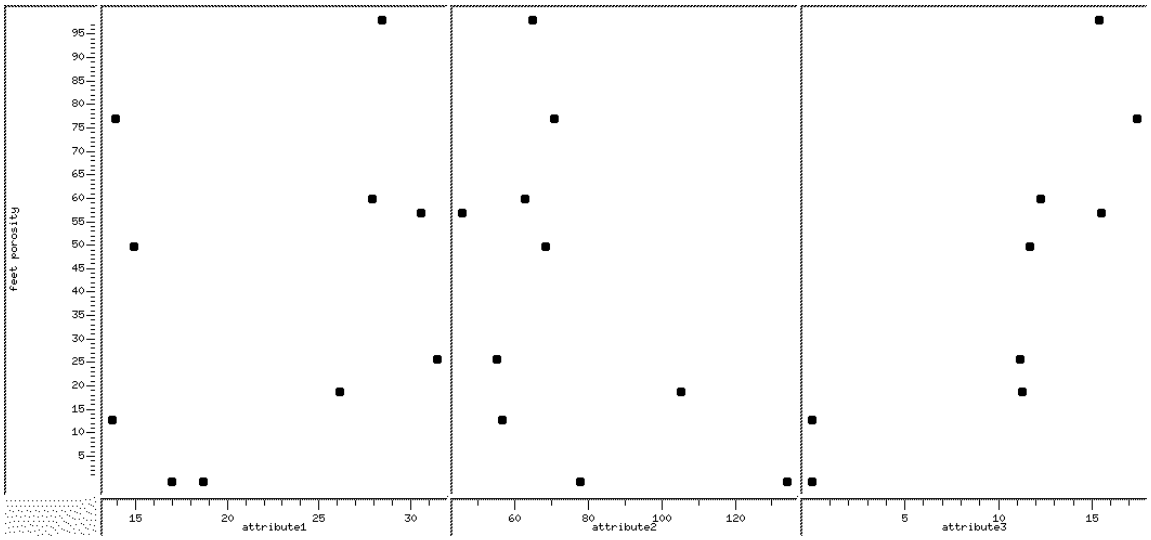

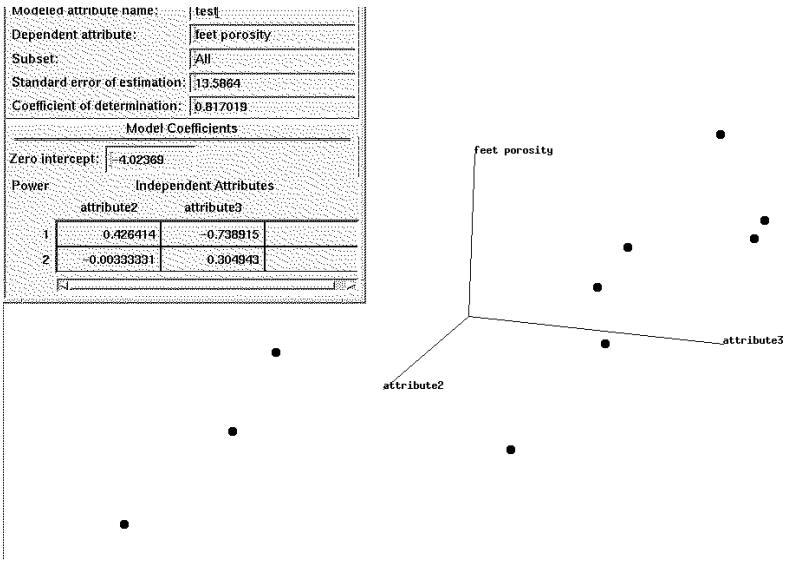

•These images show sample correlations between log-derived physical properties and seismic attributes for a real dataset. When attributes are cross-plotted against a physical property of interest, most/many such graphs show no trend (e.g., upper left). Some plots might show “broad” correlations such as the negative correlation shown in the middle image. The image at upper right shows a strong, positive correlation. The user might need to decide whether to use a first-order polynomial (i.e., linear relationship) or a higher-order polynomial to fit a curve.

•The lower image shows that it can be advantageous to use more than one attribute to predict the values of a physical property. The two attributes shown in the middle and right of the upper row are combined to predict the physical property. The regression line is curved in 3-D space.

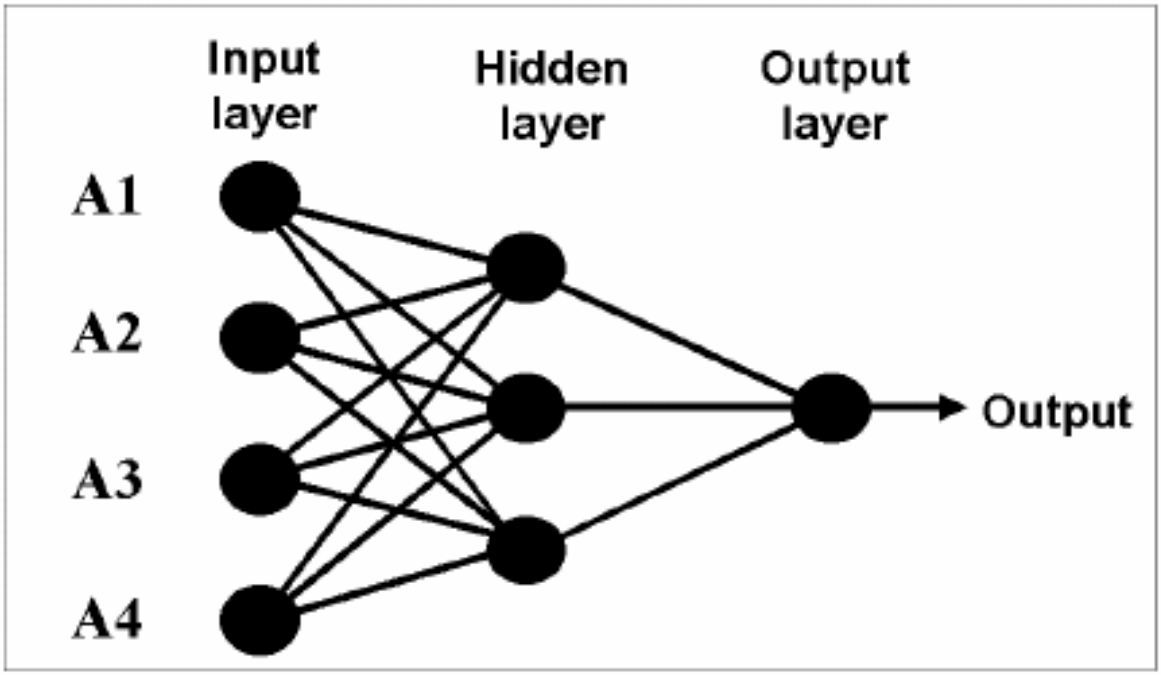

•A simple representation of a feed-forward neural network.. In this example, three layers are present: an input layer, a hidden layer and an output layer. The input layer might consist of four attributes (A1-A4). The output layer could be a prediction of porosity. The hidden layer consists of three nodes, each of which receives the four attributes and weighs them differently. The weights are defined using a training data set, with known combinations of attributes and log-derived porosity being used to determine the optimum weights for each node. This is known as “back propagation”. Once the weights have been optimized for each node, i.e. the network has been “trained”, new data (from areas in the seismic data without well control) can be input into the network to predict porosity.

•Neural networks are particularly useful when working with non-linear relationships, such as those that can sometimes be observed between attributes and physical properties. They are used in a variety of geophysical domains (e.g., first-break picking) and other fields (e.g., pattern recognition, medicine, marketing). They are useful for finding “hidden” patterns among variables. Unfortunately they can sometimes find relationships that do not exist.

•Other disadvantages of neural networks include: a) problems extrapolating beyond the range of the input data, b) they can be “overtrained”, so that they accurately predict the input data but will not adequately perform with new data, and c) their black-box character - it is difficult to examine the nature of the relationships between attributes and physical properties.

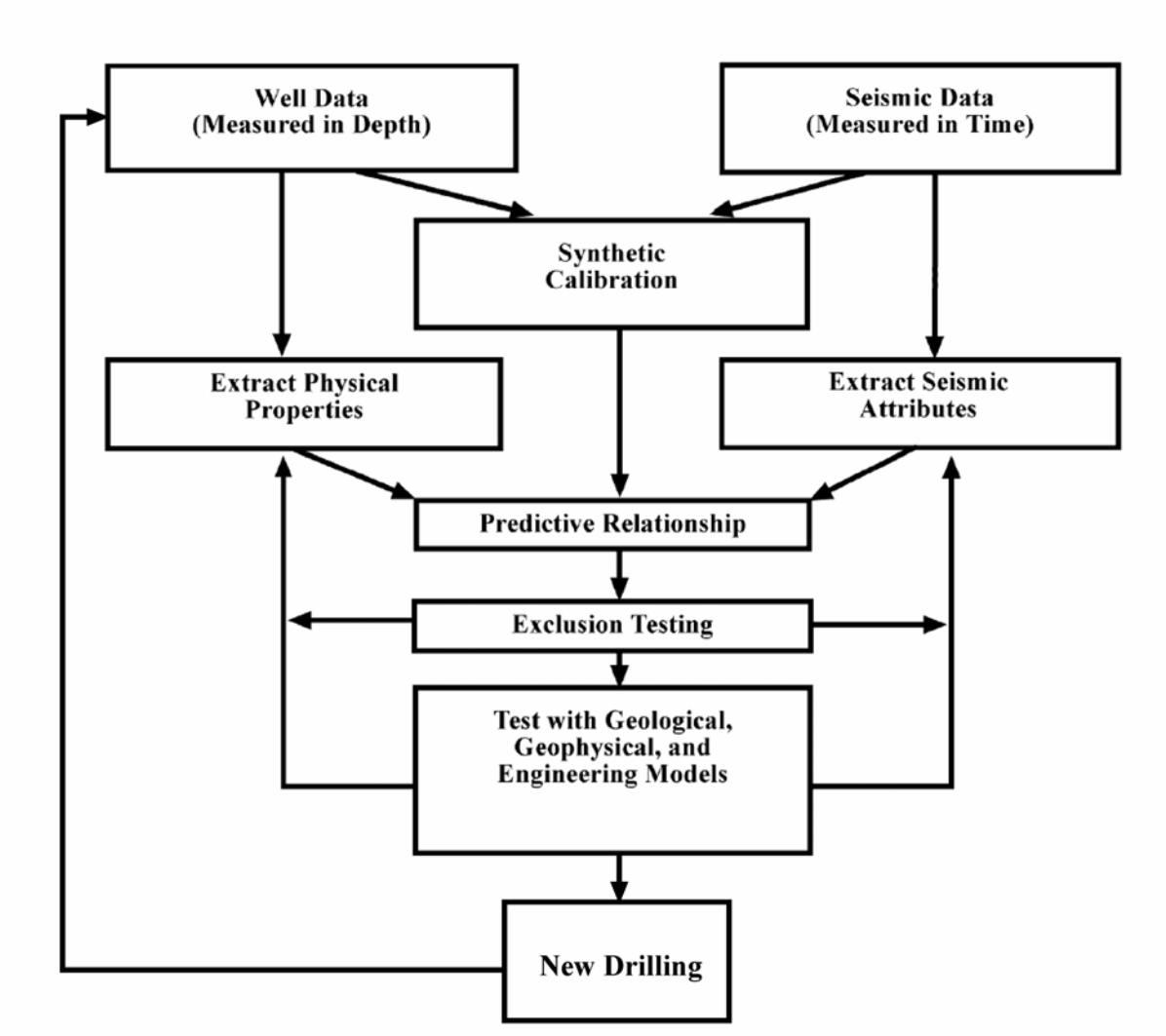

Pearson and Hart, 2004

•Workflow for a seismic attribute study. The essential inputs are well (log) data and seismic data. Calibration of log and seismic data through the generation of synthetic seismograms allows horizons to be recognized and mapped. The wells are then used to derive physical properties (porosity, lithology, etc.) and attributes are extracted from the seismic data. The attributes and logs are integrated (using neural networks, geostatistics, multivariate linear regression, etc.) to generate a predictive relationship that may be tested in a variety of ways: mathematically (e.g., exclusion testing), geologically (do the results make sense geologically?), geophysically (why are the attributes related to the physical properties of interest?) and using engineering data (are the results consistent with engineering data?). The integration of these various data types makes the solution more robust. Once these tests are completed, the results may lead to new drilling.

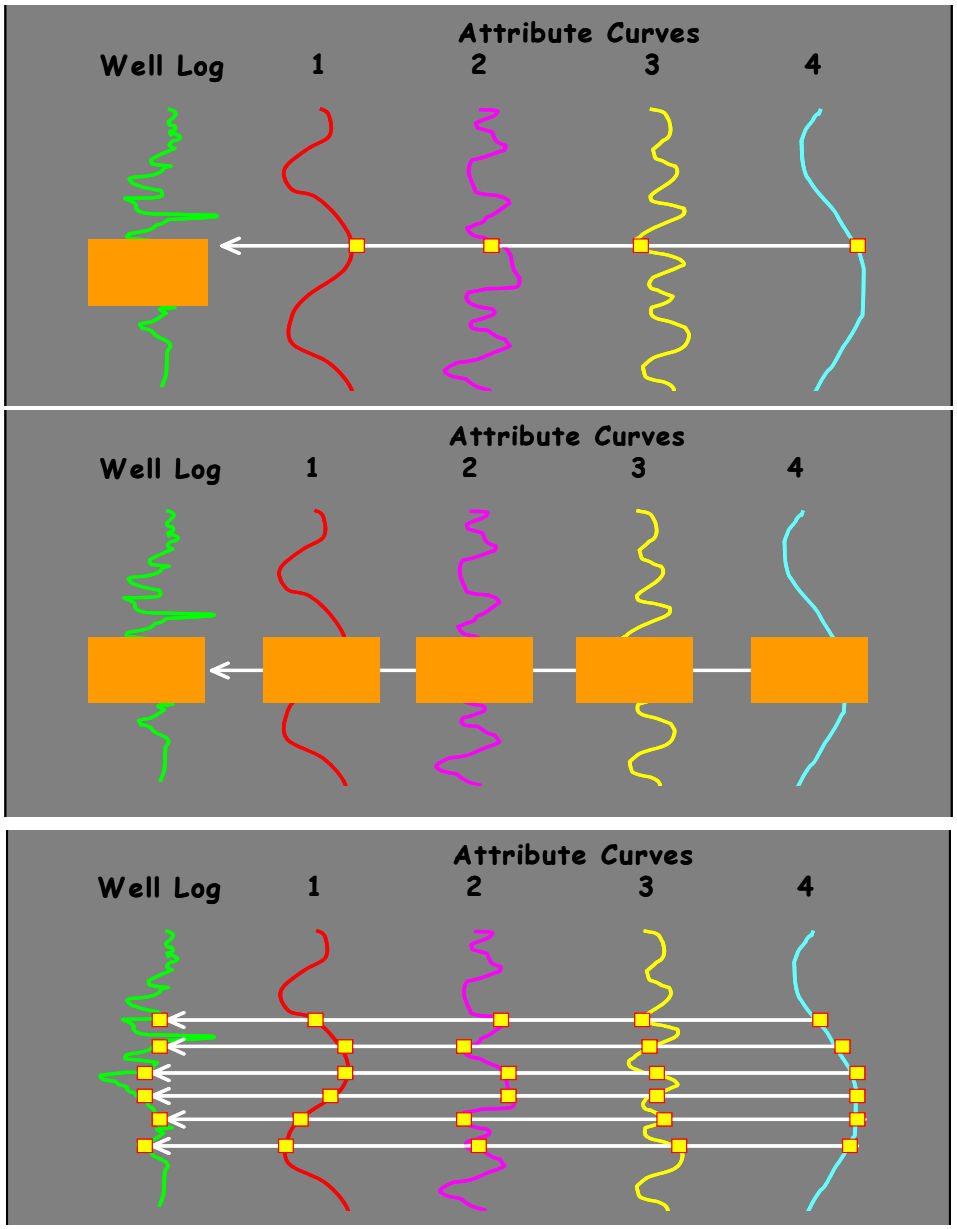

•These images, show various ways in which seismic attributes may be correlated to log-derived physical properties.

•Top – Horizon-based. Physical properties are extracted from a log and correlated to a single sample on the attribute traces. This approach yields a map. Example: Schultz et al., 1994.

•Middle – Interval based. Physical properties are extracted from a log and correlated to attributes that have been extracted over an interval. This approach yields a map. Example, Pearson and Hart, 2004.

•Bottom – Volume based. Physical properties are extracted at points along a well log that correspond to time samples in the seismic data. Correlation is done on a sample-by-sample basis. This approach generates a volume. Example: Hampson et al., 2001.

GEOPHYSICS, VOL. 66, NO. 5 (SEPTEMBER-OCTOBER 2001); P. 1349–1358, 16 FIGS., 2 TABLES.

Case History

Comparison of linear regression and a probabilistic neural network to predict porosity from 3-D seismic attributes in Lower Brushy Canyon channeled sandstones, southeast New Mexico

Daniel J. Leiphart* and Bruce S. Hart‡

ABSTRACT

The Lower Brushy Canyon Formation of the Delaware Basin, New Mexico, consists of a series of overlying sand-filled channels and associated fans separated by laterally extensive organic siltstone and carbonate interbeds. This laterally and vertically complex geology creates the need for precise interwell estimation of reservoir properties.

In this paper we integrate wireline log and 3-D seismic data to directly predict porosity in the area of an existing oil field in southeast New Mexico. The 3-D seismic data were used to interpret the location of major stratigraphic markers between wells, and these seismic horizons were used to constrain a time window for a volume-based attribute analysis. Stepwise regression and crossvalidation were used to combine seismic attributes to predict porosity in wells where the porosity was known from the well logs. The results of a linear regression porosity model showed good correlation ($r^2 = 0.74$) between seven seismic attributes and the observed porosity logs at 11 wells in the study area, but the porosity volume created from the regression model did not display the known geologic features. A probabilistic neural network was then trained to look for a nonlinear relationship between the input data (the seven attributes) and the observed porosity at the 11 wells. The correlation was better ($r^2 = 0.82$), but the biggest improvement over the linear regression model came in the more geologically realistic predicted porosity distribution.

INTRODUCTION

Predicting subsurface physical properties is a fundamental problem confronting geologists and geophysicists. We test two different means of predicting porosity between well locations using seismic attributes. Seismic attributes have been used to predict reservoir properties with success (e.g., Russell et al., 1997; Schuelke and Quirein, 1998; Pearson and Hart, 1999; Hart and Balch, 2000), and recently neural networks have been tested by geophysicists as means to increase the certainty of the predictions over standard linear regression methods (Ronen et al., 1994; Schuelke et al., 1998).

A concern among geologists is that multiattribute studies may show statistical significance between the attributes and a physical property but that there may be no theoretical basis for using the attributes, and a resulting model may be geologically and/or physically unrealistic. Following the work of others (Ronen et al., 1994; Hirsche et al., 1997; Kalkomey, 1997; Hart, 1999; Pearson and Hart, 1999), we emphasize the need for the results of an attribute-based prediction to be geologically plausible (in addition to other criteria; see below) before it is accepted. In this paper we use log and seismic data to investigate the geology of the lower Brushy Canyon in the study area. We then employ two different techniques—standard linear regression and a probabilistic neural network (PNN)—to generate porosity distribution models of the lower Brushy Canyon from seismic attributes. By comparing the results of the two methods with the geology, we conclude that the neural network provides a better image of the subsurface porosity distribution because its architecture can better capture the nonlinear

Manuscript received by the Editor June 19, 2000; revised manuscript received January 29, 2001.
*Formerly New Mexico Bureau of Mines and Mineral Resources. Presently Anadarko Petroleum Corp., Houston, Texas 77060. E-mail: dan_leiphart@anadarko.com.
‡Formerly New Mexico Bureau of Mines and Mineral Resources. Presently McGill University, Earth and Planetary Sciences, 3450 University St., Montreal, Quebec H3A 2A7, Canada. E-mail: hart@eps.mcgill.ca.
© 2001 Society of Exploration Geophysicists. All rights reserved.

relationship between seismic attributes and log-based physical properties.

GEOLOGIC SETTING

The Delaware basin is the westernmost basin in the Permian basin complex of western Texas and southeastern New Mexico. The basin is bound by the Central Basin Platform to the east,the Northwestern Shelf to the north, and the Diablo Platform to the west (Figure 1). During relative lowstands of sea level in the Permian, siliciclastic sediments bypassed the shelf and were deposited in the basin (Sageman et al., 1998; Montgomery et al., 1999). The Delaware Mountain Group, which consists of the Bell Canyon, Cherry Canyon, and Brushy Canyon Formations, in descending order, is an example of this kind of sedimentation.

The Brushy Canyon Formation includes three major facies: (1) submarine canyon fills in the underlying Victorio Peak Formation, (2) slope deposits consisting of thick successions of interbedded sandstones and siltstones, and (3) basin-floor deposits (Harms and Brady, 1996). Brushy Canyon deposition was the result of some gravity flow mechanism, such as turbidity currents or saline density currents. In addition, previously mapped Brushy Canyon channel features extend 50 miles (81 km) onto the basin floor (Basham, 1996; Montgomery et al., 1999).

The Brushy Canyon Formation consists of up to 1800 ft (549 m) of interbedded, fine-grained sandstones and siltstones and is informally subdivided into a lower, middle, and upper part. Each of these parts is separated by laterally continuous organic-rich siltstone marker beds that may be tracked throughout the basin using well-log information. The lowermost Brushy Canyon averages about 325 ft (99 m) thickness and thickens basinward. It is interpreted as a system of sand-filled feeder channels and associated fans (Sageman et al., 1998).

MATERIALS AND METHODS

Our database consisted of a time-migrated 3-D seismic survey, wireline logs from 77 wells in and around the study area, and production data. The seismic data cover an area about 16 mi^2 (41.4 km^2) with a bin size of 110 ft × 110 ft (33.5 m × 33.5 m) and a 3-s two-way traveltime (TWT) record length. The 3-D grid is laid out with cross-lines oriented approximately north–south and in-lines running west–east, perpendicular to the cross-lines. The seismic data originally consisted of two volumes that were processed into a single volume prior to our interpretation. No information regarding processing was available to us.

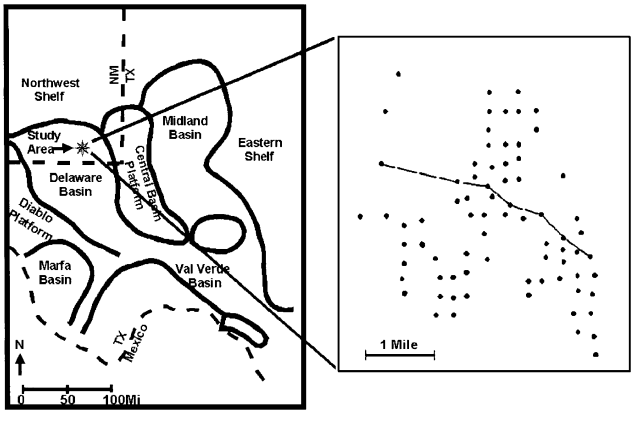

FIG. 1. Regional paleogeographic map showing the Permian basin complex (after Yang and Dorobek, 1995). Approximate location of the study area is noted by the star. Also shown are the 16 mile^2 study area, the locations of the 77 wells, and the location of the wireline log cross-section shown in Figure 3.

We analyzed digital logs for 77 wells for lithology determination and stratigraphic correlation. The main logs used in this study were gamma ray, photoelectric factor, deep resistivity, and density. Sonic logs were available for 21 wells and were used to generate the synthetic seismograms, which were then used to tie the well logs to the seismic data. The neutron porosity log was used in the multiattribute study as the target log. A good correlation ($r^2 = 0.91$) was found between neutron porosity and sonic velocity, assuring us that neutron porosity is dependent upon rock physical properties and is not biased by the presence of shales. True shales are not present in the lower Brushy Canyon in this area (Justman, 2001).

Where possible, log-based stratigraphic horizons were autotracked through the seismic data, then smoothed. These seismic horizons were then used to constrain the time window for the volume-based attribute study (e.g., Russell et al., 1997). This method was preferred over the horizon-based approach because of the geologic complexity and thickness of the lower Brushy Canyon. Attributes were extracted from the seismic data and ranked by stepwise regression, and the results were validated (Schuelke et al., 1998). We used both standard linear regression techniques and a PNN to create two predicted porosity volumes for the entire lower Brushy Canyon Formation in the study area. These two models were then evaluated by their ability to predict porosity and image stratigraphic features interpreted from the well logs.

Details of the mathematical basis for these two techniques are provided in a later section. Although we had access to a multilayered feed-forward neural network (MLFN) architecture, we did not use this method because of its black box character (Hampson et al., 2001)

STRATIGRAPHY

Lower Brushy Canyon picks

We divided the basal Brushy Canyon Formation into eight stratigraphic units based on gamma ray, photoelectric factor, deep resistivity, and density log characteristics (Figure 2). The units are named alphabetically, A through H, in descending order; each is separated vertically by organic siltstone and carbonate interbeds of varying thickness (generally <30 ft or 9.1 m). Each of these stratigraphic units has unique well-log signatures that could be correlated and tracked throughout the study area with confidence (Figure 3).

Unit A is the top unit stratigraphically. It is about 5–20 ft (1.5–6 m) below the top of the lower Brushy Canyon pick. In the central and western parts of the study area, Unit A is a massive sandstone ranging from 25 to 55 ft (7.6–16.8 m) thick (Figure 4a). In the eastern part it is characterized by a coarsening-upward package that is considerably less thick (<20 ft or 6.1 m).

Unit B is also a massive sandstone (40–65 ft or 12.2–19.8 m thick; Figure 4b) in the central and western region and a coarsening-upward sequence in the southeast (30–45 ft or 9.1–13.7 m thick).

The thickest and cleanest sandstone in the lower Brushy Canyon Formation in this area is unit C. It ranges from 35 to 100 ft (10.7–30.5 m) thick (Figure 4c) and is almost everywhere composed of 95–100% sand. Slightly higher siltstone content may be found in the extreme northwest and southeast regions.

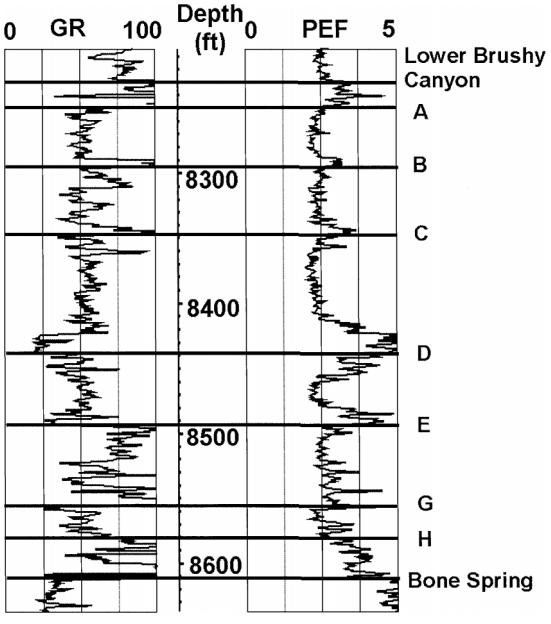

FIG. 2. Sample log through the lower Brushy Canyon in this study area. The logs, from left to right, are the gamma ray (GR) and the photoelectric factor (PEF). Note the relatively thin organic siltstone and limestone layers that separate each of the stratigraphic units. These interbeds are expressed either as abrupt increases in radioactivity as shown in the GR curve (organic siltstones) or zones of low GR values accompanied by high PEF values (limestones).

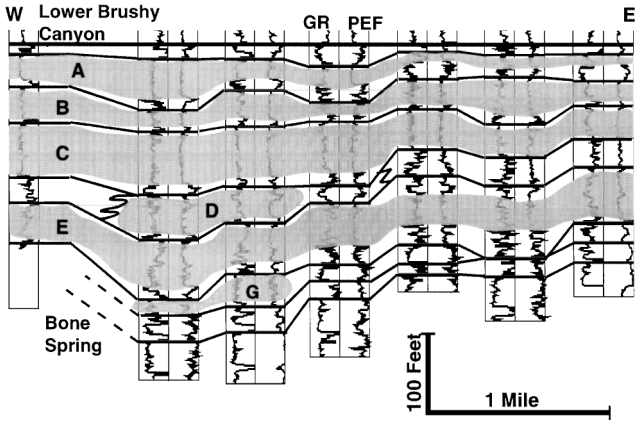

FIG. 3. Northwest–Southeast stratigraphic cross-section through the study area datumed at the lower Brushy Canyon. The location of the cross-section is shown in Figure 1. The GR (left) and PEF (right) logs are used. The shaded regions denote the significant sandstone bodies in the lower Brushy Canyon in this study area, and the letters within the shaded regions correspond to the individual stratigraphic units.

Units D and F are laterally equivalent units. Unit D consists primarily of sandstone with some limestone interbedding to the east, and it is only present in a north-northeast–south-southwest strip more than 1 mile wide in the middle of the study area (Figure 4d). Unit F is a package of approximately equal thickness that consists of organic siltstones with dolomite interbeds. It is located on both the northwest and southeast sides of unit D.

Unit E is a heterolithic unit, which complicated details of internal correlations. This unit is comprised of a massive sandstone in the northwest, a fining-upward to coarsening-upward package in the center region, and a slightly more carbonate unit in the southeast. The thickest (70 to >100 ft or 21.3 to >30.5 m) area is in the eastern to southeastern regions where the unit is characterized by a higher siltstone content (Figure 4e).

Below unit E is unit G. The thickest sandstones of this interval strike north-northeast–south-southwest (Figure 4f). To the southeast of this linear feature, unit G primarily consists of a limestone with little if any sandstone interbedding (generally <5 ft or 1.5 m).

Unit H may be considered as a transitional unit from the underlying Bone Spring Formation to the sandstone units of the basal Brushy Canyon. It is chiefly a dolomitic limestone with varying siltstone content and negligible sandstone.

Seismic horizons

Figure 5 shows a west–east transect through the center of the 3-D seismic data volume. Once the wells were accurately tied to the seismic data by way of synthetic seismograms, we could then interpret horizons of interest in the seismic data. The top of the lower Brushy Canyon is characterized by a peak that may be tracked throughout the entire data set. The top of unit C almost everywhere corresponds to the trough directly below the lower Brushy Canyon reflector. Because of the thickness and relatively low velocity of unit C, it can be

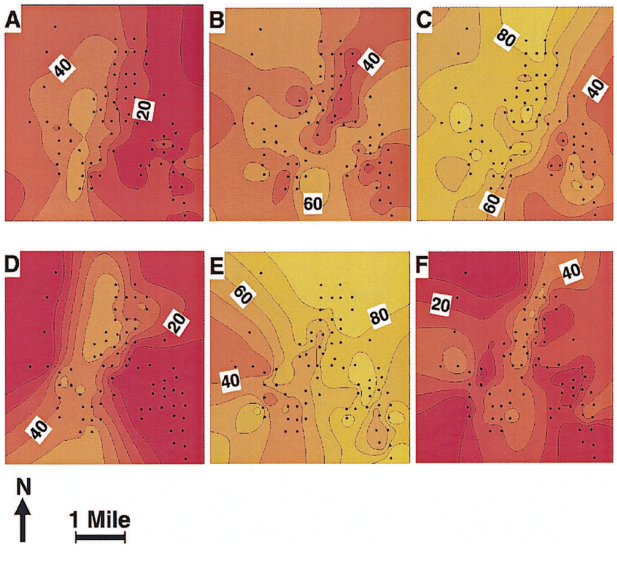

FIG. 4. Isopach maps for each of the units in the lower Brushy Canyon Formation. The contour interval is 10 ft, with yellow tones denoting thicker zones. The scale and color scheme are the same for each map.

tracked accurately throughout most of the data set as a high-amplitude trough. At most locations within this study area, the other stratigraphic units are below vertical seismic resolution because of the thinness of the bed and the relatively low acoustic impedance contrast with adjacent units.

At other locations within the Delaware basin, the Bone Spring Formation is characterized by a high-amplitude peak because of a relatively abrupt transition from the basal Brushy Canyon sandstones into the high-velocity Bone Spring carbonates (Hardage et al., 1998; Hart, 1998). However, in our study area the Bone Spring is overlain by up to 80 ft of high-velocity sandstones and carbonates (unit H and the eastern region of unit G). In this case, the top of the Bone Spring corresponds to a peak, although locally a phase reversal is present where thick carbonates overlie the formation.

Stratigraphy

The lower Brushy Canyon Formation is thought to be made up of a system of channels that transported sandy sediment to the basin floor (Basham, 1996; Sageman et al., 1998; Montgomery et al., 1999). All of the isopach, gross sand, and percent sand maps and the cross-sections show strong evidence for channel-like structures trending north–south to northeast–southwest (Figure 4). In places, isopach trends appear to be discontinuous, lacking channel geometry. This could be from the contouring algorithm's solution in areas of sparse well control or because of geologic reasons, such as preexisting sea-floor relief or postdepositional erosion by subsequent flows that affect the thickness of individual sandstone bodies.

A cross-section perpendicular to these channel trends (Figure 3) shows that the entire basal Brushy Canyon is thickest in the center region and thins to the west and the east. Furthermore, the thickest part of each succession is located in the center of the study area, with each unit becoming thinner and less sandy away from the channels. This suggests that the sediment source location and transport axes did not change significantly during the deposition of the lower Brushy Canyon in this region, as there is very little lateral shift from one channel to the next. The only exception is the addition of a new sediment source to the northeast during the deposition of unit B (Figure 4b).

The structure at the top of the underlying Bone Spring Formation appears to be the primary determining feature for the channel locations (Figure 6). Bone Spring topography is thought to have controlled basal Brushy Canyon channel locations at other areas in the Delaware Basin (Thomerson and Catalano, 1996). At this level, the study area is characterized by a prominent structural high just southeast of center. Each of the subsequent channels filled in the structural lows of the underlying unit.

The isopach maps in Figure 4 show evidence of channel sediments overflowing and spilling over the sides of the channel. This depositional pattern has been noted elsewhere in the subsurface as well as in outcrop (Basham, 1996; Gardner and Sonnenfield, 1996). The sandstone of unit D is bordered on both sides of the channel by the stratigraphically equivalent siltstones and dolomites of unit F (Figure 4d). It is possible that the channel cut into the underlying sediments of unit F; as sand filled the channel, it began to spill over the sides.

Vertical stacking and siltstone capping of channels is typical of low-stand fan deposition. Successive density currents may take similar paths, each depositing a broad, lenticular layer of sand overlain by a silty layer (Bouma, 1996). As a result, the lower Brushy Canyon consists of a vertical succession of

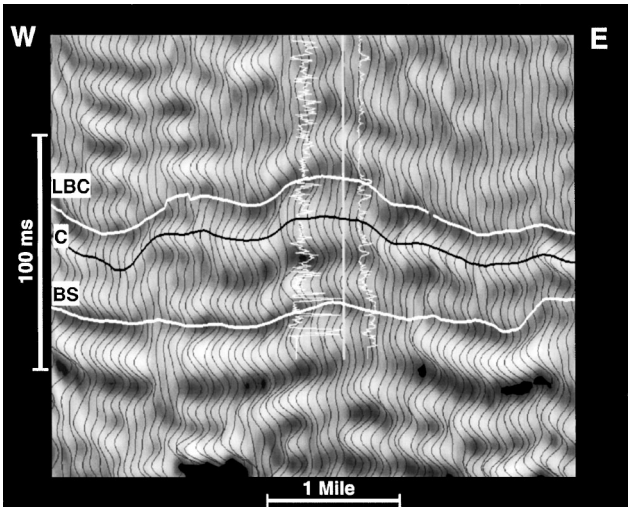

FIG. 5. West–east seismic transect near the center of the study area. The lower Brushy Canyon (LBC—white) is shown as a peak at about 1200 ms (two-way traveltime). Unit C (C—black) is characterized by a high-amplitude trough at about 1220 ms (two-way traveltime). The Bone Spring Formation (BS—white) is shown as a discontinuous peak at about 1250 ms (TWT). The wireline logs shown are the GR (left) and the PEF (right).

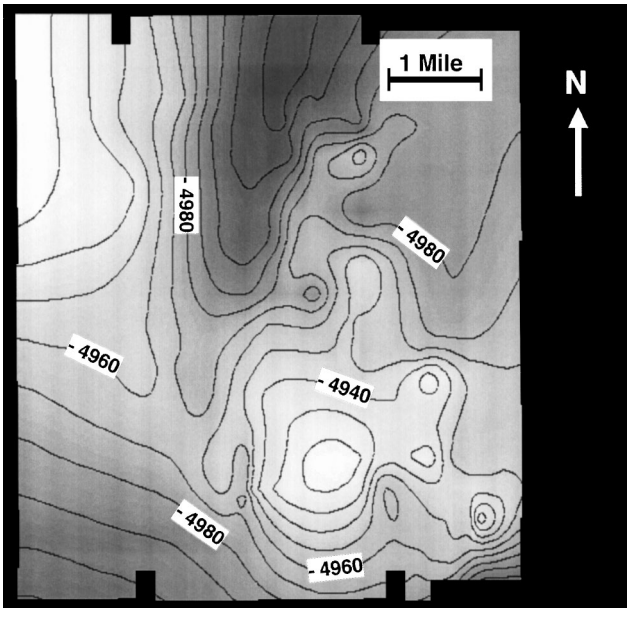

FIG. 6. Depth-converted structure map of the top of the Bone Spring Formation, calculated from the seismic data. The contour interval is 10 ft, and the color scheme is such that lighter tones depict structural highs. Note the north–south-trending valley in the center of the study area. This valley was the pathway for the unit G channel; subsequent channeling was likewise controlled by underlying structure.

channeled sandstones, each separated by a laterally extensive siltstone or carbonate layer.

SEISMIC ATTRIBUTE STUDY

Methods

Having established a stratigraphic framework for the basal Brushy Canyon in this study area, we sought a relationship between log-derived physical properties and seismic attributes. Quite simply, a seismic attribute is a derivative of a basic seismic measurement that may be extracted along a horizon or summed over a time window (Brown, 1996). Several factors go into seismic multiattribute analyses, such as whether to perform a horizon- or a volume-based analysis, the weight assigned to each attribute in the final equation, and the type and number of attributes to use.

For an attribute study to be judged successful, several criteria need to be met:

1) the results must be statistically significant,
2) a known or suspected relationship between the attribute and physical properties must exist,
3) the results must be geologically plausible, and
4) the results must agree with available engineering data.

We chose a volume-based approach because of the thickness and complexity of the lower Brushy Canyon stratigraphy and its effect on internal reflections in the seismic data. The time window from the top of the Lower Brushy Canyon Formation to the Bone Spring was chosen as the window of interest for seismic attribute extraction and all seismic-guided interpretations.

The choice of which attributes to extract was defined by the capabilities of the software. We ranked the attributes according to their correlation to the neutron porosity, and weighted appropriately, by stepwise regression following the methods of Hampson et al. (2001). The number of attributes used in this study was determined by crossvalidation. In this approach, wells are excluded one at a time, while the remaining wells are used to predict the excluded one. This technique seeks to eliminate the problem of overfitting the data associated with using too many attributes (Schuelke et al., 1998), a problem recognized by Kalkomey (1997). The point at which adding a new attribute increases the validation error and becomes too well specific is the cutoff for the optimal number of attributes to be used. Based on these results, we used a linear regression model to create a predicted porosity volume over the time window of interest.

A PNN was then trained to predict porosity over the same volume. Again, by performing the stepwise regression and validation tests before training the PNN, we eliminate the problem of overfitting the data (Schuelke et al., 1998). Ronen et al. (1994) point out that it can be important to look for nonlinear relationships between seismic attributes and rock properties. Artificial neural networks (ANNs) can be trained to determine those nonlinear relationships.

We then compared the porosity volumes created from both the standard linear regression model and the PNN model. The models were evaluated as to their statistical significance and their ability to create a porosity volume that conformed to the log-based geologic interpretations.

Results of the attribute study

The analyses were based on 246 data control points from the 11 wells in the study. We extracted 19 attributes from the seismic volume, then narrowed that list down to seven based on the stepwise linear regression and crossvalidation error analysis. These attributes are given in Table 1, along with associated application error (the average error using 11 wells with neutron porosity logs that could be accurately tied to the seismic data) and validation error (the average error leaving out one well at a time).

The smoothed inversion is a 50-ms smoothed rendering of a blocky seismic inversion. The inversion is an estimate of the seismic acoustic impedance based on the well data and the seismic wavelet. Because this inversion is based on well data, it is not a true seismic attribute. Accordingly, the inversion result is smoothed to where the well uniqueness is lost. The smoothed result keeps the low-frequency component, or trend, making it useful for predicting rock properties. Since acoustic impedance and porosity are generally inversely related, the smoothed inversion proves to be a good starting point for porosity prediction.

The integrated absolute amplitude is the running sum of the reflection strength minus a smoothed version of the reflection strength. This attribute enhances strong amplitudes, whether positive or negative, that denote high acoustic impedance contrasts. Changes in impedance contrasts may indicate stratigraphic or facies changes.

Amplitude weighted phase is the product of the reflection strength and the instantaneous phase.

Average frequency is a running average of the instantaneous frequency. The average instantaneous frequency tracks dominant frequency characteristics that may be associated with changing lithology or stratigraphy.

Instantaneous phase is independent of the reflection strength and thus emphasizes weak coherent events. In stressing the continuity of events, it can be useful in locating stratigraphic pinchouts and channel features.

Minimum continuity, or coherency, is a measure of the lowest similarity from one seismic trace to a neighboring trace over a time window. The results show abrupt contrasts in impedance because of stratigraphic or facies changes. Volumes of coherency data may be used to locate channel edges because of the variance in reflection character at the channel margins (Bahorich and Farmer, 1995).

Table 1. Seismic attributes and associated application error (includes all 11 wells) and validation error (excludes one well at a time as the target well).

Seismic attribute	Application error (% porosity)	Validation error (% porosity)
(Smoothed Inversion)^2	2.64	2.76
Integrated absolute amplitude	2.54	2.74
Amplitude weighted phase	2.45	2.71
Average frequency	2.36	2.62
Instantaneous phase	2.31	2.61
SQRT(minimum continuity)	2.25	2.59
Derivative	2.20	2.58

The derivative is the difference between the seismic trace amplitudes of one sample and the preceding sample. This emphasizes abrupt impedance contrasts that may be from stratigraphic or facies change.

The regression equation we derived had the form

$$\Phi(t) = w_0 + A_1 w_1(t) + A_2 w_2 + A_3 w_3 + A_4 w_4 + A_5 w_5 + A_6 w_6 + A_7 w_7, \quad (1)$$

where $\Phi(t)$ is porosity at sample time t, A_n is the attribute, and w_n is the weight applied to the attribute (Russell et al., 1997). The correlation coefficient for the linear regression model is $r^2 = 0.74$, with an average error (the rms difference between the target log values and the predicted values) of 2.2% (porosity units). The validation testing yielded a correlation coefficient of 0.63 with an error of 2.6% (porosity units). The regression method modeled the trends of the porosity curve, but it failed to accurately pick up the extreme values in the curve (Figure 7). Figure 8 shows that the model overpredicts the lower porosity values and underpredicts the higher values. The end model would thus be a smoothed version of the porosity curve, but the trends of high and low porosity should be adequately predicted.

Training the PNN provided better results [$r^2 = 0.82$, with an average error of 1.9% (porosity units)]. However, the validation error remained the same [$r^2 = 0.62$, with an error of 2.6% (porosity units)]. These results were obtained using the equation

$$L' = \frac{\sum_{i=1}^{n} L_i \exp(-D(x, x_i))}{\sum_{i-1}^{n} \exp(-D(x, x_i))}, \quad (2)$$

where L' is the predicted porosity value at each sample, L_i is the actual porosity value, and $D(x, x_i)$ is the distance between the input point and each of the training points (Masters, 1995; Hampson et al., 2001). This distance is measured in the multidimensional space spanned by the attributes. The PNN results are shown in Figure 9, and a crossplot of the data is shown in

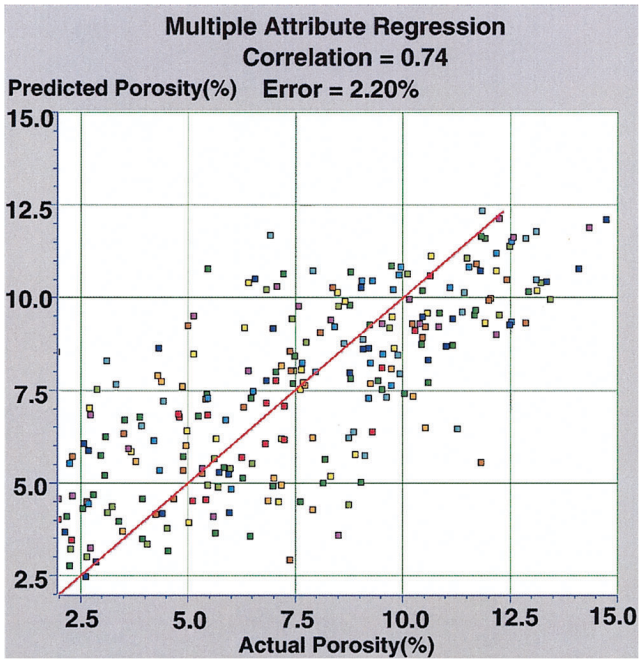

FIG. 8. Crossplot of the linear regression model results. Each data point color represents a different well. The red line is a $Y = X$ line. Note the tendency to overpredict the lower actual porosities and to underpredict the higher porosity values.

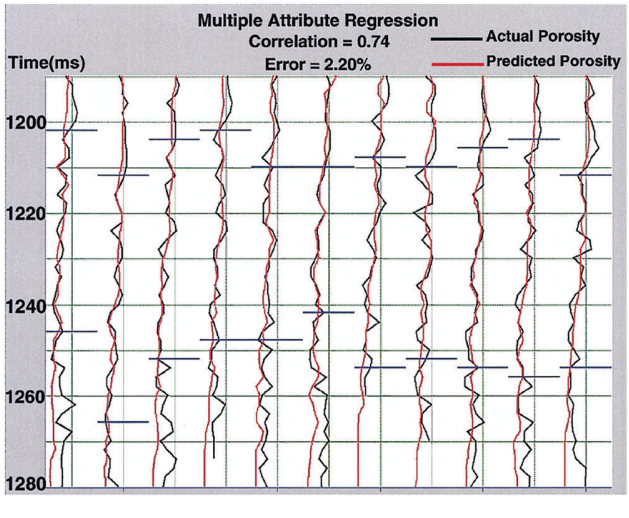

FIG. 7. Application of the linear regression method to predicting porosity. The blue horizontal lines at each well depict the time window from the lower Brushy Canyon to the Bone Spring. The model (red) adequately predicts the trends in the actual porosity curve (black) but fails to pick up the extreme porosity values. The correlation is only valid within the indicated time window.

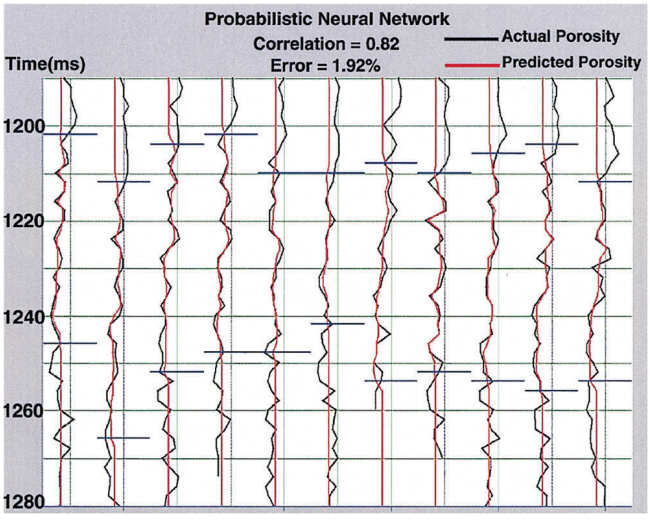

FIG. 9. Application of the PNN to predicting porosity. As in Figure 7, the blue horizontal lines depict the time window. The PNN modeled porosity curve (red) more accurately predicts the actual porosity curve (black) than the standard linear regression model. The PNN also appears to have predicted the extreme porosity values. The correlation is only valid within the indicated time window.

Figure 10. Figure 9 shows that the PNN not only predicts the trends in the porosity curves but it is also better predicts the extreme values than the linear regression model. The crossplot still reveals the tendency to smooth the porosity curve, but now we expect to see greater detail in maps generated from this model over the linear regression model.

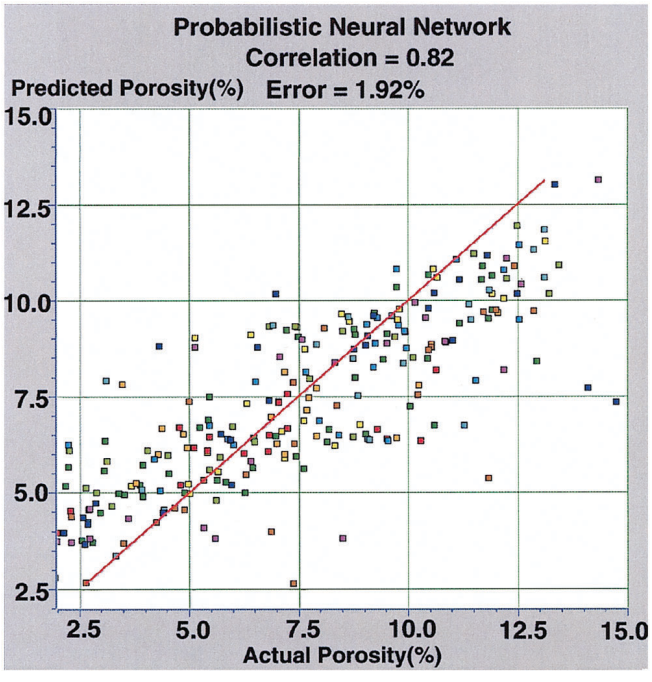

FIG. 10. Crossplot of the PNN results. Each data point color represents a different well. As in Figure 8, the model tends to overpredict the low porosities and underpredict the high porosities, but the PNN data points are arranged noticeably closer to the $Y = X$ line.

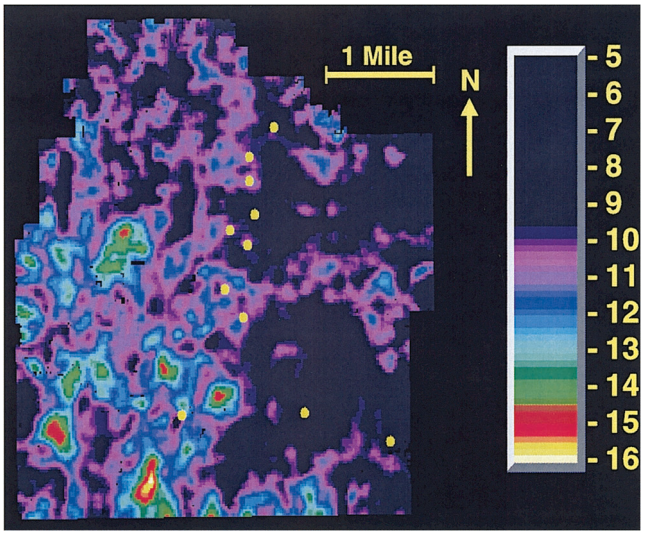

FIG. 11. Smoothed average predicted porosity map of the entire unit C time window, based on the linear regression model. Linear trends of high porosity in the northeast–southwest direction occur in the southwest but die out to the north.

Figure 11 is a smoothed average predicted porosity map of unit C based on the linear regression model. Some high-porosity north–south-striking linear features appear in the southwestern portion of the study area, but they die out to the north. The orientation of the nine wells in the center of the study area is approximately parallel to the channel of unit C (Figure 4c). The two wells in the southeastern corner are located outside the channel.

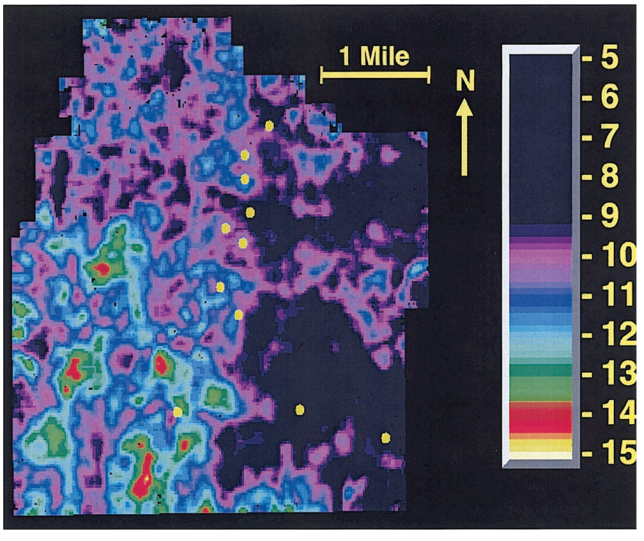

FIG. 12. Smoothed average predicted porosity map of the entire units A–D time window using the linear regression model. Because of the increased time window and the vertical stacking of channels in units A–D, channel features are now enhanced but the high porosity trends still die out to the north.

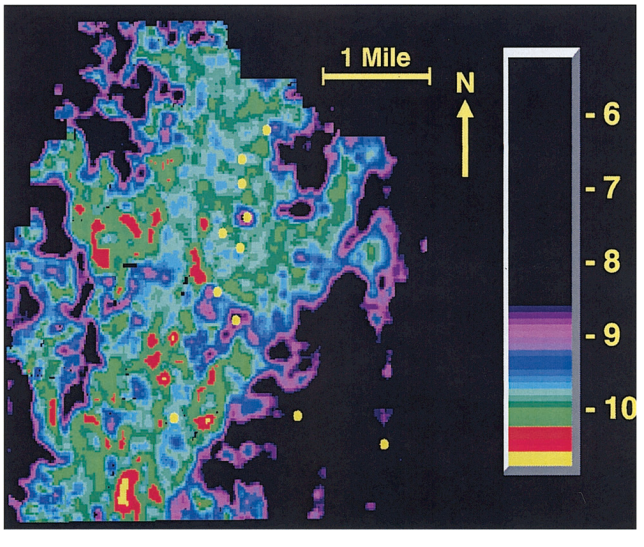

FIG. 13. Smoothed average predicted porosity map of the entire unit C time window based on the PNN model. The high-porosity zones in the southwest are diminished from 15–16% (Figure 11) to 10–11%. Other wells in this area show average unit C porosities to be about 10.2%. The PNN also predicted more uniform porosities throughout the channel and more precisely modeled the channel margins in the east and the west.

To enhance the linear features because of the vertical stacking of the channels as seen in Figure 4, we created an average predicted porosity map of units A–D (Figure 12). As expected, the north–south linear features are enhanced because of the greater time window, but the high-porosity zones still appear to die out to the north. The edge of the high-porosity zone trends north–south just east of the wells in the center of the study area. However, the porosity seems to be randomly dispersed in the western region.

Another map of the average predicted porosity of unit C was created using the PNN model (Figure 13). In addition to the more distinct north–south linear feature that runs through the center of the study area, the porosity distribution is more uniform in the southern and northern halves than in the linear regression model (Figure 11).

The PNN result was then used to create an average predicted porosity map of units A through D (Figure 14). As was the case in Figure 13, the PNN model displays more evenly distributed porosity values than the linear regression model. The edges of the high-porosity zone that runs north–south through the center of the study area are much more distinct than the those the linear regression result predicted (Figure 12).

Figure 15 shows an isopach map of unit D (Figure 4d) compared to the average predicted porosity map of the same unit based on the PNN model. The linear feature in the porosity map is identical not only in orientation to the channel in the isopach map but also in location. Stratigraphic picks on 77 well logs went into generating the isopach map on the left, while only 11 wells were used as input in making the porosity map on the right.

As a final test of the PNN prediction, we tested our results against eight wells (selected because they represent various geographic locations in the study area) that had been excluded from the multiattribute study because they lacked sonic logs. Table 2 shows the actual porosity compared with the predicted average porosity over the unit C time window using both the linear regression and the PNN models. The PNN predicted the actual average porosity within 1.4% (porosity units), whereas the regression model predicted the average porosity within 2.2% (porosity units).

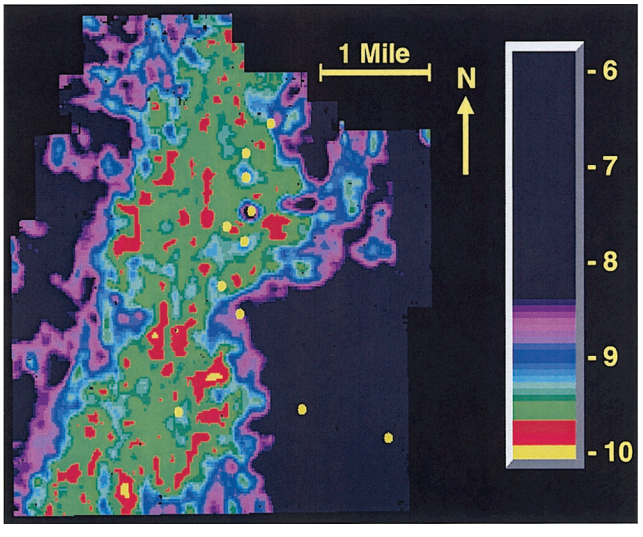

FIG. 14. Smoothed average predicted porosity map of the entire units A–D time window using the PNN model. The channel margins are now more enhanced because of the greater time window. Also, the PNN predicted more uniform porosities over the entire channel volume than the linear regression model (Figure 12), despite the same sparse well coverage in the southwest.

Discussion

The exact origin of the porosity in the lower Brushy Canyon is unknown. The most likely explanation is that porosity is a combination of depositional and diagenetic processes, with the

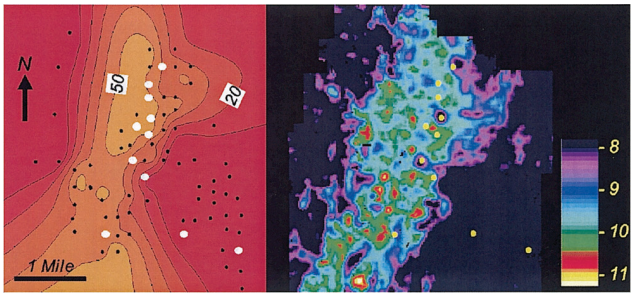

FIG. 15. Comparison of the unit D isopach (Figure 4d) with a contour interval of 10 ft and the smoothed average predicted porosity map of the entire unit D time window using the PNN model. In addition to capturing the true channel orientation, the predicted channel also appears in the same location as interpreted from the isopach map. A total of 77 wells were used to constrain the unit D sandstone channel in the porosity map. The PNN model successfully predicted the western edge of the channel, despite the fact that no wells were drilled outside the channel.

Table 2. Comparison of linear regression and PNN to predict porosity at other blind well locations.

Approximate location	Actual porosity (%)	Regression (%)	Error (%)	PNN (%)	Error (%)
South of center of main channel	10.7	12.5	1.8	10.0	−0.7
West of center of main channel	11.4	12.5	1.1	10.0	−1.4
Southwest of channel center	10.3	11.0	0.7	10.0	−0.3
Just outside channel to the west	8.1	14.0	5.9	9.5	1.4
Just outside channel to the east	10.5	7.5	−3.0	8.0	−2.5
Outside channel to the east	11.7	8.5	−3.2	9.0	−2.7
South of center of main channel	12.4	12.0	−0.4	10.0	−2.4
Northeast of channel center	10.0	11.5	1.5	10.0	0.0
Average Error			**2.2**		**1.4**

diagenetic events destroying primary porosity (Behnken, 1996; Montgomery et al., 1999). Because cleaner sandstones typically have greater original porosity than poorly sorted sandstones, we would expect to see higher predicted porosity in the high-depositional-energy channels where percent sand content is higher than outside the channels.

The most obvious difference between the linear regression porosity maps (Figures 11 and 12) and the neural network maps (Figures 13 and 14) is the more even distribution of porosity from the southern to the northern half of the study area based on the PNN model. The percent sand content maps we generated from log-based lithology interpretations to assist our channel interpretations (not shown) depicted relatively uniform sand distribution throughout the channel, and the percentages diminished with increasing distance from the channel axis. This suggests that porosity should be evenly distributed throughout the channel and decrease with distance away from the channel axis, assuming spatially uniform diagenesis. Although maps produced from both models show linear features where channels are seen on the isopach maps (Figure 4), the PNN porosity maps show a more distinct channel edge on the east and west sides.

Figure 11 shows patches of high porosity (15–16%) in the southwestern part of the study area. The actual average porosity from the well drilled in that region is 10.2%. Similar porosities are recorded in other wells in that area that were not included in the seismic attribute study because they did not have sonic logs (Table 2). A comparison with Figure 13 shows that it also has patches of higher porosity in the same region, but the values are lower (10–11%) and closer to the actual values. Porosity values predicted using the regression model were closer to the actual porosities where there was greater well control than in areas of sparse well coverage. The measured average porosity from a well in this area is 10.5%. The regression model predicted values of 10–12% in this area, which is close to the actual porosity. The PNN model in Figure 13 shows predicted porosities between 9% and 11% consistently throughout the channel. This raises the question of why the PNN predicted porosity better and more consistently than the linear regression model.

We believe the PNN predicted the porosity more accurately because the relationship between the seismic data and the well-log data was much more complex than the linear regression model predicted. The regression model accurately predicted the porosity in areas of dense well control but failed where well control was limited (the southwest). The PNN model was able to successfully determine the nonlinear relationship between the seismic data and the well data.

Another way to test the accuracy of the PNN model is to compare the predicted porosity map of a unit to its respective isopach map. Figure 15 shows the unit D isopach map (left) and the average PNN-predicted porosity over the unit D interval (right). Because the porosity on either side of the unit D channel is lower than the porosity in the channel as determined from the well logs, the porosity map should be identical with the isopach map. In addition to the near-perfect channel orientation match, we note that the channel was similar in dimensions and location despite the significant reduction of well control. There is no well control west of the unit D channel with which to constrain the channel in the PNN model. Based solely on the nonlinear relationship between well-log data and the seismic attributes, the PNN was able to predict the edge of the high-porosity zone at the western channel margin.

Table 2 lists eight wells scattered throughout the study area where the average porosity of unit C is known. Wells 4, 5, and 6 were drilled outside of the main unit C channel where well coverage is minimal. The PNN still predicted the porosity within the validation error, while the regression model greatly overpredicted the low porosity and underpredicted the higher porosities. The other five wells were drilled inside the main unit C channel, but mostly away from the dense well coverage in the north. The linear regression technique overestimated porosity in the southern half of the channel, which is inaccurate in light of the actual uniform (10–12%) channel porosity, whereas the PNN model predicted this uniformly distributed porosity trend.

ANALYSIS

The results of this work have implications that go beyond lower Brushy Canyon porosity prediction in this study area. The seismic attribute analyses allow us to gain new insights into the geology. The results show a more stratigraphically coherent distribution of physical properties than has been previously imaged in the lower Brushy Canyon using seismic attributes (Balch et al., 1998; Hardage et al., 1998). Unlike these two earlier studies, our results show channel-like features on a scale comparable to those mapped in outcrop (Basham, 1996) and in the subsurface (Thomerson and Catalano, 1996). Furthermore, we can show that the best production comes from the stacked channel succession in the center of our study area (Figure 16).

The PNN model yielded more geologically reasonable results than the linear regression model, but the physics [equation (2)] are much less intuitive. This stresses the need (a) to examine the physical basis for the seismic attribute selection

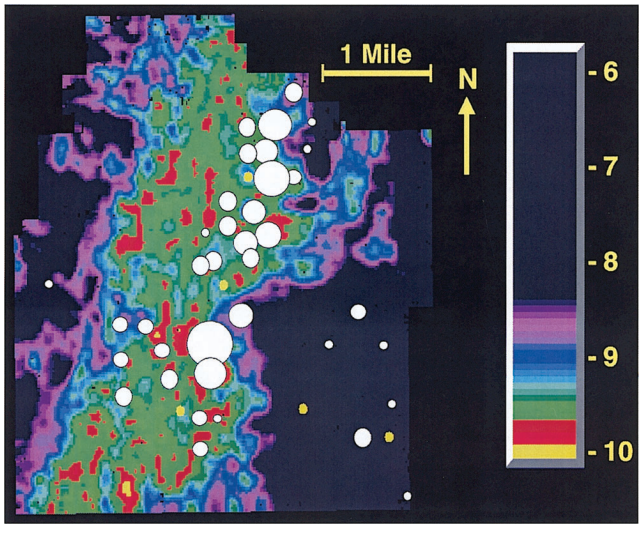

FIG. 16. PNN-based map of the average predicted porosity of the entire units A–D time window with cumulative basal Brushy Canyon production data overlain. We sorted through scout tickets to identify those wells that produce only from the lower Brushy Canyon. The larger bubbles indicate wells with better production. The best production comes from within the channel fairway, and low or moderate producers are found outside of this trend.

into the input data before the neural network is even applied and (b) to analyze the results in light of what is known about the geology of the area.

SUMMARY

This project sought to predict the porosity of the lower Brushy Canyon interval in interwell areas. To do this, we began by evaluating the geology through log-based stratigraphic analysis. The lower Brushy Canyon in this area is characterized by a vertically stacked series of channeled sandstones separated by thin layers of organic siltstones and carbonates. This vertically complex geology caused zones of extreme high and low porosity to appear in the logs. A reliable porosity model had to be able to predict the extreme values so as to not significantly overpredict the interbeds and underpredict the channel porosity.

We used both linear regression and a neural network in a volume-based approach to model porosity distribution based on seismic attribute analyses. The standard linear regression model adequately predicted the porosity in areas of greater well control but failed in areas of sparse well control. As a result, the linear regression model did not accurately portray the channels that we interpreted from well-log information.

The PNN was trained to find the best nonlinear relationship between the seven seismic attributes and the actual porosity log. The results were an all-around improvement over the regression model. Not only did the PNN yield a higher correlation coefficient, but the relationship it found greatly reduced the problem of sparse well coverage. This model also predicted edges of high-porosity zones parallel to the interpreted channel boundaries even in areas where there were no wells to constrain the location of the channel.

These results indicate that, when properly employed, PNNs can provide a means of improving subsurface physical property predictions and avoiding the pitfalls described by Schuelke et al. (1998), Hart (1999), and others.

ACKNOWLEDGMENTS

We thank Pogo Producing Co. and Burlington Resources for the well database and the 3-D seismic volume used in this project. Stratigraphic and seismic interpretations were completed using software provided by Landmark Graphics Corp. and Hampson-Russell Software Services. Robin Pearson provided assistance in understanding the capabilities of the software. Finally, we thank Jim Schuelke and two anonymous reviewers for their constructive suggestions that helped to clarify our arguments.

REFERENCES

Bahorich, M., and Farmer , S., 1995, 3-D seismic discontinuity for faults and stratigraphic features: The coherence cube: The Leading Edge, **14**, 1053–1058.

Balch, R. S., Weiss, W. W., and Wo, S., 1998, Correlating seismic attributes to reservoir properties using multi-variate non-linear regression, *in* DeMis, W. D., and Nelis, M. K., Eds., The search continues into the 21st century: West Texas Geol. Soc. Publ. **98-105**, 199–203.

Basham, W. L., 1996, Delaware Mountain group sandstone channel orientations: Implications for sediment source and deposition, *in* DeMis, W. D., and Cole, A. G., Eds., The Brushy Canyon play in outcrop and subsurface: Concepts and examples: SEPM Permian Basin Section Publ. **96-38**, 91–102.

Behnken, F. H., 1996, Reservoir characterization of the Brushy Canyon Formation sandstone (Late Permian), strata production, Nash unit #15, Nash Draw Delaware Field, Eddy County, New Mexico, *in* DeMis, W. D., and Cole, A. G., Eds., The Brushy Canyon play in outcrop and subsurface: Concepts and examples: SEPM Permian Basin Section Publ. **96-38**, 173–182.

Bouma, A. H., 1996, Initial comparison between fine- and coarse-grained submarine fans and the Brushy Canyon Formation sandstones, *in* DeMis, W. D., and Cole, A. G., Eds., The Brushy Canyon play in outcrop and subsurface: Concepts and examples: SEPM Permian Basin Section Publ. **96-38**, 41–50.

Brown, A. R., 1996, Interpretation of three-dimensional seismic data, 4th ed.: Am. Assn. Petr. Geol. Memoir 42.

Gardner, M. H., and Sonnenfield, M. D., 1996, Stratigraphic changes in facies architecture of the Permian Brushy Canyon in Guadalupe Mountains National Park, West Texas, *in* DeMis, W. D., and Cole, A. G., Eds., The Brushy Canyon play in outcrop and subsurface: Concepts and examples: SEPM Permian Basin Section Publ. **96-38**, 17–40.

Hampson, D., Schuelke, J., and Quirein, J. A., 2001, Use of multiattribute transforms to predict log properties from seismic data: Geophysics, **66**, 220–236.

Hardage, B. A., Simmons, J. L., Jr., Pendleton, V. M., Stubbs, B. A., and Uszynski, B. J., 1998, 3-D seismic imaging and interpretation of Brushy Canyon slope and basin thin-bed reservoirs, northwest Delaware basin: Geophysics, **63**, 1507–1519.

Harms, J. C., and Brady, M. J., 1996, Deposition of the Brushy Canyon Formation: 30 years of conflicting hypotheses, *in* DeMis, W. D., and Cole, A. G., Eds., The Brushy Canyon play in outcrop and subsurface: Concepts and examples: SEPM Permian Basin Section Publ. **96-38**, 51–59.

Hart, B. S., 1998, New insights on the stratigraphy and production characteristics of the Bone Spring Formation: The search continues into the 21st century: West Texas Geol. Soc. Publ. **98-105**, 119–126.

——— 1999, Geology plays key role in seismic attribute studies: Oil & Gas J., **97**, July 12, 76–80.

Hart, B. S., and Balch, R. S., 2000, Approaches to defining reservoir physical properties from 3-D seismic attributes with limited well control: An example from the Jurassic Smackover Formation, Alabama: Geophysics, **65**, 368–376.

Hirsche, K., Porter-Hirsche, J., Mewhort, L., and Davis, R., 1997, The use and abuse of geostatistics: The Leading Edge, **16**, 253–260.

Justman, H., 2001, Source rodes in the Brushy Canyon Formation (Permion), Delaware Basin, southeast New Mexico: M.Sc. thesis, New Mexico Inst. of Mining and Technology.

Kalkomey, C. T., 1997, Potential risks when using seismic attributes as predictors of reservoir properties: The Leading Edge, **10**, 11–15.

Masters, T., 1995, Advanced algorithms for neural networks: A C++ sourcebook: John Wiley & Sons, Inc.

Montgomery, S. L., Worrall, J., and Hamilton, D., 1999, Delaware Mountain group, West Texas and southeastern New Mexico, a case of refound opportunity: Part 1—Brushy Canyon: AAPG Bull., **83**, 1901–1926.

Pearson, R. A., and Hart, B. S., 1999, Convergence of 3-D seismic attribute-based reservoir property prediction and geologic interpretation as a risk reduction tool: A case study from a Permian intraslope basin: 69th Ann. Internat. Mtg., Soc. Expl. Geophys., Expanded Abstracts, 896–899.

Ronen, S., Schultz, P. S., Hattori, M., and Corbett, C., 1994, Seismic guided estimation of log properties, part 2: Using artificial neural networks for nonlinear attribute calibration: The Leading Edge, **13**, 674–678.

Russell, B., Hampson, D., Schuelke, J., and Quirein, J., 1997, Multiattribute seismic analysis: The Leading Edge, **16**, 1439–1443.

Sageman, B. B., Gardner, M. H., Armentrout, J. M., and Murphy, A. E., 1998, Stratigraphic hierarchy of organic carbon-rich siltstones in deepwater facies, Brushy Canyon Formation (Guadalupian), Delaware basin, West Texas: Geology, **26**, 451–454.

Schuelke, J. S., and Quirein, J. A., 1998, Validation: A technique for selecting seismic attributes and verifying results: 68th Ann. Internat. Mtg., Soc. Expl. Geophys., Expanded Abstracts, 936–939.

Schuelke, J. S., Quirein, J. A., and Sarg, J. F., 1998, Reservoir architecture and porosity distribution, Pegasus field, West Texas—An integrated sequence stratigraphic–seismic attribute study using neural networks: Geo-Triad, Expanded Abstracts, 142–145.

Thomerson, M. D., and Catalano, L. E., 1996, Depositional regimes and reservoir characteristics of the Brushy Canyon sandstones, East Livingston Ridge, Delaware Field, Lea County, New Mexico, *in* DeMis, W. D., and Cole, A. G., Eds., The Brushy Canyon play in outcrop and subsurface: Concepts and examples: SEPM Permian Basin Section Publ. **96-38**, 103–111.

Yang, K., and Dorobek, S. L., 1995, The Permian Basin of West Texas and New Mexico: Tectonic history of a "composite" foreland basin and its effects on stratigraphic development: SEPM Special Publication 52.

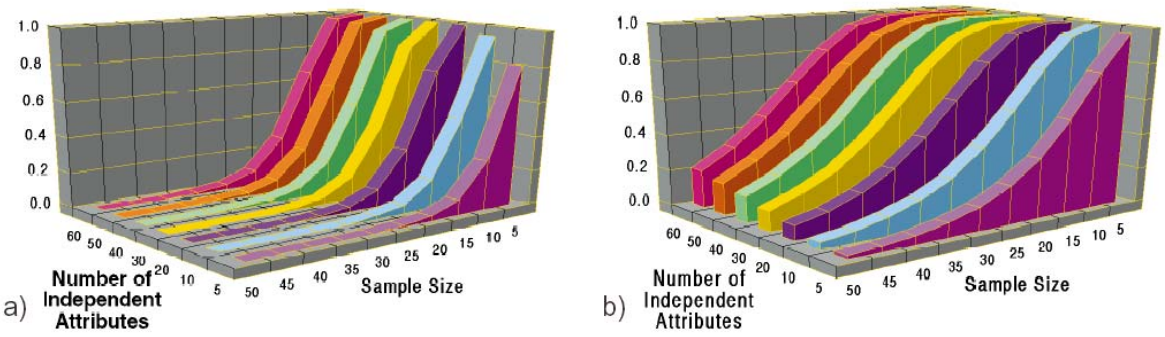

Figure 2. Probability of observing at least one spurious sample correlation of magnitude (a) E 0.6, and (b) E 0.4 when actually the well data and seismic attributes are uncorrelated.

Kalkomey, 1997

•The fact that a correlation can be found between two variables, such as a seismic attribute and a log-derived physical property, does not mean that there exists a meaningful physical basis for the relationship between those two variables. Spurious correlations are correlations that exist between two variables that are, in reality, unrelated (i.e., “coincidences”). An example of a spurious correlation might be a positive relationship between well results and the phase of the moon on spud date. For example, the best wells might have been drilled when the moon is full. Does that mean that all you need to worry about is drilling when the moon is full?

•Kalkomey (1997) showed that the chances of observing a spurious correlation between two variables depends on: a) the magnitude of the correlation coefficient, b) the number of independent attributes and c) the sample size (i.e., the number of wells). The fewer the number of wells and the greater the number of attributes, the better the chances of observing a spurious correlation.

•Attribute workers need to be careful to detect and avoid spurious correlations. The mathematical aspects f an attribute study (e.g., training neural networks, statistical testing) will not be able to identify such problems. Identification of spurious correlations must be based on: a) geological examination of the results (do they make sense geologically?), and b) geophysical assessment of the relationship between attributes and physical properties (is there a known or suspected relationship?).

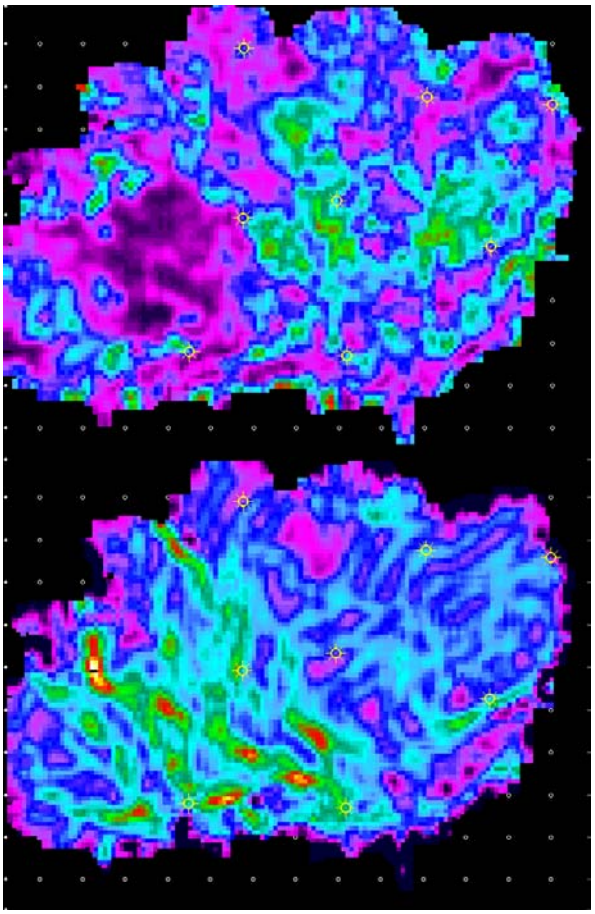

Attribute-Based Production

Upper Image: r = 0.96

Lower Image: r = 0.89

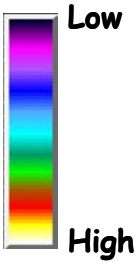

Questions:
Which map to believe?
Why?

•Hart (1999) showed these two maps that show two different predictions of production (low -> high) from a gas reservoir. In the upper image, fuzzy logic was used to identify the best combination of attributes for predicting production, and then a neural network was trained to define the predictive relationship. A correlation coefficient of 0.96 was noted between the predicted and observed production at well locations. The lower image shows a prediction, based on a different set of attributes, that also has a high correlation coefficient (0.89). The scale is the same for both maps. Although both methods yielded results with very high correlation coefficients, the maps are very different, both cannot be correct.

•Evaluation of the results using geologic and engineering data indicates that neither map can be correct. Production from this field is known to be strongly influenced by fractures that are associated with a series of normal and reverse faults (this is the Ute Dome Paradox field discussed in the case study of the structural chapter). The top map does not show the fracture trends. The lower map has suggestions of the two fracture trends, but predicts high production in the area to the southwest. However this area is low on structure and water production is a problem here. As a result, despite the statistical success, both results were rejected as being due to either a spurious correlation or over-training of the neural networks.

Time-lapse (“4-D”) Seismic

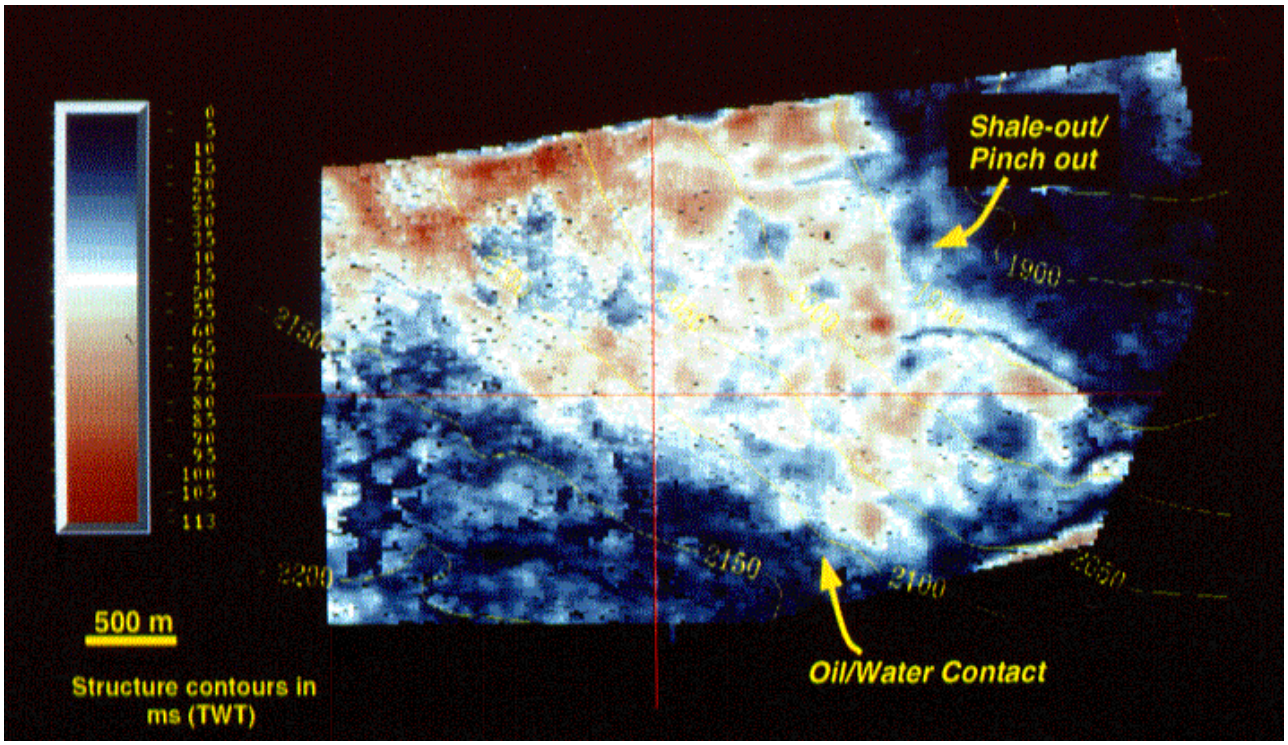

- The seismic signature of a reservoir depends on two primary elements, static reservoir rock properties (e.g., porosity and lithology) and “dynamic” time-varying properties (e.g., fluid saturation and pore pressure). The comparison of two or more 3-D surveys over the same area in effect cancels the static contribution. Therefore, any observable change is due to “dynamic” changes of the reservoir and effects of fluid flow.
- Changes in pore fluid composition (e.g., water/gas/oil saturation), pressure and temperature can all affect the velocity and density of rocks. Any of these changes might be expected when a field is being produced.
- Amplitude map above shows location of oil/water contact at the time the seismic data were collected. Perhaps a 3-D survey collected at this location another time might show the oil/water contact in a different location?

Time-lapse ("4-D") Seismic

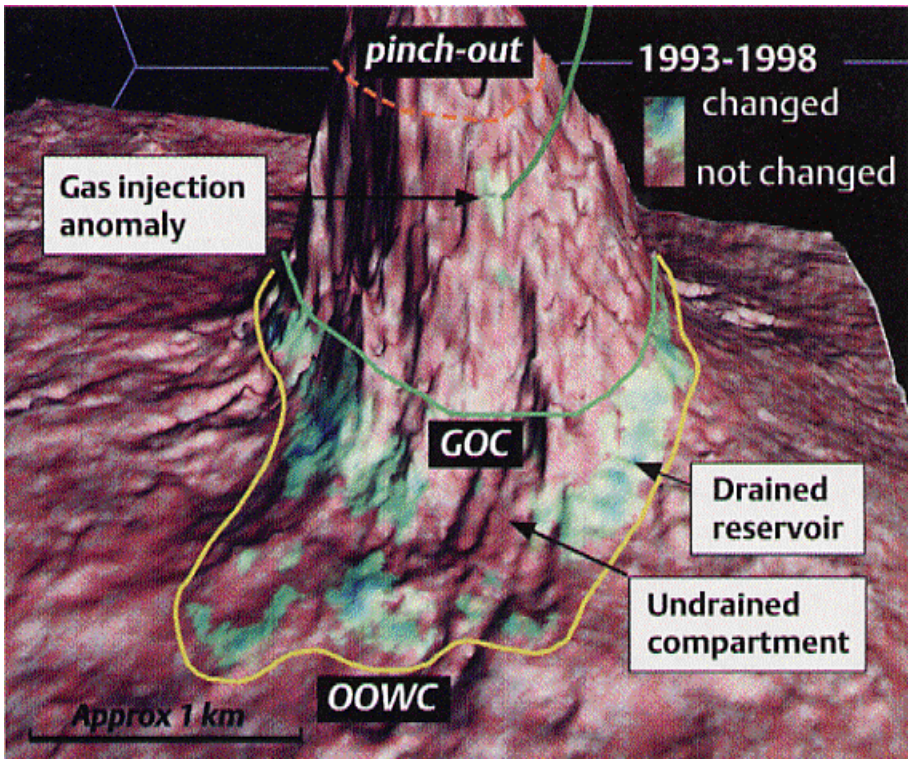

- Under the right circumstances, changes in density or velocity might be detectable seismically. These changes might manifest themselves in seismic data as changes in amplitude, changes in traveltime or changes in waveform.
- Some of the considerations for assessing the technical risk of a time-lapse study include: a) porosity, b) rock compressibility, c) change in fluid saturation, d) fluid properties, e) seismic image quality, f) repeatability of seismic imaging.
- Also need to consider economics.
- Time-lapse seismic techniques use various "differencing" techniques to identify areas where changes have occurred. This can help maximize drainage efficiency (new producers, injectors, etc.)
  - Image shows predicted changes in a North Sea reservoir.

Multicomponent Seismic

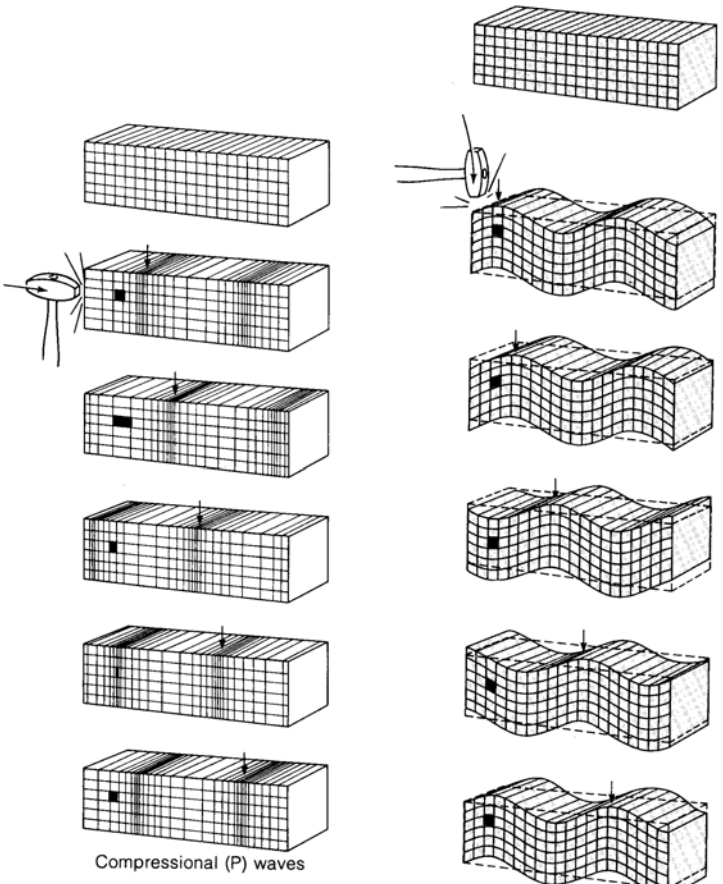

Figure 17-30

- Most seismic data collected involve the generation and recording of p waves (left).
- Multicomponent (generation and/or recording of both p and s waves) surveys may be useful in some circumstances, since some rock bodies may be invisible to p waves but not to s waves.
- Other uses include fracture identification.

Multicomponent Seismic

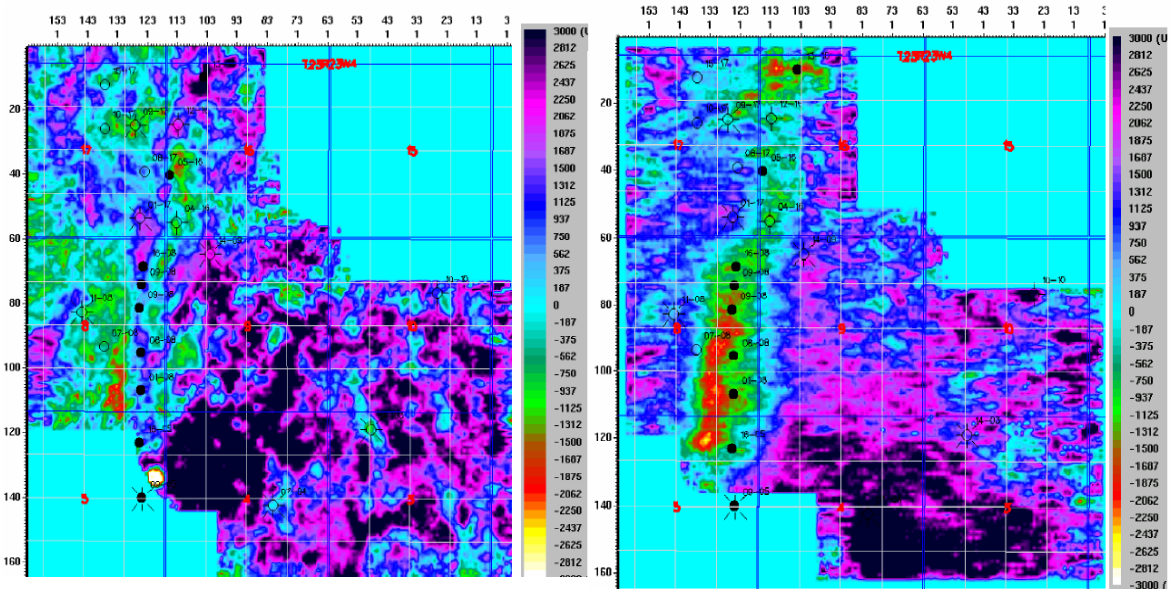

- Multicomponent seismic surveys may involve using p wave sources and geophones together, and s wave sources and geophones together. Additionally, mode converted waves (p-s) might be recorded.
- These two images show timeslices through 3-D seismic data from Alberta. On the left is a timeslice through a p-p wave volume at the approximate level of a Cretaceous channel. On the right is an equivalent timeslice through a p-s volume. Note how the channel is apparent in the p-s data but not the p-p data.

Multicomponent Seismic

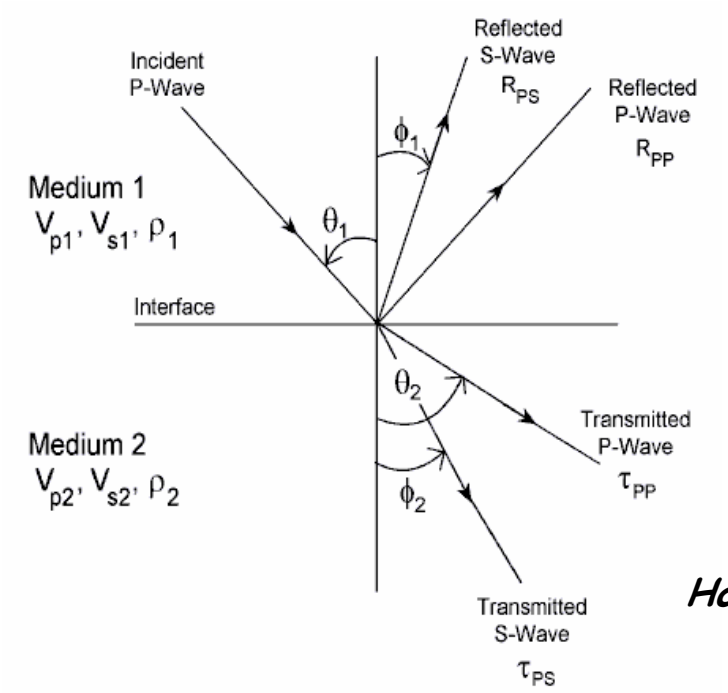

Hampson-Russell

- Converted wave surveys (p-s data) have several applications, including seeing through gas clouds and distinguishing between lithologies that have the same acoustic impedance but different rigidities (shear wave velocities).
- There are some problems that need to be faced when working with converted wave surveys. These include:
  - As shown above, the angle of incidence for the downgoing p-wave is different from the angle of the upgoing s-wave ($\Theta_1 \neq \varphi_1$ in the image above). As such, the reflection does not come from a point mid-way between the source and receiver. The reflection therefore does not represent a midpoint but rather a conversion point. Knowledge of p- and s-wave velocity fields is needed to accurately map the location of these points for stacking
  - Unlike conventional p-wave data that travel up and down at the same velocity, converted waves travel up at a slower velocity (s-wave) than the downgoing p-wave. As such, reflection times are different for the two types of survey. Along with differences in reflection character, the different times can cause problems in carrying horizons from one type of data to the other.

Inversion

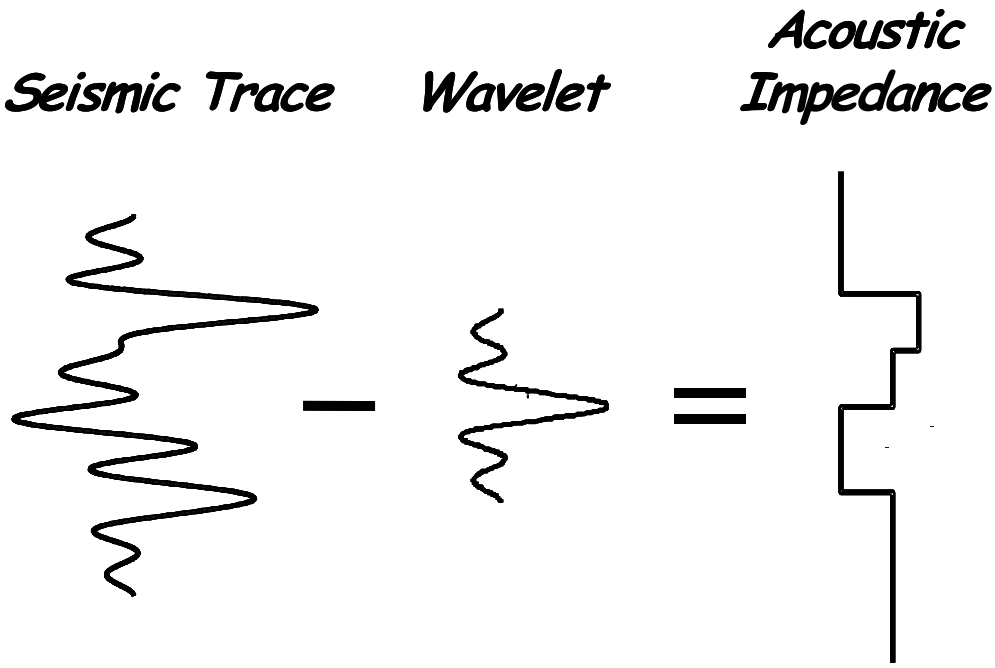

- Conventional seismic data image the change in physical properties at interfaces between layers of different acoustic impedance
- What we are really interested in are the physical properties of the layers themselves
- Conceptually, as shown above, what we want to do is remove the seismic wavelet from our data so that we end up with acoustic impedance traces
  - Acoustic impedance is a layer property that is closely associated with lithology, porosity and pore fill
  - By removing the seismic wavelet we enhance resolution, minimizing tuning effects
  - The result more closely resembles a geologic cross-section

Inversion

- The three most commonly used types of inversion are:

- **Recursive**
  - Seismic trace known
  - Each sample of the seismic trace is assumed to be a reflection coefficient
  - Integration along seismic trace produces acoustic impedance trace
- **Model-Based**
  - Wavelet and seismic trace known
  - Initial model obtained from well data and or other data
  - Model convolved with wavelet and compared with seismic trace
  - Iterate until acceptable match obtained
- **Sparse-Spike**
  - Assume earth is a set of discrete layers the boundaries represented by reflection coefficients
  - Wavelet known
  - Seismic trace known
  - Extract reflection coefficients from largest down
  - Invert reflectivity sequence

- Each of these methods has limitations and advantages.
  - Recursive: lacks low-frequency information, but can be used when well data are not available
  - Model-based: sensitive to choice of wavelet and input model, non-unique solutions
  - Sparse-spike: sensitive to choice of wavelet, non-unique solutions

Inversion

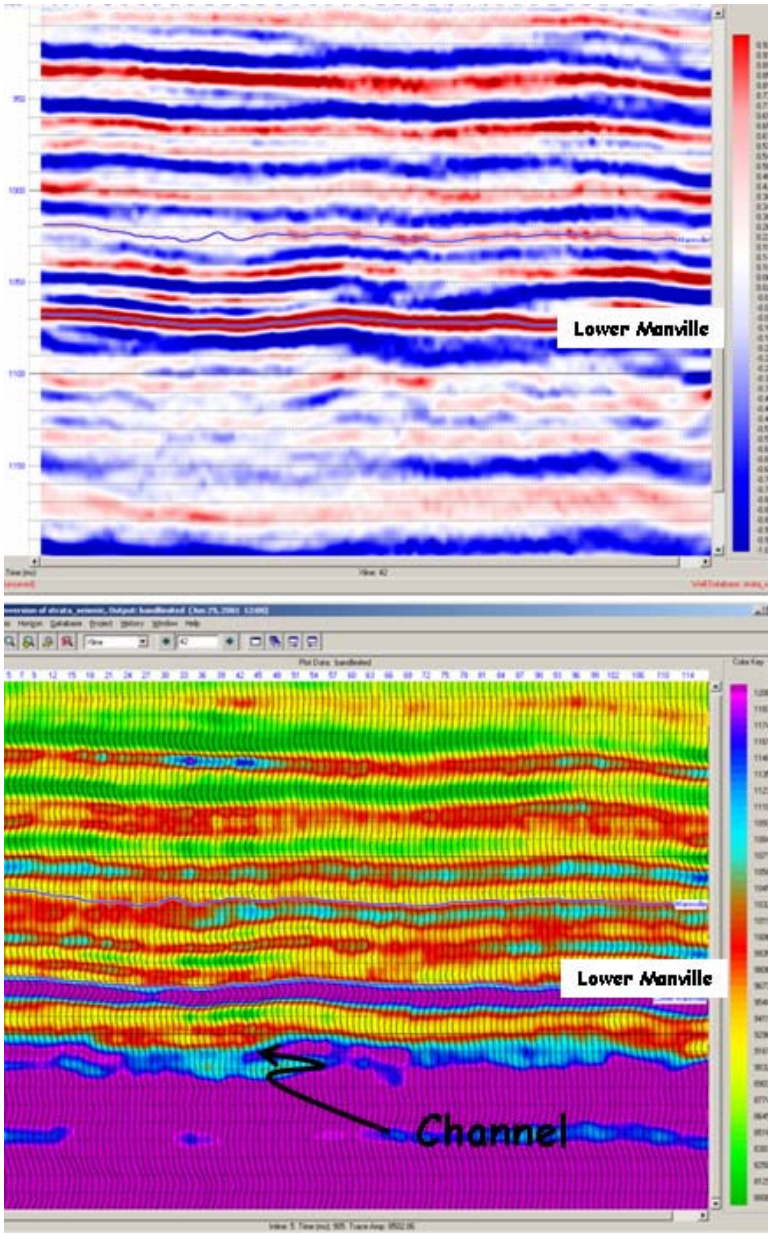

Comparison of amplitude data (top) and inversion results (bottom). Inversion results clearly show relatively low impedance clastic channel (yellow/red) incised into high-impedance carbonates (purple/blue) along pre-Cretaceous unconformity. Try to find this channel in the amplitude data.